

Defining the mechanisms of inflammation that underlie the pathogenesis of ovine footrot

Grazieli Maboni, DVM, MSc

Thesis submitted to the University of Nottingham for the degree of Doctor of Philosophy

March 2017

Abstract

Ovine footrot is a bacterial infection of the ovine interdigital skin with a significant welfare and economical concern for the sheep industry globally. Footrot is a major cause of lameness in sheep and it is characterised by two different clinical presentations, interdigital dermatitis (ID) and under-running footrot. The aetiology of this disease is complex with *Dichelobacter nodosus* as the essential pathogen initiating under-running footrot lesions, however the role of other bacteria, including *Fusobacterium necrophorum* and *Treponema* spp., and the roles of other bacterial populations in healthy, ID and footrot feet remain unclear. The severity of footrot is thought to be exacerbated by the intense inflammatory response against the infection; nevertheless, there is little information in the literature regarding the ovine immune response to this disease. In this context, the hypothesis of this study is that the pathology of footrot is a host mediated expression of local immune responses, in association with bacterial colonisation, leading to severe inflammation that can progress to under-running lesions. This hypothesis was investigated through the determination of bacterial prevalence and load using qPCR and host gene expression studies using RT-qPCR and RNA sequencing. Moreover, a 3D skin explant model was developed for *in vitro* infection studies. Key findings include that the highest prevalence and load of *D. nodosus* was on feet with ID and the vast majority of samples from UK sheep contained virulent *D. nodosus* strains; notably, the more pathogenic subspecies of *F. necrophorum*

was found in these samples. In addition, a comparison of bacterial colonisation on the ovine interdigital skin surface and within the skin demonstrated that bacterial prevalence and load differed between those two locations. Gene expression analysis revealed that inflammation, as marked by mRNA expression levels of *CXCL8* and *IL1β*, central mediators of immune response in the skin, were associated with virulent *D. nodosus* in footrot affected feet. This suggests that *D. nodosus* colonisation may impact on the inflammatory mechanisms involved in footrot. The global gene expression study (RNA sequencing) showed 34 significantly expressed genes in footrot samples indicating upregulation of the local inflammatory and innate immune responses, whilst little association of the local adaptive immune response. A 3D skin model culture was developed and infection with *D. nodosus* strains for 28h was demonstrated by qPCR and FISH and resulted in the release of IL1β and CXCL8 in the culture media. Hence, this confirms a role for IL1β and CXCL8 in the early local response to *D. nodosus* infection. Taken together, the data presented in this thesis may potentially endorse our hypothesis that the separation of the hoof horn from the sensitive underlying tissue is led by the host expression of local immune responses in association with bacterial colonisation.

Acknowledgments

First and foremost, I would like to express my gratitude to my supervisor Dr Sabine Tötemeyer for the opportunity to work on this project and for being always supportive since our first contact by e-mail. It was an extraordinary educational experience. I am eternally grateful.

I would like to thank the sheep abattoir staff for their essential support in obtaining biopsies from sheep feet. Also Dr Rodrigo Nova, Melissa Bexon, Michael Agbaje, Dr Adam Blanchard, Nikki Bollard and Wayne Sanders for helping in the abattoir visits.

This study would not be completed without the help of Dr Sara Frosth and Dr Anna Aspan. Thank you for the tremendously support, for sharing experiences and for the countless emails and exchange of ideas. Especially, thank you for the opportunity to visit Uppsala and for everything I learned in that week.

I also would like to thank Professor Richard Emes for the guidance in RNAseq analysis. Dr Tim Jensen and the research group from the Danish Technical University for teaching me the FISH analysis. Moreover, I would like to thank Dr Kerstin Baiker, Dr Catrin Rutland, Alan Lasslett, Aziza Alibhai and Ceri Staley for histological and technical support.

Thank you Felipe for the unconditional support during the years of my PhD.

Thanks to my flatmate Ivonne and to my office colleague Aouatif, for sharing the daily joys and frustrations. You were the closest association with `family' and `home' during my time in Nottingham.

Thank you to all my friends from the Vet School with whom I shared lunch, coffees and stimulating discussions in and out of work. A special thanks to Rob, Sandie, Ramzi, Diego and Abril. You have earned a special place in my heart.

To my Masters supervisor, Dr Agueda C. de Vargas for the opportunity to work at LABAC (Brazil), where I was introduced to the fantastic world of bacteriology. Thank you for the inspiration and support.

Franciele, Thiago, Ana and Valdir: thank you for everything. Fran, thank you for your support during my high school, I am eternally grateful for your help!

Last but not least, I would like to express my gratitude for CAPES (Brazilian government) and The University of Nottingham for the PhD scholarship.

Dedication

I would like to dedicate this work to my mother Ana, for understanding my absence.

Table of contents

1. General Introduction **1**

1.1 Ovine footrot 1

1.1.2 Clinical presentations 2

1.1.3 Footrot aetiology 3

1.1.3.1 *D. nodosus* 5

1.1.3 Footrot epidemiology and transmission 12

1.1.5 Treatment and vaccination 13

1.1.6 Control program in the UK 15

1.2 Skin structure 16

1.2.1 Epidermis 17

1.2.2 Dermis 21

1.2.3 Histology and anatomy of the ovine hoof 22

1.3 Innate immune response in the skin 23

1.4.1 Innate immune response in the epidermis 26

1.4.2 Innate immune response in the dermis 27

1.4.2.1 Dermal DCs 29

1.4.2.2 Mast cells 29

1.4.2.3 Skin macrophages 30

1.4.2.4 Fibroblasts 30

1.4.2.5 Natural killer (NK) cells 31

1.5 Toll like receptors 31

1.5.1 TLRs involved in bacterial recognition 36

1.5.1.1 TLR2 forms heterodimers with TLR1 and TLR6 36

1.5.1.2 TLR4 37

1.5.1.3 TLR5 38

1.5.1.4 TLR9 38

1.5.1.5 TLR11 38

1.5.1.6 TLR13 39

1.5.2 TLRs in sheep 39

1.5.2.1 TLRs in healthy ovine tissues and cells 43

1.5.2.2 TLRs in ovine tissues and cells during disease process 44

1.6 Cytokines and chemokines 45

1.6.1 Chemokines 46
1.6.1 Ovine cytokines and chemokines 47
1.7 Summary and thesis aims 50
1.8 Hypothesis and aims 52
2. General materials and methods 54
2.1 Collection of tissue biopsies 54
2.2 DNA extraction 57
2.3 Real-time PCR assays for bacterial quantification 57
2.4 RNA extraction 61
2.5 cDNA synthesis and quality control of genomic DNA contamination 61
2.6 Quantification of ovine gene expression 62
2.7 Normalisation analysis of RT-qPCR data 63
3. Ovine footrot: new insights into bacterial colonisation... 65
3.1 Introduction 67
3.2 Materials and methods 70
3.2.1 DNA extraction and real-time PCR assays 71
3.2.2 Statistical analysis 72
3.3 Results 72
3.3.1 Prevalence and load of *D. nodosus*, *F. necrophorum* and *Treponema* spp. in tissues from the ovine interdigital skin 72
3.4 Discussion 77
3.5 Conclusions 81
4. Investigating bacterial colonisation on the ovine interdigital skin surface and within the skin layers 82
4.1 Introduction 82
4.2 Materials and methods 85
4.2.1 Study design 85
4.2.2 qPCR data normalisation and statistical analysis 88
4.2.3 Bacterial 16S rRNA sequencing 88
4.3 Results 89
4.3.1 Bacterial prevalence in biopsies vs. swabs 89
4.3.2 Bacterial load in biopsies vs. swabs 93
4.3.3 Bacterial 16S rRNA sequencing 97

4.4 Discussion 99
4.5 Future work 103
4.6 Conclusions 103
5. Identification of novel and reliable reference genes for RT-qPCR studies on ovine interdigital skin 105
5.1 Introduction 107
5.2 Materials and methods 110
5.2.1 Study design 110
5.2.3 Analysis of reference gene stability and co-regulatory function 111
5.3 Results 111
5.3.1 mRNA expression levels of candidate reference genes 111
5.3.2 Expression stability analysis 113
5.3.3 Co-regulation of candidate reference genes 118
5.4 Discussion 119
5.5 Conclusions 123
6. Expression of TLRs and pro-inflammatory cytokines in the ovine interdigital skin 124
6.1 Introduction 125
6.2 Materials and methods 127
6.2.1 Statistical analysis 127
6.3 Results 128
6.3.1 mRNA expression of cytokines in the ovine interdigital skin 128
6.3.2 Association of the host immune response and virulent *D. nodosus* colonisation 132
6.4 Discussion 137
6.5 Conclusions 141
7. Global gene expression in the ovine interdigital skin 142
7.1 Introduction 142
7.2 Materials and methods 144
7.2.1 Selection of samples for RNAseq 145
7.2.2 Sequencing and analysis of RNAseq data 146
7.2.3 Hierarchical cluster analysis and pathway analysis 147
7.2.4 Validation of RNAseq results using RT-qPCR 148

7.3 Results 149
7.3.1 Read mapping statistics 149
7.3.2 Determination of differently expressed genes among healthy, ID and footrot samples.....150
7.3.3 Validation of differently expressed genes of RNAseq using RT-qPCR 154
7.3.4 Hierarchical cluster analysis.....157
7.3.5 Grouping of differently expressed genes according to biological function using Ingenuity Pathway Analysis.....159
7.4 Discussion.....164
7.5 Conclusions.....171
8. Development of a 3D skin model culture to investigate ovine footrot 173
8.1 Introduction 173
8.2 Materials and methods 176
8.2.1 EVOC model optimization 176
8.2.2 EVOC model viability.....179
8.2.2.1 Tissue fixing, processing & staining.....180
8.2.2.2 TUNEL staining for cell viability detection.....184
8.2.3 EVOC exposure to *D. nodosus*.....185
8.2.3.1 Fluorescent *in situ* Hybridization (FISH) for.....187
D. nodosus 187
8.2.3.2 Cytokine measurement by Enzyme-Linked Assay (ELISA) 189
8.2.4 Statistical analysis.....190
8.3 Results 190
8.3.1 Optimisation of EVOC model 190
8.3.2 Tissue integrity and cell viability over a 76h mock infection 194
8.3.3 Ovine interdigital skin explant as an infection model.....198
for *D. nodosus* 198
Detection of D. nodosus by qPCR.....198
8.3.3.1 Tissue integrity and cell viability after 28h of bacterial infection.....202
8.3.3.2 Release of cytokine in the media supernatants following infection with *D. nodosus* 204
8.4 Discussion.....207

8.5 Future work and EVOC applications 214
8.6 Conclusions 218
9. General discussion 219
9.1 Overview 219
9.1.1 Events involved in healthy ovine feet leading to disease initiation (Figure 9.1 A) 223
9.3 Events involved in ID stage (Figure 9.1 B) 226
9.4 Events leading to the separation of the hoof from the sensitive underlying tissue (Figure 9.1 C) 227
9.5 Events involved in established footrot lesion (Figure 9.1 C) ...228
Appendix 263

List of Tables

Table 1.1 Recognized pathogen ligands (PAMPs) of Toll-like receptors (TLRs) 1-13……34

Table 1.2 Toll-like receptors (TLRs) mRNA expression in ovine tissues and cells in healthy conditions……..41

Table 1.3 Toll-like receptors (TLRs) mRNA expression in ovine tissues and cells during bacterial disease process……..…42

Table 1.4 Ovine cytokines investigated in bacterial infections…….48

Table 2.1 Ovine foot scoring system (provided by Dr Jasmeet Kaler, University of Nottingham)……55

Table 2.2 PCR mastermix reaction used in the quantitative PCR assays……..58

Table 2.3 Primers and probes details……60

Table 3.1 Number of visits to the abattoir and number of biopsies collected from healthy, interdigital dermatitis and footrot feet…….71

Table 4.1 Details of the matched samples included in this study. Swabs and biopsies were collected from the ovine interdigital skin space……87

Table 4.2 McNemar's test analysis of bacterial prevalence on matched-pair samples of swabs and biopsies collected from the ovine interdigital skin……..90

Table 5.1 Studies on reference genes available in the literature for normalisation of RT-qPCR data using ovine cells and tissues…….109

Table 5.2 Standard curve data of RT-qPCR assays for reference genes……..112

Table 5.3 Gene expression stability analysis using RefFinder software of 10 candidate reference genes for normalisation of RT-qPCR studies of the ovine interdigital skin……115

Table 6.1 Standard curve data for RT-qPCR assays……..128

Table 7.1 Samples selected for RNA sequencing (n=18) based on ovine feet clinical conditions, quality and yield of RNA, inflammatory background (IL1β expression) and presence of *D. nodosus*…….146

Table 7.2 RNAseq reads for 18 biopsy samples from the ovine interdigital skin. Total reads: number of raw reads generated from RNAseq. Mapped reads: sequence reads that were confidently mapped to reference ovine genome……150

Table 7.3 List of differentially expressed genes in healthy and footrot samples (n=18) from RNAseq……152

Table 7.4 Standard curve data for RT-qPCR assays used to validate RNAseq results……155

Table 7.5 Functional analysis of the genes differently expressed in healthy and footrot samples by Ingenuity Pathway Analysis. Category: inflammatory response……160

Table 7.6 Functional analysis of the genes differently expressed in healthy and footrot samples by Ingenuity Pathways Analysis. Category: dermatological diseases and conditions……161

Table 8.1 Transport medium components……177

Table 8.2 Washing medium components……178

Table 8.3 Qualitative, semi-quantitative scoring system used to evaluate skin tissue viability for both epidermis and dermis. Provided by Dr Kerstin Baiker……..……..182

Table 8.4 Components of infection media without antibiotics……185

Table 8.5 Components of infection media with antibiotics…..……..186

List of Figures

Figure 1.1 Clinical signs of footrot……3

Figure 1.2 Isolation, identification and morphology of *D. nodosus*……..10

Figure 1.3 H&E stained section showing the layers of the epidermis and dermis of the ovine interdigital skin……..18

Figure 1.4 Anatomy of the healthy ovine hoof……23

Figure 1.5 Cells involved in the innate immune response in the skin……25

Figure 1.6 Skin-resident immune cells in epidermis and dermis and their role in the immune response……..28

Figure 1.7 Toll-like receptors (TLRs) mediated immune responses……..35

Figure 2.1 Skin-hoof interface site at which tissues and swabs were collected……..56

Figure 3.1 Bacterial prevalence in the ovine interdigital skin from healthy, interdigital dermatitis and footrot feet biopsies……75

Figure 3.2 Bacterial load in the ovine interdigital skin from healthy, interdigital dermatitis and footrot feet biopsies……76

Figure 4.1 Bacterial prevalence in biopsies compared to swabs collected from the ovine interdigital skin……92

Figure 4.2 Total percentage of eubacteria DNA extracted from tissue biopsies (A) and from swabs (B)……..94

Figure 4.3 *Dichelobacter nodosus* load in biopsies compared to swabs collected from the ovine interdigital skin……..95

Figure 4.4 *Fusobacterium necrophorum* load (A) and *Treponema* spp. load (B) in biopsies compared to swabs collected from the ovine interdigital skin……..96

Figure 4.5 Microbiota analysis of the ovine interdigital skin using two approaches, swabs (surface) and biopsies (deeper skin layers)……..98

Figure 5.1 Gene expression stability analysis using RefFinder software……..116

Figure 5.2 Intergroup variation of gene expression using Comprehensive Analysis of RefFinder software ……117

Figure 5.3 Co-expression analysis for ten candidate reference genes performed with Ingenuity Pathway Analysis (IPA)……..118

Figure 6.1 mRNA expression levels of *TLR2* (A), *TLR4* (B), *IL1β* (C), *IL6* (D), *CXCL8* (E) and *IL17* (F) in healthy, mild ID (interdigital dermatitis), moderate/severe ID and footrot biopsies……130

Figure 6.2 mRNA expression levels of *IL1β* (A), *CXCL8* (B), *IL6* (C) and *IL17* (D) across the different ovine foot conformation/integrity scores……..131

Figure 6.3 Correlation analysis between pro-inflammatory cytokines relative mRNA expression and virulent *D. nodosus* load ……..134

Figure 6.4 Healthy samples: expression values of pro-inflammatory cytokines associated with virulent *D. nodosus* load……135

Figure 6.5 Footrot samples: expression values of pro-inflammatory cytokines associated with virulent *D. nodosus* load……136

Figure 7.1 Volcano plot showing the relationship between the –log10 P value for each gene and the magnitude of the difference in expression values of the samples in healthy, interdigital dermatitis (ID) and footrot groups……151

Figure 7.2 RT-qPCR validation of RNAseq data for differently expressed genes between healthy and footrot samples……156

Figure 7.3 Heat-map showing hierarchical clustering of global gene expression detected through RNAseq in healthy, interdigital dermatitis (ID) and footrot (FR) ovine interdigital skin samples…158

Figure 7.4 Differentially expressed genes (P<0.05 and fold change >2) grouped by Ingenuity Pathway Analysis……..163

Figure 8.1 Aseptic collection of biopsies from the ovine interdigital skin under a laminar flow cabinet……178

Figure 8.2 Assembling the EVOC model……179

Figure 8.3 Timeline of the EVOC model viability experiment……180

Figure 8.4 H&E images illustrating the qualitative, semi-quantitative scoring system used to evaluate skin tissue viability for both epidermis and dermis……183

Figure 8.5 Timeline of the EVOC infection experiments……187

Figure 8.6 Schematic overview of EVOC model optimization and improvements……192

Figure 8.7 Final EVOC protocol……193

Figure 8.8 Increased DNA fragmentation (TUNEL) in epidermal cells of biopsies from the EVOC model over 76h of incubation……196

Figure 8.9 Comparison of cell viability (TUNEL) and tissue integrity (H&E scores)……197

Figure 8.10 EVOC model infection with *Dichelobacter nodosus* virulent and benign strains……200

Figure 8.11 Fluorescent *in situ* hybridization (FISH) on ovine interdigital skin biopsies from the EVOC model (B, C, D, E, F and G)……201

Figure 8.12 Tissue integrity and cell viability after 28h of infection with *D. nodosus*……203

Figure 8.13 Preliminary experiment. Release of IL1β (A) and CXCL8 (B) in the media supernatants following infection with *D. nodosus*……204

Figure 8.14 Detection of IL1β in the media supernatants of the EVOC model by ELISA……206

Figure 9.1 Key events involved in the host-pathogen mechanisms leading to ovine footrot in the presence of virulent *D. nodosus*……222

List of Abbreviations

DNA	Deoxyribonucleic acid
16S rRNA	16S ribosomal Ribonucleic Acid
18S rRNA	18S ribosomal Ribonucleic Acid
3D	Three Dimensional
HEPES	4-(2-hydroxyethyl)-1-piperazineethanesulfonic acid
ACTB	Actin Beta
ASCC2	Activating signal cointegrator 1 complex subunit 2
ADORA3	Adenosine A3 receptor
ANXA1	Annexin A1
bp	Base pairs
BHLHE40	Basic Helix-Loop-Helix Family Member E40
CTSW	Cathepsin W
°C	Celsius
cm	Centimetre
C3ORF58	Chromosome 3 open reading frame 58
COPZ1	Coatomer protein complex, subunit zeta
cDNA	complementary Deoxyribonucleic Acid
CI	Confidence Interval
DDX54	DEAD (Asp-Glu-Ala-Asp) box polypeptide 54
DC	Dendritic cell
DMEM	Dulbecco's Modified Eagle's medium
ELISA	Enzyme-linked Immunosorbent Assay
EVOC	*Ex vivo* Organ Culture
FAWC	Farm Animal Welfare Committee
FAA	Fastidious Anaerobe Agar
FISH	Fluorescence *in situ* Hybridization
FC	Fold Change
GAPDH	Glyceraldehyde-3-Phosphate Dehydrogenase
HDAC1	Histone deacetylase 1
HA	Hoof Agar
h	hours
IPA	Ingenuity Pathway Analysis

ID	Interdigital dermatitis
IL	Interleukin
KLK6	Kallikrein-related
LC	Langerhans Cell
LPS	Lipopolysaccharide
MgCl2	Magnesium Chloride
mRNA	Messenger Ribonucleic Acid
µl	Microlitre
µm	Micrometre
µM	MicroMolar
mg	Milligrams
Ml	Millilitres
mm	Millimetres
mM	MiliMolar
MIQE	Minimum Information for Publication of Quantitative Real-Time PCR Experiments
M	Molar
ng	Nanograms
NK	Natural Killer cell
NFAM1	NFAT activating protein with ITAM motif 1
N°	Number
PAMP	Pathogen-associated molecular pattern
PRR	Pattern Recognition Receptors
PPIA	Peptidylprolyl isomerase A
PBMC	Peripheral Blood Mononuclear Cell
PLCXD2	Phosphatidylinositol-specific phospholipase C, X domain containing 2
PCR	Polymerase Chain Reaction
Cq	Quantification cycles
qPCR	Quantitative PCR
RTX	Repeats-in-toxin
RT-qPCR	Reverse Transcriptase-Quantitative PCR
RNA	Ribonucleic Acid
rRNA	Ribosomal Ribonucleic Acid

RIN	Ribonucleic Acid Integrity Number
RNAseq	Ribonucleic Acid sequencing
SD	Standard Deviation
SVMS	School of Veterinary Medicine and Science
TLR	Toll Like Receptor
TMEM79	Transmembrane protein 79
TUBA	Tubulin Alfa
TNF	Tumour Necrosis Factor
vs.	Versus
v/v	Volume/Volume
w/v	Weight/Volume

Chapter 1

1. General Introduction

1.1 Ovine footrot

Footrot is a contagious disease that affects the interdigital skin and the hoof of sheep that is caused primarily by an anaerobic bacterium, *Dichelobacter nodosus* (Beveridge, 1941). It is one of the most common ovine diseases and the greatest welfare and economical concern for sheep farmers and veterinarians worldwide (Goddard et al. 2006). Footrot is the main cause of lameness in sheep flocks in the UK (Farm Animal Welfare Council (FAWC) 2011) with over 90% of farmers reporting it on their farms (Wassink et al. 2010). Footrot has also been reported in many other countries such as Australia (Beveridge, 1941), Sweden (Frosth et al. 2012), Norway (Gilhuus et al. 2013), Switzerland (Stäuble et al. 2014), Spain and Portugal (Lorenzo et al. 2012), New Zealand (Bennett et al. 2009), Brazil (Aguiar et al. 2011), India (Vinod Kumar et al. 2016) and Buthan (Gurung et al. 2006). In addition to sheep welfare concerns, footrot has significant financial impact on the meat and wool industries. This is mainly associated with reduced production and wool strength, and the costs related to treatment and prevention of this disease (Green & George 2008). The cost of footrot in the UK is approximately £24-84 million per year in treatment and loss of production (Nieuwhof & Bishop 2005; Wassink et al. 2010).

1.1.2 Clinical presentations

In the UK, footrot is classified in two different clinical presentations, interdigital dermatitis (ID) and underrunning footrot (Figure 1.1). These two clinical presentations are considered by UK researchers as part of one disease process, called footrot (Clifton & Green 2016). The terminology for ID and footrot differs between countries; for instance in Australia, mild/benign footrot is also used synonymously for ID and underrunning footrot is called virulent footrot (Raadsma & Dhungyel 2013). Footrot begins as ID, which is characterized by an initial inflammation of the interdigital skin where the superficial epidermal layers are inflamed, damaged and slough off irregularly. ID may or may not develop into footrot depending on animal susceptibility, environmental conditions and virulence factors (proteases) of *D. nodosus* (Graham and Egerton, 1968; Stewart et al. 1986; Kennan et al. 2010). Footrot is characterized by the separation of the hoof horn from the sensitive underlying tissue (`underrunning lesion') (Beveridge, 1941; Egerton et al. 1969), which begins at the junction of the skin fold with the heel that spreads anteriorly to the abaxial wall and causes the hoof horn to separate from the foot laminae (Abbott & Lewis 2005). Underrunning footrot lesions usually result in discharge of greyish exudate with a characteristic foetid odour (Beveridge, 1941). These clinical presentations and lameness are the basis of footrot diagnosis in the field; however, in both presentations, affected sheep can present lameness and it is not possible to distinguish clinically lame sheep with ID and those with early signs of footrot (Winter, 2004).

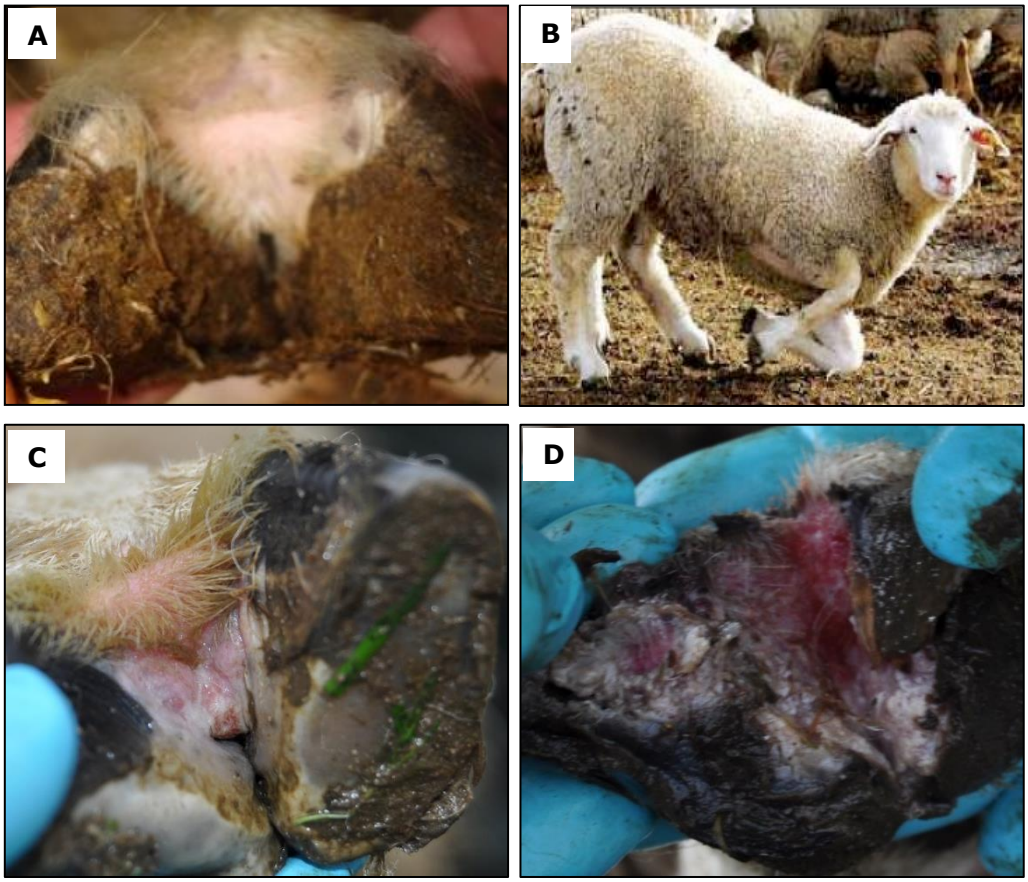


Figure 1.1 Clinical signs of footrot. Healthy ovine feet (A); Signs of lameness in the front feet (B); Interdigital dermatitis characterized by erythema in the interdigital skin (C); Footrot characterized by the separation of the hoof and skin (underrunning) (D) (Photos A, C, D: Dr Adam Blanchard, SVMS). (B: Hagedorn, 2007).

1.1.3 Footrot aetiology

D. nodosus is the essential causative agent of ovine footrot as shown through experimental challenges by Beveridge (1941), Egerton et al. (1969) and Kennan et al. (2010). It was initially reported that *D. nodosus* was the only microorganism that could initiate the hoof disease when applied as a pure bacterial culture, but the disease was more severe when other bacterial species including *Fusobacterium necrophorum* and Spirochaetes were present (Beveridge, 1941; Egerton et al., 1969; Roberts and Egerton, 1969). Beveridge (1941)

reported that Spirochaetes potentially contributed to the pathogenesis of footrot, since typical lesions failed to develop in sheep infected experimentally in the absence of Spirochaetes (Beveridge, 1941). More recently, *in vivo* trials showed that virulent strains of *D. nodosus,* in comparison to benign strains, are essential to initiate underrunning lesions (Kennan et al. 2010). Further information on *D. nodosus* is discussed in section 1.1.3.1.

The role of *F. necrophorum*, also a Gram-negative anaerobic bacterium, in the pathogenesis of footrot has been discussed over the years with two hypotheses raised. Since damage to the epithelium of the interdigital skin is a requirement for the initiation of disease (Beveridge, 1941), the first hypothesis is that *F. necrophorum* facilitates disease development by further damaging the interdigital skin and promoting ID that subsequently permits replication of *D. nodosus* (Egerton et al. 1969; Roberts & Egerton 1969). The second hypothesis is that *F. necrophorum* plays an opportunistic or secondary role, rather than a causal role in disease initiation, since it was found that *F. necrophorum* load increases once footrot has developed (Beveridge, 1941; Witcomb et al. 2014). In ovine footrot, two subspecies of *F. necrophorum* were identified, *F. n.* subspecies *necrophorum* and subspecies *funduliforme* (Frosth et al. 2015); *F. n.* subspecies *necrophorum* is reported to be more pathogenic due to a higher lipopolysaccharide content and higher leucotoxin production (Tan et al. 1996). In addition, Spirochetes (Beveridge, 1941) and more specifically *Treponema* spp., were also identified in sheep feet

affected by ID and/or footrot, although the role of these microorganisms in this disease is unknown (Calvo-Bado et al. 2011; Frosth et al. 2015).

In addition to *D. nodosus*, *F. necrophorum* and *Treponema* spp., more than 27 different bacterial groups were identified in the interdigital space of healthy, ID and footrot feet using pyrosequencing of the *16S rRNA* gene in a small set of ovine feet biopsies (Calvo-Bado et al. 2011). In this study, healthy feet were associated mainly with *Peptostreptococcus* spp., ID feet were associated mostly with *Corynebacterium* spp., and feet with footrot were associated mainly with *Staphylococcus* spp. (Calvo-Bado et al. 2011). These findings therefore suggest that the clinical disease status of the interdigital skin impacts on the abundance and prevalence of commensal bacterial communities.

In summary, it is well known that *D. nodosus* is essential to initiate footrot, but many other bacteria may also play a role in the lesions development and exacerbation. Footrot is considered by many a polymicrobial disease with a complex aetiology, but how the bacterial communities of the hoof interact with *D. nodosus* and affect the disease remains unclear.

1.1.3.1 *D. nodosus*

D. nodosus is a Gram negative and anaerobic bacterium initially described and known as *Fusiformis nodosus* (Beveridge, 1941) or

Bacteroides nodosus (Mraz, 1963). This bacterium has the smallest genome sequenced among anaerobic bacteria with a size of 1.4 Mb containing 1,389,350 bp (Myers et al. 2007). In terms of virulence factors, *D. nodosus* relies mainly on type IV fimbriae and extracellular serine proteases (Kennan et al. 2001). In addition, the RTX (repeat in toxin) toxin gene (Myers et al. 2007), outer membrane protein genes (Myers et al. 2007) and some molecular markers of virulence such as *vap* (virulence associated proteins), *vrl* (virulence related locus) (Katz et al. 1991; Rood et al. 1996) and *intA* gene (Cheetham et al. 2006) have also been reported; however, their precise role is not fully understood.

Serogroups and type IV fimbriae

D. nodosus fimbriae are very immunogenic and provide the basis of the classification of *D. nodosus* into serogroups (Claxton, 1989). *D. nodosus* strains are currently classified in 10 serological groups (A–I and M), which are subdivided into 19 serotypes (Claxton, 1989; Ghimire et al. 1998). In the UK, a multi-serogroup infection can occur at the flock and even at the foot level (Moore et al. 2005). *D. nodosus* fimbriae are classified as type IV due to their highly conserved amino-terminal region, polar location and association with twitching motility. The type IV fimbriae of *D. nodosus* are required for twitching motility and are essential for virulence, protease secretion and natural competence (Kennan et al. 2001). Twitching motility is required for the translocation of the bacterium into a more anaerobic

microenvironment, which is necessary for subsequent bacterial growth and extracellular protease production (Han et al. 2008).

Extracellular proteases

Other important virulence factors of *D. nodosus* are the extracellular subtilisin-like serine proteases, which are involved in the degradation of keratin, collagen and elastin of the interdigital skin and hoof (Kennan et al. 2010). Virulent strains of *D. nodosus* produce three closely related extracellular proteases, the acidic proteases, AprV2 and AprV5, and the basic protease, BprV. These proteases exhibit great thermostability and elastase activity and are involved in footrot tissue damage (Riffkin et al. 1995). AprV2 protease was reported to be important in footrot development since the results of an *in vivo* sheep study demonstrated that AprV2, AprV5 and BprV mutants did not initiate underrunning footrot; however, complementation with AprV2 wild type gene caused footrot, hence fulfilling Koch's postulates (Kennan et al. 2010). Benign strains of *D. nodosus* produce AprB2, AprB5 and BprB, which are thermolabile proteases and are unable to digest elastin (Riffkin et al. 1995). The virulent AprV2 protease differs from its benign counterpart AprB2 by a single amino acid change (Tyr92Arg) (Riffkin et al. 1995). A recent study using whole genome sequencing of 103 *D. nodosus* strains isolated from eight different countries identified that *D. nodosus* has a global conserved bimodal population, which correlates with virulent and benign phenotypes (Kennan et al. 2014). It is important to highlight that the presence of AprV2 or AprB2 in *D. nodosus* strains does not always correlate with

severity of clinical presentations since *D. nodosus* AprV2 positive has also been identified in ID cases and in sheep without any clinical sign (Moore et al. 2005; Stäuble et al. 2014). Further evidence was provided by the presence of benign *D. nodosus* strains (AprB2) in underrunning footrot lesions of Swedish sheep (Frosth et al. 2015).

Other virulence factors associated with D. nodosus

D. nodosus also has four outer membrane protein genes (*omp1A*, *omp1B*, *omp1C* and *omp1D*), which encode proteins that are thought to interfere with the immune response of the host (Myers et al. 2007). Site-specific inversions within these genes result in highly antigenic and phase-variant outer membrane proteins. This phase variance may allow *D. nodosus* to have antigenic shifts and evade the immune system of the host (Kennan et al. 2010). Furthermore, *D. nodosus* has a putative RTX (Repeat in Toxin) toxin gene, which could cause necrosis in the ovine foot (Myers et al. 2007). Additionally, *D. nodosus* has mobile genetic elements that are linked with virulence, the best studied are *vrl* (Rood et al. 1996) and *intA* (Cheetham et al. 2006). *Vrl* is found in 87% (670/771) of virulent isolates and 6% (46/771) of benign clinical isolates from Australian sheep. *IntA* was found in 98% of virulent strains and 28% of benign strains (Rood et al. 1996). Despite the *intA* and *vrl* regions being previously thought to be associated with virulence, their exact role in footrot pathogenesis is unclear. Importantly, a recent study did not find a correlation between the *intA* gene and virulence in ovine footrot (Dhungyel et al. 2013).

Identification and characterization of D. nodosus

Different methods are used to identify and characterize *D. nodosus* including culture and more recently molecular assays. In culture, *D. nodosus* needs particular growth requirements, such as anaerobic growth conditions and specific media such as hoof agar, Eugon agar (Stewart & Claxton, 1993) or Trypticase-Arginine-Serine agar (Skerman, 1975) (Figure 1.2). In addition, putative *D. nodosus* isolated colonies can be subcultured and maintained in Fastidious Anaerobe agar. In hoof agar, for instance, *D. nodosus* colonies are recognised by their granulated outer zones, and distinct bands of apparently no growth between the outer and central part of the colony (Frosth, 2016) and have a typical "ground glass" appearance (Thorley, 1976) in a format of `nodes` (Figure 1.2). *D. nodosus* is a slightly curved Gram negative rod, 3–10μm long and 0.6–0.8μm wide at the centre and 0.8μm to 1.2μm at the ends (Beveridge, 1941).

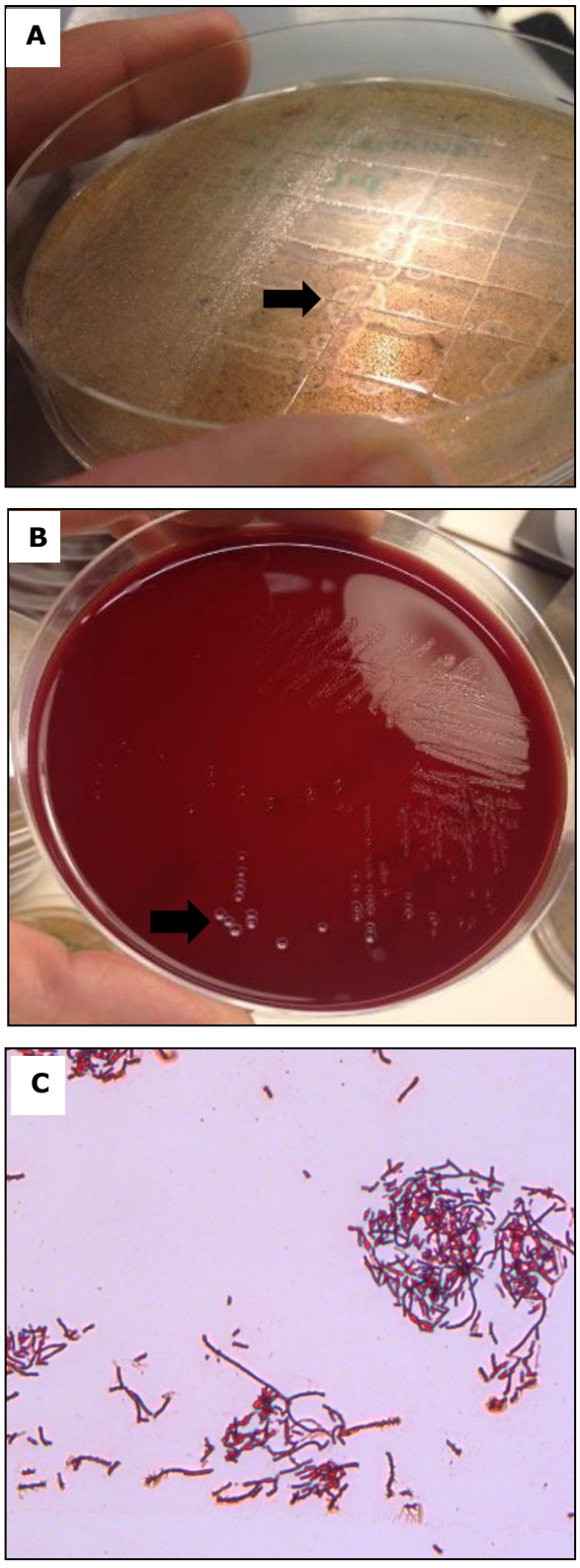


Figure 1.2 Isolation, identification and morphology of *D. nodosus*. Black arrows indicate colonies growing between the grids on Hoof agar in a format of `nodes`(A) and *D. nodosus* colonies sub cultured on Fastidious Anaerobe agar, characterized as small translucent greyish white colonies without haemolysis (B). Gram stain of *D. nodosus* colonies, magnification 100x (C).

Molecular methods can also identify *D. nodosus* since culture is difficult and time consuming given the fastidious nature of the bacterium. Conventional PCR was found to be 17% more sensitive than culture for the detection of *D. nodosus* from footrot lesions (Moore et al. 2005). Moreover, recent studies demonstrated that quantitative PCR (qPCR) is a promising and specific tool in identifying *D. nodosus* based on the *16S rRNA* gene (Frosth et al. 2012), and on the RNA polymerase sigma-70 factor gene (*rpoD*) (Calvo-Bado et al. 2011).

The classification of *D. nodosus* into virulent and benign strains is important since the virulent strains have the potential to initiate underrunning lesions (Kennan et al. 2010). *In vitro* tests used to identify virulent strains of *D. nodosus* include the elastase test, which measures the quantitative activity of proteases (Stewart, 1979), and the gelatine gel test, which measures a difference in protease thermo stability between benign and virulent strains. Thermo stable strains retain their ability to hydrolase gelatine after heating to 68°C, whereas benign strains produce a protease that is susceptible to heat inactivation and does not retain gelatinase activity (Palmer, 1993). More recently, two competitive real-time PCR assays based on allelic discrimination of the protease genes aprV2 and aprB2 were developed (Stäuble et al. 2014; Frosth et al. 2015). Both assays allow direct detection and differentiation of virulent and benign *D. nodosus* in a single and rapid test with 100% specificity. An independent study compared both assays using swabs from the interdigital skin of

Australian sheep and found that the assay developed by Frosth et al. (2015) was more sensitive when compared to the assay developed by Stäuble et al. (2014) and McPherson et al. (2017).

1.1.3 Footrot epidemiology and transmission

The main risk factors associated with the occurrence of footrot in addition to the presence of virulent *D. nodosus* include poor foot conformation (Kaler et al. 2010), superficial skin damage (Egerton et al. 1969), sheep breed (Emery et al. 1984) and presence of co-infecting bacteria such as *F. necrophorum* (Egerton et al. 1969; Roberts & Egerton 1969). In addition, other factors associated with farm management may also play an important role in the transmission and occurrence of footrot. The introduction of new sheep into a flock represents a major risk factor (Grøneng et al. 2014) and high stocking rates (>8.8 ewes/hectare) were found to be associated with ID occurrence (Wassink et al. 2004). Foot trimming was linked to an increased risk of footrot in UK farms since this practice may damage the sensitive dermis of the foot (Kaler et al. 2010). Furthermore, footrot occurrence is highly favoured by feet exposure to moisture and damp, which may explain the high incidence of footrot in the UK. The climate in this country is optimal for *D. nodosus* to thrive; it is wet and damp under-foot, with temperatures of approximately 10°C and a high rate of precipitation (Graham & Egerton, 1968). In other countries with different weather conditions such as Australia, footrot tends to occur more seasonally (Green & George 2008).

D. nodosus is not thought to be ubiquitous in soil or present in ovine faeces, although it was initially estimated that this bacterium could survive for a maximum of 7–10 days on pasture and for up to 6 weeks in hoof horn clippings (Whittington, 1995). Under optimal conditions *D. nodosus* survived for 24 days at 5°C (Cederlöf et al. 2013). A recent study demonstrated that *D. nodosus* was detectable for 40 days in different soil types and a temperature of 5°C compared with 25°C allowed better survival of *D. nodosus* than the previously reported studies (Muzafar et al. 2016). Unlike *D. nodosus*, *F. necrophorum* is ubiquitous in soil and it is a commensal bacterium in the alimentary tract, which can be shed in faeces and hence contaminate sheep feet (Roberts & Egerton 1969; Smith et al. 1997).

Transmission of footrot between sheep may occur by soil, pasture or bedding (Beveridge, 1941). It was recently shown that swabs taken from the feet of new-born lambs were negative for *D. nodosus*, but a few hours after birth *D. nodosus* was detectable on their feet. Moreover, the same *D. nodosus* strains were detected on their mother's feet, on the feet of other ewes and on the straw bedding (Muzafar et al. 2015). These results confirm that the environment has an important role in the transmission of *D. nodosus* between animals.

1.1.5 Treatment and vaccination

Traditional treatments for footrot include foot trimming, which is a common practice to remove excessive horn growth, and foot bathing, that is the application of antibacterial solutions such as zinc sulphate

and formalin to the sheep feet. These traditional methods might be detrimental since foot paring can delay recovery from footrot by exposing deep tissues to environmental *D. nodosus* (Kaler & Green 2009). Even though these methods were reported not to be fully effective, foot trimming and foot bathing are included in the most common treatments used by UK farmers (Wassink et al. 2010).

Antibiotic injection and spray are effective against footrot and achieve a cure in more than 85% of treated sheep (Wassink et al. 2010). Antibiotics from the tetracycline group are used to effectively treat ovine footrot. To date, the recommendations for treatment and control of this disease include the isolation of lame sheep from the flock and treatment of diseased sheep with parenteral or topical antibiotics. These procedures were associated with a decrease in footrot prevalence (Kaler & Green 2009). However, farmers consider individual treatments as time consuming (Wassink et al. 2010), another disadvantage associated with antibiotic usage includes the resistance to antimicrobials. Significantly high resistance rates of *D. nodosus* to oxytetracycline (43%) and tetracycline (50%), which are predominantly used against footrot, were reported in Portugal and Spain (Jiménez et al. 2004).

Vaccination plays an important role in the prevention and control of footrot. The commercial multivalent vaccine (Footvax) licensed in the UK contains nine serogroups of *D. nodosus* (A, B1, B2, C, D, E, F, G and H) and has limited efficacy when used alone (62%) with a

maximum duration of protection of five months (Duncan et al. 2012). This vaccine is also used worldwide as a control measure and is the only multivalent vaccine produced commercially. Some farmers reported that vaccination reduces the number of new cases and the severity of cases that occur, nevertheless, there are other reports that vaccination does not improve the severity or incidence of footrot and it can cause abscesses at the site of injection (Wassink et al. 2005). The limited duration of protection and partial protection of this multivalent vaccine is not well understood, possible reasons might be due to antigenic competition between bacterial strains, failure to induce cross-serogroup protection or the use of a sub-optimal adjuvant (Hunt et al. 1994). Therefore, Footvax vaccine should be used in combination with other control and treatment strategies in a sheep flock. Further studies are necessary to investigate potential *D. nodosus* antigens that could be targeted in a new vaccine composition, and whether the addition of other bacteria involved in footrot, for instance *F. necrophorum*, would enhance the protection of a vaccine.

1.1.6 Control program in the UK

A control plan has been recommended to UK farmers to reduce the occurrence of lameness in ovine flocks, and consequently the occurrence of ID and footrot (Farm Animal Welfare Committee, 2011). A Five Point Plan was designed to tackle infectious bacterial diseases that are causes of lameness and it was initially implemented on a UK sheep farm over a four-year study period. The adoption of the

measures recommended resulted in significant lameness reduction and consequently benefits in welfare and animal production (Clements & Stoye 2014). In 2011, the Farm Animal Welfare Committee aimed to reduce lameness in the UK through the implantation of this plan to less than 5% until 2016, and to less than 2% by 2021. The Five Point Plan includes:

i. CULLING of badly or repeatedly affected animals
ii. QUARANTINE of new sheep introduced into the flock for a minimum of 28 days, and the inspection of all new stock for signs of foot lesions
iii. TREATMENT of all lame sheep with parenteral injection of antibiotics and topical antibiotic spray
iv. AVOID propagation of infection on farm by adopting management practices, for instance, reducing the accumulation of infection around mineral buckets or troughs by moving them regularly and thinking carefully about where and how sheep are handled
v. VACCINATE biannually the whole-flock during winter and coincide this with housing or pregnancy scanning. Carry out summer vaccination around shearing time.

1.2 Skin structure

Since footrot and ID are skin diseases of the foot, this section will focus on the skin structure and the function of cells present in each skin layer. Skin forms the external covering of the body and is the largest organ, constituting 15 to 20% of its total mass (Ross & Pawlina

2006). The main role of the skin is to prevent loss of water and protect the body from environmental insults. In addition, the skin has important immune and sensory functions and helps to regulate body temperature (Maxie & Yussef 2007). The skin tissues are organized in three main layers; the epidermis, dermis and hypodermis that work together to provide strength and flexibility and execute the functions of the skin. During embryonic development, the main layers of the skin have different origins, the epidermis is derived from ectoderm and the dermis and hypodermis are derived from mesoderm (Ross & Pawlina 2006). The basic structure of the skin is similar in all mammals but skin thickness differs between regions of the body and different species. The dermis contributes most to the difference in skin thickness. The epidermis varies less, but it is generally thinner in areas with thick hair and thicker in areas without hair (Maxie & Yussef 2007).

1.2.1 Epidermis

The epidermis is composed of stratified squamous epithelium and is the outermost layer of the skin with five histologically distinct layers; stratum basale, stratum spinosum, stratum granulosum, stratum corneum and lucidum (Figure 1.3). The main functions of the epidermis are to limit water loss from the body, reduce the absorption of chemicals from the environment and prevent microbial infection (Aughey & Frye 2001; Ross & Pawlina 2006).

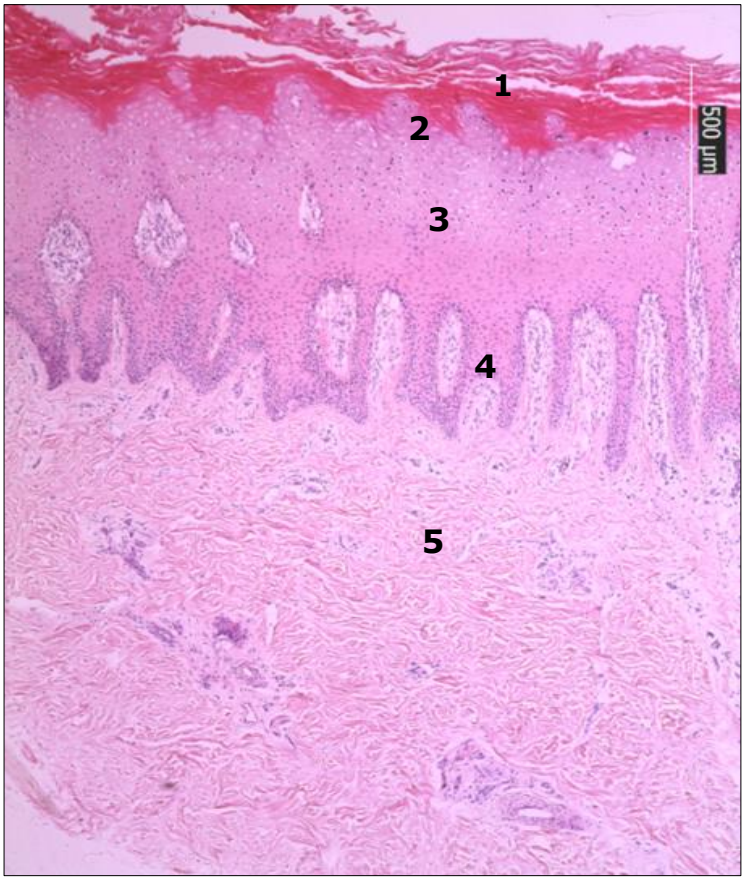


Figure 1.3 H&E stained section showing the layers of the epidermis and dermis of the ovine interdigital skin. (1) Stratum corneum; (2) Stratum granulosum; (3) Stratum spinosum; (4) Stratum basale; (5) Dermis. Adapted from Davenport et al. (2014).

The stratum basale is the deepest layer of the epidermis and it is composed of a single cell layer, which resides on the basal lamina (Maxie & Yussef 2007; Ross & Pawlina 2006). This layer contains stem cells that proliferate and differentiate into keratinocytes and migrate to upward layers to replenish these layers with new cells. The epidermal stem cells in the stratum basale are connected to each other and to keratinocytes by cell junctions formed by desmosomes (Maxie & Yussef 2007).

The stratum spinosum is above the stratum basale. The cells are slightly flattened and they are connected by desmosomes (Gawkrodger, 2002; Maxie & Yussef 2007). In addition, these cells are larger than those of the stratum basale and they exhibit cytoplasmic processes or spines, which give the name of this layer (Ross & Pawlina 2006). In large animals, these cells are organized in four or more layers and in dogs and cats in one or two layers (Maxie & Yussef 2007). The stratum granulosum is above the stratum spinosum (Ross & Pawlina 2006). This stratum contains keratinocytes that migrate towards the surface and accumulate basophilic granules of keratohyalin in the cytoplasm. These granules are a keratin precursor (Gawkrodger, 2002).

The stratum corneum is the outermost region of the epidermis. The cells in this layer are called corneocytes, which are the most differentiated cells in the skin since they are flattened, desquamating, anucleated and filled with keratin filaments (Nishifuji & Yoon 2013). The stratum lucidum is composed of several layers of squamous cells, translucent and anucleate, which do not have keratohyalin granules and sometimes is considered a subdivision of the stratum corneum (Ross & Pawlina 2006). This layer is present in the epidermis of the planum nasale of many species, the footpads of carnivores and the skin of the teat (Aughey & Frye 2001).

The basic cell types in the epidermis are keratinocytes, melanocytes, Langerhans cells (LCs) and Merkel cells. Keratinocytes are considered

the main cells of the epidermis (Gawkrodger, 2002), representing approximately 85-90% of the cells (Maxie & Yussef 2007). Keratinocytes have two essential functions; the production of keratin (Gawkrodger, 2002; Maxie & Yussef 2007; Ross & Pawlina 2006), and formation of the epidermal water barrier, which maintains the epithelium dry and the body homeostasis (Ross & Pawlina 2006). Keratin forms the cytoskeleton of keratinocytes and it is responsible for the shape of the cells and the structural integrity of the epidermis (Mills, 2007). It is also the main component of the stratum corneum, hair and nails (Gawkrodger, 2002). Furthermore, epidermal keratinocytes have immune functions, as discussed in section 1.4.1 (Mills, 2007; Nestle et al. 2009). Melanocytes are mainly located in the stratum basale of the epidermis and close to the hair follicles. These cells can have long and dendritic processes (Maxie & Yussef 2007). The function of melanocytes is to produce a pigment (melanin), which is important to protect the organism against the detrimental effects of solar radiation (Ross & Pawlina 2006). Even though the melanin is mainly present in the stratum basale, it can also be present throughout the epidermis in animals with dark skin (Maxie & Yussef 2007).

LCs are present in the stratum basale and in the stratum spinosum, depending on species and region of the skin. Like melanocytes, LCs have dendritic processes that extend in different directions. These cells are characterized by cytoplasmic granules called Birbeck granules (Gawkrodger, 2002; Maxie & Yussef 2007; Ross & Pawlina

2006), which are present in pigs, cats, cattle, sheep, goats, horses, and humans, but not in dogs (Maxie & Yussef 2007). Merkel cells are localized in the stratum basale and have dense-core cytoplasmic granules, which facilitate their identification (Aughey & Frye 2001). Their density in the epidermis is variable and they are in highest numbers in areas involved with sensory perception. Merkel cells may also have neuroendocrine effects and may be involved in control of the hair cycle. These cells are present in sheep, pigs, dogs, cats, monkeys, birds, reptiles and amphibians (Maxie & Yussef 2007).

1.2.2 Dermis

The dermis has an important role in maintenance and repair of the skin and is responsible for its elasticity (Maxie & Yussef 2007). It is composed of collagen, elastic and reticular fibers and it contains dermal cellular elements, hair follicles, glands, muscles (arrector muscle of hair), nerves, blood and lymphatic vessels (Nestle et al. 2009). The most important cells in the dermis are fibroblasts, macrophages and mast cells. This skin layer also contains dendritic cells (DCs) subsets and small numbers of T-helper lymphocytes and natural killer cells (NK) (Nestle et al. 2009). In contrast to human and pigs where the dermis is subdivided into papillary and reticular dermis, the dermis of domestic animals lacks papillae and is divided into superficial and deep dermis (Maxie & Yussef 2007). Many structural and functional differences between the dermis layers have been reported, such as the collagen types, organization of collagen fibers, elastic fiber structure, cellular populations, vessel and nerve

patterns. The superficial dermis consists of loose connective tissue that is beneath the epidermis. The collagen fibers contained in this part have mostly type I and type III collagen molecules. This layer is relatively thin and contains blood vessels and sensory nerves, which terminate in the dermis or penetrate the basal lamina to enter the epithelial compartment. The deep dermis forms the bulk of the dermis. This portion is thicker and less cellular than the superficial layer and it is characterized by type I collagen and by elastic fibers (Maxie & Yussef 2007).

1.2.3 Histology and anatomy of the ovine hoof

The ovine hoof consists of two digits separated by the interdigital skin. The hoof wall (or horn) is a hard and thick surface. It is derived from the epidermis, where skin becomes hoof, which is named coronary band. The point where the hoof wall is bound to the sole is called the white line and it is a junction between the sole and wall, which allow the hoof to be more flexible during the animal movement (Figure 1.4) (Frandson, 2009; Dyce, 2002).

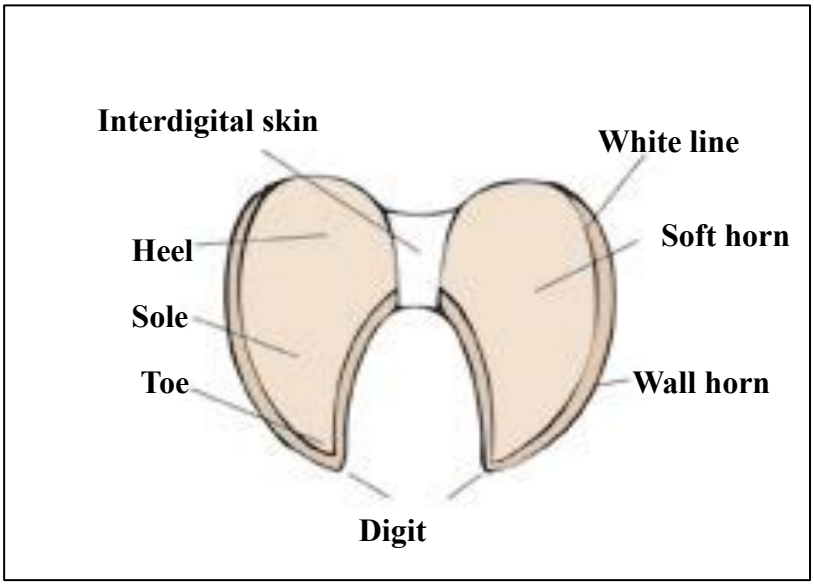


Figure 1.4 Anatomy of the healthy ovine hoof. (EBLEX Ltd. Sheep BRP Manual 7).

1.3 Innate immune response in the skin

The skin immune system consists of innate immune and adaptive immune responses. The initial innate defence mechanisms of the host are physical and chemical barriers represented by the skin, mucous membranes and antimicrobial substances. If microorganisms break these barriers, critical mechanisms of the immune response of the skin are activated initiating an inflammatory response (Afshar & Gallo 2013). Some of these microorganisms are destroyed initially by phagocytosis through phagocytic cells, such as neutrophils and macrophages, which are attracted to the site of microbial invasion and then they ingest and kill the microorganisms through oxidative burst or lytic enzymes. Moreover, these microorganisms can also be destroyed by other components of the immune system such as antimicrobial peptides or the complement system, which activates a

cell-killing membrane attack complex forming pores in the membrane of the pathogen destroying it directly by osmotic lysis. Other innate immune mechanisms will help to eliminate the remaining microorganisms (discussed in the next sections).

The innate immune system has developed a series of pattern recognition receptors (PRRs) that can recognize conserved pathogen-associated molecular patterns (PAMPs) such as lipopolysaccharide (LPS), peptidoglycan, flagellin and nucleic acids. Examples of PRRs are Toll-like receptors (TLR), C-type lectin receptor and NOD-like receptors (nucleotide-binding oligomerization domain receptors). TLRs are the best studied of these receptors and the interactions of TLRs and PAMPs lead to the activation of host cell signalling pathways by cytokines and chemokines (Nestle et al. 2009). Cytokines play a role in the following immune responses acting as signalling molecules that regulate immunity and inflammation and chemokines induce migration of inflammatory and non-inflammatory cells to the appropriate tissues (discussed in section 1.7).

The resident cells in the skin can act as sentinels against the invasion of microorganisms. Resident cells in the epidermis and dermis, such as keratinocytes, LCs, DCs, mast cells, macrophages, fibroblasts and NK cells provide an early protection system releasing cytokines and chemokines through recognition of PAMPs by PRRs (Nestle et al. 2009; Kupper & Fuhlbrigge 2004) (Figure 1.5).

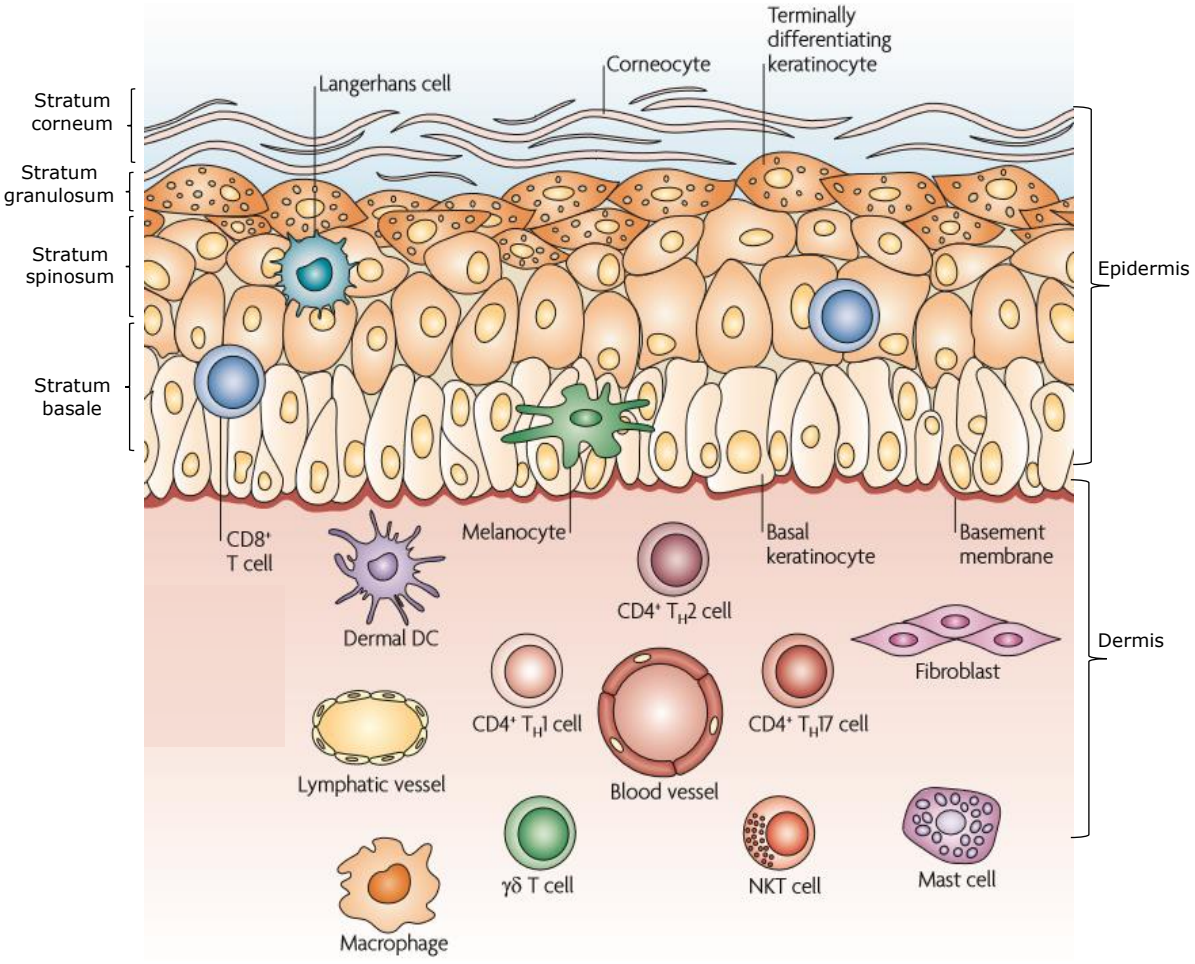


Figure 1.5 Cells involved in the innate immune response in the skin. Specialized cells in the epidermis include melanocytes and Langerhans cells. Rare T cells, mainly CD8+ cytotoxic T cells, can be found in the stratum basale and stratum spinosum. The dermis contains dendritic cell (DC) subsets, including dermal DCs, and T cell subsets, including CD4+ T helper 1 (TH1), TH2 and TH17 cells, γδ T cells and natural killer T (NKT) cells. Adapted from Nestle et al. (2009).

1.4.1 Innate immune response in the epidermis

Immune components in the epidermis are the first to enter in contact with microbial antigens and function as both physical barrier and an early warning system. For instance, keratinocytes play a role in this initial response reacting to harmful insults by the production of IL1β, IL6, IL10, CXCL8, Tumor Necrosis factor (TNFα) and antimicrobial peptides such as β-defensins, hence they modulate an immune response by attracting different cell types into the skin that will also function to eliminate the harmful insults. In addition, keratinocytes present antigens to T lymphocytes cells expressing Major Histocompatibility Complex class II (MHC-II) molecules in several skin disorders (Nestle et al. 2009). Nevertheless, keratinocytes can support the anti-inflammatory response producing immunosuppressive factors and cytokines capable of blocking inflammatory mechanisms (Albanesi et al. 2005).

Similar to keratinocytes, LCs are among the first to contact microbial antigens in the epidermis. These cells have long dendrites that form a tight network in tissues, which help to detect foreign antigens in the environment. They are the main DCs in the epidermis and when activated they release chemokines, cytokines and work as an antigen presenting cells (Nestle et al. 2009). Furthermore, LCs transport antigens from the skin to regional lymph nodes where they are presented in MHC-I and MHC-II to naive T cells, thus initiating adaptive cutaneous immune responses (Nestle et al. 2009; Igyártó & Kaplan 2013). LCs express specific TLRs such as TLR1, 2, 3, 6 and 7,

low levels of TLR8, but not TLR4, 5 or 9 (Flacher et al. 2006). It suggests that epidermal LCs might react to viruses but not to Gram-negative or flagellated bacteria (van der Aar et al. 2007). This low response to bacteria can be related to their localization since LCs are the first to encounter bacteria in the skin and it prevents a strong adaptive immune response to commensal bacteria. Hence, it prevents continuous inflammation since LCs do not respond to every bacterium that invades the skin (van der Aar et al. 2007). In summary, LCs not only have a role in the innate response in the epidermis expressing TLRs, cytokines and chemokines, but also play a role in the adaptive immune response acting as an antigen presenting cell.

1.4.2 Innate immune response in the dermis

There are many cells in the dermis cooperating with epidermal cells in the local inflammatory response and most of them play a role in the skin innate system as antigen presenting cells and secreting chemokines and cytokines (Figure 1.6). For example, keratinocytes (epidermal cell), fibroblasts and natural killer cells (dermal cells) play a role in the activation of dermal DC producing cytokines such as IL1β, IL6, CXCL8 (IL8) and TNF.

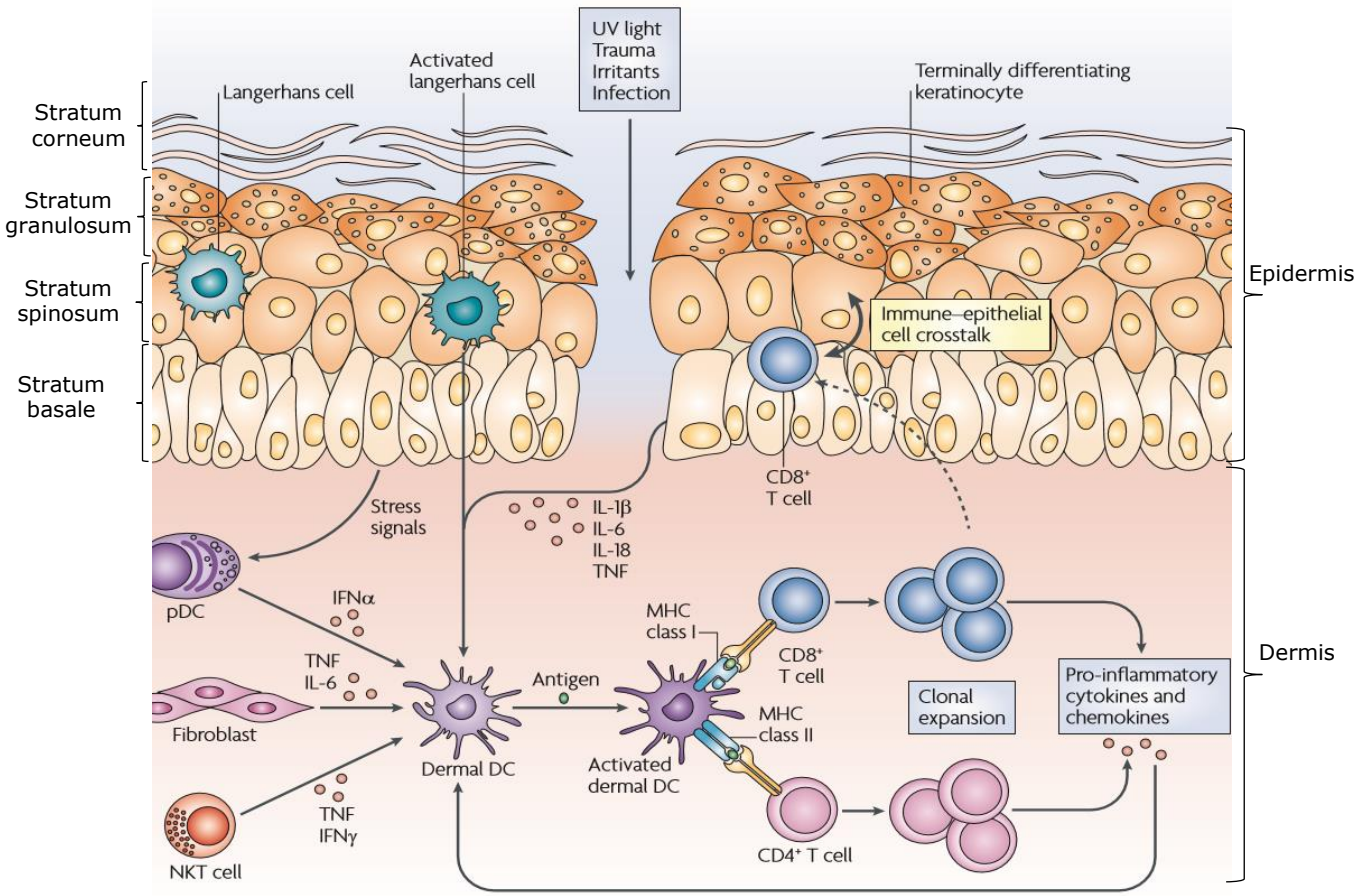


Figure 1.6 Skin-resident immune cells in epidermis and dermis and their role in the immune response. Ultraviolet (UV) light, trauma, irritants or infection (essentially any type of barrier disruption) triggers a coordinated immune response to maintain skin homeostasis. Skin-resident immune cells are key sentinels for restoring homeostasis but can also be effector cells during tissue pathology. Moreover, skin-resident T cells can migrate into the epidermis, engaging in an immune epithelial cell crosstalk. Adapted from Nestle et al. (2009).

1.4.2.1 Dermal DCs

In the dermis, activated dermal DCs are able to present antigens for skin resident $CD8^+$ and $CD4^+$ T lymphocytes, which will also help in the elimination of the microbial antigens producing pro-inflammatory cytokines and chemokines that can interact with epidermal and dermal cells (Nestle et al. 2009). Dermal DCs reside in the dermis and migrate rapidly to skin-draining lymph nodes in response to inflammation, there they present antigen to T cells (Kaplan, 2010). Beside the function as antigen presenting cells, dermal DCs are involved in the inflammatory response by secreting cytokines and chemokines to generate a cytokine network (Nestle et al. 2009).

1.4.2.2 Mast cells

Essential components of the immune response in the dermis are mast cells, since they contain inflammatory molecules in the cytoplasm that are released when they are stimulated by several factors including microorganisms. In the skin, mast cells contain inflammatory molecules such as histamine and heparin that promote important vascular alterations for the inflammatory process (Reber & Frossard 2014). Additionally, they participate in the innate response releasing IL1β, IL4, IL5, IL6, IL13, TNF and granulocyte–macrophage colony-stimulating factor (GM-CSF) in response to various TLR ligands (Kupper & Fuhlbrigge 2004). In contrast, mast cells can suppress immune reactions against some bacteria, for instance IL10 derived

from mast cells can have an immunosuppressive role in infection with uropathogenic *Escherichia coli* (Chan et al. 2013).

1.4.2.3 Skin macrophages

Skin macrophages are predominantly sessile dermal cells but they can migrate to lymph nodes under inflammatory conditions. They exhibit different immunological functions in the skin, including phagocytosis and presentation of antigens. Additionally, macrophages produce many cytokines and chemokines that stimulate new capillary growth, collagen synthesis and fibrosis, thus macrophages are considered one of the most important immune cells involved in wound healing (Delavary et al. 2011).

1.4.2.4 Fibroblasts

Fibroblasts play a structural role in the skin, producing collagens and other connective components for the tissue within which it resides. They are also sentinel cells in the dermis and when activated by substances released during tissue injury or by microorganisms, they produce chemokines that initiate the recruitment of bone-marrow-derived cells (Smith et al. 1997). Fibroblasts synthesize TNF, IL1β, IL6 and CXCL8, thereby linking the innate and adaptive immune response and initiating a cascade of events involved in wound healing and clearance of invading microorganisms (Buckley et al. 2001; Nestle et al. 2009). Moreover, fibroblasts have a role in the establishment of chronic inflammation since a failure to switch off the

inflammatory response of fibroblasts can result in the retention of leukocytes in the inflamed tissue (Buckley et al. 2001). A potential role of dermal fibroblasts in the immune response to ovine footrot was reported by Davenport et al. (2014). In this study, fibroblasts stimulated with LPS or heat-killed extracts of *D. nodosus* showed elevated levels of IL1β mRNA expression.

1.4.2.5 Natural killer (NK) cells

These cells are important components of the dermis. They are recognized for participating in regulation and coordination of immunity (Nestle et al. 2009). They are best known for cytotoxic defence against viral infections and tumour cells, but NK cells can also secrete TNF and it can modulate DC trafficking from the skin to lymph nodes in a contact hypersensitivity mouse model (Gorbachev & Fairchild 2006).

1.5 Toll like receptors

The TLR family plays an important role in the innate immune response against bacterial infection, as well as the subsequent induction of adaptive immune mechanisms. TLRs recognize bacterial PAMPs triggering inflammatory responses and DC maturation, which result in a response against the invading bacteria (Nestle et al. 2009). TLRs comprise a family of receptor proteins present on cells. In skin, they are expressed by keratinocytes and LCs in the epidermis, macrophages, DC, T and B lymphocytes, mast cells and fibroblasts in

the dermis, and endothelial cells of the skin microvasculature (Miller & Modlin 2007). TLRs are type I transmembrane proteins that contain an amino-terminal leucine-rich repeat (LRR) domain and a carboxyl-terminal Toll-interleukin-1 receptor (TIR) domain. The LRR domain is responsible for the recognition of PAMPs, whereas the TIR domain is required for initiating intracellular signalling (Suresh & Mosser 2013). PAMPs are conserved structures and important for the survival of the pathogen, whereby mutations or loss of PAMPs can reduce their adaptive ability. These structures are produced only by microbes and not by host cells (Medzhitov, 2001). After recognition of PAMPs, TLRs trigger intracellular signalling pathways that result in the activation of various transcription factors such as nuclear factor kB (NFkB), activator protein-1 (AP-1) and interferon regulatory factors, which activates expression of cytokines, type I interferon (IFN) and chemokines, thus, driving a specific immune response. The signalling pathways depend on adapter molecules, which are associated with TIR domain of TLR. MyD88 (myeloid differentiation primary response protein 88) is used by all TLRs, except TLR3. Other adapter molecules that interact with TLRs in the signalling pathways are MAL/TIRAP (My88-like/TIR domain-containing adaptor protein), TRIF (TIR-domain-containing adaptor inducing interferon) and TRAM (TRIF-related adaptor molecule). Despite the common use of several signalling molecules by TLRs, different TLRs utilize different adapter proteins. The difference in adapters leads to activation of distinct signalling pathways that contribute to different cellular responses (Kawai & Akira 2006).

There are two major consequences of PAMP recognition by TLRs. The first is the initiation of a cascade of responses in the form of cytokines or antimicrobial compounds. Second, it induces the competency of selected cells to present antigen to T cells, which is necessary to initiate adaptive immune responses. For instance, the stimulation of TLRs results in DC maturation, migration to draining lymph nodes and presentation of antigen to naive T cells, thus providing a link between the innate and adaptive immune systems (Kawai & Akira 2006). In conclusion, the consequences of PAMPs recognition by TLRs can initiate innate immune responses to kill pathogens directly or it can initiate specific adaptive immune responses to provide a second layer of protection, which occurs when cytokines responses are not sufficient to eliminate the pathogen (Suresh & Mosser 2013).

Thirteen TLRs (TLR1–13) have so far been reported in mammals, although TLR11, 12 and 13 are absent from the human genome (Table 1.1). TLRs can also be classified into two groups based on cellular location. TLRs 1, 2, 4, 5 and 6 are found on the cell membrane and can be activated by extracellular PAMPs. In contrast, TLRs 3, 7, 8 and 9 are found in membranes of intracellular compartments. The intracellular location of TLRs 3, 7, 8 and 9 enable them to detect nucleic acids (DNA or RNA) that have been released from viruses or bacteria degraded within endosomes and lysosomes inside the cell (Miller & Modlin 2007) (Figure 1.7).

Table 1.1 Recognized pathogen ligands (PAMPs) of Toll-like receptors (TLRs) 1-13.

TLR	Pathogen ligands (PAMP)
TLR1 (heterodimer with TLR2)	Bacteria: peptidoglycan, lipoproteins, LTA Fungi: zymosan
TLR2 (heterodimer with TLR6)	Bacteria: lipoproteins
TLR3	Viruses: dsRNA
TLR4	Bacteria: LPS Viruses: RSV fusion protein Fungi: manann, glucuronoxylomannan Protozoa: glycoinositolphospholipids
TLR5	Bacteria: flagellin
TLR7 and TLR8	Viruses: ssRNA
TLR9	Bacteria: CpG DNA Viruses: CpG DNA Protozoa: CpG DNA, haemozoin
TLR10	To date, specific ligands remain unknown. However, it has been shown to recognize *Listeria monocytogenes*
TLR11	Uropathogenic bacteria Protozoa: profilin-like molecule
TLR12	Protozoa: profilin-like molecule
TLR13	Bacteria: ssRNA Viruses: recognize VSV

sRNA: double-stranded RNA; LPS: lipopolysaccharide; LTA: lipoteichoic acid; RSV: respiratory syncytial virus; ssRNA: single-stranded RNA; VSV: vesicular stomatitis virus. Source: (Regan et al. 2013), (Mills 2011).

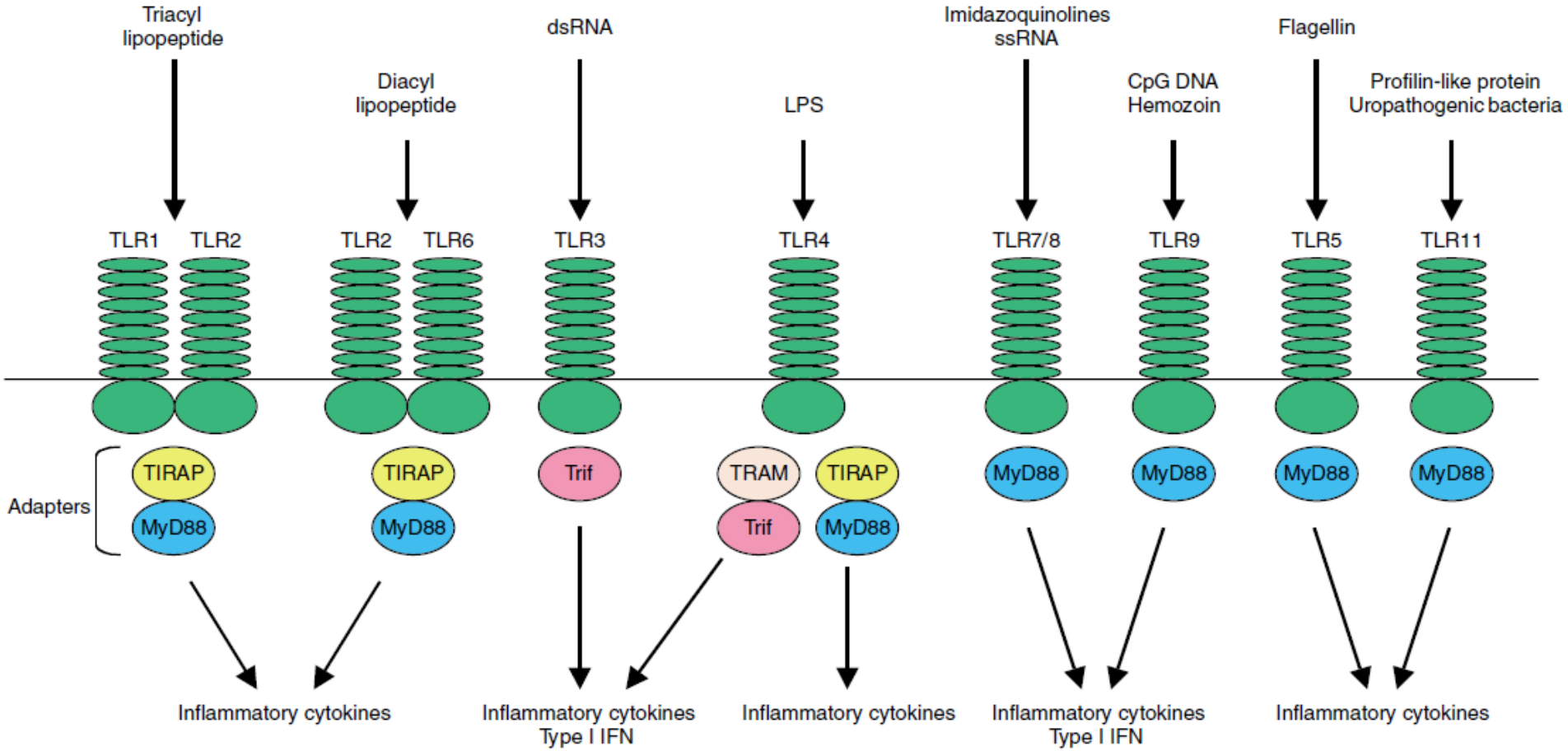


Figure 1.7 Toll-like receptors (TLRs) mediated immune responses. Specific pathogen-associated molecular patterns (PAMPs) recognized by TLRs and the following signalling pathways that result in the different activation of immune molecules. Adapted from (Kawai & Akira 2006).

1.5.1 TLRs involved in bacterial recognition

There are specific TLRs involved in bacterial recognition. Currently, the TLRs identified as receptors for bacterial PAMPs include TLR1, TLR2, TLR4, TLR5, TLR6, TLR9, TLR10, TLR11, and TLR13.

1.5.1.1 TLR2 forms heterodimers with TLR1 and TLR6

TLR2 co-operates with TLR1 or TLR6 amplifying the diversity of ligands that are recognized, thus leading to a wide range of inflammatory cascades. TLR2, in concert with TLR1 or TLR6, recognizes various bacterial components, including peptidoglycan, lipopeptide and lipoprotein of Gram-positive bacteria and mycoplasma lipopeptide (Medzhitov, 2001). TLR6-deficient mice did not show any production of cytokines in response to mycoplasma-derived diacyl lipopeptides. However, they showed normal production of cytokines in response to triacyl lipopeptides derived from Gram-negative bacteria (Takeuchi et al. 2001). In contrast, TLR1-deficient mice showed a normal response to mycoplasma-derived diacyl lipopeptides, but did not respond to triacyl lipopeptides (Takeuchi et al. 2002). These reports demonstrated that TLR1 and TLR6 in association with TLR2 differentiate between diacyl and triacyl lipopeptides, respectively. Furthermore, TLR2 is involved in the recognition of atypical LPS which differs from typical LPS in the number of acyl chains in the lipid A (Takeda, 2004). TLR2 has been shown to interact with atypical LPS from *Leptospira interrogans*, *Porphyromonas gingivalis*, *Helicobacter pylori and Fusobacterium nucleatum* (Werts et al. 2001; Mandell et al. 2004; Kikkert et al.

2007). TLR2 may also recognize the footrot bacterium *F. necrophorum,* which is a close relative of *F. nucleatum* and, hence, likely to have atypical LPS.

1.5.1.2 TLR4

TLR4 is present on a variety of cell types, mostly in cells of the immune system, including macrophages and DCs. LPS is potent immunoactivator of TLR4, which can be activated by a very small amount of LPS (Takeda, 2004). Macrophages and B cells from TLR4-deficient mice did not respond to LPS, demonstrating that TLR4 is an essential receptor for bacterial LPS recognition (Morrison & Ryan 1980). This recognition is complex and requires several accessory molecules. Firstly, LPS binds to a serum protein, LPS-binding protein (LBP), which transfers LPS monomers to CD14 that is a high-affinity LPS receptor. Additionally, another accessory molecule is the protein expressed on the cell surface, MD2, which is expressed in association with the ectodomain of TLR4. MD2 is required for LPS recognition by TLR4 (Schromm et al. 2001). RP105 is another protein that can cooperate in this process and it is expressed on the surface of B cells (Medzhitov, 2001). Furthermore, TLR4 is involved in the recognition of endogenous ligands, such as heat shock proteins (HSP60 and HSP70), the extra domain A of fibronectins, oligosaccharides of hyaluronic acid, heparan sulfate and fibrinogen. Nevertheless, these endogenous ligands require very high concentrations to activate TLR4 (Gao & Tsan 2003).

1.5.1.3 TLR5

TLR5 is involved in the recognition of flagellin, a conserved protein that forms bacterial flagella contributing to virulence through chemotaxis, adhesion, and invasion of host surfaces. The structural conservation and the important function of flagellin for bacterial mobility explain why it was selected as a target for recognition by TLRs (Medzhitov, 2001).

1.5.1.4 TLR9

is involved in the recognition of unmethylated CpG motifs in bacterial DNA, which are potent stimulators of the immune system and differs from CpG motifs in the vertebrate genome since bacteria lack cytosine methylation, thus, unmethylated CpG motifs are prevalent in bacteria but not in vertebrates. Signalling by CpG DNA requires its internalization into endosomal or lysosomal compartments of the cell and this intracellular delivery of bacterial DNA increases the immunostimulatory potential (Dalpke et al. 2006).

1.5.1.5 TLR11

TLR11 is involved in the recognition of a specific group of bacteria, urophatogenic *Escherichia coli*. This receptor is expressed in macrophages and liver, kidney, and bladder epithelial cells. Mice lacking TLR11 are highly susceptible to infection of the kidney by uropathogenic bacteria (Zhang et al. 2004) and *Salmonella* Typhi (Mathur et al. 2012), indicating a potentially important role for TLR11 in preventing these infections.

1.5.1.6 TLR13

TLR13 is responsible for detecting the 23S ribosomal RNA of both Gram-negative and Gram-positive bacteria. A short sequence of 23S rRNA is necessary and sufficient to trigger the TLR13 pathway. Thus, TLR13 is different from other TLRs involved in the recognition of nucleic acids since it recognizes a specific RNA sequence (Li & Chen 2012). Moreover, TLR13 was recently shown to be triggered by *Streptococcus pyogenes* infection in mice (Fieber et al. 2015), which provides further evidence of TLR13 role in bacterial-mediated infections.

1.5.2 TLRs in sheep

Different TLR patterns observed among animal species and these differences reflect the selective pressure on each host to adapt to new environments and pathogens. Ovine TLRs are similar to those in cattle, with 92-98% amino acid sequence identity (Menzies & Ingham 2006; Nalubamba et al. 2007). Moreover, sheep TLRs share high amino acid sequence similarity with other species such as human, mouse and pig suggesting that they are likely derived from the same ancestral sequence (Chang et al. 2009). Analysis of the full-length sequences of all TLR genes of sheep compared with cattle, human, mouse and pig sequences suggested that TLR7 is the most conserved gene among these mammals (80-98% amino acid identity) whereas TLR2 and TLR4 are the most different. It might be related to the diversity of ligands that each TLR recognizes, for instance TLR2 and

TLR4 are bacterial sensors whilst TLR7 detects single-stranded viral RNA that might be more conserved in structure (Chang et al. 2009).

Different tissues and cell populations express distinct repertoires of TLRs and consequently each tissue has distinct defensive properties depending on the identity and abundance of each receptor. In sheep, there is limited information published on expression levels of TLRs in different tissues and cells in normal conditions or during disease processes. Currently, in sheep tissues or cells TLR1 to 10 have been identified. Most of the studies related to the expression of TLRs during a pathological process are focused on Johne`s disease (paratuberculosis), and so far, only one study investigated TLRs in the ovine skin. Table 1.2 and 1.3 summarizes the results of studies present in the literature regarding the expression levels of TLRs in sheep.

Table 1.2 Toll-like receptors (TLRs) mRNA expression in ovine tissues and cells in healthy conditions.

		Ovine healthy tissues and cells	
Toll like receptors	**Expression levels**	**Local**	**Ref.**
TLR1	**(+/-)**	Jejunum, Peyer`s patch, mesenteric lymph node, kidney*, skin*, urinary bladder*, $CD4^+$ and $CD8^+$ T lymphocyte, interdigital skin	A; B; E
	(++)	Lung*, dendritic cells, keratinocytes, prescapular lymph node*	B; C
	(+++)	Lymphocyte B, alveolar macrophages, PBMCs, cornea epithelial cells, mesenteric lymph node*	B; C ; D
TLR2	**(+/-)**	Jejunum, mesenteric lymph node, kidney*, skin*, lung*, urinary bladder*, $CD4^+$ and $CD8^+$ T lymphocyte	A; B
	(++)	Peyer`s patch, keratinocytes, prescapular lymph node*, interdigital skin	A; C; E
	(+++)	Mesenteric lymph node*, alveolar macrophages, PBMCs, B lymphocytes, cornea epithelial cells	B; C; D
TLR3	**(+/-)**	Peyer`s patch, mesenteric lymph node, skin*, B lymphocytes, $CD4^+$ and $CD8^+$ T lymphocyte	A; B
	(++)	Lung*, keratinocytes, PBMC, prescapular lymph node*	B; C
	(+++)	Jejunum, urinary bladder*, kidney*, cornea epithelial cells, keratinocytes, alveolar macrophage	B; D
TLR4	**(+/-)**	$CD8^+$ T lymphocyte, lung*, skin*, urinary bladder*, peyer`s patch, jejunum, mesenteric/prescapular lymph nodes	A; B
	(++)	Kidney*, keratinocytes, PBMCs, interdigital skin	C; E
	(+++)	B lymphocytes, $CD4^+$ T lymphocyte, cornea epithelial cells, alveolar macrophages	B; C; D
TLR5	**(+/-)**	$CD8^+$ T lymphocyte, $CD4^+$ T lymphocyte, B lymphocytes, mesenteric/prescapular lymph node*	B
	(++)	Kidney*, peyer`s patch, mesenteric lymph node, alveolar macrophages, keratinocytes, PBMC	A; B; C
	(+++)	Urinary bladder*, kidney*, skin*, lung*, cornea epithelial cells, jejunum	B, D
TLR6	**(+/-)**	$CD8^+$ T lymphocyte, interdigital skin	B; E
	(++)	Prescapular lymph nodes*, lung*, skin*, keratinocytes	B; C
	(+++)	$CD4^+$ T lymphocyte, B lymphocytes, urinary bladder*, kidney*, peyer`s patch, cornea epithelial cells, jejunum, mesenteric lymph nodes, alveolar macrophages, PBMCs	A; B; C; D
TLR7	**(+/-)**	$CD8^+$ T lymphocyte, Mesenteric/prescapular lymph nodes*, lung*, skin*, kidney*, urinary bladder*, jejunum, keratinocytes	A; B; C
	(++)	$CD4^+$ T lymphocyte, cornea epithelial cells, alveolar macrophages, PBMCs	A; B; C; D
	(+++)	B lymphocytes, peyer`s patch, mesenteric lymph node	A; B; C
TLR8	**(+/-)**	$CD8^+$ T lymphocyte, prescapular lymph node*, lung*, skin*, kidney*, urinary bladder*, peyer`s patch, mesenteric lymph nodes, jejunum, cornea epithelial cells, keratinocytes	A; B; C; D
	(++)	B lymphocytes, alveolar macrophages	B; C
	(+++)	$CD4^+$ T lymphocyte, mesenteric lymph node*, PBMCs	B; C
TLR9	**(+/-)**	$CD4^+$ and $CD8^+$ T lymphocyte, prescapular lymph node*, lung*, skin*, kidney*, urinary bladder*, peyer`s patch, mesenteric lymph nodes, jejunum	A; B
	(++)	Alveolar macrophages, keratinocytes, PBMC	C
	(+++)	B lymphocytes, mesenteric lymph node*, cornea epithelial cells	B; D
TLR10	**(+/-)**	$CD8^+$ T lymphocyte, mesenteric/prescapular lymph node*, lung*, skin*, kidney*, urinary bladder*, jejunum, cornea epithelial cells, keratinocytes	A; B; C; D
	(+++)	$CD4^+$ T lymphocyte, B lymphocytes, Peyer`s patch, mesenteric lymph nodes, alveolar macrophages, PBMCs	A; B; C

(+/-): very low or absent expression levels, (++): medium expression levels detected, (+++): strong expression levels detected in comparison with control groups. PBMC: peripheral blood mononucleated cell. *Expression levels in comparison with spleen samples. (Ref.) References: A (Menzies &

Ingham 2006); B (Nalubamba et al. 2007); C (Chang et al. 2009); D (Dhanasekaran et al. 2010); E (Davenport et al. 2014).

Table 1.3 Toll-like receptor (TLR) mRNA expression in ovine tissues and cells during bacterial disease.

Tissues and cells	Disease stage (from farms with MAP)	Increased expression	Unchanged expression	Inconsistent results	References
Ileum	Asymptomatic		*TLR1 to TLR8*	*TLR2, TLR3, TLR4, TLR8*	A
		TLR2 to TLR4, TLR8, TLR9	*TLR1, TLR5 to TLR7, TLR10*		B
			TLR6		C
	Paucibacillary	*TLR1 to TLR6, TLR8*	*TLR7*	*TLR1, TLR5*	A
		TLR2 to TLR4, TLR6, TLR8	*TLR1, TLR5, TLR7, TLR9, TLR10*		B
		TLR6			C
	Multibacillary	*TLR1 to TLR8*		*TLR1, TLR6*	A
		TLR2 to TLR4, TLR8, TLR9	*TLR1, TLR5, TLR7, TLR10*		B
		TLR6			C
Jejunum	Asymptomatic	*TLR3, TL5 to TLR8*	*TLR1, TLR2, TLR4*	*TLR6*	A
			TLR6		C
	Paucibacillary	*TLR1 to TLR8*			A
		TLR6			C
	Multibacillary	*TLR1 to TLR8*			A
		TLR6			C
PBMC	Asymptomatic	*TLR1, TLR3, TLR5 to TLR8*	*TLR2, TLR4*		A
		TLR6			C
	Paucibacillary	*TLR1, TLR2, TLR6 to TLR8*	*TLR3 to TLR5*	*TLR6*	A
			TLR6		C
	Multibacillary	*TLR1, TLR2, TLR6 to TLR8*	*TLR3 to TLR5*		A
		TLR6			C
Tissues and cells	**Disease stage**	**Increased expression**	**Unchanged expression**	**References**	
Interdigital skin	Interdigital dermatitis/ Footrot	*TLR2, TLR4*	*TLR1, TLR6*	Davenport et al. (2014)	
Fibroblast	*In vitro* response to *Dichelobacter nodosus*	*TLR2*	*TLR1, TLR4, TLR6*		
Ovine bronchial epithelial cells	*In vitro* response to *Mycobacterium bovis*	*TLR2, TLR6, TLR8*	*TLR4*	(Ma et al. 2016)	
Ovine bronchial epithelial cells	*In vitro* response to *Mycoplasma ovipneumoniae*	*TLR2, TLR4, TLR6*	*TLR8*	Xue et al. (2015)	

MAP: *Mycobacterium avium* subsp. *paratuberculosis*; PBMC: peripheral blood mononucleated cell. References: A (Taylor et al. 2008); B (Nalubamba et al. 2008); C (Plain et al. 2010).

1.5.2.1 TLRs in healthy ovine tissues and cells

Among the TLRs investigated so far, the most highly expressed receptor in different tissues was *TLR6*, followed by *TLR1*, *3*, *5* and *10*. *TLR2* and its heterodimers *TLR1* and *TLR6* were highly expressed in B lymphocytes, alveolar macrophages, PBMCs, corneal epithelial cells and mesenteric lymph nodes. In contrast, *TLR2* and its heterodimers were expressed in low levels in $CD8^+$ T lymphocytes (Table 1.2).

The expression pattern of TLRs among skin tissues and keratinocytes was similar. In general, TLR transcripts in healthy ovine skin were found at low levels, only *TLR5* and *TLR6* showed a medium to high expression in skin and keratinocytes. These results were unexpected since the skin is in constant contact with the environment. *TLRs 3*, *5* and *6* were highly expressed in ovine jejunum. It suggests that gut, kidney and urinary bladder epithelium can respond to viral TLR3 and motile bacterial infections TLR5 (Nalubamba et al., 2007; Chang et al. 2009). TLRs investigated in lung tissues and in alveolar macrophages did not show a similar expression pattern since all TLRs were expressed in a medium to high level in alveolar macrophages and presented a low expression in lung tissues (Nalubamba et al. 2007). Ovine corneal epithelial cells expressed high levels of all TLRs, except *TLR8* and *TLR10* (Dhanasecaran et al. 2010). The only study available on expression of TLRs in ovine skin showed that *TLR1*, *2*, *4* and *6* are expressed in healthy ovine interdigital skin (Davenport et al. 2014). Despite the healthy clinical appearance of the sheep used in these studies, a potential limitation could be underlying

asymptomatic diseases in these animals at time of sample collection. Under those circumstances, the high expression of some TLRs in certain tissues might be in response to the presence of unidentified pathogenic microorganisms in the samples used.

1.5.2.2 TLRs in ovine tissues and cells during disease process

Since there is limited information about TLR gene expression in skin diseases of sheep, this section will also discuss studies regarding the TLR gene expression in intestinal and lung infections. The gene expression of TLRs in diseases of sheep was investigated in paratuberculosis (Johne`s disease) caused by *Mycobacterium avium* subsp. *paratuberculosis* (MAP). mRNA expression was analysed in the ileum, jejunum and peripheral blood cells from unexposed animals and infected flocks with MAP (Table 1.3). An increased expression of *TLR 1*, *2*, *3*, *4* and *8* in ileum and jejunum was observed among infected animals, suggesting that TLRs can play an important role in the immune response against MAP in sheep (Taylor et al. 2008; Nalubamba et al. 2008). *TLR2* and *TLR6* were both found to have a similar pattern of increased expression in ileum of sheep infected with MAP suggesting a possible role of *TLR2*/*TLR6* heterodimers in paratuberculosis (Taylor et al. 2008; Nalubamba et al. 2008; Plain et al. 2010). A specific qPCR assay was developed to identify *TLR6* gene expression based on the complete mRNA sequence of ovine *TLR6*. Reanalysis suggested that the previous assays would cross-react with ovine *TLR1*, since the partial sequences used to identify *TLR1* and *TLR6* had identical homology (Plain et al. 2010). It can explain the

inconsistent results found between previous studies and Plain et al. (2010), which differently showed an increased expression of *TLR6* in the ileum and jejunum of sheep infected with MAP (Taylor et al. 2008; Nalubamba et al. 2008).

Moreover, the role of TLRs in sheep during disease processes was investigated during lung infections of sheep. Ma et al. (2016) and Xue et al. (2015) reported that expression levels of *TLR2*, *TLR6* and *TLR8* in bronchial epithelial cells were increased in the presence of *Mycobacterium bovis* and *TLR2*, *TLR4* and *TLR6* in the presence of *Mycoplasma ovipneumoniae*. The first study to investigate the role of TLRs in bacterial infection of the ovine interdigital skin demonstrated the differential expression of TLR1, 2, 4 and 6 in interdigital dermatitis (ID) and footrot. TLR2 and TLR4 were significantly increased in both ID and footrot. Additionally, the immunological role of dermal fibroblasts was investigated by stimulating these cells with LPS from *D. nodosus* and *F. necrophorum*. TLR2 was highly expressed; however, there was no effect on TLR4 and TLR6 and a slight decrease in expression of TLR1. This suggests that dermal fibroblasts may play an important role in the inflammatory response to ID and footrot in sheep (Davenport et al. 2014).

1.6 Cytokines and chemokines

Cytokines are proteins that can act locally or systemically affecting several cells at the same time and are able to synergise or antagonize the function of other cytokines. They have several functions in relation

to their inflammatory role; they can impact on antigen presentation, bone marrow differentiation, cellular recruitment and activation (Borish & Steinke 2003). Cytokines function as ligands to their receptors on the cellular surface leading to signal transduction. Different cytokines activate distinct signal transduction pathways that result in the activation of various repertoires of transcription factors. Cytokines and their receptors can be classified based on the three-dimensional structure of the receptors. Examples of this classification include the following groups of receptors for cytokines that can play a role in the skin: (1) interleukin type I cytokine receptors for cytokines: IL-4, IL-6, IL-13, IL-21 and IL-23. (2) interleukin type II cytokine receptors for cytokines: IL-19, IL-20, IL-22 and IL-24. (3) immunoglobulin (Ig) superfamily receptors including IL-1α and IL-1β. (4) tumour necrosis factor receptor (TNFR) family receptors including, for instance, TNF-α (Hänel et al. 2013).

1.6.1 Chemokines

Chemokines are a group of cytokines that induce cell migration or chemotaxis of neutrophils, monocytes, lymphocytes, eosinophils, fibroblasts and keratinocytes. In addition, they can have homeostatic functions acting on haematopoiesis, immune surveillance and organ development. In general, homeostatic chemokines are expressed in specific tissues, while inflammatory chemokines are expressed in many different cells present in several locations (Commins et al. 2010). Host cells express multiple chemokine receptors that can induce specific signals, suggesting that each receptor signals through

different pathways. The receptors can bind more than one chemokine, thus permitting extensive connection between the chemokine functions (Locati et al. 2005). Chemokines contain cysteine residues and are subdivided into four families based on the positioning of the cysteine residues. The largest group of chemokines, the C-C subfamily, has the first two cysteines in an adjacent position and attracts mainly eosinophils, monocytes and T cells. The C-X-C subfamily is characterized by the separation of the first two cysteines by an amino acid; they can be angiogenic or angiostatic and mainly attract neutrophils. A third family of chemokines, the C subfamily, lacks the first and third cysteines, containing only a single cysteine residue including XCL1 and XCL2, which act as lymphocyte-specific chemotactic molecules (lymphotactin). A fourth subfamily (CX3C) has the two cysteine residues separated by three amino acids acting mainly on monocytes and T lymphocytes (Commins et al. 2010).

1.6.1 Ovine cytokines and chemokines

There are several cytokines/chemokines involved in inflammatory reactions in response to bacterial infection, which result from TLR recognition and secretion of specific cytokines that stimulate local inflammation. In sheep, there are several studies regarding the expression and role of cytokines in pathological conditions; however, few studies have been conducted in sheep bacterial infections. The main results of these studies and their references are summarized in Table 1.4.

Table 1.4 Ovine cytokines investigated in bacterial infections.

Disease/bacteria	Cytokine	Location	Reference
Corynebacterium pseudotuberculosis	*IL1β* and *TNF-α* were highly expressed in the site were *C. pseudotuberculosis* was inoculated. *IL2* and *IL4* were more expressed in lymph nodes. *IL1β* and *CXCL8* were highly expressed in sheep with pyogranulomas	Skin (inoculation site) and lymph nodes	Pepin et al. (1997)
Mastitis	*TNFα* and *CXCL8* were highly expressed after inoculation of *Staphylococcus aureus* and *Escherichia coli*. *IL1β* was detected mainly in response to *S. aureus. GM-CSF* was detected in low levels	Milk and teat cistern tissue	(Persson-Waller et al. 1997)
Chlamydia psittaci	Infected macrophages release *IL1β*, *CXCL8* and *GM-CSF*. Heat-treated *Clamydia* did not induce *IL1β*	Alveolar lavage	(Entrican et al. 1999)
Paratuberculosis	In pauci-and multibacillary forms of paratuberculosis the levels of *IL1β*, *TNFα*, *CXCL8* were increased. No changes were seen in *IL1α* levels	Ileum	(Smeed et al. 2007)
Ureoplasma parvum (foetal skin inflammation)	Skin response to 7 days of *U. parvum* exposure is characterized by high expression of *MCP-1*, *TNFα* and *IL10*. Cultured foetal keratinocytes increase the expression of *MCP-1*, but not *IL1β*, *IL6*, *CXCL8* and *TNFα*	Skin from the left groin and keratinocytes	(Kemp et al. 2011)
LPS from Escherichia coli (foetal skin inflammation)	Inflamed foetal skin increases the expression of *IL1β*, *CXCL8*, *TNFα*, *MCP-1* up to 15 days, causing prolonged in utero inflammatory response	Skin from the left groin	(Zhang et al. 2012)
Footrot	Increased expression of *TNFα* and *IL1β* in ID and footrot samples	Interdigital skin	(Davenport et al. 2014)
Dichelobacter nodosus/ Fusobacterium necrophorum	Increased expression of *TNFα* and *IL1β* after stimulation with heat-killed extracts of bacteria	Dermal fibroblasts	(Davenport et al. 2014)
Mycoplasma ovipneumoniae	Increased expression of *IL6*, *CXCL8*, *IL10, IL18, IL12β*, *IL33*. No changes were seen in IL1α and TGF-β	Bronchial epithelial cells	(Xue et al. 2015)
Chlamydia abortus	Increased expression and production of CXCL8. No changes seen for *IL1β* or *TNFα*	Oro-nasal turbinate cells	(Doull et al. 2015)

GM-CSF (Granulocyte-Macrophage Colony-stimulating Factor); MCP-I (Monocyte Chemoattractant Protein). TGF-β (Transforming Growth Factor Beta). ID: interdigital dermatitis.

TNFα has an important inflammatory role in bacterial infection, and in the skin it stimulates local dendritic cells to leave the tissues and migrate to the local lymph node (Nestle et al. 2009). Increased levels of *TNFα* were found in skin ovine bacterial diseases including ID and footrot, inflamed foetal skin in response to LPS and skin infection in response to *Ureaplasma parvum* (Davenport et al. 2014; Kemp et al. 2011). Moreover, *TNFα* was also significantly expressed in other bacterial infections such as mastitis caused by *S. aureus* and *Escherichia coli* and in response to *Corynebacterium paratuberculosis* (Persson-Waller et al. 1997; Pepin et al. 1997).

Similar to TNFα, IL1β plays an important role in the skin inflammatory response (Nestle et al. 2009). In ovine skin bacterial infections, the expression of *IL1β* was reported to be increased in response to ID and footrot, after stimulation with heat-killed extracts of *D. nodosus* and *F. necrophorum* and in inflamed foetal skin (Davenport et al. 2014; Zhang et al. 2012); in contrast, it was not increased in keratinocytes in response to *U. parvum* (Kemp et al. 2011). IL1β also plays a role in mastitis, in response to *C. paratuberculosis* and in response to *Chlamydia psittaci* (Pepin et al. 1997; Entrican et al. 1999). Moreover, IL6 is a pro-inflammatory cytokine induced by bacterial LPS along with TNFα and IL1β (Zuber Shaikh, 2011). In sheep, both *IL6* and *IL10* were highly expressed in foetal skin inflammation in response to *U. parvum* and *Mycoplasma ovipneumoniae* (Kemp et al. 2011; Xue et al. 2015).

An important pro-inflammatory chemokine is CXCL8 which is the most potent chemoattractant for neutrophils (Zuber Shaikh 2011). *CXCL8* showed similar expression pattern of *TNFα* and *IL1β* (Table 1.4), being highly expressed in almost all studies (Pepin et al. 1997; Persson-Waller et al. 1997; Entrican et al. 1999; Zhang et al. 2012; Xue et al. 2015; Doull et al. 2015), except in response to paratuberculosis and *U. parvum* (Smeed et al. 2007; Kemp et al. 2011). Monocyte chemotactic protein 1 (MCP1 or CCL2) also functions as a chemotactic molecule, attracting monocytes, memory T cells, and DCs to the sites of inflammation caused by infection (Borish & Steinke 2003). *MCP1* was highly expressed in response to LPS and *U. parvum* in ovine skin tissues and in keratinocytes (Kemp et al. 2011).

Most of the studies available in the literature investigated the expression of specific cytokines such as *IL1β*, *TNFα*, *CXCL8* and *IL6*. The expression levels of these cytokines were increased in the presence of bacterial infections in a wide range of ovine cells and organs; further studies are warranted to raise further information of the potential role of these cytokines in interdigital skin affected by footrot.

1.7 Summary and thesis aims

Footrot is a highly prevalent and costly bacterial infectious disease of the ovine interdigital skin with a significant welfare and economical concern worldwide. Footrot aetiology is complex and so far the majority of studies have focused on bacterial colonisation, targeting

mainly *D. nodosus* to understand virulence mechanisms and disease progression. However, other bacteria such as *F. necrophorum* and *Treponema* spp. might also be linked to disease severity, but their role in footrot remains unclear. In the UK, the last cross sectional field study on bacterial prevalence of ovine footrot was performed in 2005 by Moore et al. In this context, further investigations on bacterial colonisation of the ovine interdigital skin are warranted. Regarding the skin immune responses, very little is known about the inflammatory processes of bacterial infections in sheep, as previously discussed in this literature review. In footrot, the skin inflammatory response is thought to play an important role in the exacerbation of the lesions and to be responsible for the sloughing of necrotic tissues (Egerton et al. 1969). A more recent study characterized aspects of the inflammatory response in footrot demonstrating an increase of transcript levels of *TLR2* and *4* and pro-inflammatory cytokines in a small set of footrot samples (Davenport et al. 2014). However, there is no further information regarding the ovine immune response to this disease. Research on immune molecules and their association with the bacterial load can result in more detailed information of the disease process. This information is anticipated to advance diagnostic methods as well as control strategies such as the design of an efficacious and affordable vaccine.

Currently, research on footrot relies on *in vivo* trials or on the availability of abattoir samples. *In vivo* trials raise several ethical and legal issues due to the use of animals in research, and in the UK,

animal research is strictly regulated involving a long and bureaucratic process. Another limitation is that commonly used rodent models in research cannot be applied to ovine footrot studies due to feet anatomical differences. Therefore, there is a need to develop new alternatives to model the infection *in vitro,* which can realistically mimic the *in vivo* infection without using animal trials or relying on abattoir post-mortem explants.

1.8 Hypothesis and aims

The hypothesis of this project is that the pathology of footrot is a host mediated expression of local immune responses, in association with bacterial colonisation, leading to severe inflammation that can progress to underrunning footrot. This hypothesis was investigated through the following aims:

Bacterial colonisation in the interdigital skin:

1.8.1 Aim 1. To investigate the colonisation of *D. nodosus, F. necrophorum, Treponema* spp. and eubacteria, and to characterize the virulence of *D. nodosus* in a cross section of healthy, ID and footrot abattoir biopsies from the ovine interdigital skin.

1.8.2 Aim 2. To compare the prevalence and load of *D. nodosus, F. necrophorum, Treponema* spp. and eubacteria on the ovine interdigital skin surface using swabs and within the skin using abattoir biopsies.

Identification of reference genes for RT-qPCR studies of ovine interdigital skin:

1.8.3 Aim 3. To determine the stability of a range of reference genes to identify the most stable genes for normalisation of RT-qPCR data according to MIQE guidelines in an effort to improve the quality and normalization of RT-qPCR data for ovine interdigital skin samples.

Host immune response:

1.8.4 Aim 4. To investigate whether clinical conditions, foot conformation or *D. nodosus* load have impact on the expression levels of specific genes of interest, such as *TLR2*, *TLR4* and pro-inflammatory cytokines previously reported to be important in the skin (*IL1β*, *IL6*, *CXCL8* and *IL17*).

1.8.5 Aim 5. To characterize the transcriptomic profile of ovine interdigital skin samples from healthy, ID and footrot affected feet using RNA sequencing and a combined network and pathway approach.

Modelling footrot *in vitro* using a 3D skin explant model:

1.8.6 Aim 6. To develop a 3D skin model using ovine interdigital skin explants to study the infection with *D. nodosus*. This allows the investigation of bacterial invasion into the interdigital skin layers and the early inflammatory response to this infection in an *in vitro* environment that simulates the *in vivo* infection.

Chapter 2

2. General materials and methods

2.1 Collection of tissue biopsies

This study included 241 ovine interdigital post-slaughter biopsies collected at an abattoir using a convenience sampling approach due to variable availability of the clinical conditions at slaughter. Mud and faeces were removed from the foot and the interdigital space was cleaned with detergent and a paper towel. Disease status of the feet was scored by two different scorers with one of the scorers (the author of this thesis) present during all visits in order to ensure observer consistency. The scoring system was adapted from Parsonson et al. (1967), allowing classification into healthy, ID or footrot feet according to established scoring criteria (details of the scoring system were provided by Dr Jasmeet Kaler, Table 2.1).

Table 2.1 Ovine foot scoring system (provided by Dr Jasmeet Kaler, University of Nottingham).

Score type	Area of the foot	Score	Description
Conformation	Sole and heel/Wall of each digit	0	Undamaged sole and heel area
		1	Mildly damaged sole and heel (<25%)
		2	Moderately damaged/misshapen sole and/or heel area of the digit (>25% and <75%)
		3	Severely damaged/misshapen sole and/or heel area of the digit (>75%)
Interdigital dermatitis (ID)	Interdigital space	0	Clean interdigital region with no dermatitis (scald) lesions or fetid smell
		1	Slight ID, irritation of the skin, but dry
		2	Slight interdigital dermatitis with a fetid smell (<5% affected)
		3	Moderate interdigital dermatitis with a fetid smell (5 to 25% affected)
		4	Severe interdigital dermatitis with a fetid smell (>25% affected)
Footrot lesions	Sole and heel/Wall of each digit	0	No underrunning of the heel and sole area
		1	Active footrot lesion with a degree of under-running of the heel and/or sole area of the digit (<50%)
		2	Active footrot lesion with a marked degree of under-running of the heel and/or sole area of the digit (>50% and <100%)
		3	Active footrot lesion with complete under-running of heel and/or sole (100%)

After scoring, tissues were collected from the ovine interdigital space (Figure 2.1) using disposable 6mm biopsy punches (National Veterinary Services) and then stored in 2ml of RNALater (Sigma-Aldrich, Dorset, UK) for at least 12h at 4°C to allow RNALater to penetrate within the tissue prior to longer term storage at -20°C. Each biopsy was cut in two parts, one used for DNA and one for RNA extraction.

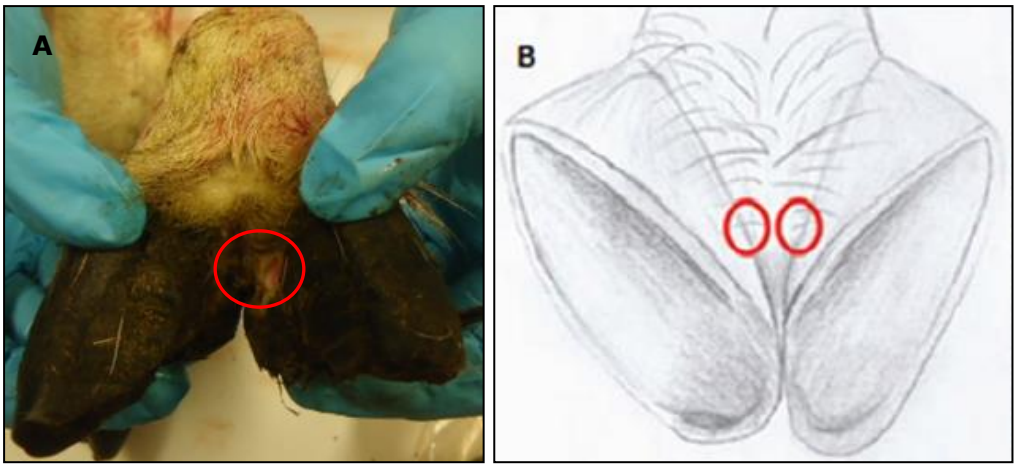


Figure 2.1 Skin-hoof interface site at which tissues and swabs were collected. (A) photo; (B) schematic drawing (provided by C. Heawood and R. Davenport).

The entire sample set included 79 healthy, 38 mild ID, 27 moderate/severe ID (joined scores 2, 3 and 4 due to similarity of lesion extension), and 97 footrot samples. Of these, 40 animals had all four feet sampled; total of 160 samples. During two visits to the abattoir (01/11/2013 and 04/11/2013) it was not possible to follow the same animal on the processing line; therefore 78 feet biopsies were collected without knowing if they belonged to the same sheep. Since the animals were sampled in the processing line of the abattoir, no information regarding sheep breed or other characteristics were available for this study. In one of the visits to the abattoir, 36 swab samples, 14 healthy, 9 ID and 13 footrot affected feet, were collected using Liquid Amies Elution Swab (ESwab) Collection and Transport System (BD diagnostics, Oxford, UK) from the skin-hoof interface (Figure 2.1).

2.2 DNA extraction

Half of the biopsy tissue was cut into small pieces and incubated with 180µl of ATL buffer and 20µl of proteinase K (20mg/ml) (QIAGEN, Hilden, Germany) at 56°C for 3h for enzymatic digestion. DNA was isolated using the QIAamp Cador Kit according to manufacturer's recommendations and eluted in 50µl of AVE buffer (QIAGEN). The final DNA concentration was determined using NanoDrop (Thermo Fisher Scientific, Paisley, UK).

2.3 Real-time PCR assays for bacterial quantification

The quantity of *D. nodosus* DNA was assessed by Real-time PCR using primers and probe targeting the *16S rRNA* gene of *D. nodosus* (Frosth et al. 2012). The following DNA concentrations were used for standard curves: 10ng/5µl, 1ng/5µl, 100pg/5µl, 10pg/5µl, 1pg/5µl and 100fg/5µl. DNA samples were diluted to 10ng/µl; except for DNA extracted from healthy samples, which was diluted to 100ng/µl. Samples were subjected to initial denaturation at 95°C for 10 minutes, followed by 45 cycles at 95°C for 15 seconds and 60°C for 60 seconds. Total eubacterial DNA was quantified using primers and probe targeting the *16S rRNA* gene (Strub et al. 2007). The following DNA concentrations were used for standard curves: 100ng/5µl, 10ng/5µl, 1ng/5µl, 100pg/5µl and 10pg/5µl. For both assays, all samples were tested in triplicate. Samples were subjected to initial denaturation at 50°C for 2 minutes and 95°C for 10 minutes, followed by 40 cycles at 95°C for 15 seconds and 60°C for 2 minutes. Every

qPCR plate included a standard curve and a no-template control in the form of master mix, without DNA. The qPCR components used for both assays are summarized in Table 2.2. The assays were performed using the PCR LightCycler 480 (Roche Applied Science, West Sussex, UK) and the results were analysed by absolute quantification using the Fit Points method (LightCycler 480 software). Standard curve graphs were generated using Excel software and linear regression (log10 dilution vs. quantification cycles). Efficiency was calculated using the equation E(%)=10(-1/slope)x100%. The specificity of all primer pairs was confirmed by melting curve analysis and DNA electrophoresis of PCR amplicons. The experiments were designed and reactions were performed according to MIQE guidelines (Bustin et al. 2009; Bustin et al. 2010). Details of primers and probes are summarised in Table 2.3.

Table 2.2 PCR mastermix reaction used in the quantitative PCR assays.

PCR mastermix	***D. nodosus* assay**	**Eubacteria assay**
2x Roche LightCycler master mix	10µl	10µl
Primer forward (100pmol)	(1µl) 0.4µM	(1µl) 6µM
Primer reverse (100pmol)	(1µl) 0.4µM	(1µl) 6µM
Probe (100pmol)	(1µl) 0.15µM	(1µl) 3 µM
qPCR quality water	2µl	2µl
DNA	5µl	5µl
Total	20µl	20µl

Assays targeting *Treponema* spp., *F. necrophorum* subspecies and virulent/benign *D. nodosus* were performed at the National Veterinary Institute (Sweden) by Dr Sara Frosth. qPCR for *Treponema* spp. targeted the intergenic spacer region 2 (ISR2) containing a *tRNAIle* gene for *Treponema* spp. (Frosth et al. 2015). qPCR for *F. n.* subsp.

necrophorum and *F. n.* subsp. *funduliforme* targeted the *gyrB* gene (Frosth et al. 2015). Differentiation between virulent and benign *D. nodosus* was performed based on the presence of *aprV2* (virulent) and *aprB2* (benign) genes (Frosth et al. 2015). For all bacterial targets used in this study, the qPCR data was normalised as percentage of bacteria present in the total eubacteria DNA extracted.

Table 2.3 Primers and probes details.

Gene	Strand	Sequence 5`-3`	Accession	Reference
D. nodosus 16S	F R P	CGGGGTTATGTAGCTTGCTATG TACGTTGTCCCCCACCATAA FAMTGGCGGACGGGTGAGTAATATATAGGA ATC-TAMRA	M35016	(Frosth et al. 2012)
Eubacteria 16S	F R P	TCCTACGGGAGGCAGCAGT GGACTACCAGGGTATCTAATCCTGTT 6-FAM-CCAGCAGCCGCGGTA-MGB	HE985141	(Strub et al. 2007)
*GAPDH**	F R	CCACCAACTGCTTGGCCCCC GGACACGTTGGGGGTGGGGA	AF022183.1	(Davenport et al. 2014)
ACTB	F R	TGTGCGTGACATCAAGGAGAA CGCAGTGGCCATCTCCTG	NM_001009784	(Hughes et al. 2011)
18S rRNA	F R	GCAATTATTCCCCATGAACG CAAAGGGCAGGGACTTAATC	DQ013885	(Taylor et al. 2008)
α-Tubulin	F R	CCAGATGGTGAAATGTGACC GCATTGACATCTTTGGGAAC	AF251146	(Taylor et al. 2008)
PPIA	F R	CATACAGGTCCTGGCATCTTGTC TGCCATCCAACCACTCAGTCT	AY251270	(Lloyd et al. 2012)
GAPDH	F R	TCCGTTGTGGATCTGACCTG TGCTTCACCACCTTCTTGATCTC	AF030943	(Hughes et al. 2011)
ASCC2	F R	AGGAGGCTTGAAGACAGCAA GTTGTCACAGCTGCTTTCCA	XM_04017467	This study
BHLHLE40	F R	CTACCAGGGATGGATTTTGC TCCGGTCACGTCTCTTTTTC	NM_001129741	This study
C3ORF58	F R	TGGTGCTACAGAGTTTTCCAT GCGAGGTCAACTCGTTTCTC	XM_012130530	This study
DDX54	F R	GAAGCTGGGACCTGGTAGAC GTTCTGAGCTCGCACCATCT	XM_012098176	This study
TMEM79	F R	CATTGTACTGGGGATCCTGGT ATGAAGAGCTGGACCGACTG	XM_004002610	This study
IL1β	F R	TTCTGCATGAGCTTCGTACAA GGGTCGGTGTATCACCTTTTT	X56972.1	(Darlay et al. 2011)
IL17	F R	GAGTCTGGTGGCTCTTGTGA TGCTGTGGGAAGTTCTTGTC	XM_004018887	This study
CXCL8	F R	GAGAAGTCCTCTGGGACAGC CAGCCAGCTTGGAAGTCATA	NM_001009401	This study
IL6	F R	AATTTCCTGCAGTTCAGCCT GTTTCTGACCAGAGGAGGGA	NM_001009392	This study
TLR2	F R	CATCTTTGTGCTTTCGGAGA AAGAGACGGAAGTGGGAGAA	AM981300.1	Davenport et al. 2014
TLR4	F R	AGAAACCTCCGCTACCTTGA CAGGGAGCAAGTTGTTCTGA	NM_001135930 .1	Davenport et al. 2014
ANXA	F R	GAAAGGAAAGCCCCTGGA TCAAACTGGGCTGGAGTTTT	XM_004004305	This study
KLK6	F R	GCGAGTGACAGGAATGGC TGTAGAGGGCAGCTTGGTAG	XM_012190747	This study
PLCXD2	F R	GGTCCACAGGAATCTTCC GGCAAAGTCCACCAGGTCT	XM_004002907	This study
16S V3	F 341	TCGTCGGCAGCGTCAGATGTGTATAAGAGACAG CCTACGGGNGGCWGCAG		(Klindworth et al. 2013)
16S V4	R 534	CTCGTGGGCTCGGAGATGTGTATAAGAGACA GTGGACTACHVGGGTATCTAATCC		(Klindworth et al. 2013)

All primers were used for qPCR except *Primers, which were used in the conventional PCR reaction for quality control of cDNA synthesis. F: forward primer; R: reverse primer; P: probe.

2.4 RNA extraction

The second half of each tissue biopsy was homogenised using a 5mm stainless steel bead (QIAGEN) for 4 minutes, at 30 oscillations per second. RNA was extracted using NucleoSpin RNA isolation kit (Machery-Nagel, Düren, Germany) following the manufacturer's recommendations. RNA was eluted in 40µl of RNAse free water. RNA concentration and quality were analysed using the RNA 6000 Nano Kit Bioanalyser (Agilent technologies, Ratingen, Germany).

2.5 cDNA synthesis and quality control of genomic DNA contamination

RNA was diluted in RNAse/DNAse free water (Thermo Fisher Scientific) to 100ng/µl and cDNA synthesised using M-MLV Reverse Transcriptase (50,000 units) and random primers (20µg) (Promega), according to manufacturers instructions. The final volume of each reaction was diluted with 75µl of RNAse/DNAse free water (Thermo Scientific, Paisley, UK). To identify any residual genomic DNA contamination, reactions with and without reverse transcription enzyme were performed and PCR amplified using primers targeting the *GAPDH* gene (Details of primers in Table 2.3). Each 50µl reaction contained 1.25 units GoTaq polymerase and 1x Green GoTaq flexi buffer (Promega), 1µM primers, 2mM MgCl2 and 5ng of cDNA. The PCR program consisted of an initial denaturation at 95ºC for 3 minutes, 25 cycles of 95ºC for 10 seconds, 55ºC for 1 minute, 72ºC for 1 minute and a final extension at 72ºC for 10 minutes.

2.6 Quantification of ovine gene expression

Ovine mRNA expression levels of *β-Actin* (*ACTB*), *Glyceraldehyde-3-Phosphate Dehydrogenase* (*GAPDH*), *α-Tubulin* (*TUBA*), *Cyclophilin* (*PPIA*) and *Eukaryotic 18S ribosomal RNA* (*18S rRNA*), *Activating signal cointegrator 1 complex subunit 2* (*ASCC2*), *basic helix-loop-helix family, member e40* (*BBHEL*), *Transmembrane protein* 79 (*TMEM79*), *DEAD (Asp-Glu-Ala-Asp) box polypeptide 54* (*DDX54*) and *chromosome 3 open reading frame 58* (*C3ORF58*), *IL1β*, *IL6*, *CXCL8* and *IL17* were investigated by RT-qPCR using a LightCycler 480 system (Roche Applied Science). Primers for *ASCC2*, *BBHEL*, *TMEM79*, *DDX54* and *C3ORF58* were designed using Primer3Plus (version 0.4.0); for each gene, a minimum of three forward and three reverse primers were designed and assessed by RT-qPCR. All assays were performed with manual reaction setup using the LightCycler 480 system (Roche Applied Science). Reactions contained 5µl of cDNA (1:100 dilutions) in 1× SYBR green qPCR master mix (Sigma-Aldrich) with 1µM of forward and reverse primers (Sigma-Aldrich) (Table 2.3). All standard dilutions, samples and no template controls were performed in triplicates. For *ASCC2*, *BBHEL*, *TMEM79*, *DDX54* and *C3ORF58*, samples were subjected to initial denaturation at 95°C for 20 minutes, followed by 45 cycles at 95°C for 5 seconds, 60°C for 20 seconds and 72°C for 30 seconds and a continuous dissociation step at 97°C to obtain a melt curve. For *ACTB*, *GAPDH*, *TUBA*, *PPIA*, *18S rRNA*, *IL1β, IL6, CXCL8* and *IL17*, the samples were subjected to initial denaturation at 95°C for 10 minutes, followed by 45 cycles at 95°C for 10 seconds, 60°C for 50 seconds and 72°C for 1 minute and a final dissociation step at 97°C.

The specificity of all primer pairs was confirmed by melting curve analysis and DNA electrophoresis of PCR amplicons. The experiments were designed and reactions were performed according to MIQE guidelines (Bustin et al. 2009; Bustin et al. 2010).

2.7 Normalisation analysis of RT-qPCR data

Normalised expression of RT-qPCR data of cytokines and TLRs was calculated using the following formula: CT+ (NT-CT`) * S/S` with S= target gene slope; S`= reference gene slope; CT= Cq value of targeted gene for each sample; CT`= Cq value of reference gene for each sample; NT= mean of Cq values of reference gene for all samples (Hughes et al. 2007). Data were normalised using *ACTB* and *PPIA* as reference genes.

2.8 Isolation and DNA extraction of *D. nodosus* strains

D. nodosus strains were isolated from swabs collected from the interdigital skin of post-slaughter sheep in an abattoir as described in section 2.1 and according to instructions from the SVA, Sweden (http://www.sva.se/analyser-och-produkter/provtagningsinstruktioner/provtagning-fotrota). A total of 39 swabs were collected (healthy n=7, ID scores 3 and 4 n= 27, footrot n= 5).

All swabs were cultured on 4% Hoof Agar provided by the SVA (Sweden) (Appendix 4). A sterile tooth pick was used to make grids from the streaked area across the agar plate to allow *D. nodosus* to

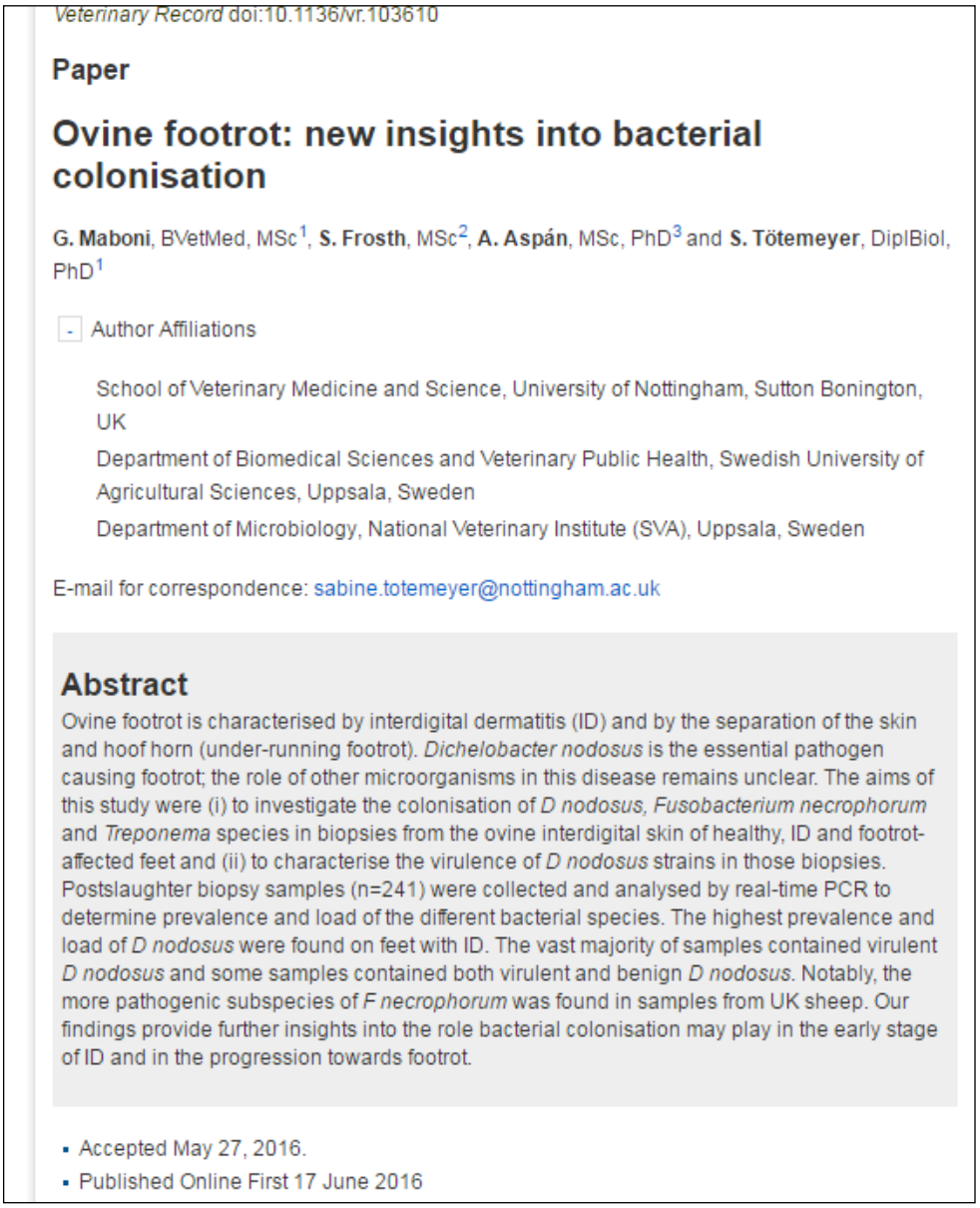
grow in between the grid lines. The plates were incubated anaerobically (Oxoid, AnaeroGen, Thermo Scientific, Waltham, USA) at 37ºC for five days. Colonies resembling *D. nodosus* were selected, sub cultured on 4% Hoof Agar and incubated anaerobically for 3-4 days. Pure *D. nodosus* cultures were maintained on Fastidious Anaerobe agar (EO labs, Bonnybridge, UK) for 3-4 days under anaerobic conditions. *D. nodosus* colonies were stored at -80ºC using two methods: (1) Eugon Glycerol Broth, which consisted of Bacto Eugon broth (Sparks, MD, USA) 0.2% yeast extract and 50% glycerol), and (2) CryoBeads (Hardy Diagnostics, Santa Maria, USA).

For DNA extraction from *D. nodosus*, putative colonies grown on Fastigious Anaerobe agar were selected and DNA was extracted using boiling method. The colonies were transferred into a tube containing 1ml distilled water, boiled for 10 minutes at 90ºC in water bath and followed by centrifugation for 5 minutes at 8,000 g (Heraeus Pico 17, Thermo Scientific, Waltham, USA). The pellet was discarded and the supernatant was stored at -20ºC to be further used in the qPCR reaction targeting *D. nodosus*.

Chapter 3

3. Ovine footrot: new insights into bacterial colonisation

This chapter presents the work previously published in a paper format `Ovine footrot: new insights into bacterial colonisation. Maboni, G. et al (2016) Veterinary Record.' doi:10.1136/vr.103610 (Appendix 1).



Veterinary Record doi:10.1136/vr.103610

Paper

Ovine footrot: new insights into bacterial colonisation

G. Maboni, BVetMed, MSc[1], **S. Frosth**, MSc[2], **A. Aspán**, MSc, PhD[3] and **S. Tötemeyer**, DiplBiol, PhD[1]

- Author Affiliations

School of Veterinary Medicine and Science, University of Nottingham, Sutton Bonington, UK

Department of Biomedical Sciences and Veterinary Public Health, Swedish University of Agricultural Sciences, Uppsala, Sweden

Department of Microbiology, National Veterinary Institute (SVA), Uppsala, Sweden

E-mail for correspondence: sabine.totemeyer@nottingham.ac.uk

Abstract

Ovine footrot is characterised by interdigital dermatitis (ID) and by the separation of the skin and hoof horn (under-running footrot). *Dichelobacter nodosus* is the essential pathogen causing footrot; the role of other microorganisms in this disease remains unclear. The aims of this study were (i) to investigate the colonisation of *D nodosus, Fusobacterium necrophorum* and *Treponema* species in biopsies from the ovine interdigital skin of healthy, ID and footrot-affected feet and (ii) to characterise the virulence of *D nodosus* strains in those biopsies. Postslaughter biopsy samples (n=241) were collected and analysed by real-time PCR to determine prevalence and load of the different bacterial species. The highest prevalence and load of *D nodosus* were found on feet with ID. The vast majority of samples contained virulent *D nodosus* and some samples contained both virulent and benign *D nodosus*. Notably, the more pathogenic subspecies of *F necrophorum* was found in samples from UK sheep. Our findings provide further insights into the role bacterial colonisation may play in the early stage of ID and in the progression towards footrot.

- Accepted May 27, 2016.
- Published Online First 17 June 2016

Author's contributions

Grazieli Maboni conceived and designed the experiments, collected samples, performed DNA extraction and qPCR assays for *D. nodosus 16S* and total eubacteria, analysed the data, wrote the manuscript, prepared figures and tables and reviewed drafts of the manuscript.

Dr Sara Frosth performed qPCR assays for virulent/benign *D. nodosus*, *F. necrophorum* and *Treponema* spp., and reviewed drafts of the manuscript.

Dr Anna Áspan supervised S. Frosth during development of qPCR assays, discussed the data and reviewed drafts of the manuscript.

Dr Sabine Totemeyer conceived and designed the experiments, supervised G. Maboni during laboratory experiments, manuscript writing and preparation of figures and tables, and reviewed drafts of the manuscript.

3.1 Introduction

Ovine footrot is a major cause of lameness affecting sheep welfare worldwide (Goddard et al. 2006), it is characterized by two different clinical presentations, interdigital dermatitis (ID) and underrunning footrot. ID is an initial inflammation of the interdigital skin where the superficial epidermal layers are inflamed, damaged and slough off irregularly and it may develop into underrunning footrot, which is characterized by the separation of the hoof horn from the sensitive underlying tissue (Beveridge 1941; Egerton et al. 1969). In Australia, mild/benign footrot is also used synonymously for ID and underrunning footrot is called virulent footrot (Raadsma & Dhungyel 2013).

Footrot is a complex disease and its occurrence is associated with different factors such as farm management (Green et al. 2007), environmental conditions (Wassink et al. 2005; Muzafar et al. 2016), initial damage in the epithelium of the interdigital skin (Beveridge 1941; Egerton et al. 1969) and virulence of *Dichelobacter nodosus,* a Gram negative anaerobic bacterium that is essential in causing underrunning footrot (Egerton et al. 1969, Kennan et al. 2001, Kennan et al. 2010), and *D. nodosus* load increasing in ID feet prior to footrot (Witcomb et al. 2014). Furthermore, *D. nodosus* was reported to play a role in the development of ID and footrot, therefore driving the early stages of this disease (Witcomb et al. 2014; Witcomb et al. 2015).

Whole genome sequencing demonstrated that *D. nodosus* has a global conserved bimodal population, correlating with virulent and benign

phenotypes (Kennan et al. 2014). A large number of virulent *D. nodosus* strains were identified in Australia (Kennan et al. 2014), while in Scandinavian countries, such as Sweden, mainly benign strains have been found (Frosth et al. 2015). In UK flocks, virulent *D. nodosus* was more prevalent than benign in swabs from sheep with ID and footrot (Moore et al. 2005). Virulent and benign *D. nodosus* strains differ in their ability to degrade the extracellular matrix of the host due to enzymatic activity of extracellular proteases (Riffkin et al. 1995). The acidic protease AprV2 is responsible for the overall elastase activity of virulent strains and was shown to be essential for the development of footrot, while the acidic protease AprB2 is associated with a benign phenotype (Kennan et al. 2010). Importantly, the presence of virulent *D. nodosus* strains does not always correlate with severity of clinical presentations since virulent *D. nodosus* has also been identified in sheep without any clinical signs and in ID cases (Stäuble et al. 2014, Moore et al. 2005).

In addition, *Fusobacterium necrophorum*, *Treponema* spp. and a range of other bacterial genera have been identified in the ovine interdigital skin (Roberts & Egerton, 1969; Bennett et al. 2009; Calvo-Bado et al. 2011; Frosth et al. 2015). The role of *F. necrophorum* in this disease still needs to be fully understood, with two hypotheses currently discussed: (1) *F. necrophorum* is important to establish ID prior to *D. nodosus* infection and hence initiates the disease (Egerton et al. 1969), or (2) *F. necrophorum* is involved in the persistence and severity of footrot, once the underrunning lesion has developed, playing a role as

an opportunistic, secondary pathogen (Witcomb et al. 2014). *F. necrophorum* is divided into subspecies *necrophorum* and *funduliforme*, the first is described to be more pathogenic (Tan et al. 1996).

Treponema spp. are usually free living organisms, but they have been associated with contagious ovine digital dermatitis (CODD) (Sullivan et al. 2015) and bovine digital dermatitis (BDD) (Gomez et al. 2012). BDD and CODD have polytreponemal aetiology with different *Treponema* species involved in their pathogenesis (Sullivan et al. 2015). *Treponema* spp. were also identified in a sheep with ID lesions from a flock with footrot history (Calvo-Bado et al. 2011) and were found in both flocks and feet, with and without footrot (Frosth et al. 2015), hence suggesting that further investigation is warranted to elucidate their role and whether different species of *Treponema* can be identified in ovine footrot.

Taken together, current data suggest that footrot is a polymicrobial disease and *D. nodosus* and other microorganisms might have a synergistic relationship. However, the role of bacterial diversity and load and how that differs between healthy, ID and footrot feet remains unclear. In this context, the aims of this study were (i) to investigate the colonisation of *D. nodosus, F. necrophorum, Treponema* spp. and eubacteria, and (ii) to characterize the virulence of *D. nodosus* strains in a cross section of healthy, ID and footrot abattoir biopsies from the ovine interdigital skin.

3.2 Materials and methods

This study included 241 ovine interdigital post-slaughter biopsies collected at an abattoir using a convenience sampling approach due to variable availability of the clinical conditions at slaughter. The entire sample set included 79 healthy, 39 mild ID (slight lesion with ≤5 per cent of the interdigital skin space affected), 26 moderate/severe ID (interdigital skin lesions with ≥5 per cent of the interdigital space affected) and 97 footrot samples (Table 1). Of these, 40 animals had all four feet sampled, total of 160 samples. During two visits to the abattoir (November 1, 2013, and November 4, 2013), it was not possible to follow the same animal on the processing line; therefore, 78 feet biopsies were collected without the information if they belonged to the same sheep (Table 1). Since the animals were sampled in the processing line of the abattoir, no information regarding sheep breed or other characteristics was available for this study. At the abattoir, all feet disease status was scored by two different scorers with one of the scorers present during all visits in order to standardise the sampling and scoring method; for details, see Table 3.1. The scoring system was adapted from Parsonson et al. (1967), allowing classification into healthy, ID or footrot feet according to established scoring criteria: absence of interdigital skin lesion=healthy; slight interdigital skin lesion (≤5 per cent affected)= mild ID; moderate-to-severe ID lesion (>5 per cent affected); presence of under-running lesion= footrot. Tissues were collected as described previously (Davenport et al. 2014) and placed into RNALater (Sigma-Aldrich) at 4°C before long-term storage at −20°C.

Table 3.1 Number of visits to the abattoir and number of biopsies collected from healthy, interdigital dermatitis and footrot ovine feet.

Date of visit to abattoir	N° of healthy feet	N° of ID feet	N° of footrot feet	N° of sheep with all four feet sampled	N° of samples collected
21/10/2013 [1,2]	32	6	2	10	40
01/11/2013*[1,2]	0	20	20	0	40
04/11/2013*[1,2]	4	4	30	0	38
13/12/2013[1,2]	14	7	19	10	40
16/12/2013[1,2]	10	19	10	10	39
19/01/2015[1,3]	19	9	16	10	44
Total	**79**	**65**	**97**	**40**	**241**

ID= interdigital dermatitis
*It was not possible to follow the same animal in the processing line
[1-3] Scorer 1 (Grazieli Maboni), scorer 2 (Melissa Bexon), scorer 3 (Michael Agbaje)

3.2.1 DNA extraction and real-time PCR assays

For enzymatic digestion, each tissue was cut into small pieces and incubated with 180µl of ATL buffer and 20µl of proteinase K (20mg/ml) (QIAGEN) at 56°C for 3 hours. DNA was isolated using the QIAamp cador kit according to manufacturer's recommendations and eluted in 50µl AVE buffer (QIAGEN). The final DNA concentration was determined using NanoDrop (Thermo Fisher Scientific). Bacterial load was quantified using real-time PCR based on *16S rRNA* gene for eubacteria (Strub et al. 2007) and *D. nodosus* (Frosth et al. 2012) and the intergenic spacer region 2 (ISR2) containing a tRNAIle gene for *Treponema* spp. (Frosth et al. 2015). Real-time PCR for *F. n.* subsp. *necrophorum* and *F. n.* subsp. *funduliforme* targeted the *gyrB* gene (Frosth et al. 2015). Differentiation between virulent and benign *D. nodosus* was performed based on the presence of *aprV2* (virulent) and *aprB2* (benign) genes (Frosth et al. 2015). *D. nodosus* and eubacteria

assays were performed using PCR Lightcycler® 480 (Roche Applied Science). Virulent and benign *D. nodosus*, *F. necrophorum* and *Treponema* spp. assays were carried out in an Applied Biosystems® 7500 Fast Real-Time PCR System (Thermo Fisher Scientific).

3.2.2 Statistical analysis

Fisher's exact test was performed for bacterial prevalence and One-way ANOVA followed by Dunn's multiple comparisons test for bacterial load using GraphPad Prism® (Version 6.0, La Jolla, USA). Confidence intervals of the prevalence data were calculated using Graphpad Software (http://graphpad.com/quickcalcs/confInterval2/). A P-value ≤0.05 was considered significant.

3.3 Results

3.3.1 Prevalence and load of *D. nodosus*, *F. necrophorum* and *Treponema* spp. in tissues from the ovine interdigital skin

The prevalence of *D. nodosus*, *F. necrophorum*, *Treponema* spp. and eubacteria was investigated in the ovine interdigital skin biopsies. All samples were positive for eubacteria (100% of prevalence). Both total *D. nodosus* and virulent *D. nodosus* were significantly more prevalent in mild ID ($P<0.05$ and $P<0.01$, respectively), moderate/severe ID ($P<0.001$ and $P<0.0001$, respectively) and footrot ($P<0.05$ and $P<0.01$, respectively) in comparison with healthy feet. Among all clinical conditions, *D. nodosus* showed the highest prevalence in moderate/severe ID samples. Moreover, total *D. nodosus* and virulent

D. nodosus were significantly more prevalent in moderate to severe ID than in footrot samples (Figure 3.1 A, Appendix 1 Table 1). In contrast, benign *D. nodosus* was only detected in 7% (17/241) of the samples (Figure 3.1 B). Mixed populations of benign and virulent *D. nodosus* strains were found in a small number of samples across all clinical conditions (Figure 3.1 B).

F. necrophorum was detected in 15% (36/241) of the samples, with 14.5% (35/241) positive for *F. necrophorum* subsp. *necrophorum*, only two samples positive for *F. necrophorum* subsp. *funduliforme* and one sample positive for both subspecies. *F. necrophorum* was significantly more prevalent in footrot than in healthy feet ($P<0.05$) (Figure 3.1 C). Presence of both *D. nodosus* and *F. necrophorum* in the same tissue sample or virulent *D. nodosus* and *F. necrophorum* in the same tissue was significantly higher in footrot compared to healthy feet ($P<0.01$ and $P<0.01$, respectively). *Treponema* spp. prevalence was very low (8%, 20/241) and similar across all clinical conditions (Figure 3.1 D) (Appendix 1 Table 1).

A similar proportion of eubacterial DNA was detected at around 0.06%±0.020 (mean ± standard error of the mean) of total DNA for all samples, with 0.07%±0.041 for healthy samples, 0.028%±0.007 mild ID, 0.027±0.011 for moderate/severe ID and 0.073±0.039 for footrot samples. *D. nodosus* load was significantly higher in moderate/severe ID and footrot in comparison to healthy feet ($P<0.0001$ for both) (Figure 3.2 A). Virulent *D. nodosus* load was

significantly increased in mild ID, moderate/severe ID and footrot compared with a healthy feet (P=0.001, P<0.0001 and P<0.0001, respectively), with highest load in moderate/severe ID (Figure 3.2 B). *F. necrophorum* load was significantly increased in footrot but not in ID samples (P=0.022) (Figure 3.2 C). The highest *Treponema* spp. load was found in footrot followed by healthy feet (Figure 3.2 D).

In summary, while eubacterial load were similar in all feet, both prevalence and load of total and virulent *D. nodosus* were highest in moderate to severe ID, while *F. necrophorum* were highest in footrot samples.

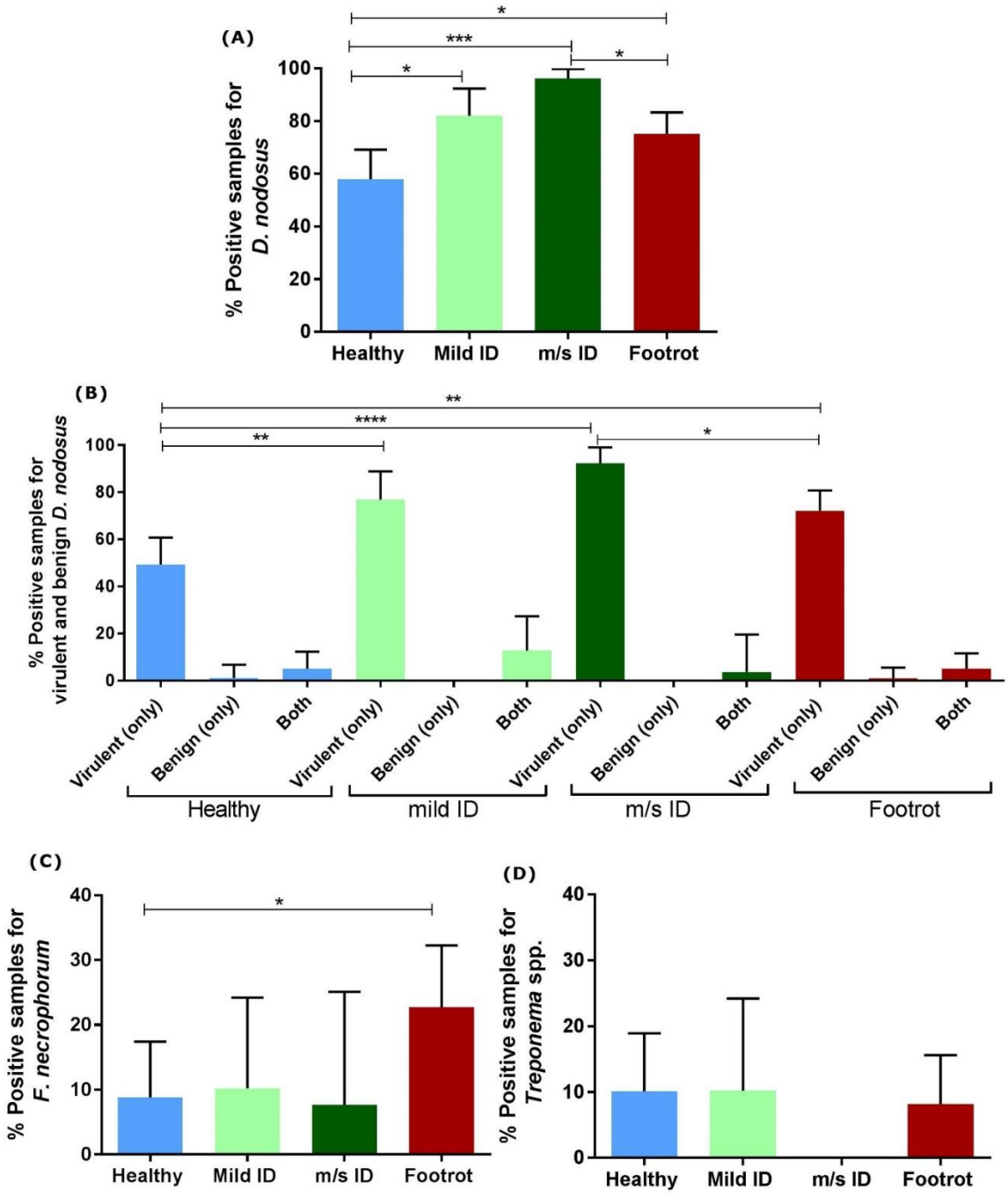


Figure 3.1 Bacterial prevalence in the ovine interdigital skin from healthy, interdigital dermatitis and footrot feet biopsies. Prevalence of total *Dichelobacter nodosus* (A); Prevalence of virulent and benign *D. nodosus* (B); Prevalence of *Fusobacterium necrophorum* (C); Prevalence of *Treponema* spp. (D). Mild ID (interdigital dermatitis score 1); m/s ID (moderate to severe ID scores 2, 3 and 4). Data were analysed by Fisher's Exact Test. *P ≤0.05, **P ≤0.01, ***P ≤0.001, ****P ≤0.0001.

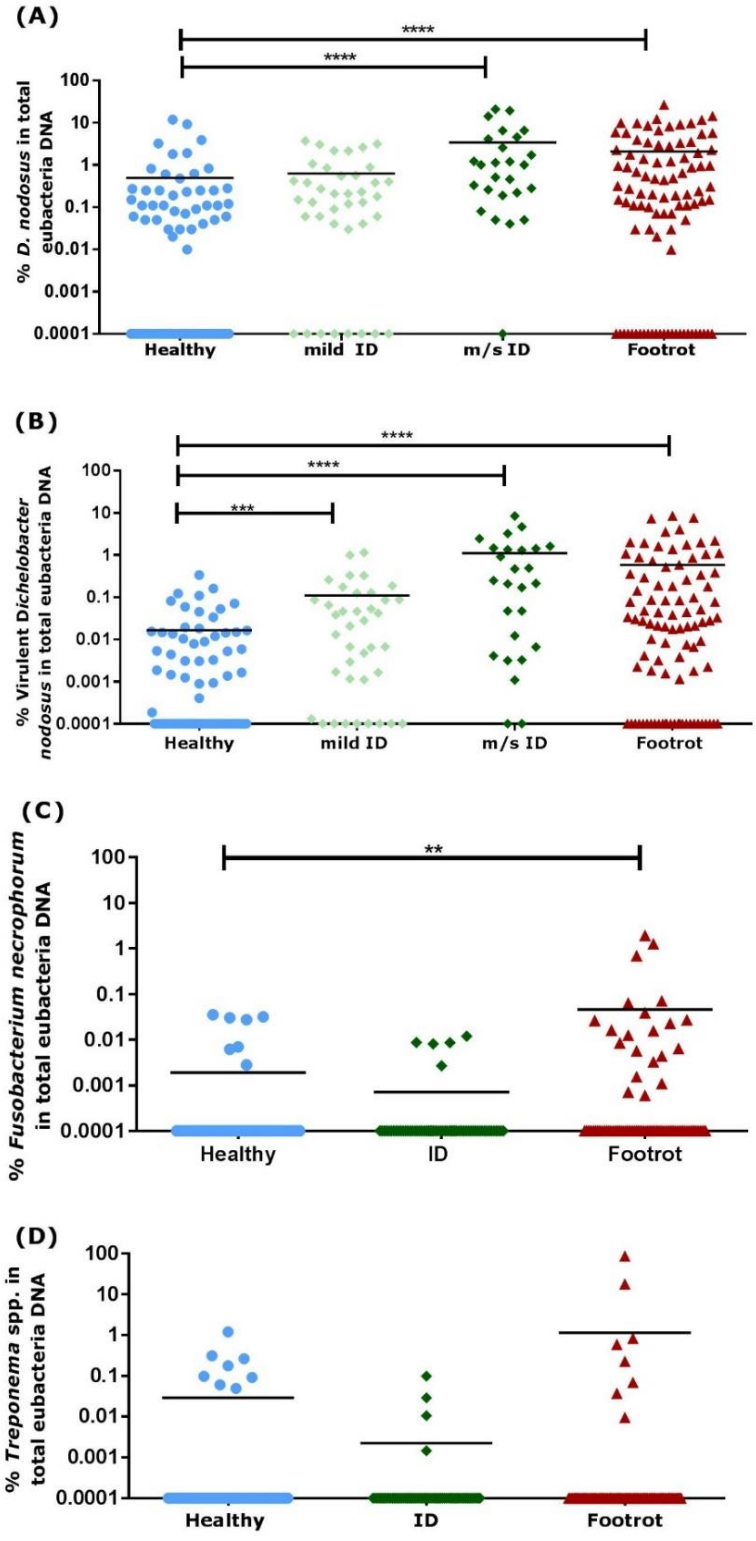


Figure 3.2 Bacterial load in the ovine interdigital skin from healthy, interdigital dermatitis and footrot feet biopsies. Load of total *Dichelobacter nodosus* (A), virulent *D. nodosus* (B), *F. necrophorum* (C) and *Treponema* spp. (D) as percentage of total eubacterial DNA. Healthy= 79 samples; mild ID= 39 samples; m/s ID= 26 samples; footrot= 97 samples. Mean is indicated by a black horizontal line. Data were analysed by Dunn's multiple comparisons test. *P ≤0.05, **P ≤0.01, ***P ≤0.001, ****P ≤0.0001. Number 0.001 (y axis): results below of the detection limit. Mild ID score 1; ms ID: moderate to severe ID scores 2, 3 and 4.

3.4 Discussion

In this study we provided further insights into the bacterial colonisation present in healthy, ID and footrot ovine feet. We found similar patterns regarding the prevalence and load of *D. nodosus* and *F. necrophorum* in post slaughter biopsies from the interdigital space as previous studies in UK sheep flocks using swabs and biopsies (Moore et al. 2005; Calvo-Bado et al. 2011; Witcomb et al. 2014; Witcomb et al. 2015).

As expected, the highest *D. nodosus* prevalence and load found in this study was in ID samples, hence supporting the hypothesis that *D. nodosus* drives the development of the early stages of footrot (Witcomb et al. 2014; Witcomb et al. 2015). Interestingly, *D. nodosus* was found in a large proportion of biopsy samples from healthy feet (58%, 46/79), suggesting it might be present in the stratum corneum (horny layer) but not necessarily causing disease. It is also possible that these visibly healthy feet might have had subclinical footrot and may have developed underrunning lesions in the following days. Risk factors for the development of underrunning footrot in addition to the presence of virulent *D. nodosus* include poor foot conformation (Kaler et al. 2010), superficial skin damage (Egerton et al. 1969), sheep breed (Emery et al. 1984) and presence of co-infecting bacteria such as *F. necrophorum* (Egerton et al. 1969; Roberts & Egerton 1969).

In this study, the majority of *D. nodosus* present in the ovine interdigital skin biopsies were virulent strains. Similarly, a high prevalence of virulent *D. nodosus* in the UK sheep was identified

previously using gelatinase gel protease assay (Moore et al. 2005). Therefore, these studies demonstrate that virulent strains are currently circulating in UK flocks. In contrast, in Sweden where underrunning footrot is not endemic, most of the *D. nodosus* were found to be benign (Frosth et al. 2015). We found a mixed population of benign and virulent *D. nodosus* strains in the same feet, a potential synergistic role of benign and virulent strains needs still to be investigated.

F. necrophorum prevalence and load were higher in footrot than in ID and healthy samples. These results, together with other published data that also found an increased presence of *F. necrophorum* in footrot lesions (Beveridge, 1941; Bennett et al. 2009; Witcomb et al. 2014; Witcomb et al. 2015), support the hypothesis that *F. necrophorum* contributes to the pathogenesis of underrunning footrot. *F. necrophorum* was presumed to facilitate *D. nodosus* invasion (Egerton et al. 1969), in the present study we found that the presence of both *D. nodosus* and *F. necrophorum* in the same tissue was significantly higher in footrot than in healthy feet; nevertheless, the exact nature and the role of the synergy between *F. necrophorum* and *D. nodosus* remains unclear.

Only a small number (9%, 7/79) of healthy biopsy samples were positive for *F. necrophorum* in this study. Similarly, Witcomb et al. (2015) found low prevalence of *F. necrophorum* in swabs (8%, 1/12) and biopsies (8%, 1/12) from healthy feet, but in an earlier study where swabs were repeatedly collected from 18 sheep during 5 weeks,

F. necrophorum was found in 62% (140/225) of healthy feet (Witcomb et al. 2014). This suggests that the prevalence of *F. necrophorum* in healthy feet varies according to sampling structure and collection methods. *F. necrophorum* is a commensal in the alimentary tract (Smith & Thornton 1997) and might be present in faeces contaminating ovine feet. Moreover, it was also detected on swabs taken from the oral cavity of sheep and suggested it might be transmitted from the mouth of sheep to the paddock (Bennet et al. 2009); hence, the significance of *F. necrophorum* in healthy ovine interdigital skin remains unclear, it may colonise healthy skin as a commensal microorganism without causing any skin disease, while in damaged skin, *F. necrophorum* colonisation may initiate ID and, thus, predispose the invasion of *D. nodosus*. Whether *D. nodosus* essentially requires *F. necrophorum* colonisation to facilitate its skin invasion remains unclear.

F. necrophorum is divided into subspecies *necrophorum* and *funduliforme*, the first is described to be more pathogenic due to a higher lipopolysaccharide content and higher production of leukotoxin (Tan et al. 1996). In this study, the majority of positive samples for *F. necrophorum* was subsp. *necrophorum*. Previous studies investigating this bacterium in UK flocks did not differentiate the subspecies of *F. necrophorum* (Witcomb et al. 2014, Witcomb et al. 2015). Therefore, despite the fact that this sample set is small, this is the first study suggesting that *F. necrophorum* subsp. *necrophorum* may be the more prevalent subspecies circulating in UK flocks. Since

F. n. subsp. *necrophorum* is described to be more virulent than *F. n.* subsp*. funduliforme* (Tan et al. 1996) and considering the fact that this bacterium may exacerbate footrot lesions, there might be an association between the high prevalence of severe footrot lesions in the UK and the presence of *F. n*. subsp. *necrophorum*. In contrast, in Swedish flocks where most of the footrot lesions were associated with mild footrot, *F. n.* subsp. *funduliforme* was more prevalent than *F. n.* subsp. *necrophorum* (Frosth et al. 2015).

Spirochaetes have also been identified in ID and/or footrot lesions (Beveridge, 1941; Calvo-Bado et al. 2011; Frosth et al. 2015). In the present study, a small number of biopsies were positive for *Treponema* spp. with similar prevalence in healthy, ID and footrot feet. Similarly, low detection of *Treponema* spp. in ovine biopsies from UK sheep was also reported by Calvo-Bado et al. (2011); moreover, no significant association between *Treponema* spp. and footrot was reported by Frosth et al. (2015). Hence, whether the low detection of *Treponema* spp. reflects its importance in the footrot pathogenesis remains an open question to be further elucidated. We amplified treponemal DNA using a genus-specific qPCR and not a species-specific assay, hence detecting free living as well as pathogenic *Treponema* spp.*;* therefore more studies are warranted to characterize the *Treponema* species commonly present in ovine footrot*.* In contrast to early investigations reporting that an initial infection with *D. nodosus* is often followed by an infection with *Treponema* spp. (Beveridge, 1941; Thomas, 1962),

we only found 3% of the biopsies (8/241) positive for both virulent *D. nodosus* and *Treponema* spp.

A limitation of using abattoir samples is that it is impossible to investigate the progression of the disease and thus verify whether healthy or ID feet positive for *D. nodosus* would develop footrot lesions. On the other hand, an advantage of using abattoir samples is the ability to collect biopsies from animals that are slaughtered for other purposes than this study and detect bacteria localized within tissues.

3.5 Conclusions

The results presented in this study, together with other published data confirm that *D. nodosus* is mainly associated with ID stage, and *F. necrophorum* with footrot stage; therefore supporting that *D. nodosus* drives the early stages of footrot and *F. necrophorum* plays a role in the pathogenesis of ovine footrot. Moreover, virulent *D. nodosus* population is more prevalent than benign in UK flocks. *Treponema* spp. was detected in few samples; hence further studies are warranted to provide more detailed information about the role *Treponema* spp. may have in ovine footrot. Additionally, this study reports novel results regarding the higher prevalence of *F. necrophorum* subsp. *necrophorum* than subsp. *funduliforme* in sheep from the UK, and a mixed population of virulent and benign *D. nodosus* present in the same skin biopsy.

Chapter 4

4. Investigating bacterial colonisation on the ovine interdigital skin surface and within the skin layers

4.1 Introduction

In footrot little is known about the skin localisation of the main bacteria involved in the disease. *D. nodosus* was primarily reported to be restricted to the superficial epidermal layers of the ovine skin, whereas *F. necrophorum* was reported to be located in deep skin layers (Egerton et al. 1969). A recent study provided new evidence showing that the majority of *F. necrophorum* and *D. nodosus* cells were located in the epidermis of fluorescently *in situ* hybridized ovine skin sections, but one *F. necrophorum* and one *D. nodosus* cell were detected in the dermis (Witcomb et al. 2015). These results were carefully interpreted due to limitations of sample size. Moreover, Witcomb et al. (2015) hypothesised that *D. nodosus* and *F. necrophorum* when located in dermal layers may act as potential reservoirs for chronic infection.

Other evidence of bacteria on the surface and within skin layers of the interdigital skin is that *D. nodosus*, *F. necrophorum* and *Treponema* spp. have been detected from both swabs (Moore et al. 2005; Bennett et al. 2009; Witcomb et al. 2014; Frosth et al. 2015;

Witcomb et al. 2015) and biopsies (Calvo-Bado et al. 2011; Witcomb et al. 2015; Maboni et al. 2016), demonstrating that these bacteria are present on both skin surface and in deeper skin layers. None of these studies investigated how effective are swabs in comparison with biopsies and whether the results obtained by both methods differ in terms of bacterial prevalence and load. These studies were performed using different sampling sizes in various countries, hence with specific disease epidemiology and bacterial prevalence; however, independent of using swabs or biopsies they share similar outcomes such as high prevalence of *D. nodosus* in ID samples (Moore et al. 2005; Witcomb et al. 2014 and 2015; Maboni et al. 2016), *F. necrophorum* in footrot samples (Bennet et al. 2009; Witcomb et al. 2014; Witcomb et al. 2015; Maboni et al. 2016) and few samples positive for *Treponema* spp. (Calvo Bado et al. 2011; Frosth et al. 2015; Maboni et al. 2016).

The advantages and disadvantages of using swabs or biopsies for sampling the ovine interdigital skin were recently discussed in the literature (Witcomb et al. 2014; Egerton, 2014). Biopsies provide the possibility to collect bacterial cells present on the skin surface and also those localized within the tissue, then represent the activity of organisms colonising all layers of the skin (Egerton, 2014). However, biopsies have the disadvantage of being invasive, compromising animal welfare, and when taken over time, may predispose sheep feet to infection and change the natural progression of disease. In contrast, swabs have the advantage of being non-invasive, which is

essential for longitudinal sampling (*in vivo* studies) (Witcomb et al. 2014), and are an important approach for footrot routine diagnosis. In countries like Sweden where laboratory diagnosis of footrot is a common practice, swabbing is the recommended approach to collect specimens for laboratory tests (Dr Sara Frosth, personal communication). Another advantage of using swabs is the larger superficial area that is sampled in comparison with 6mm biopsies, therefore expecting to detect a higher number of bacterial cells. The main disadvantage is that swabs do not represent organisms with invasive tissue behaviour.

In addition to *D. nodosus*, *F. necrophorum* and *Treponema* spp., 27 bacterial genera were found in a microbiota study using a pyrosequencing approach. *Peptostreptococcus* was the most abundant genus in healthy interdigital skin, with *Corynebacterium* mainly associated with ID and *Staphylococcus* the most abundant genera in footrot samples (Calvo-Bado et al. 2011). Nevertheless, little is known about the role of other bacterial groups as well as their localisation within the ovine interdigital skin.

In this context, two main questions regarding bacterial localisation in the ovine interdigital skin remain to be elucidated. (i) Where is the main location of bacteria involved in footrot. (ii) How effective are swabs compared to biopsies when applied to epidemiological studies of ovine footrot? Therefore, this study aimed to compare the prevalence and load of total eubacteria, *D. nodosus, F. necrophorum*

and *Treponema* spp. on the ovine interdigital skin surface using swabs and within the skin using biopsies (matched samples). Furthermore, microbial communities were also investigated in the matched swabs and biopsies using sequencing of the prokaryotic 16S ribosomal RNA (Miseq, Illumina).

4.2 Materials and methods

Collection of swabs and biopsies from the ovine interdigital skin is described in section 2.1, DNA extraction is described in section 2.2 and qPCR assays for bacterial quantification are described in section 2.3 (Chapter 2 and 3).

4.2.1 Study design

The design included the collection of samples from the ovine interdigital skin surface using swabs, prior to collecting biopsies from the same skin area. After swab collection, the interdigital space was cleaned with detergent, 70% ethanol and a paper towel in order to remove any remaining bacteria present on the skin surface before collection of biopsies. A convenience sampling approach was used due to variable availability of the clinical conditions at the abattoir, which resulted in 14 healthy, 9 ID and 13 footrot samples (36 swabs & 36 biopsies) from 9 different sheep (Table 4.1). Detection and quantification of total *D. nodosus* (targeting *16S rRNA* gene), virulent and benign *D. nodosus, F. necrophorum, Treponema spp.* and total eubacteria were assessed by qPCR in swabs and biopsies. As part of

a preliminary investigation, DNA samples from 30 swabs and 30 biopsies (matched samples) were sent to the National Veterinary Institute (Sweden) for bacterial 16S rRNA sequencing in an attempt to investigate differences in the microbial populations present on the surface and within the ovine interdigital skin. Virulent/benign *D. nodosus*, *F. necrophorum* and *Treponema* spp. qPCR assays were performed by Dr Sara Frosth.

Table 4.1 Details of the matched samples included in this study. Swabs and biopsies were collected from the ovine interdigital skin space.

Sheep	Sample	Clinical condition	Conformation score	ID Score	Footrot score
Sheep 1	MM205	Footrot	2	0	1
	MM206*	Healthy	1	0	0
	MM207*	ID	1	1	0
	MM208*	Footrot	2	0	1
Sheep 2	MM209	Footrot	2	3	1
	MM210*	Healthy	1	0	0
	MM211*	ID	1	1	0
	MM212*	ID	1	1	0
Sheep 3	MM213*	Healthy	2	0	0
	MM214*	Footrot	2	1	1
	MM215*	Footrot	1	4	1
	MM216*	Footrot	2	1	1
Sheep 4	MM217*	Healthy	1	0	0
	MM218*	ID	0	3	0
	MM219*	Healthy	0	0	0
	MM220	Footrot	2	4	2
Sheep 5	MM221*	Healthy	1	0	0
	MM222*	Footrot	2	3	2
	MM223*	ID	1	1	0
	MM224*	Healthy	0	0	0
Sheep 6	MM225*	Footrot	3	1	3
	MM226*	Healthy	0	0	0
	MM227*	ID	0	1	0
	MM228*	ID	1	1	0
Sheep 7	MM229	Healthy	1	0	0
	MM230	Healthy	1	0	0
	MM231*	Healthy	1	0	0
	MM232*	Healthy	0	0	0
Sheep 8	MM233*	Healthy	1	0	0
	MM234*	ID	2	1	0
	MM235*	Footrot	1	1	1
	MM236*	Footrot	3	4	4
Sheep 9	MM237*	ID	1	1	0
	MM238*	Healthy	1	0	0
	MM239	Footrot	1	2	1
	MM240*	Footrot	2	1	1

ID= interdigital dermatitis
* Samples included in the microbial population analysis (16S rRNA sequencing)
For details of conformation, ID and footrot scoring system see Table 2.1 (Chapter 2)

4.2.2 qPCR data normalisation and statistical analysis

The qPCR data for total eubacterial load were normalised as % of pg of total eubacteria DNA present in the total pg of DNA extracted from each tissue biopsy or swab. The qPCR data for *D. nodosus* (*16Sr RNA* gene, virulent and benign), *F. necrophorum* and *Treponema* spp. were normalised as % of eubacterial DNA obtained for each tissue biopsy or swab.

McNemar's test for matched-pair samples was carried out for bacterial prevalence comparison of biopsies vs. swabs (total number of samples) and for comparison between the different clinical conditions. Wilcoxon matched-pairs signed rank test (non-parametric T test) was carried out for comparison of bacterial load in biopsies vs. swabs. All analyses were performed using Graphpad Prism. A P-value ≤ 0.05 was considered significant.

4.2.3 Bacterial 16S rRNA sequencing

DNA extracted from swabs and biopsies (as described in Chapter 2) was subjected to a 16S rRNA V3/V4 variable region amplification by standard PCR using the Illumina metagenomic library preparation kit and primers 341F and 534R (Primer details, Table 2.3, Chapter 2). The libraries were sequenced using an Illumina MiSeq at the National Veterinary Institute (Sweden). The generated reads where parsed through Trimmomatic (version 0.36) (Bolger et al. 2014) to remove Illumina sequencing adaptors and 16S rRNA primer contamination

based on Klindworth et al. (2013). Remaining sequences were also assessed and filtered using a 15bp sliding window approach for quality scores (phred >30) and were required to be of a minimum length of 50bp. The trimmed high quality reads where classified using RDPTools taxonomic classification system (Wang et al. 2007). Microbial diversity at phylum level was assessed by calculating the Shannon index and Pielou's Evenness test (Bioinformatics analysis was performed by Dr Adam Blanchard).

4.3 Results

4.3.1 Bacterial prevalence in biopsies vs. swabs

All samples were positive for total eubacteria (100% of prevalence). A higher number of biopsy samples were positive for total *D. nodosus* (78%, 28/36) in comparison with swabs (61%, 22/36), but this difference was not statistically significant (Table 4.2). In contrast, virulent *D. nodosus* was significantly more prevalent in swabs (64%, 23/36) than biopsies (36%, 13/36, P= 0.0162) (Table 4.2). A similar number of positive samples for benign *D. nodosus* were detected in biopsies (22%, 8/36) and swabs (19%, 7/36) (Table 4.2); however, as the number of positive samples for benign *D. nodosus* is small, these results might not be representative. Moreover, *F. necrophorum* was significantly more detected in swabs (70%, 25/36) than in biopsies (17%, 6/36) (P=0.0004) (Table 4.2). *Treponema* spp. was significantly more detected in biopsies (36%, 13/36) than in swabs (11%, 4/36) (P=0.0159) (Table 4.2). In summary, virulent *D.*

nodosus was more often detected in swabs, and benign *D. nodosus* detection was similar in both biopsies and swabs. Furthermore, *F. necrophorum* was more often detected in swabs, whereas *Treponema* spp. was more frequently detected in biopsies. An overall agreement was obtained from swabs and biopsies where both presented positive results or both presented negative results for total *D. nodosus*, virulent/benign *D. nodosus* and *Treponema* spp., except for *F. necrophorum* (Table 4.2).

Table 4.2 McNemar's test analysis of bacterial prevalence on matched-pair samples of swabs and biopsies collected from the ovine interdigital skin.

Swabs/Biopsies	**Total DN**	**Virulent DN**	**Benign DN**	**FN**	**Treponema**
+/+	21/36	11/36	3/36	5/36	3/36
-/-	7/36	11/36	24/36	13/36	22/36
+/-	1/36	12/36	4/36	17/36	1/36
-/+	7/36	2/36	5/36	1/36	10/36
P-value:	0.0771	**0.0162**	1	**0.0004**	**0.0159**
More Prevalent?	Biopsies	**Swabs**	Similar	**Swabs**	**Biopsies**

DN: *Dichelobacter nodosus*. FN: *Fusobacterium necrophorum*. **+/+**= sample positive for the targeted bacterium in both swab and biopsy (agreement between both methods). **-/-**= sample negative for the targeted bacterium in both swab and biopsy (agreement between both methods). **+/-**= positive in swab and negative in biopsy (disagreement between both methods). **-/+**= negative in swab and positive in biopsy (disagreement between both methods). Biopsies n= 36; Swabs n= 36. P-value ≤0.05 was considered significant (in bold). Confidence intervals: 0.14(95%CI 0.003-1.1) for *D. nodosus*; 6(95%CI 1.33-55) for virulent *D. nodosus*; 0.8(95%CI 0.15-3.7) for benign *D. nodosus*; 0.05(95%CI 0.001-0.37) for *F. necrophorum*; 0.1(95% CI 0.002-0.7) for *Treponema* spp. Analysis were performed using Graphpad Prism.

In addition, these data were further analysed in the context of the clinical conditions (i.e. healthy, ID and footrot affected feet) (Figure 4.1). For both biopsies and swabs, a similar number of total *D. nodosus* as well as benign *D. nodosus* was detected among healthy,

ID and footrot (Figure 4.1 A, C). In contrast, a higher percentage of virulent *D. nodosus* was found on swab samples of all clinical conditions (healthy 50% 7/14; ID 78%, 7/9; footrot 70%, 9/13) than in biopsies (healthy 28%, 4/14; ID 33%, 3/9; footrot 46%, 6/13) (Figure 4.1 B), but these results were not statistically significant. *F. necrophorum* was statistically more prevalent in healthy swab samples (71%, 10/14) than in healthy biopsies (7%, 1/14) (P=0.0269); but, *F. necrophorum* was not significantly more often detected in ID and footrot swab samples (55%, 5/9 and 76%, 10/13, respectively) than in biopsy samples (11%, 1/9 and 31%, 4/13, respectively) (Figure 4.1 D). *Treponema* spp. was only detected in healthy (28%, 4/14), ID (33%, 3/9) and footrot biopsy samples (46%, 6/13), while healthy and ID swabs were negative (31%, 4/13) (Figure 4.1 E). In summary, no major differences of bacterial prevalence on the skin surface (swabs) and within skin layers (biopsies) were observed among healthy, ID and footrot matched samples, except for *F. necrophorum*.

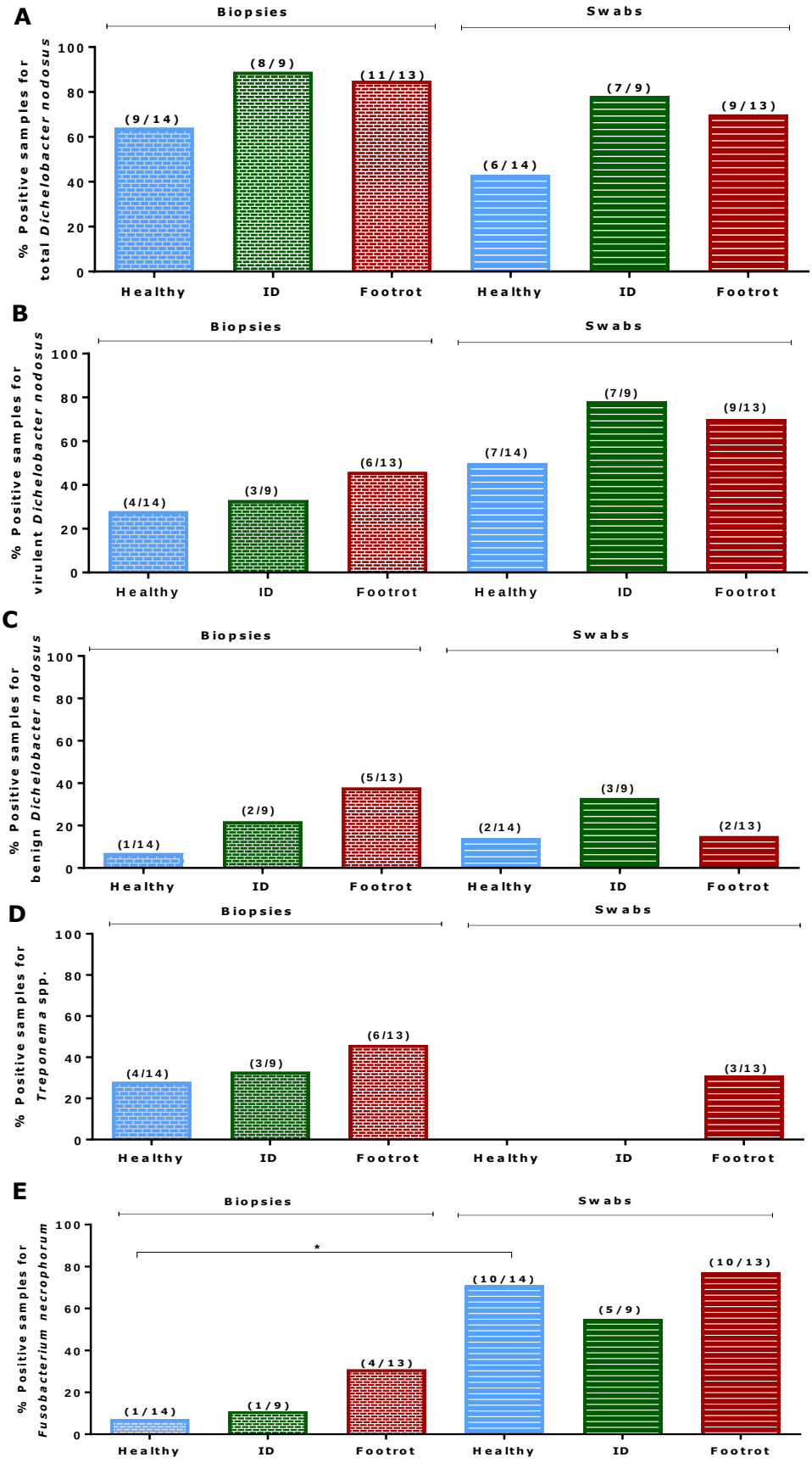


Figure 4.1 Bacterial prevalence on biopsies compared to swabs collected from the ovine interdigital skin. Prevalence of *Dichelobacter nodosus* (A); virulent *D. nodosus* (B); benign *D. nodosus* (C); *Treponema* spp. (D) and *Fusobacterium necrophorum* (E). Data were analysed using McNemar's test for matched-paired samples (Graphpad Prism). *P<0.05 considered significant.

4.3.2 Bacterial load in biopsies vs. swabs

To determine the load of total eubacterial DNA, swabs and biopsies were subjected to quantitative measurements of *16S rRNA* gene with bacterial universal primers. A higher load of total eubacterial DNA was found in swabs (1.6%, ±1.04) than in biopsies (0.02%, ±0) (Figure 4.2 A, B), suggesting bacterial detection in tissue samples may be less sensitive due to the lower proportion of bacterial DNA. Similar loads of eubacterial DNA were quantified in healthy, ID and footrot from both biopsies and swab samples (Figure 4.2 A, B).

D. nodosus, *F. necrophorum* and *Treponema* spp. load varied according to clinical conditions. The load of total *D. nodosus,* but not virulent *D. nodosus,* was significantly higher in biopsy tissues than in swabs collected from healthy ($P \leq 0.01$), ID ($P \leq 0.01$) and footrot affected feet ($P \leq 0.001$) (Figure 4.3 A, B). Benign *D. nodosus*, *F. necrophorum* and *Treponema* spp. did not show any significant differences between clinical conditions, which is likely due to the low number of positive samples for these bacteria (Figure 4.3 C, and 4.4 A, B). Taken together, bacterial prevalence and load differ on the surface and within layers of the ovine interdigital skin. Virulent *D. nodosus* and *F. necrophorum* prevalence and load tended to be higher in swabs, whereas *Treponema* spp. prevalence and load tended to be higher within the skin layers (biopsies).

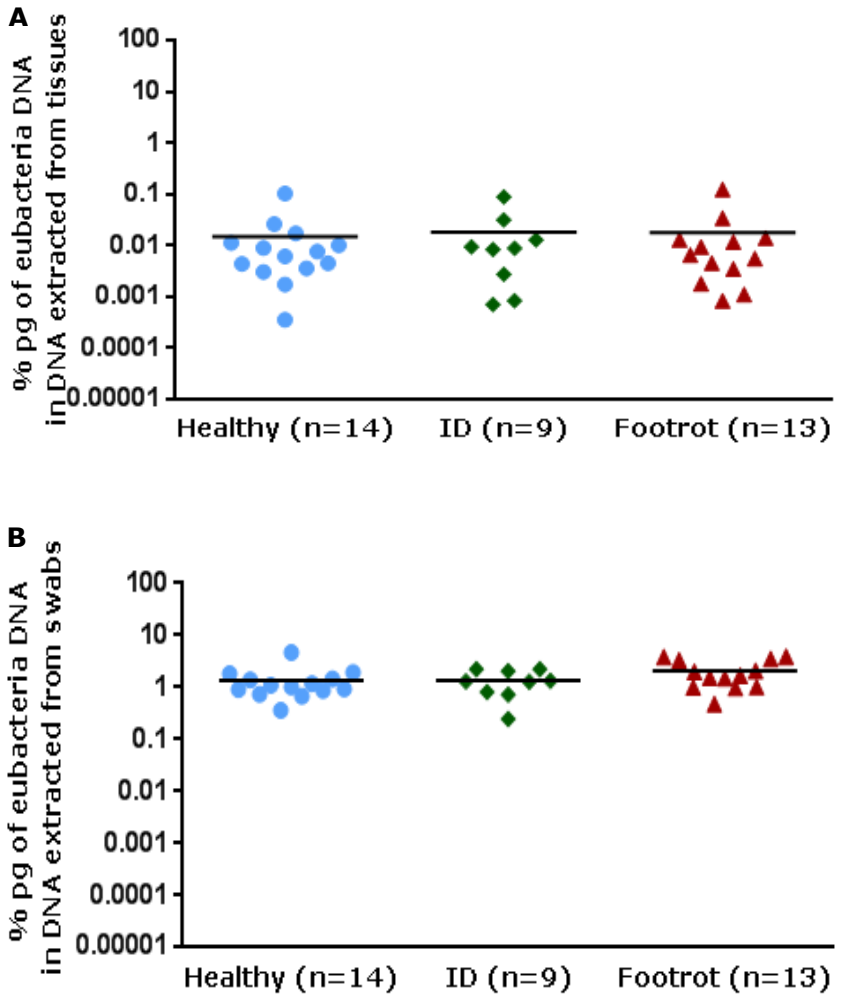


Figure 4.2 Total percentage of eubacterial DNA extracted from tissue biopsies (A) and from swabs (B). Mean is indicated by a black horizontal line. Data were analysed by Dunn's multiple comparison test. Number 0.00001 (y axis): results below of the detection limit.

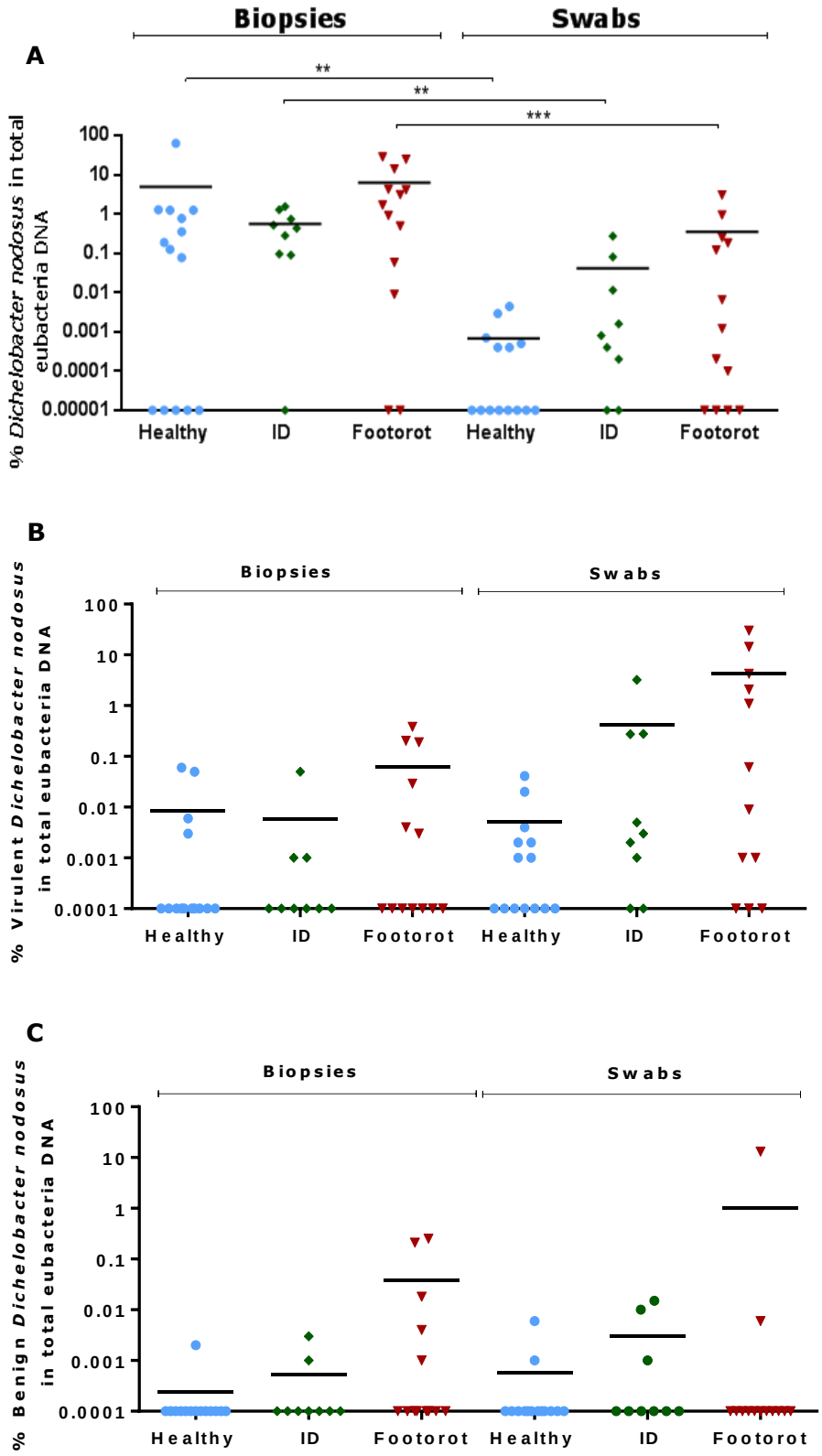


Figure 4.3 *Dichelobacter nodosus* load in biopsies compared to swabs collected from the ovine interdigital skin. Total *Dichelobacter nodosus* (targeting *16S rRNA* gene) (A); virulent *D. nodosus* (B), benign *D. nodosus* (C). Total number of healthy samples=19, ID=9 and footrot=13. Mean is indicated by a black horizontal line. Data were analysed by Wilcoxon matched-pairs signed rank test (non-parametric T test) using Graphpad Prism. **P≤0.01, ***P≤0.001. Number 0.00001 (y axis): results below of the detection limit. ID= interdigital dermatitis.

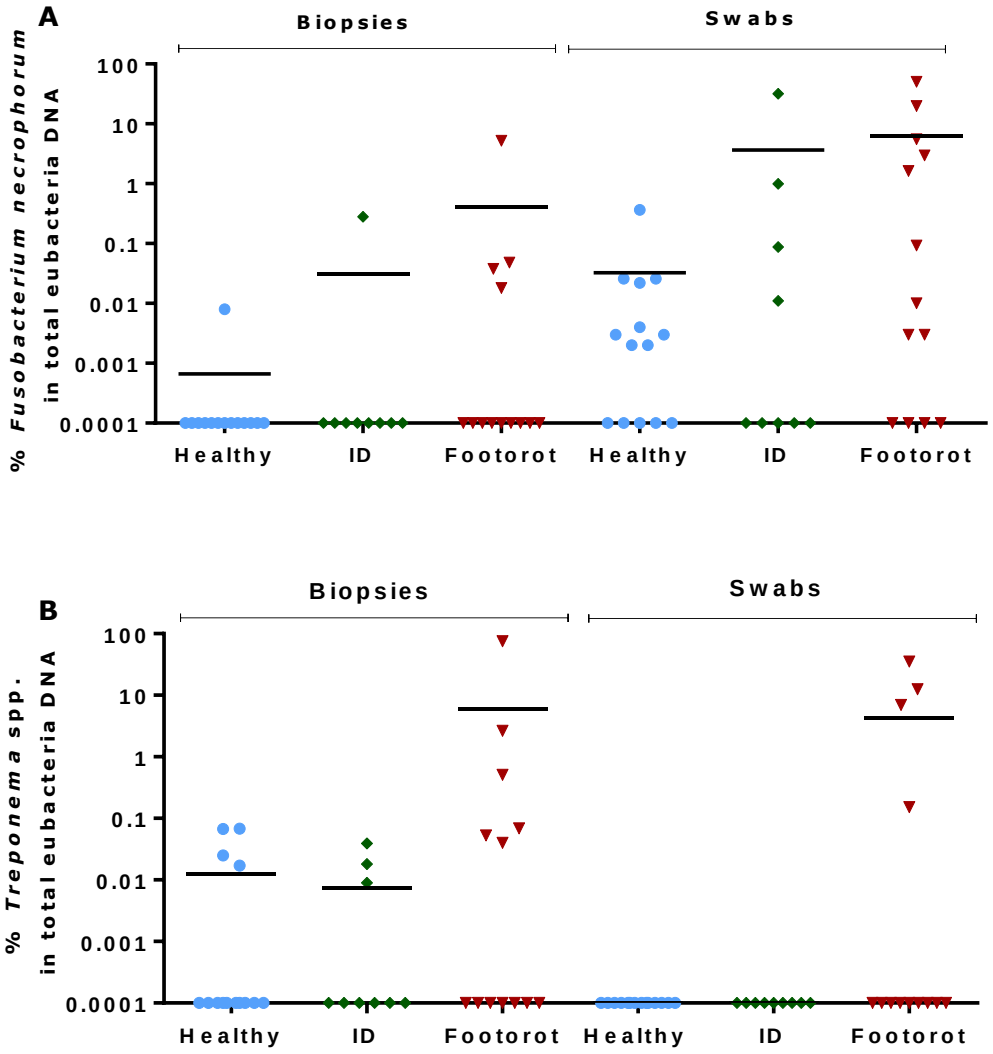


Figure 4.4 *Fusobacterium necrophorum* load (A) and *Treponema* spp. load (B) in biopsies compared to swabs collected from the ovine interdigital skin. Total number of healthy samples=19, ID=9 and footrot=13. Mean is indicated by a black horizontal line. Data were analysed by Wilcoxon matched-pairs signed rank test (non-parametric T test) using Graphpad Prism. Number 0.00001 (y axis): results below of the detection limit. ID= interdigital dermatitis.

4.3.3 Bacterial 16S rRNA sequencing

Bacterial 16S rRNA sequencing was used to investigate whether bacterial communities present on the skin surface differ from those present within skin layers. An initial analysis focused on differences at phyla level showed that the most abundant phyla present on the skin surface (swabs) were Proteobacteria (91%), Firmicutes (4%), Bacteroidetes (3%) and Actinobacteria (0.7%). The same bacterial phyla were found as the most abundant within the skin layers (biopsies), but in different proportions, for instance, Firmicutes (49%), Actinobacteria (26%), Bacteriodetes (10%) and Proteobacteria (9%) (Figure 4.5). This preliminary analysis revealed that bacterial communities were more diverse in healthy biopsies than swabs, even though the total eubacterial load in biopsies was lower than in swabs.

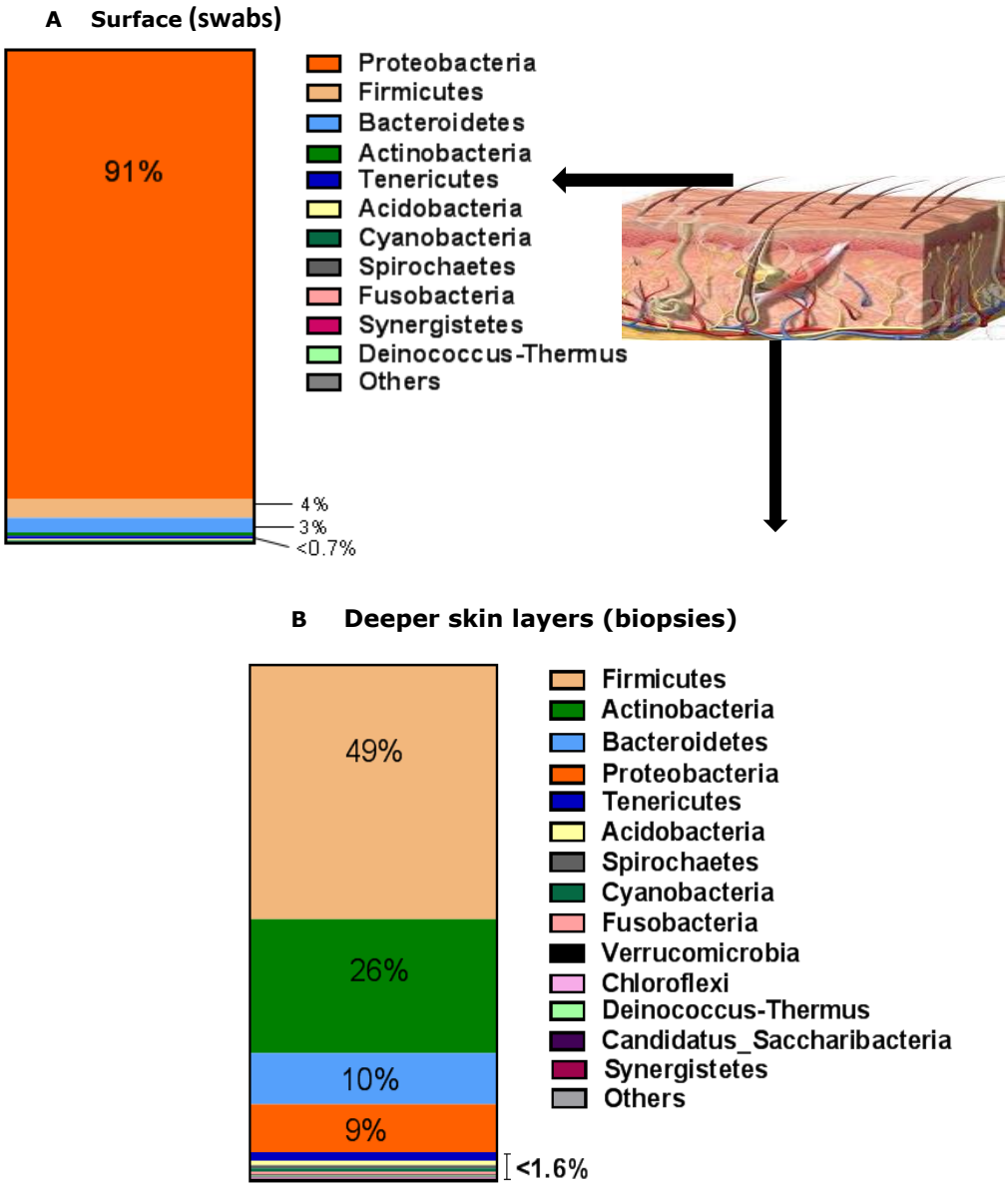


Figure 4.5 Preliminary microbiota analysis of the ovine interdigital skin using two approaches, swabs (surface) and biopsies (deeper skin layers). Relative abundance (% of reads) of phyla bacterial groups present on the skin surface (A) and in deeper skin layers (B). Sequencing of the prokaryotic 16S ribosomal RNA (Miseq, Illumina) was used in this study.

4.4 Discussion

This study compared bacterial prevalence and load on the skin surface and within skin layers using swabs and tissue biopsies. The key findings included that total eubacterial DNA as well as DNA from *D. nodosus*, *F. necrophorum* and *Treponema* spp. were detected on both skin surface and within layers of healthy and disease affected skin. Moreover, bacterial prevalence and load differ on the skin surface compared to within skin layers. Total *D. nodosus* and *Treponema* spp. were more frequently detected in biopsies, while virulent *D. nodosus* and *F. necrophorum* were more detected in swabs (Table 4.2). Therefore, we provided further evidence of the presence of both *D. nodosus* and *F. necrophorum* not only on the skin surface but also within skin layers, hence supporting earlier findings (Egerton et al. 1969; Witcomb et al. 2015). It should be noted that this study does not prove that live bacteria inhabit the skin surface or within layers, as qPCR cannot distinguish between viable or dead cells. Also as biopsies are an invasive method, we used biopsies taken from an abattoir, therefore sheep sampled for this study were slaughtered for a different purpose and they were naturally infected.

A higher load of eubacteria was more detected in swabs than in biopsies

As expected, the total eubacterial DNA present in biopsies was considerably lower (0.02% of eubacteria in total DNA) compared with swabs (1.6% of eubacteria in total DNA), which is likely to be

associated with constant skin surface exposure to faecal and soil bacteria. Moreover, swab samples were collected from exactly the same area prior to biopsy collection, which removed part of the bacteria present on the superficial layer. Interestingly, eubacterial DNA was detected in all healthy ovine skin biopsies (Figure 4.2 A). It has been shown recently that healthy human skin biopsies contained bacterial DNA (analysing *16S rRNA* genes by qPCR) in deep skin compartments (Nakatsuji et al. 2013). Hence, as previously revealed in human skin, the healthy ovine skin may not maintain a complete barrier to bacterial entry, and bacteria may penetrate and reside below the stratum corneum. The approaches used in this study did not allow differentiation of the location of bacteria within skin layers. A more exact localisation of bacterial *16S rRNA* genes within different interdigital skin compartments is currently in progress as part of another PhD project.

D. nodosus, Treponema spp. and F. necrophorum detection on swabs compared to biopsies

Total *D. nodosus,* as well as virulent and benign *D. nodosus,* were detected in biopsies and swabs, demonstrating it has the ability to colonize both surface and within the skin layers. Prevalence of virulent *D. nodosus* was significantly higher in swabs than biopsies (Table 4.2). As virulent *D. nodosus* is the definitive pathogen of footrot, swabs might represent an appropriate method for epidemiological and *in vivo* studies of this disease. Based on these findings, we could postulate that virulent *D. nodosus* inhabit mainly the superficial skin

layer where it initiates underrunning footrot lesions (Kennan et al. 2010), and other bacteria, with a more invasive nature, might inhabit within the skin layers playing a role in the lesion exacerbation. *Treponema* spp., for instance, was more frequently within the skin layers than on the skin surface, which might be related to an tissue invasive nature of these bacteria (Edwards et al. 2003). *Treponema* spp. involved in bovine digital dermatitis and in human periodontitis were reported to have a high capability for penetrating and adhering to both bovine and human tissue layers (Edwards et al. 2003). Therefore, we postulate that *Treponema* spp. identified in the ovine interdigital skin might have the same invasive behaviour. As the number of positive samples was small (biopsies n=13), further studies are necessary to investigate this hypothesis as well as to understand the mechanisms by which the ovine skin permits bacteria to enter across the epidermal barrier. Importantly, this study applied a qPCR approach at genus specific level since there is no characterisation of treponemal species involved in footrot.

F. necrophorum was significantly more prevalent in swabs than biopsies, suggesting this bacterium may inhabit predominantly the most superficial layers of the ovine interdigital skin. *F. necrophorum* was significantly more prevalent in healthy swabs than in healthy biopsies. In contrast, Witcomb et al. (2015) found the same prevalence of *F. necrophorum* in swabs (8%, 1/12) and biopsies (8%, 1/12) in healthy ovine feet, but these were unmatched samples. In an earlier longitudinal study where swabs were repeatedly collected

from a larger sample set, *F. necrophorum* was found in 62% (140/225) of healthy feet (Witcomb et al. 2014). The results presented in this study, together with data presented by Witcomb et al. (2014, 2015), confirm that the prevalence of *F. necrophorum* in healthy feet varies according to sampling structure and collection methods. *F. necrophorum* is a commensal in the alimentary tract (Smith and Thornton, 1997) and in the mouth of sheep (Bennett et al. 2009), which may cross contaminate the environment and then the animal`s feet, hence explaining the high detection of *F. necrophorum* on the surface of healthy skin.

D. nododus, F. necrophorum and Treponema spp. residing within the skin layers may interact with epidermal and dermal immune cells

Another reason to investigate bacterial localisation within the skin layers is that it extends our understanding of the influence of these microorganisms in the host immune response. The epidermis and dermis are composed of many different specialized cell types that express pattern recognition receptors, which will actively respond when exposed to microorganisms. *In vitro* culture of deep skin cells, such as dermal fibroblasts, were shown to interact with *D. nodosus* and *F. necrophorum* to give increased levels of IL1β mRNA expression after bacterial challenge (Davenport et al. 2014). Based on the interaction between the reported to be surface microorganisms, *F. necrophorum* and *D. nodosus* (Egerton et al. 1969; Rasmussen et al. 2012; Witcomb et al. 2015) with immune functions of dermal fibroblasts, we hypothesize that these bacteria might penetrate below

the stratum corneum and possibly below the epidermal basement membrane, hence influencing the host immune response. Therefore, information on *D. nodosus*, *F. necrophorum* and *Treponema* spp. localisation may provide the basis for new approaches to understand the interaction of bacteria and the ovine immune system.

4.5 Future work

As this work is a pilot study, the small sample size is a major limitation. While not part of this PhD project, a new and larger sample set could be included to obtain a more representative data set. Further analysis of the sequencing data will be performed to investigate (i) the microbiota on the surface and within the skin in the four feet of the same sheep, (ii) bacterial community abundance according to clinical conditions i.e. healthy, ID and footrot, (iii) and a comparison between the results obtained by qPCR and the abundance of *D. nodosus*, *F. necrophorum* and *Treponema* spp. in the 16S rRNA sequencing data. Finally, microbiota analysis will provide further insights into the localisation of other bacterial communities that might also be involved in footrot aetiology and pathogenesis.

4.6 Conclusions

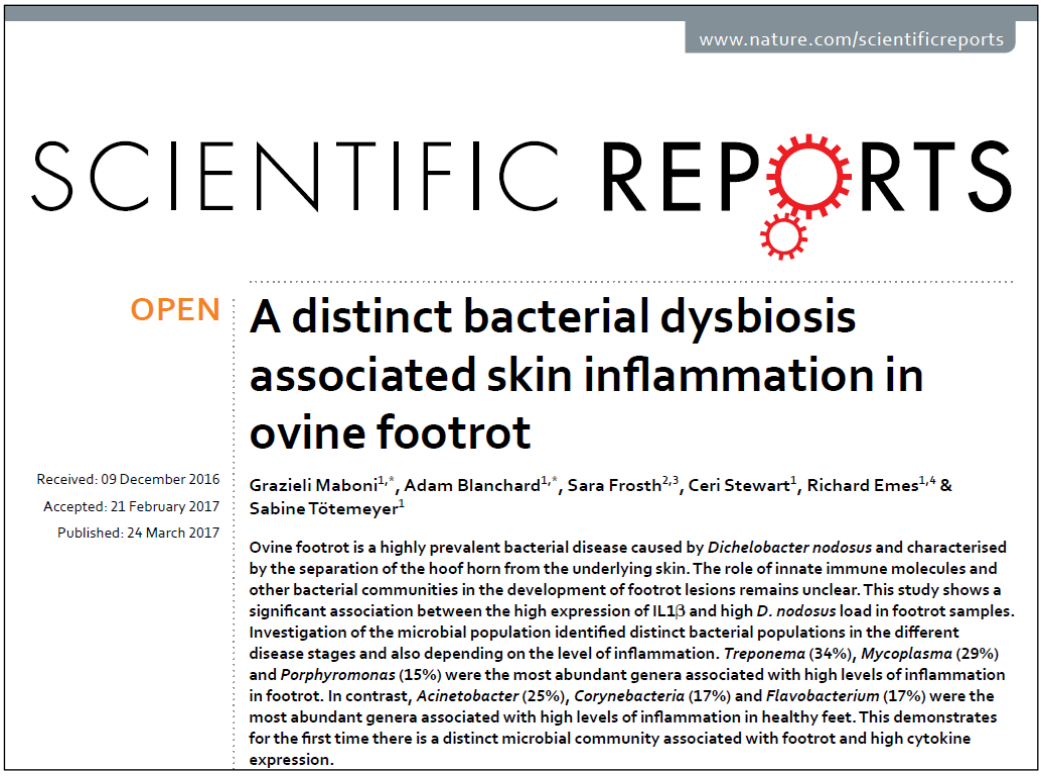
To our knowledge, this is the first study to describe the detection, quantification and localisation on the surface and within ovine interdigital skin layers of *D. nodosus, F. necrophorum, Treponema spp.* and total eubacteria. We also present evidence that bacterial

prevalence and load differ on the surface (swabs) and within the skin layers (biopsies). The first question raised in this study was where the main bacteria involved in footrot are located? The data here presented suggest that virulent *D. nodosus* and *F. necrophorum* were mainly located on the skin surface (swabs), whereas *Treponema* spp. within the skin layers (biopsies). The second question was how effective is swabbing method in comparison to biopsies when applied in epidemiological studies of this disease? Here, we could postulate that as virulent *D. nodosus* and *F. necrophorum*, the two main microorganisms of footrot, were more detected in swabs, this method might represent an appropriate approach for epidemiological and *in vivo* studies of the disease. Moreover, the presence of all bacterial species within the skin layers (biopsies) may favour the interaction of these microorganisms with deeper skin cells, hence influencing the host immune response. This provides the basis for new approaches to understanding this skin infection.

Chapter 5

5. Identification of novel and reliable reference genes for RT-qPCR studies on ovine interdigital skin

This chapter is an extension of the data on ovine reference genes previously described and published in a paper format `A distinct bacterial dysbiosis associated skin inflammation in ovine footrot'. DOI: 10.1038/srep45220 (Appendix 2).



www.nature.com/scientificreports

SCIENTIFIC REPORTS

OPEN

Received: 09 December 2016
Accepted: 21 February 2017
Published: 24 March 2017

A distinct bacterial dysbiosis associated skin inflammation in ovine footrot

Grazieli Maboni[1,*], Adam Blanchard[1,*], Sara Frosth[2,3], Ceri Stewart[1], Richard Emes[1,4] & Sabine Tötemeyer[1]

Ovine footrot is a highly prevalent bacterial disease caused by *Dichelobacter nodosus* and characterised by the separation of the hoof horn from the underlying skin. The role of innate immune molecules and other bacterial communities in the development of footrot lesions remains unclear. This study shows a significant association between the high expression of IL1β and high *D. nodosus* load in footrot samples. Investigation of the microbial population identified distinct bacterial populations in the different disease stages and also depending on the level of inflammation. *Treponema* (34%), *Mycoplasma* (29%) and *Porphyromonas* (15%) were the most abundant genera associated with high levels of inflammation in footrot. In contrast, *Acinetobacter* (25%), *Corynebacteria* (17%) and *Flavobacterium* (17%) were the most abundant genera associated with high levels of inflammation in healthy feet. This demonstrates for the first time there is a distinct microbial community associated with footrot and high cytokine expression.

Author's contributions

Grazieli Maboni conceived and designed the experiments, collected samples, performed DNA and RNA extraction, cDNA synthesis, primer design, optimized RT-qPCR assays for reference genes and cytokines/TLRs, analysed the data, prepared figures and tables, wrote the manuscript and reviewed drafts of the manuscript.

Dr Adam Blanchard performed bioinformatics analysis, analysed the data, wrote the manuscript and reviewed drafts of the manuscript.

Dr Sara Frosth performed qPCR assays for virulent *D. nodosus*, prepared libraries for sequencing on the Illumina MiSeq system, and reviewed drafts of the manuscript.

Ceri Stewart optimized RT-qPCR assays for cytokines/TLRs as part of a 3rd year research project at School of Veterinary Medicine and Science.

Professor Richard Emes performed bioinformatics analysis and reviewed drafts of the manuscript.

Dr Sabine Tötemeyer conceived and designed the experiments, supervised G. Maboni during laboratory experiments, analysed the data and prepared microbiota figures, wrote the manuscript and reviewed drafts of the manuscript.

5.1 Introduction

RT-qPCR is a precise and sensitive method to provide mRNA gene expression profiles (Bustin, 2002). The accuracy of RT-qPCR is determined by a number of factors, such as mRNA quality, reverse transcription and PCR amplification efficiency. Moreover, the selection of suitable reference genes, also called housekeeping genes, for normalization of Cq values is a crucial step to obtain reliable RT-qPCR results (Bustin et al. 2010). Originally, there was an assumption by researchers that essential metabolic genes could be suitable reference genes as they were thought to be constitutively expressed; however, there is increasing evidence that the expression of these essential metabolic genes can vary significantly in certain conditions (Bustin 2000; Hruz et al. 2011). Studies have demonstrated that the expression of commonly used reference genes varies according to cell type, origin of tissue sample, disease condition and treatments (Thellin et al. 1999; Hruz et al. 2011). Reference genes are often selected from other published studies without taking into account the sample origin, treatments and all other variabilities that may influence the gene expression stability. Other studies have focused on validating a small subset of commonly used reference genes for specific conditions; however, it has been argued that reference genes should be ideally selected from the complete genome rather than from a small set of commonly used reference genes (Hruz et al. 2011). In order to ensure high quality RT-qPCR data a 'Minimum Information for Publication of Quantitative Real-Time PCR

Experiments' (MIQE) guidelines highlight the critical importance of proper selection and evaluation of reference genes for particular tissues or cell types using the specific experiment in question (Bustin et al. 2010).

Stable reference genes for ovine tissues have been investigated in a range of different samples including intestinal tissues, pulmonary artery, lung, whole blood, circulating neutrophils, oocytes, mandibular condyle and efferent leucocytes (Taylor et al. 2008; Passmore et al. 2009; Serrano et al. 2011; Peletto et al. 2011; O'Connor et al. 2013; Vorachek et al. 2013; Jiang et al. 2015; Puech et al. 2015; Mahakapuge et al. 2016). Table 5.1 summarises the main findings of these studies highlighting that a diverse set of candidate reference genes was investigated in earlier studies and their expression stability varies according to different ovine tissues and cell types. A study investigating reference genes stability for intestinal ovine tissues found *HK5.1* as the most stable candidate gene (Taylor et al. 2008). The most stable genes for whole blood were *SDHA*, *YWHAZ* (Passmore et al. 2009), *RPS18* and *SDHA* (Serrano et al. 2011), while in circulating neutrophils the most stable candidate genes were *G6PD*, *YWHAZ*, *GAPDH* and *RPL19* (Vorachek et al. 2013) and in PBMC were *ACTB* and *YWHAZ* (Puech et al. 2015). *PPIA* and *ACTB* were the most stable genes for pulmonary artery and lung tissues (Passmore t al. 2009) and these genes also presented stable expression on interdigital skin samples (Davenport et al. 2014). Jiang et al. (2015) investigated gene expression stability for ovine

mandibular condyle samples and found *RPL19*, *ACTB* and *PGK1* as the most stable candidate reference genes (Table 5.1).

Table 5.1 Studies on reference genes available in the literature for normalisation of RT-qPCR data using ovine cells and tissues.

Ovine sample	**Method of analysis**	**Most stable genes**	**Least stable genes**	**Reference**
Intestinal tissues	SD of Cq values	*HK5.1*	*ACTB*,*18S*, *GAPDH*	(Taylor et al. 2008)
Pulmonary artery/lung	geNorm	*PPIA, ACTB*	*HGPRT,GAPDH, PGK1*	(Passmore et al. 2009)
Whole blood	geNorm, NormFinder	*SDHA, YWHAZ*	*TFRC, PGK1*	(Peletto et al. 2011)
Whole blood	Maximum Likelihood method	*RPS18, SDHA*	*ACACA, RPL13A*	(Serrano et al. 2011)
Circulating neutrophils	geNorm, NormFinder, BestKeeper, Delta CT method	*G6PD, YWHAZ, GAPDH, RPL19*	*PGK1, ACTB, B2M*	(Vorachek et al. 2013)
Oocytes	geNorm	*SDHA,TUBB, PPIA*	*ACTB, GAPDH*	(O'Connor et al. 2013)
Interdigital skin	geNorm	*ACTB*	*18S, TUBA, B2M*	(Davenport et al. 2014)
Mandibular condyle	RefFinder	*RPL19,ACTB, PGK1*	*HPRT,SDHA, YWHAZ*	(Jiang et al. 2015)
PBMC	geNorm, NormFinder	*ACTB, YWHAZ*	*PPIA*	(Puech et al. 2015)
Efferent leucocytes	geNorm, NormFinder	*PGK1,GAPDH YWHAZ*	*RPL-13A,HPRT, SDHA, ACTB, B2M*	(Mahakapuge et al. 2016)

SD: standard deviation; Cq: quantification cycle; PBMC: peripheral blood mononuclear cells

An initial investigation of reference genes stability was previously performed by our group (Davenport et al. 2014). *ACTB* was the most stable of 6 candidate genes according to geNorm analysis using a small set of 28 biopsies (Davenport et al. 2014) (Table 5.1). That is the only study available in the literature addressing reference genes stability for the ovine interdigital skin. Prior to investigating the

expression of targeted genes associated with interdigital skin diseases in sheep, a wider investigation and selection of appropriate reference genes are essential. In an effort to improve the quality and normalization of RT-qPCR data for ovine interdigital skin samples, this study expanded the analysis performed by Davenport et al. (2014) aiming to investigate 10 candidate reference genes in a large set of healthy, ID and footrot samples. Moreover, a novel approach, RefFinder software, was applied to rank the stability of candidate reference genes. This approach integrates all currently available major algorithms (geNorm, Normfinder, BestKeeper, and the Comparative Delta CT method) to rank reference gene stability.

5.2 Materials and methods

Collection of biopsies from ovine interdigital skin is described in section 2.1, RNA extraction is described in section 2.4, cDNA synthesis in section 2.5 and RT-qPCR assays are described in section 2.6 (Chapter 2). Primer details are described in Table 2.3 (Chapter 2).

5.2.1 Study design

Five commonly used reference genes in ovine RT-qPCR normalisation studies were selected from the literature, including *ACTB* (Hughes et al. 2011; Davenport et al. 2014)*, GAPDH* (Hughes et al. 2011)*, TUBA* (Taylor et al. 2008), *PPIA* (Lloyd et al. 2012) and *18S rRNA* (Taylor

et al. 2008). Additional 5 genes, not previously tested in ovine interdigital skin, were selected from the ovine transcriptome including *TMEM79, ASCC2, C3ORF58, BHLHE40* and *DDX54*. The expression stability of all 10 candidate reference genes was compared using cDNA from a sample set of 10 healthy, 10 mild ID, 10 moderate/severe ID and 10 footrot samples (For ovine feet scoring system used in this study see table 2.1).

5.2.3 Analysis of reference gene stability and co-regulatory function

Analysis of reference gene stability was performed using RefFinder in order to compare and rank the tested candidate reference genes (Xie et al. 2012) (http://fulxie.0fees.us/?t ype=reference, accessed in September 2015). RefFinder also integrates a `comprehensive analysis', which integrates the results of geNorm, NormFinder, BestKeeper, and the Delta CT method in one overall analysis. Potential co-regulatory function of the 10 candidate reference genes was analysed using Ingenuity Pathway Analysis software (IPA, Qiagen Redwood City). Provided by the Advanced Data Analysis Centre (ADAC, University of Nottingham).

5.3 Results

5.3.1 mRNA expression levels of candidate reference genes

mRNA expression levels of *ACTB, GAPDH, TUBA*, *PPIA*, *18S rRNA*, *TMEM79, ASCC2, C3ORF58, BHLHE40* and *DDX54* were examined in

40 ovine interdigital skin biopsies by RT-qPCR. PCR products from all primer pairs were confirmed by sequencing. All targets showed amplification efficiencies within the ranges of an optimised RT-qPCR assay (90%-105%, Bustin et al. 2010), except for *TUBA* (122%). Slope values obtained from the standard curves ranged from -3.250 to -3.586 and the coefficient of correlation values (R^2) ranged from 0.865-0.998 (Table 5.2). No template controls did not show any amplification and melt curves showed single peaks of amplification. Overall, the mean of quantification cycle values for all genes were similar among healthy, mild ID, moderate/severe ID and footrot samples.

Table 5.2 Standard curve data of RT-qPCR assays for reference genes.

Gene	Cq values range	Slope	R^2	Efficiency	Melt curve peaks
18S rRNA	11 - 13	-3.423	0.998	96%	Single
ACTB	22- 29	-3.563	0.997	91%	Single
TUBA	31 - 37	-4.45	0.865	122%	Single
PPIA	23 - 49	-3.586	0.961	90%	Single
GAPDH	20 - 34	-3.464	0.870	94%	Single
TMEM79	27 - 30	-3.413	0.963	96%	Single
ASCC2	30 - 35	-3.466	0.985	94%	Single
C3ORF58	30 - 32	-3.250	0.953	103%	Single
BHLHE40	27 - 30	-3.559	0.998	91%	Single
DDX54	29 - 32	-3.410	0.997	96%	Single

ACTB: *β-Actin*; *PPIA*: *cyclophilin*; *18S rRNA*: *eucariotic 18S ribossomal RNA*; *TUBA*: *α-tubulin*; *GAPDH*: *Glyceraldehyde-3-Phosphate Dehydrogenase*; *TMEM79*: Transmembrane protein 79; *ASCC2: Activating signal cointegrator 1 complex subunit 2*; *C3ORF58*: *chromosome 3 open reading frame 58*; *BHLHE40: basic helix-loop-helix family, member e40*; *DDX54: DEAD (Asp-Glu-Ala-Asp) box polypeptide 54*. Cq= quantification cycles. Slope/Efficiency: Ideally the efficiency (E) of a PCR should be 100%, meaning that for each cycle the amount of product doubles (E=2). The efficiency was calculated from the slope of the standard curve according to the following formula:
$E = 10(-1/slope)-1$. R^2 is the coefficient of correlation obtained from the standard curve and should ideally be >0.99.

5.3.2 Expression stability analysis

The expression data of 10 candidate reference genes were analysed using RefFinder software in order to rank the gene expression stability and to identify the most stable genes in the ovine interdigital skin in accordance with the MIQE guidelines (Bustin et al. 2010). According to RefFinder Comprehensive analysis, *ACTB, DDX54* and *PPIA* were the most stable reference genes and *TUBA*, *18S rRNA* and *GAPDH* were ranked as the least stable (Table 5.3 and Figure 5.1). The four algorithms incorporated by RefFinder showed slightly different gene ranking orders individually; however, *ACTB, DDX54* and *PPIA* were ranked as the three most stable genes in all algorithms, while *DDX54* was a novel candidate gene. Among the different software applications incorporated in RefFinder, BestKeeper showed a distinctly different gene ranking stability, except for the first three most stable genes (Table 5.3).

This study included samples from four different clinical disease conditions status such as healthy, mild ID, moderate/severe ID and footrot. Considering that NormFinder identifies the best genes with minimal inter- and intragroup expression variation, while other algorithms tend not to take into account group variation, we also performed the Comprehensive analysis for each clinical condition individually (Figure 5.2). No major differences between the different clinical conditions were observed. The top ranked genes for the entire set of samples, *ACTB, PPIA* and *DDX54,* were also classified as the

most suitable genes when investigating healthy, mild ID, moderate/severe ID and footrot samples separately.

Table 5.3 Gene expression stability analysis using RefFinder software of 10 candidate reference genes for normalisation of RT-qPCR studies of the ovine interdigital skin.

geNorm		**NormFinder**		**BestKeeper**		**Delta CT**		**Comprehensive analysis**	
Gene	Stability value	Gene	Stability value	Gene	Stability value	Gene	Stability value	Gene	Stability value
ACTB	0.348	*DDX54*	0.323	*ACTB*	0.514	*DDX54*	1.374	*ACTB*	1.414
PPIA	0.348	*ACTB*	0.365	*PPIA*	0.534	*ACTB*	1.396	*DDX54*	1.732
DDX54	0.582	*PPIA*	0.428	*DDX54*	0.565	*PPIA*	1.413	*PPIA*	2.06
C3ORF58	0.717	*C3ORF58*	0.56	*TMEM79*	0.706	*C3ORF58*	1.488	*C3ORF58*	4.427
ASCC2	0.848	*ASCC2*	0.857	*18S rRNA*	0.723	*ASCC2*	1.627	*ASCC2*	5.623
BHLHLE40	0.995	*BHLHLE40*	1.278	*C3ORF58*	0.727	*BHLHLE40*	1.813	*BHLHLE40*	6.236
TUBA	1.16	*TUBA*	1.499	*BHLHLE40*	0.76	*TUBA*	1.993	*TMEM79*	7.348
GAPDH	1.301	*GAPDH*	1.518	*ASCC2*	0.91	*GAPDH*	2.022	*TUBA*	7.454
TMEM79	1.629	*TMEM79*	2.621	*TUBA*	0.967	*TMEM79*	2.884	*18S rRNA*	8.409
18S rRNA	1.899	*18S rRNA*	2.712	*GAPDH*	1.584	*18S rRNA*	2.978	*GAPDH*	8.459

ACTB: *β-Actin*; *PPIA*: *cyclophilin*; *18S rRNA*: *eucariotic 18S ribossomal RNA*; *TUBA*: *α-tubulin*; *GAPDH*: *Glyceraldehyde-3-Phosphate Dehydrogenase*; *TMEM79: Transmembrane protein 79*; *ASCC2: Activating signal cointegrator 1 complex subunit 2*; *C3ORF58*: *chromosome 3 open reading frame 58*; *BHLHE40: basic helix-loop-helix family, member e40*; *DDX54: DEAD (Asp-Glu-Ala-Asp) box polypeptide 54*. Samples from all clinical conditions were included in this analysis (n=40). Low stability values in the table represents high gene expression stability.

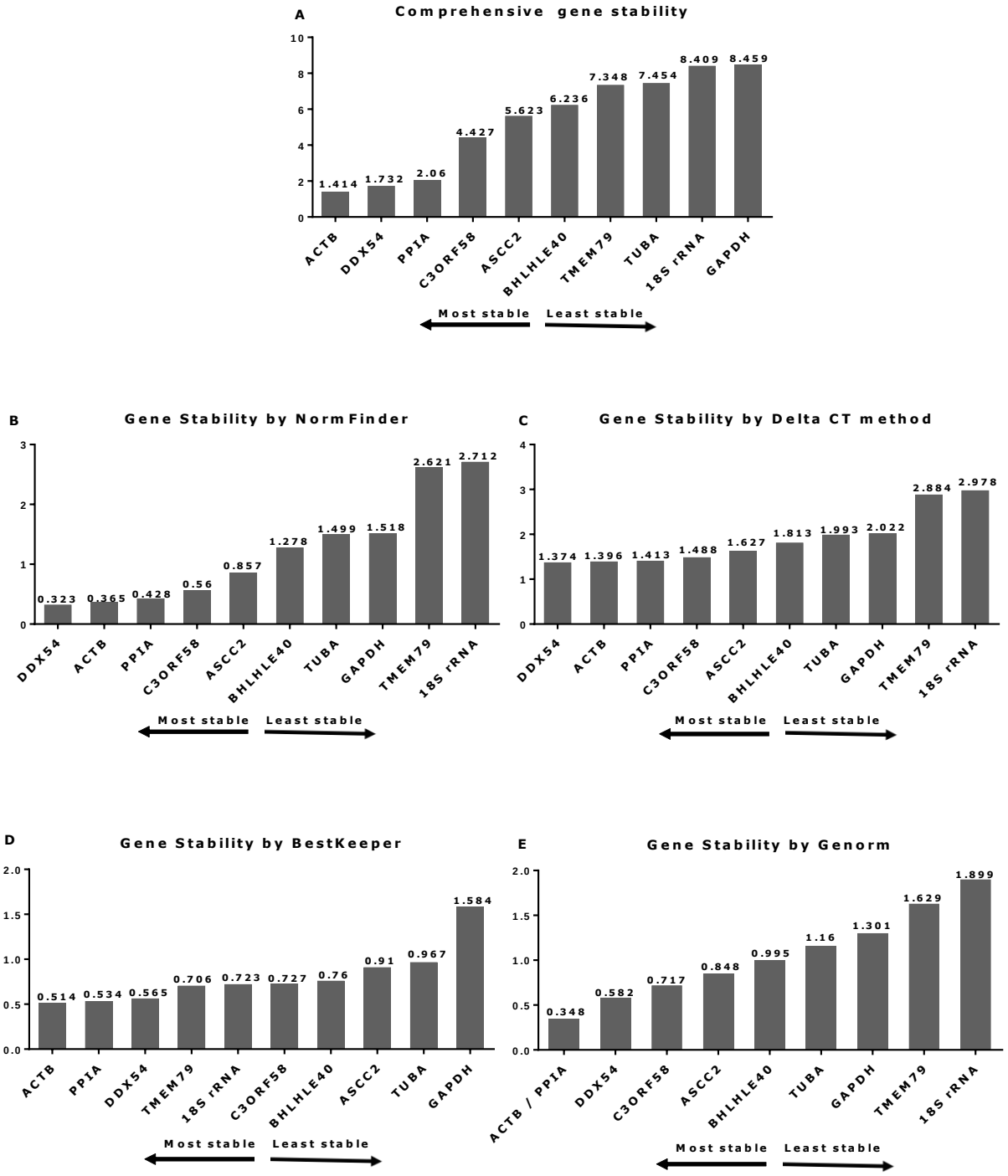


Figure 5.1 Gene expression stability analysis using RefFinder software. All samples from all clinical conditions were included in this analysis (n=40). Comprehensive analysis (A); Gene stability analysis by NormFinder (B); Gene stability analysis by Delta CT method (C); Gene stability analysis by BestKeeper (D); Gene stability analysis by geNorm (E). *ACTB*: *β-Actin*; *PPIA*: *cyclophilin*; *18S rRNA*: *eukaryotic 18S ribosomal RNA*; *TUBB*: *α-tubulin*; *GAPDH*: *Glyceraldehyde-3-Phosphate Dehydrogenase*; *TMEM: Transmembrane protein 79*; *ASCC2: Activating signal cointegrator 1 complex subunit 2*; *C3ORF58*: *chromosome 3 open reading frame 58*; *BHLHE40: basic helix-loop-helix family member e40*; *DDX54: DEAD (Asp-Glu-Ala-Asp) box polypeptide 54*.

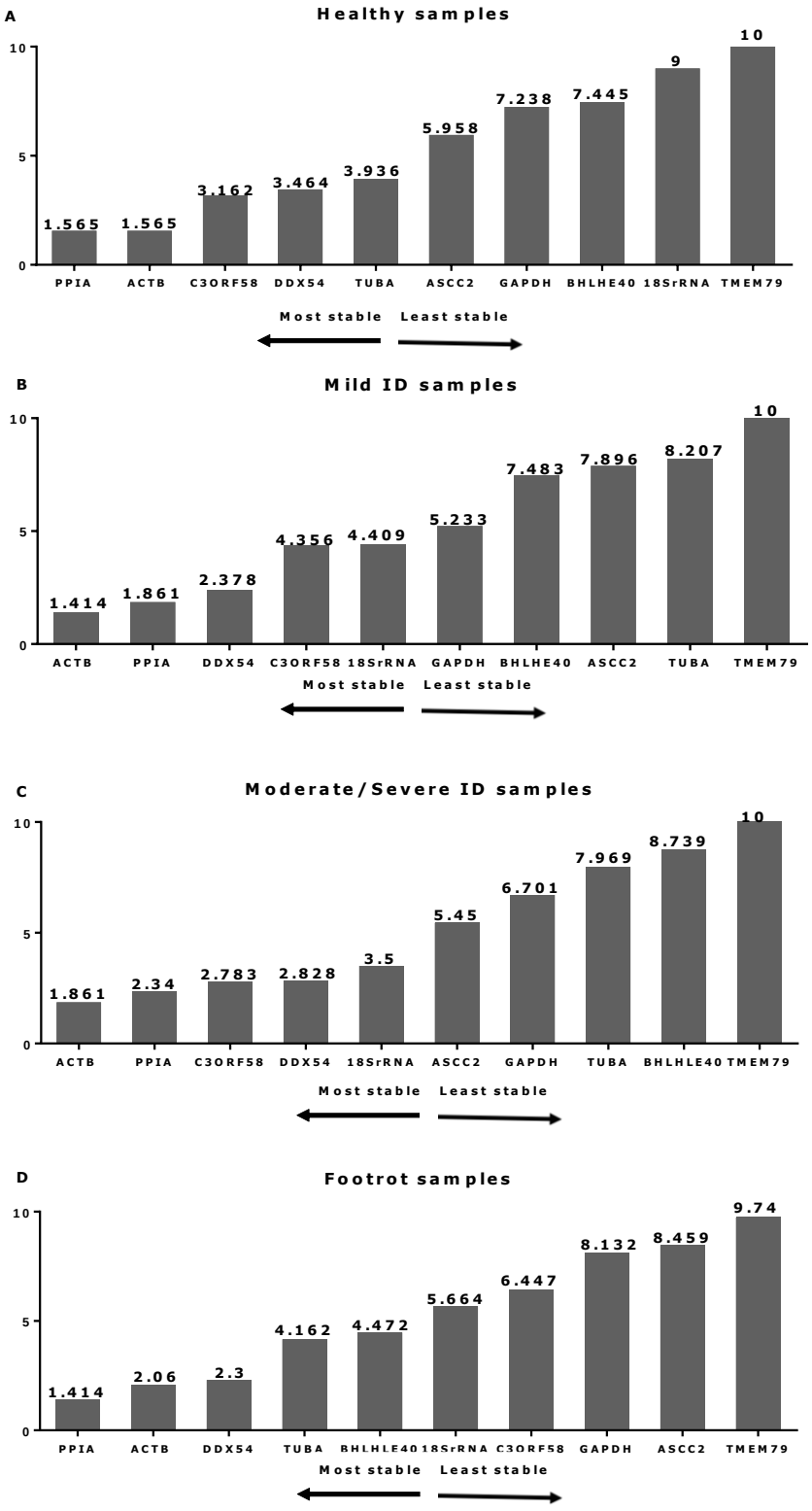


Figure 5.2 Intergroup variation of gene expression using comprehensive analysis of RefFinder software. Each group represents different clinical conditions of the ovine interdigital skin and contained 10 samples. *ACTB*: *β-Actin*; *PPIA*: *cyclophilin*; *18S rRNA*: *eucariotic 18S ribossomal RNA*; *TUBA*: *α-tubulin*; *GAPDH*: *Glyceraldehyde-3-Phosphate Dehydrogenase*; *TMEM79: Transmembrane protein 79*; *ASCC2: Activating signal cointegrator 1 complex subunit 2*; *C3ORF58*: *chromosome 3 open reading frame 58*; *BHLHE40: basic helix-loop-helix family, member e40*; *DDX54: DEAD (Asp-Glu-Ala-Asp) box polypeptide 54*.

5.3.3 Co-regulation of candidate reference genes

Gene expression stability analysis is based on the assumption that the tested genes belong to different functional classes and are not co-regulated through common upstream regulators (Vandesompele et al. 2002; Andersen et al. 2004). Hence, we investigated whether the candidate genes are likely to be independent using IPA. This analysis revealed that *TUBA*, *ACTB* and *GAPDH* share some upstream regulators, as do *DDX54* and *C3orf58*. In contrast, no direct co-regulator was known between *ACTB*, *DDX54* and *PPIA*, which were identified as the most reliably stable genes by RefFinder Comprehensive analysis (Figure 5.3).

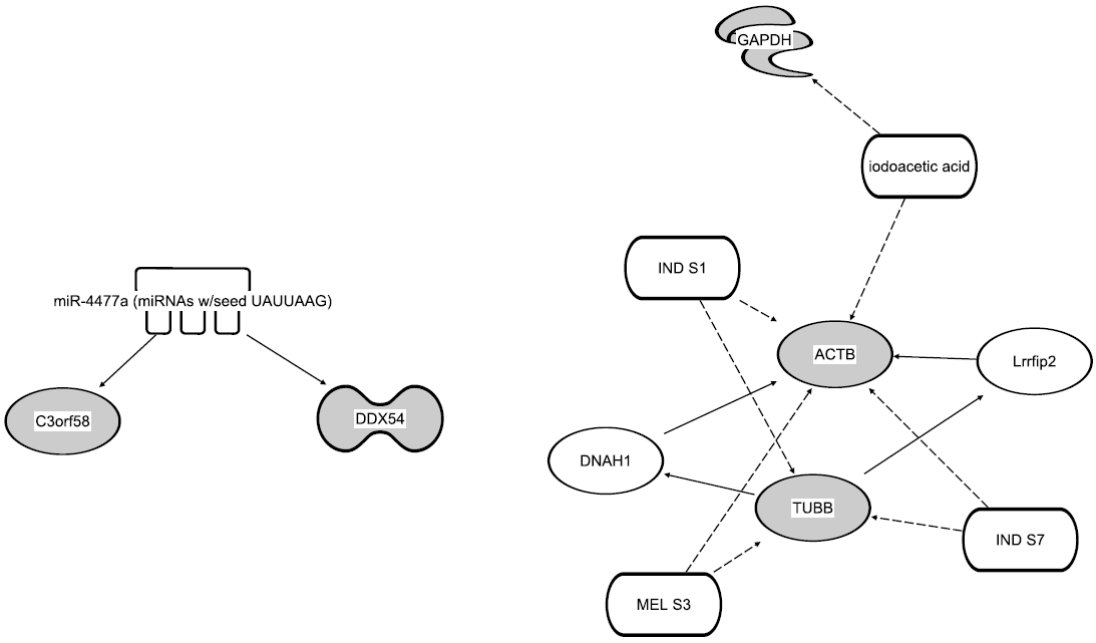


Figure 5.3 Co-expression analysis for ten candidate reference genes performed with Ingenuity Pathway Analysis (IPA). Analysis included all 10 candidate reference genes. Only *TUBB*, *ACTB* and *GAPDH* share common upstream regulators. *ACTB: β-Actin*; *TUBB*: *α-tubulin*; *GAPDH*: *Glyceraldehyde-3-Phosphate Dehydrogenase*; *C3ORF58*: *chromosome 3 open reading frame 58*; *DDX54: DEAD (Asp-Glu-Ala-Asp) box polypeptide 54*.

5.4 Discussion

This study investigated the stability of 10 candidate reference genes for normalization of RT-qPCR data of ovine interdigital skin samples in accordance with MIQE guidelines (Bustin et al. 2010). Once candidate reference genes were screened for mRNA expression levels using RT-qPCR, the expression stability among healthy, ID and footrot samples was further analysed using RefFinder software. *ACTB*, *DDX54* and *PPIA* were ranked as the most stable reference genes among the different clinical conditions, suggesting the best choice of reference genes. Using other types of ovine cells and tissues, similar ranking positions to our study include *ACTB* and *PPIA* as the most suitable candidates for sheep PBMC samples (Puech et al. 2015) and for pulmonary artery (Passmore et al. 2009).

Importance of selecting reference genes for a particular type of samples

As the role of immune response in footrot pathogenesis remains unclear, further gene expression analysis may be vital in our understanding of the disease. The validation of reference genes for normalisation of gene expression studies was little explored in the context of footrot. The two studies available in the literature investigated the stability of traditional reference genes in interdigital skin biopsies (Davenport et al. 2014) and in circulating neutrophils from footrot affected sheep (Vorachek et al. 2013). Davenport et al. (2014) reported altered immune molecules gene expression in footrot samples normalized to *ACTB*, which was ranked as the most stable reference gene by geNorm among other 5 candidate

genes (*TUBA*, *18S rRNA*, *GAPDH*, *PPIA* and *B2M*). The present research was an extension of the Davenport et al. (2014) study, therefore confirming the stability of *ACTB* in a wider range of samples and higher number of candidate genes. In contrast, the study on circulating neutrophils from footrot affected sheep found *ACTB* as unstable and *GAPDH* as the most stable gene (Vorachek et al. 2013). These divergent results might be associated with differences in sample origin and types, i.e. skin biopsies vs. circulating neutrophils. In the present study, *GAPDH, 18S rRNA* and *TUBA* presented low expression stability. This contrasts with other studies in sheep, which reported these genes as stable using different sample types. For instance, *GAPDH* was reported to be a suitable reference gene for ovine PBMC samples and efferent leucocytes (Peletto et al. 2011; Mahakapuge et al. 2016), *18S rRNA* for ovine fetal liver (Xu et al. 2015) and *TUBA* for ovine oocytes (O'Connor et al. 2013) (Table 5.1). Taken together, these results suggest that if some of the previously reported studies were to be used as a source of reference genes for ovine interdigital skin, our RT-qPCR data could have been negatively affected; hence it highlights the importance of selecting reference genes for particular type of samples using the specific experiment in question as suggested by Bustin et al. (2010).

Gene expression stability analysis by different algorithms

MIQE guidelines recommend at least one algorithm to verify gene expression stability and therefore identify suitable reference genes (Bustin et al. 2010). Different algorithms based on distinct methods

have been developed; the most popular are geNorm, NormFinder, BestKeeper and Comparative Delta CT method (Vandesompele et al. 2002; Andersen et al. 2004; Pfaffl et al. 2004; Silver et al. 2006). geNorm provides a measure of gene expression stability by calculating the mean pairwise variation of each reference gene from all the other reference genes (Vandesompele et al. 2002). In contrast, NormFinder identifies the best stable combination of reference genes ranking a set of genes according to their expression stability measure (Andersen et al. 2004). The Delta CT method assesses gene expression stability by calculating pair-wide differences of CT values, and the BestKeeper program analyses the stability of a candidate reference gene based on the standard deviation (SD) of the Ct values (Pfaffl et al. 2004). It is presumed that a comparison of different algorithms allows for better evaluation of the most suitable reference genes (Tong et al. 2009). Hence, to comprehensively investigate the stability of 10 candidate reference genes, we employed RefFinder, which integrates all those algorithms in the same computational program (Xie et al. 2012). Moreover, RefFinder analysed the results obtained from all algorithms in one overall Comprehensive analysis based on the rankings obtained from each algorithm. For this analysis, RefFinder assigns an appropriate weight to an individual gene, and calculates the geometric mean of these weights, in order to obtain an overall final ranking (Xie et al. 2012; Jiang et al. 2015). While all algorithms agreed on the three most stable expressed genes, *ACTB, DDX54* and *PPIA,* differences were observed regarding ranking positions shown by the different algorithms, especially BestKeeper, which showed the most different gene ranking position

among all algorithms (Figure 5.1, D). Considering that each statistical algorithm applies distinct methods to verify the gene expression stability, these small differences in lower ranking positions can be expected.

Co-regulation analysis of the candidate reference genes

This study also investigated co-regulation among the candidate reference genes, which confirmed that the top ranked genes, *ACTB*, *PPIA* and *DDX54*, do not share common upstream regulators. The co-regulation study was performed because gene expression stability analysis is based on the assumption that the tested genes belong to different functional classes and are not co-regulated through common upstream regulators (Vandesompele et al. 2002; Andersen et al. 2004). For instance, geNorm ranks genes according to the similarity of their expression profiles across the entire sample set (Vandesompele et al. 2002), thus genes sharing common classes will tend to display similar expression profiles, and then be the top ranked genes (Andersen et al. 2004). In contrast, NormFinder identifies the best genes with minimal inter- and intragroup expression variation, and hence it is assumed to be less sensitive to co-regulation of candidate reference genes (Andersen et al. 2004).

Despite the fact that *ACTB* and *PPIA* are commonly used reference genes and were indicated as the most stable genes by all algorithms, most of the novel candidate reference genes selected in the current study

showed a better performance than the traditional reference genes, *GAPDH, TUBA* and *18S rRNA*. Similarly, recent research in human ovary, rice and soybean samples showed that some novel, non-traditional, candidate reference genes showed more stable expression than traditional reference genes (Scarlet et al. 2015; Xu et al. 2015). This suggests it is important to investigate the stability of new reference genes and not be focused only on those that have been traditionally used to normalise data of the cell/tissue of interest.

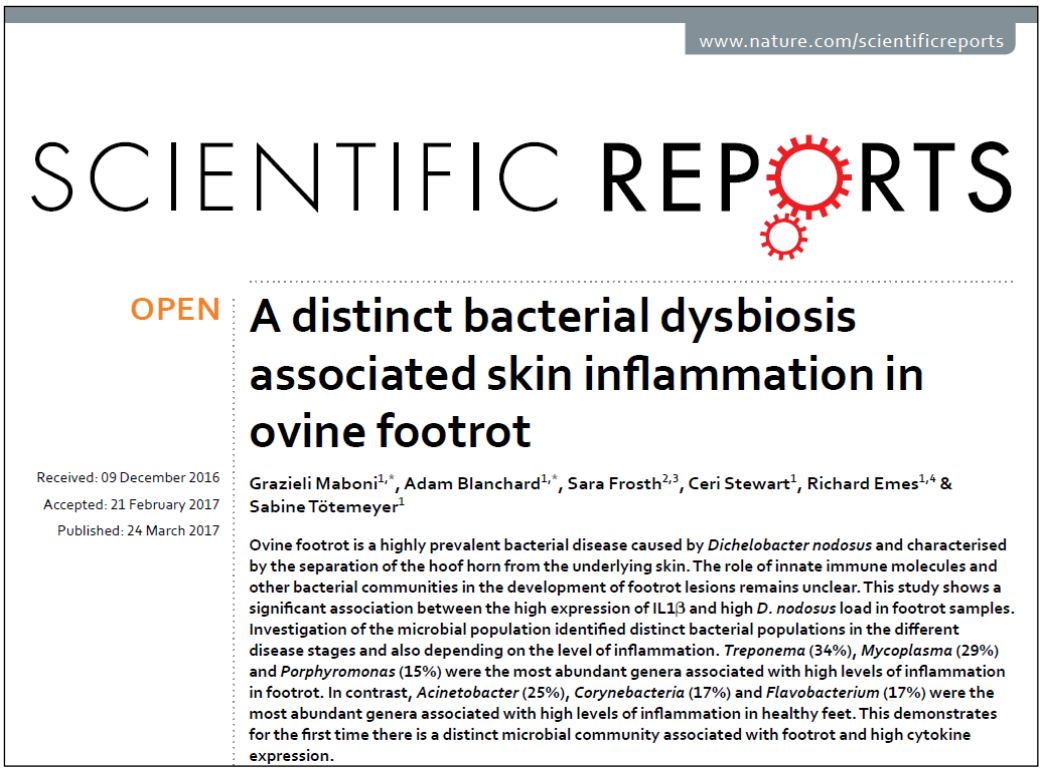
5.5 Conclusions

According to RefFinder Comprehensive analysis, *ACTB*, *PPIA* and *DDX54* were the most stable genes in ovine interdigital skin samples from healthy, ID and footrot cases. The consistency of the results obtained from all algorithms and the lack of common upstream co-regulators for *ACTB, DDX54* and *PPIA*, clearly demonstrated their robustness as candidate reference genes. In contrast, mRNA expression levels of *GAPDH, TUBA* and *18S rRNA* were not stable, suggesting they are not suitable reference genes for normalisation of RT-qPCR data on ovine interdigital skin. The present findings will facilitate the correct interpretation of RT-qPCR data in further studies that explore the molecular mechanisms related to ovine interdigital infections.

Chapter 6

6. Expression of TLRs and pro-inflammatory cytokines in the ovine interdigital skin

This chapter is an extension of the data on mRNA expression of cytokines and TLRs previously described and published in a paper format `A distinct bacterial dysbiosis associated skin inflammation in ovine footrot'. DOI: 10.1038/srep45220 (Appendix 2).



www.nature.com/scientificreports

SCIENTIFIC REPORTS

OPEN

Received: 09 December 2016
Accepted: 21 February 2017
Published: 24 March 2017

A distinct bacterial dysbiosis associated skin inflammation in ovine footrot

Grazieli Maboni[1,*], Adam Blanchard[1,*], Sara Frosth[2,3], Ceri Stewart[1], Richard Emes[1,4] & Sabine Tötemeyer[1]

Ovine footrot is a highly prevalent bacterial disease caused by *Dichelobacter nodosus* and characterised by the separation of the hoof horn from the underlying skin. The role of innate immune molecules and other bacterial communities in the development of footrot lesions remains unclear. This study shows a significant association between the high expression of IL1β and high *D. nodosus* load in footrot samples. Investigation of the microbial population identified distinct bacterial populations in the different disease stages and also depending on the level of inflammation. *Treponema* (34%), *Mycoplasma* (29%) and *Porphyromonas* (15%) were the most abundant genera associated with high levels of inflammation in footrot. In contrast, *Acinetobacter* (25%), *Corynebacteria* (17%) and *Flavobacterium* (17%) were the most abundant genera associated with high levels of inflammation in healthy feet. This demonstrates for the first time there is a distinct microbial community associated with footrot and high cytokine expression.

6.1 Introduction

Research on footrot has been focused on bacterial colonisation targeting mainly *D. nodosus* and *F. necrophorum* in an attempt to understand virulence mechanisms and, thus, the disease progression. An initial report on the inflammatory response to footrot hypothesised that the intense skin inflammatory response played an important role in the exacerbation of the lesions being responsible for the sloughing of necrotic tissues (Egerton et al. 1969). Further investigations has not been performed and little is known about the ovine inflammatory response to footrot, which may also play a fundamental role in the disease process.

Several pro-inflammatory cytokines and chemokines are expressed in the skin including *IL6*, *CXCL8*, *IL1β* (Lai & Gallo 2008) and *IL17* (Jin & Dong 2013). IL1β has a range of stimulatory effects on immune cells playing a key role in the innate immunity of the skin (Arend et al., 2008). Similarly, IL6 is involved in key immune processes such as monocyte and T-cell recruitment, survival and differentiation (Scheller et al. 2011). IL17 leads to the release of pro-inflammatory cytokines and immune cell recruitment (Jin & Dong 2013). CXCL8 is a classical chemokine involved in the recruitment of neutrophils and proliferation of keratinocytes (Seow et al. 1994, Tuschil et al. 1992). In the ovine interdigital skin, the mRNA expression of *TLR2*, *TLR4* and *IL1β* was found to be significantly elevated in severe ID and footrot, suggesting they may play a role in the recognition and response to

the bacteria involved in footrot development (Davenport et al. 2014). Other studies so far have been focused on the investigation of the systemic ovine inflammatory response to footrot in the context of vaccination and experimental infection with *D. nodosus* (Roberts & Egerton 1969; Bhardwaj et al. 2014; Raadsma et al. 1994; Schwartzkoff et al., 1993). Following experimental infection with *D. nodosus* and vaccination no changes in *TLR4* mRNA expression in peripheral blood leukocytes was observed. In contrast, *TLR2* mRNA expression levels increased in peripheral blood in leukocyte responses to both infection and vaccination (Bhardwaj, 2012).

In this context, it was hypothesised that the pathology of footrot is a host mediated expression of local immune responses. In association with bacterial colonisation, it leads to severe inflammation that can progress to underrunning footrot. Moreover, in addition to IL1β, we also postulated that commonly expressed pro-inflammatory cytokines in the skin such as IL6, CXCL8, and IL17 may be expressed in the ovine interdigital skin and be involved in the inflammatory mechanisms of footrot. Hence, this study aimed to investigate whether clinical conditions (healthy, ID and footrot) and the sheep foot conformation/integrity have an impact on the mRNA expression of specific genes of interest, such as *TLR2*, *TLR4*, *IL1β*, *IL6*, *CXCL8* and *IL17.* Moreover, this study also aimed to investigate whether high virulent *D. nodosus* load are associated with high levels of *IL1β* expression in the ovine interdigital skin.

6.2 Materials and methods

Collection of biopsies from the ovine interdigital skin is described in section 2.1, RNA extraction in section 2.4, cDNA synthesis in section 2.5, RT-qPCR assays and normalisation targeting *TLR2*, *TLR4*, *IL1β*, *IL6*, *CXCL8*, *IL17* are described in sections 2.6 and 2.7 and quantification of virulent *D. nodosus* by qPCR in section 2.3 (Chapter 2).

6.2.1 Statistical analysis

Interquartile ranges (IQR) was determined using Excel (Version 14.0.7166.5, Westerville, USA) in order to classify samples in a range between the 25th and 75th percentiles according to their relative mRNA expression of *IL1β*, *IL6*, *CXCL8* and *IL17*. Kruskal-Wallis test (Mann Whitney test) was performed to verify the association between low and high virulent *D. nodosus* load (pg DNA/100µg of total DNA) and low and high expression of *IL1β*, *IL6*, *CXCL8* and *IL17* (quartiles). Kruskal-Wallis test (Dunn`s multiple comparison test) was used to verify the association between TLRs and cytokines mRNA expression with clinical conditions and foot integrity scores. Pearson correlation coefficient was used to investigate the correlation between virulent *D. nodosus* (pg DNA/100µg of total DNA) and mRNA expression of *IL1β*, *IL6*, *CXCL8* and *IL17*. All analyses were performed using GraphPad Prism (Version 6.0, La Jolla, USA) and a P-value ≤0.05 was considered significant.

6.3 Results

6.3.1 mRNA expression of cytokines in the ovine interdigital skin

To investigate the host immune response to interdigital dermatitis and footrot, the mRNA expression levels of *TLR2*, *TLR4*, *IL1β*, *IL6*, *CXCL8* and *IL17* were analysed in 53 visually healthy, 30 mild ID, 25 moderate/severe ID and 83 footrot samples. PCR products from all primer pairs were confirmed by sequencing. All targets showed amplification efficiencies within the ranges of an optimised RT-qPCR assay (90%-105%, Bustin et al. 2010). Slope values obtained from the standard curves ranged from -3.282 to -3.489 and the coefficient of correlation values (R^2) ranged from 0.709-0.998. Non-template controls did not show any amplification and melt curves showed single peaks of amplification (Table 6.1).

Table 6.1 Standard curve data for RT-qPCR assays.

Gene	Cq values range	Slope	R^2	Efficiency	Melt curve peaks
TLR2	23-33	-3.282	0.939	101.6%	Single
TLR4	25-36	-3.422	0.943	96%	Single
IL1β	23-37	-3.482	0.963	93.7%	Single
IL6	26-38	-3.321	0.709	100%	Single
CXCL8	26-32	-3.489	0.998	93.5%	Single
IL17	25-34	-3.460	0.905	94.5%	Single

Cq= quantification cycles. Slope/Efficiency: Ideally the efficiency (E) of a PCR should be 100%, meaning that for each cycle the amount of product doubles (E=2). The efficiency was calculated from the slope of the standard curve according to the following formula: E = 10(-1/slope)-1. R^2 is the coefficient of correlation obtained from the standard curve and should ideally be >0.99.

mRNA expression of all targets was detected in the ovine interdigital skin samples. Healthy samples showed a wide and marked inflammatory background. No differential gene expression of any inflammatory mediator in the context of clinical conditions was identified in healthy samples (Figure 6.1). In this context, we investigated whether foot conformation could be a non-infectious factor that affects the expression levels of cytokines in the ovine interdigital skin considering that foot integrity might indicate underlying damage or disease. All ovine foot samples were classified according to an integrity score on a 0-3 scale, independent of diseases status (Table 2.1, Chapter 2). There was a slightly, but not significantly increased expression of *IL1β*, *IL6* and *CXCL8* in samples from feet with conformation scores two and three (Figure 6.2 C-F). The expression levels of *TLR2* and *TLR4* were very similar across the different foot conformation scores (Figure 6.2 A, B).

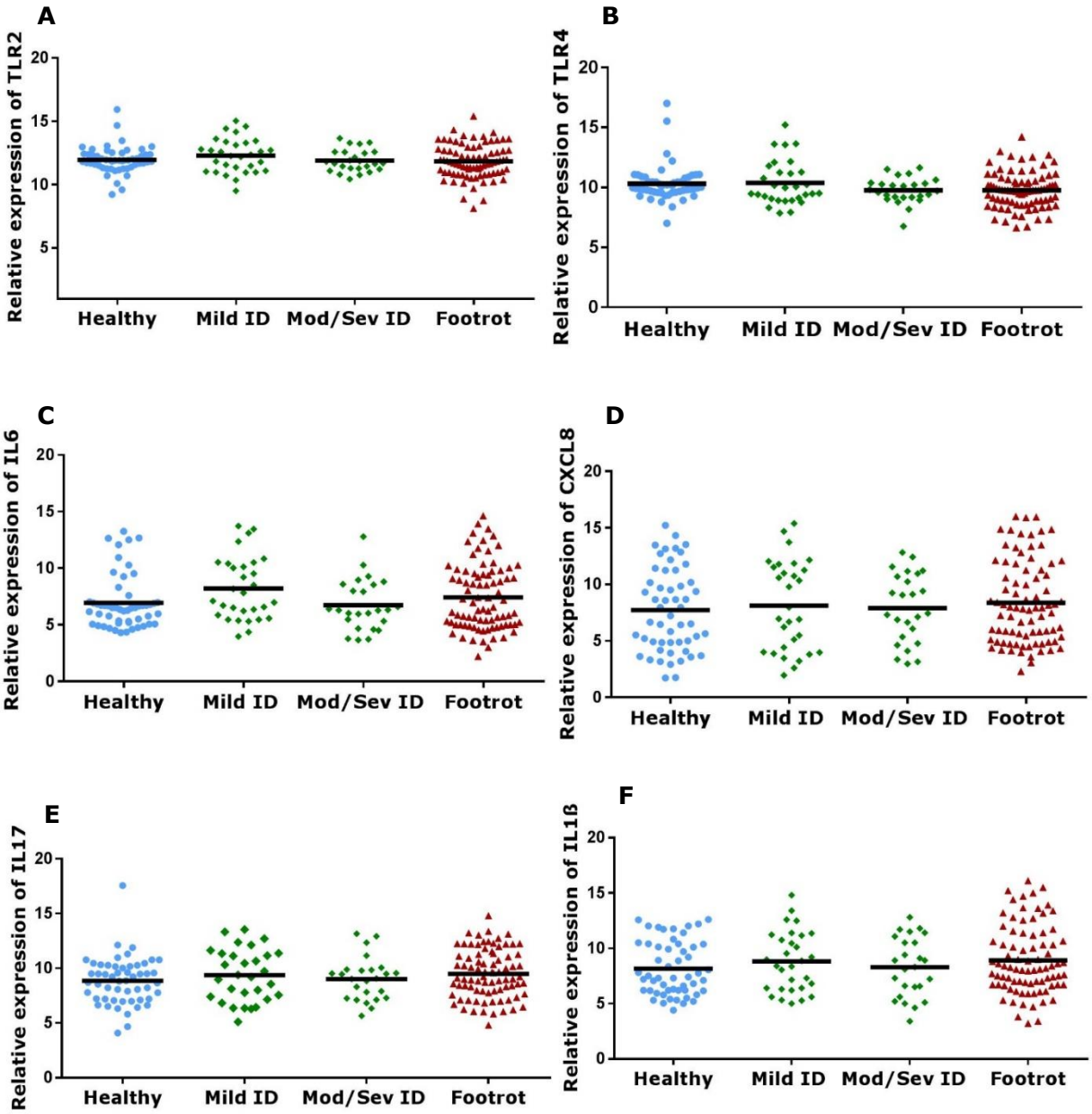


Figure 6.1 Similar mRNA expression levels of *TLR2* (A), *TLR4* (B), *IL16* (C), *IL8* (D), *IL17* (E) and *IL1β* (F) across the different clinical conditions of biopsies from the ovine interdigital skin. Mean is represented by black bars. Each circle represents a single biopsy. Healthy n=53, mild interdigital dermatitis (ID)=30, moderate/severe ID=25, footrot=83. Data were analysed by Dunn's multiple comparisons test. Analyses were performed using GraphPad Prism.

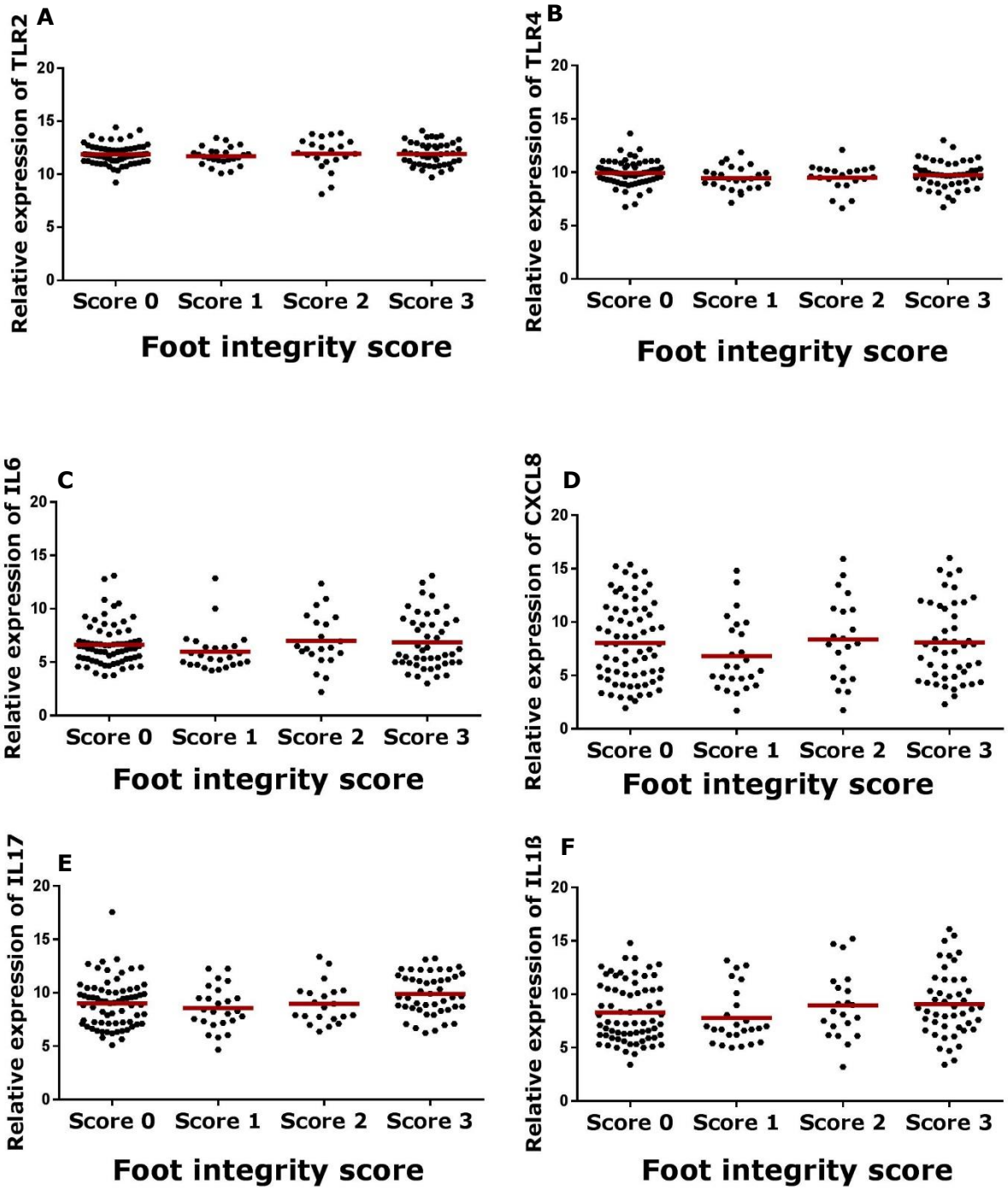


Figure 6.2 mRNA expression levels of *TLR2* (A), *TLR4* (B), *IL6* (C), *IL8* (D), *IL17* (E) and *IL1β* (F) across the different ovine foot conformation/integrity scores. Ovine foot scoring system conformation of the sole and heel/wall of each digit: 0= undamaged sole and heel area with a perfect shape. 1= mildly damaged/misshapen sole and/or heel area of the digit (<25%). 2= moderately damaged/misshapen sole and/or heel area of the digit (>25% and <75%). 3= severely damaged/misshapen sole and/or heel area of the digit (>75%). Mean is represented by red bars. Data were analysed by Dunn's multiple comparisons test. Analyses were performed using GraphPad Prism.

6.3.2 Association of the host immune response and virulent *D. nodosus* colonisation

We also investigated whether the load of the causative bacterium of underrunning footrot, virulent *D. nodosus*, is associated with differential expression of inflammatory markers. Low but significant correlations of virulent *D. nodosus* load and cytokine mRNA expression were identified for *IL1ß* (P=0.039) and *CXCL8* (P=0.046) in samples from footrot affected feet (Figure 6.3 E, F). No significant correlations were found for *D. nodosus* and *IL1ß* and *CXCL8* in healthy samples (Figure 6.3 A, B), as well as for IL6 and IL17 in healthy and footrot samples (Figure 6.3 C, D, G, H). To further investigate the association between mRNA expression of cytokines and *D. nodosus* load, healthy and footrot samples with *IL1β*, *IL6*, *CXCL8* and *IL17* expression values within the 25th (low) and 75th (high) quartiles were selected to investigate the *D. nodosus* load (Figure 6.4 and 6.5 A, B, C and D). As ID can be considered an intermediate stage between healthy and footrot, and might not be associated with a marked inflammatory background, ID samples were not included in this analysis. While in healthy samples the *D. nodosus* load is similar in the low and high inflammation groups (Figure 6.4 E, F, G, H), footrot samples with high levels of *IL1β* expressions also have significantly higher *D. nodosus* load (P=0.036) (Figure 6.5 E). However, footrot samples with high levels of *IL6*, *CXCL8* and *IL17* did not have significantly higher levels of *D. nodosus* (Figure 6.5 F, G, H). In summary, inflammation as marked by mRNA expression levels of

CXCL8 and *IL1β* are associated with virulent *D. nodosus* in footrot affected feet.

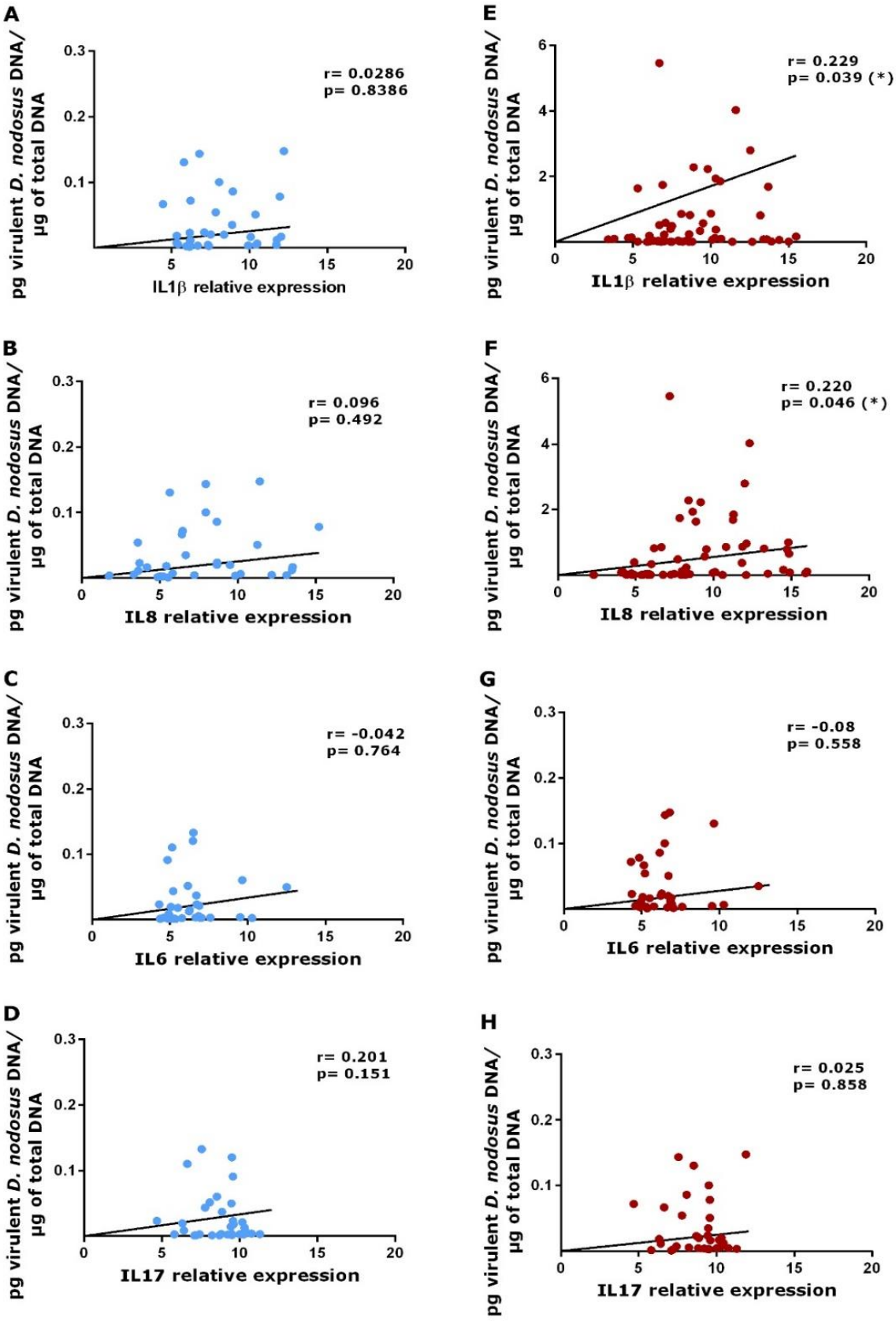


Figure 6.3 Correlation analysis between pro-inflammatory cytokines relative mRNA expression and virulent *D. nodosus* load. Analysis of healthy ovine interdigital skin samples between virulent *D. nodosus* load and *IL1β* (A), *CXCL8* (B), *IL6* (C) and *IL17* (D) (blue circles). Analysis of footrot samples between virulent *D. nodosus* and *IL1β* (E), *CXCL8* (F), *IL6* (G) and *IL17* (H) (red circles). r: Pearson's correlation coefficient. *P-value ≤0.05. Analyses were performed using GraphPad Prism.

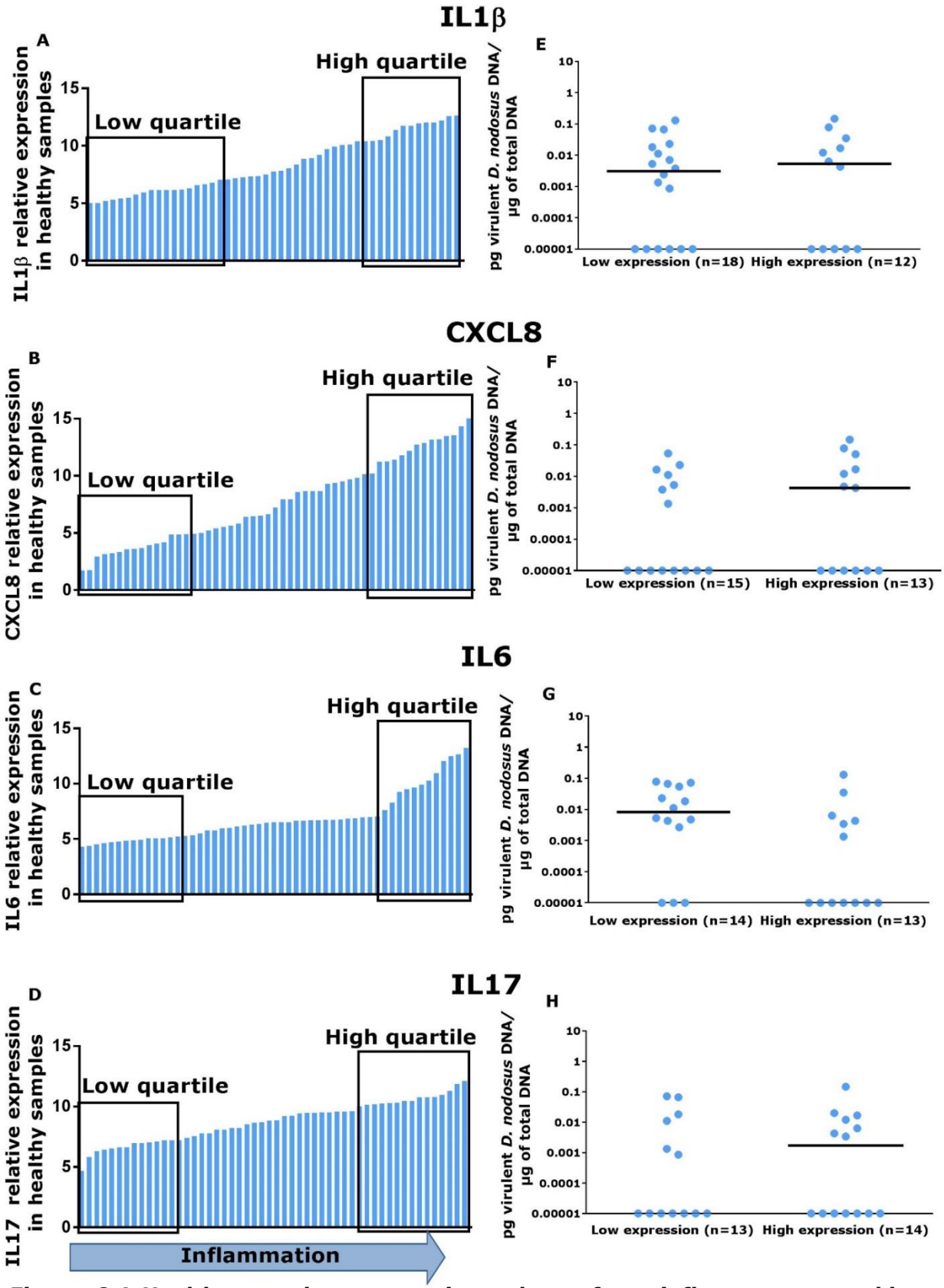


Figure 6.4 Healthy samples: expression values of pro-inflammatory cytokines associated with virulent *D. nodosus* load. Range of mRNA expression values of *IL1β* (A), *CXCL8* (B), *IL6* (C) and *IL17* (D); Black boxes highlight the expression values within the 25th (low) and 75th (high) quartiles. Association of low and high expression values of *IL1β* (E), *CXCL8* (F), *IL6* (C) and *IL17* (H) with virulent *D. nodosus* load. Data were analysed by Kruskal-Wallis test (Mann Whitney test) using GraphPad Prism.

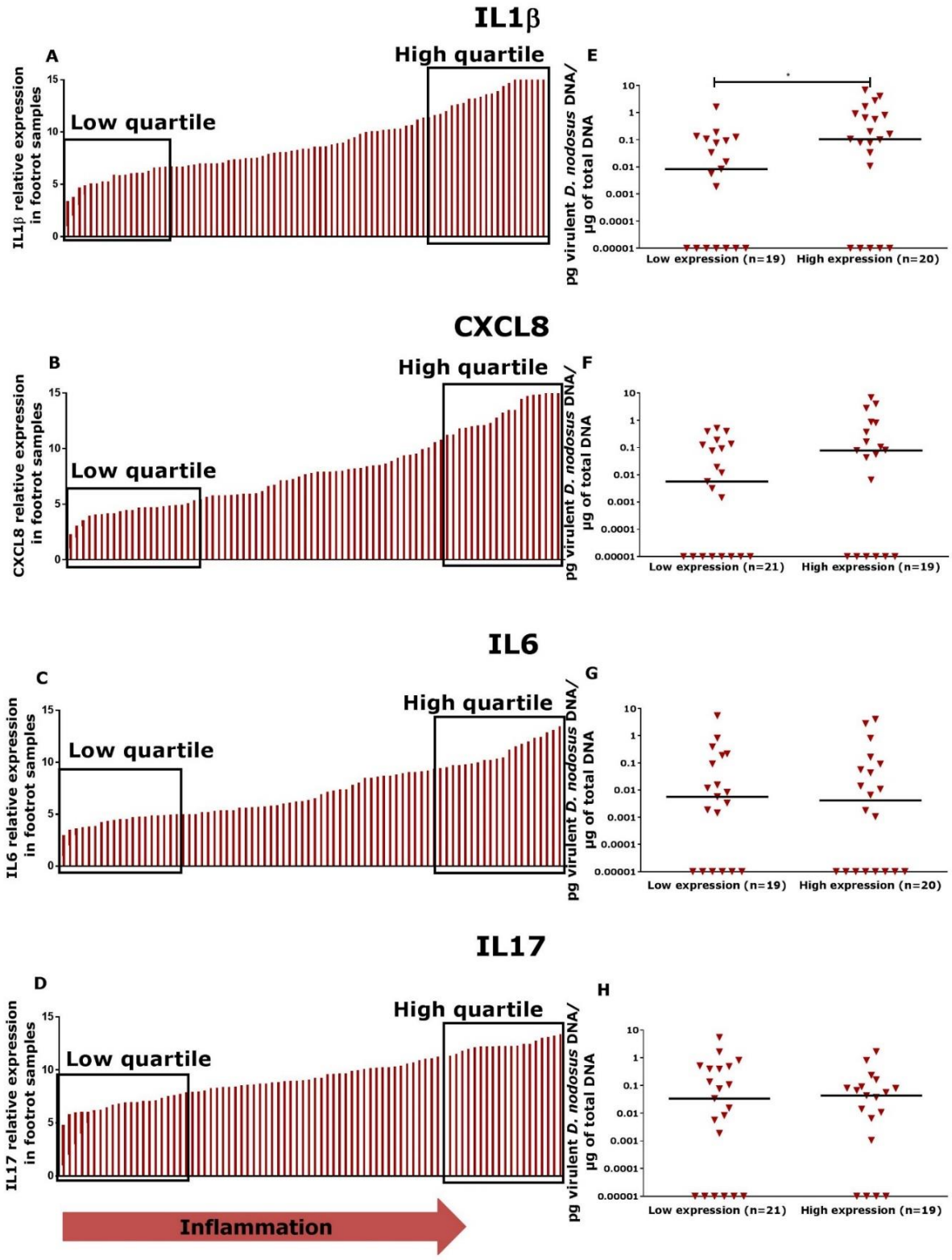


Figure 6.5 Footrot samples: expression values of pro-inflammatory cytokines associated with virulent *D. nodosus* load. Range of mRNA expression values of *IL1β* (A), *CXCL8* (B), *IL6* (C) and *IL17* (D); Black boxes highlight the expression values within the 25th (low) and 75th (high) quartiles. Association of low and high expression values of *IL1β* (E), *CXCL8* (F), *IL6* (C) and *IL17* (H) with virulent *D. nodosus* load. Data were analysed by Kruskal-Wallis test (Mann Whitney test) using GraphPad Prism. * P-value ≤0.05.

6.4 Discussion

This study investigated the mRNA expression of a panel of six genes in ovine interdigital skin biopsies in order to verify whether feet clinical condition, foot conformation or *D. nodosus* load are associated with expression levels of TLRs and pro-inflammatory cytokines known to play a role in skin bacterial infections. Feet clinical condition and non-infectious factors such as foot conformation seemed not to impact on the inflammatory response to footrot. In contrast, virulent *D. nodosus* load was associated with expression levels of pro-inflammatory cytokines.

Association of TLRs and cytokines expression and clinical disease conditions

The six inflammatory genes investigated in this study were previously reported to have a likely role in skin immune responses in sheep and cattle (Davenport et al. 2014; Refaai et al. 2013; Scholey et al. 2013). Surprisingly, in the context of foot disease, no differential expression of *TLR2*, *TLR4*, *IL1β*, IL6, CXCL8 and IL17 was identified in ID and footrot compared to healthy samples. Using a smaller sample set (n=28), our previous work has shown *IL1β* to be elevated in severe ID and footrot in relation to healthy samples (Davenport et al. 2014). These divergent results can be associated with a higher expression of *IL1β* in healthy samples found in this study than was observed by Davenport et al. (2014). Samples for the present study were collected between autumn and winter and it was noted that the weather had

been significantly wetter than when samples were collected for the previous study (Sabine Tötemeyer, personal communication). Wetter environmental conditions might impact on the basal levels of inflammation and may favour inflammation in the interdigital skin of apparently healthy samples. The wide inflammatory background seen in healthy samples might also be associated with the presence of subclinical disease that may have subsequently developed into ID and footrot in the next few days. However, using abattoir samples limits the investigation of the progression of the disease and thus verify whether healthy feet expressing high levels of pro-inflammatory cytokines would develop footrot lesions. These sheep might also have had footrot previously and the wide inflammatory response could be related to a healing process.

Association of TLRs and cytokines expression and foot conformation

Infectious as well as non-infectious factors might be associated with inflammatory responses in the skin. Particularly in the context of footrot, poor foot conformation could be a non-infectious factor leading to a higher expression of inflammatory genes indicating underlying damage and disease. Sheep with damaged sole and heel area have an increased susceptibility to become lame and consequently develop footrot (Kaler et al. 2010). In the present study, we showed that the effects of poor foot conformation were not directly associated with a higher inflammatory response, since slightly higher

but not significant mRNA expression levels of cytokines was present in feet with poor conformation.

Association of D. nodosus load and mRNA expression of cytokines

A significant association between samples with high expression of IL1β and high *D. nodosus* load in footrot samples as well as significant correlations between *CXCL8* and *IL1β* with *D. nodosus* in footrot samples, but not in healthy samples, further confirmed that *D. nodosus* infection could play a key role in the development of an inflammatory microenvironment characterised by those pro-inflammatory cytokines. It is important to highlight that based on these experiments, it is not possible to conclude whether *D. nodosus* triggers the expression of *CXCL8* and *IL1β* or if the inflammation in the skin facilitates the invasion of this bacterium. In our previous study, *IL1β* levels were elevated in ovine dermal fibroblasts stimulated with LPS or heat-killed extracts of *D. nodosus*, suggesting that both *IL1β* and fibroblasts play a key role in the host response to footrot (Davenport et al. 2014). *CXCL8* production is part of the initial immune response and plays a role in the recruitment of neutrophils, as well as having an effect on the proliferation of keratinocytes (Tuschil et al. 1992). Keratinocytes are key cells synthesising the potent pro-inflammatory cytokine *IL1β* (Mizutani et al. 1991). This may explain the thickened epidermal layer of ovine interdigital skin observed in histological studies of footrot (Egerton et al. 1969). Both cytokines, *CXCL8* and *IL1β*, were highly expressed in sheep with skin

pyogranulomas (Pepin et al. 1997), in response to inflamed foetal ovine skin (Zhang et al. 2012) and also in bovine digital dermatitis lesions in cattle feet (Refaai et al. 2013).

Initial reports on ovine immune response to footrot suggested that the inflammatory destruction of the epidermal matrix, rather than the direct action of bacteria might be the main factor contributing to the separation of the horn observed in footrot lesions (Egerton et al. 1969). Based on this initial hypothesis, this study further speculated that the intense inflammatory destruction of the epidermal matrix, in association with bacterial colonisation, leads to severe inflammation that can progress to underrunning lesions. Taking the results of the present study together, we can hypothesise that both inflammatory response and *D. nodosus* colonisation might be potential risk factors playing a synergistic role and thus contributing to the exacerbation of footrot lesions.

As previously discussed, in addition to *D. nodosus*, *F. necrophorum* and *Treponema* spp., more than 27 different bacterial genera were identified in ovine interdigital skin samples using pyrosequencing analysis (Calvo-Bado et al. 2011). Therefore, it was postulated that other microbial communities could be involved in footrot pathogenesis and could also be associated with high and low levels of inflammation in the interdigital skin. While not part of this PhD project, the data presented in this chapter leaded to the subsequent analysis of microbial communities in association with clinical conditions (healthy

and footrot), and with high and low levels of *IL1β* expression (Maboni et al. 2017 - Appendix 2).

6.5 Conclusions

In summary, *TLR2*, *TLR4*, *IL1β*, *IL6*, *CXCL8* and *IL17* were found to be expressed in all healthy, ID and footrot samples. The key findings of this study suggest that clinical conditions and foot conformation do not impact on the expression levels of TLRs and cytokines in the ovine interdigital skin. However, this study showed for the first time that inflammation, as marked by mRNA expression levels of *CXCL8* and *IL1β*, central mediators of immune response in the skin, were associated with virulent *D. nodosus* in footrot affected feet. This suggests that *D. nodosus* colonisation may impact on the inflammatory mechanisms involved in footrot.

Chapter 7

7. Global gene expression in the ovine interdigital skin

7.1 Introduction

Gene expression studies can be targeted and/or genome-wide. When genes of interest are already known, RT-qPCR can be employed to investigate the gene expression of a targeted set of genes. In contrast, when genes of interest are unknown or an unbiased analysis is required, genome-wide technologies such as RNA sequencing (RNAseq) can be employed as a strategy to ascertain which genes are expressed in a particular tissue or cell of interest (Wang et al. 2009). The initial approach applied in this project was RT-qPCR aiming to investigate a targeted set of cytokines and TLRs previously reported to play a role in the immune response of skin infections (as described in Chapter 6). The results of this previous investigation showed that there is no association of expression of the targeted molecules with the clinical condition of the interdigital space, hence a genome-wide approach was used to provide further insights into genes associated with ID and footrot inflammatory mechanisms.

RNAseq is a Next Generation Sequencing technology that is highly informative and allows the analysis of thousands of genes to provide a quantitative profile of the cell or tissue of interest (Wang et al.

2009). Currently the most commonly used technique is provided by the Illumina. This technology is based on detecting and recording light that is emitted when a complementary nucleotide is added to a particular fragment of cDNA. The light detected will determine the identity of the nucleotide (`base calling') and then the sequence of the whole `read'. The many short reads generated can either be mapped to a reference genome or assembled *de novo* to produce the transcriptome. RNAseq revolutionised transcriptomics research due to its relative low cost associated with its high throughput (Wang et al. 2009). Additional advantages include the use of the sequencing data not only for wide gene expression profiling, but also for investigating single nucleotide polymorphisms (Lalonde et al. 2011), discovery of novel transcripts (Guttman et al. 2010) and the elucidation of gene pathways and networks (Emmert-Streib & Glazko 2011). This technique has been increasingly used as an integral part of transcriptomics research (Wang et al. 2009). However, it is important to note that RNAseq generates a massive amount of data that requires specialist methods to extract significant biological information from it.

RNAseq studies on sheep have been used to study different traits. These includes the elucidation of the molecular mechanism of wool follicle development on skin tissues (Yue et al. 2015), to study the mechanisms of resistance to *Haemonchus contortus* in abomasal mucosal surfaces (Guo et al. 2016), to evaluate the global gene expression profile of *Mycoplasma agalactiae* infection on mammary

gland (Chopra-Dewasthaly et al. 2017) and on blood cells from sheep infected with *Fasciola hepatica* (Fu et al., 2016). RNAseq was also employed to study immune pathways and to identify differential gene expression in bovine interdigital skin biopsies affected by digital dermatitis, which is a similar disease to ovine footrot (Scholey et al. 2013). No RNAseq studies have been reported on ovine interdigital skin.

The initial hypothesis of this project states that the pathology of footrot is a host mediated expression of local immune responses, in association with bacterial colonisation, leading to severe inflammation that can progress to underrunning footrot. As discussed in previous chapters, little is known regarding the mechanisms by which the immune response is instigated in ovine footrot. Therefore, in order to provide a greater understanding of this initial hypothesis and to obtain novel information on ovine expression of local immune responses, this study aimed to characterize the transcriptomic profile of ovine interdigital skin samples from healthy, ID and footrot affected feet using RNAseq and a combined network and pathway approach.

7.2 Materials and methods

Collection of biopsies from the ovine interdigital skin is described in section 2.1, RNA extraction in section 2.4 and cDNA synthesis is described in section 2.5 (Chapter 2).

7.2.1 Selection of samples for RNAseq

Eighteen biopsies from the ovine interdigital skin, including 9 healthy, 4 ID and 5 footrot were selected for RNAseq. The selection criteria included a RNA yield above 150ng/µl, RIN number above 6.5 (in order to ensure that the quality and quantity of total RNA was sufficient to generate cDNA libraries and consequently transcriptome reads of good quality), *IL1β* mRNA levels differently expressed between healthy and diseased samples in order to select healthy samples with low inflammatory background, samples positive or negative for *D. nodosus* and the clinical condition of sheep with all four feet sampled to allow further analysis and associations between RNAseq data, clinical conditions and *D. nodosus* load (Table 7.1).

Table 7.1 Samples selected for RNA sequencing (n=18) based on ovine feet clinical conditions, quality and yield of RNA, inflammatory background (IL1β expression) and presence of *D. nodosus*.

Clinical condition/ Sheep	**Sample**	**Clinical condition/ sample**	**RNA ng/µl**	**RIN number**	**IL1β (Cq)**	***D. nodosus***
Animal 1 (all conditions)	MM209	Footrot	176	9.2	10.2	Positive
	MM210	Healthy	354	9.7	5.1	Positive
	MM211	ID score 2	266	9.4	7.6	Positive
Animal 2 (all conditions)	MM233	Healthy	445	10.0	6.3	Negative
	MM234	ID score 1	431	6.5	6.8	Positive
	MM235	Footrot	853	8.9	9.3	Positive
Animal 3 (footrot and healthy)	MM213	Healthy	158	7.9	7.1	Positive
	MM215	Footrot	1607	9.3	12.7	Positive
	MM216	Footrot	1055	8.3	11.1	Positive
Animal 4 (footrot and healthy)	MM190	Footrot	715	9.6	9.6	Negative
	MM191	Healthy	685	9.6	5.4	Negative
Animal 5 (all conditions)	MM157	Healthy	823	9.2	6.20	Negative
	MM158	ID score 2	929	8.9	11.70	Positive
Animal 6 (healthy and ID)	MM200	Healthy	808	9.4	7.8	Positive
	MM198	ID score 2	476	9.4	11.4	Positive
Animal 7 (all healthy)	MM05	Healthy	365	9.1	5.9	Positive
	MM07	Healthy	858	9.2	7.5	Positive
Individual feet	MM103	Healthy	1014	9.6	4.4	Positive

IL1β mRNA expression values: normalised quantification cycles (Cq); ID= interdigital dermatitis; RIN= RNA integrity number. For foot scoring system details see table 2.1 (Chapter 2).

7.2.2 Sequencing and analysis of RNAseq data

RNAseq was performed at The University of Edinburgh, Ashworth Laboratories, Edinburgh Genomics using HiSeq 2500 Illumina. Samples (n=18, 100ng/µl of RNA) were prepared using TruSeq stranded mRNA-seq kit. Full details of the sample preparation are described in (http://support.illumina.com/content/dam/illumina-support/documents/documentaion/chemistrydocumentation/sampleprepstruseq/truseqstrandedmrna/truseq-stranded-mrna-sample-pr

ep-guide-15031047-e.pdf). The libraries were then sequenced on 1 lane of Illumina HiSeq 2500 using v4 High Output mode to produce 125 base paired end reads. Sequence files were returned as FASTQ files for further analysis. Full details of sequencing protocol are described in (htpp://www.illumina.com/systems/hiseq2500150 0/performancespecifications.html).

Quality control, alignment of transcripts and determination of differently expressed genes analysis were performed by ADAC (Advanced Data Analysis Centre, University of Nottingham) (Described in Chapter 2). Briefly, adapter sequences were removed from Fastq files using Cutadapt (version 1.2.1), then trimmed sequences were aligned to the genome assembly (Ovis Aries Oarv3.1) and SAM files of samples were then merged into counts files using HTSeq (version 0.6.1). edgeR software (version 3.6.8) was used for differential expression analysis between healthy, ID and footrot samples. R scripts used in this study are described in Appendix 6. Ovine uncharacterised proteins were investigated using BLAST Protein NCBI (https://blast.ncbi.nlm.nih.gov, May 2017).

7.2.3 Hierarchical cluster analysis and pathway analysis

A heat-map was generated to visualise differently expressed genes among healthy, ID and footrot samples using ADAC R scripts.

Pathway analysis was conducted using Ingenuity Pathway Analysis knowledgebase (IPA, Qiagen Redwood City) in order to identify

functional clusters and biological interactions between the gene products. The human database was used as reference in the IPA analysis since sheep database was not available. Orthologous sheep Ensembl identifiers were obtained via the Ensembl biomart database. Only those genes with a defined 1:1 relationship were used. Hence, the list of differently expressed genes with their Ensembl identifiers corresponding to human gene orthologues was imported into the IPA. Clustering and enrichment analysis was conducted by IPA statistical algorithm based on its proprietary knowledge base. IPA calculates an enrichment P value using the right-tailed Fisher Exact Test; P-value ≤ 0.05 indicates a statistically significant result.

7.2.4 Validation of RNAseq results using RT-qPCR

Three differentially expressed genes were selected for validation by RT-qPCR. *ANXA1* and *KLK6* expression was significantly increased in footrot samples and both genes are associated with inflammation in the functional analysis (Further information described in Table 7.3, results section), while *PLCXD2* expression was downregulated in footrot samples. Primer design and optimization of RT-qPCR assays were performed by the author of this thesis together with a veterinary student from the University of Nottingham as part of an undergraduate research project. The RT-qPCR assays were performed using cDNA from the 18 RNA samples originally sent for sequencing. Primers for *ANXA1, KLK6* and *PLCXD2* were designed using Primer3Plus (version 0.4.0); for each gene, a minimum of three

forward and three reverse primers were designed and assessed by RT-qPCR (Table 2.3 for primers details, Chapter 2). Reactions contained 5µl of cDNA (diluted 1:10 for *KLK6*, 1:100 for *ANXA1*, 1:30 for *PLCXD2*) in 2× LuminoCt SyBR Green qPCR ready mix (Sigma-Aldrich) with 0.5µM of forward and reverse primers (Sigma Aldrich). Samples were subjected to initial denaturation at 95°C for 20 minutes, followed by 45 cycles at 95°C for 05 seconds, 60°C for 20 seconds and 72°C for 30 seconds and a continuous dissociation step at 97°C to obtain a melt curve. Normalization of Cq values was performed with two reference genes, *ACTB* and *PPIA* (For reference genes identification see Chapter 5). Further details of the RT-qPCR assays are described in Chapter 2 (sections 2.6 and 2.7). The Gene expression values of differently expressed genes between healthy and footrot obtained by RT-qPCR were analysed by Kruskal-Wallis test (Mann Whitney test, non-parametric). Analysis was performed using GraphPad Prism (Version 6.0, La Jolla, USA) and a P value of ≤0.05 was considered significant.

7.3 Results

7.3.1 Read mapping statistics

The number of raw reads obtained after sequencing and the number of mapped reads obtained after quality control and mapping to reference genome are shown in Table 7.2. Among the 18 samples, a range of 85.9%-88.9% of mapped reads were obtained after mapping to the reference genome.

Table 7.2 RNAseq reads for 18 biopsy samples from the ovine interdigital skin. Total reads: number of raw reads generated from RNAseq. Mapped reads: sequence reads that were confidently mapped to reference ovine genome.

Sample	Clinical Condition	Total reads	Mapped reads
MM209	Footrot	20828520	18226600
MM235	Footrot	15985434	13969530
MM215	Footrot	20029725	17605514
MM216	Footrot	18683515	16117050
MM190	Footrot	12079170	10460913
MM158	ID score 2	15438573	13555064
MM198	ID score 2	12099957	10552295
MM234	ID score 1	19462571	16785044
MM158	ID score 2	15438573	13555064
MM213	Healthy	17333607	14934929
MM191	Healthy	11233777	9882573
MM157	Healthy	14290741	12456223
MM210	Healthy	17496257	15402963
MM05	Healthy	12150513	10725790
MM07	Healthy	10287393	9071378
MM103	Healthy	10686400	9338712
MM233	Healthy	16637151	14690202
MM200	Healthy	13807683	12104093

ID: interdigital dermatitis

7.3.2 Determination of differently expressed genes among healthy, ID and footrot samples

Further analysis of the 25,198 genes annotated in the ovine genome included the determination of genes with increased mRNA expression (upregulated) or decreased mRNA expression (downregulated) among healthy, ID and footrot samples. Using $P < 0.05$ and log2-fold change >1 as cut-off to determine differently expressed genes, the expression of 34 genes were found to be significantly different between healthy and footrot samples. Among those genes, the mRNA expression of 31 was increased in footrot samples (upregulated), and

3 genes showed decreased mRNA expression in footrot samples in comparison to healthy samples (downregulated) (Figure 7.1, Table 7.3). There were no significant differences between healthy and ID samples (Figure 7.1). Out of 34 genes, five genes represented uncharacterized proteins (Table 7.3). Further investigations revealed that four of these genes were fully characterized in other animal species. For instance, *LOC100744607* (*TAF5-like RNA polymeraseII p300/CBP-associated factor-associated factor*) bovine gene, which shares 88% of identity with sheep; *IGHG3* (*Immunoglobulin heavy constant gamma 3*) bovine gene, which shares 79% of identity with sheep; *IGL* (*Immunoglobulin lambda light chain*) gene from goat, sharing 80% of identity with sheep, and *PIK3R2* (*Phosphatidylinositol 3-kinase regulatory subunit beta*) bovine gene, sharing 82% of identity with sheep (Table 7.3).

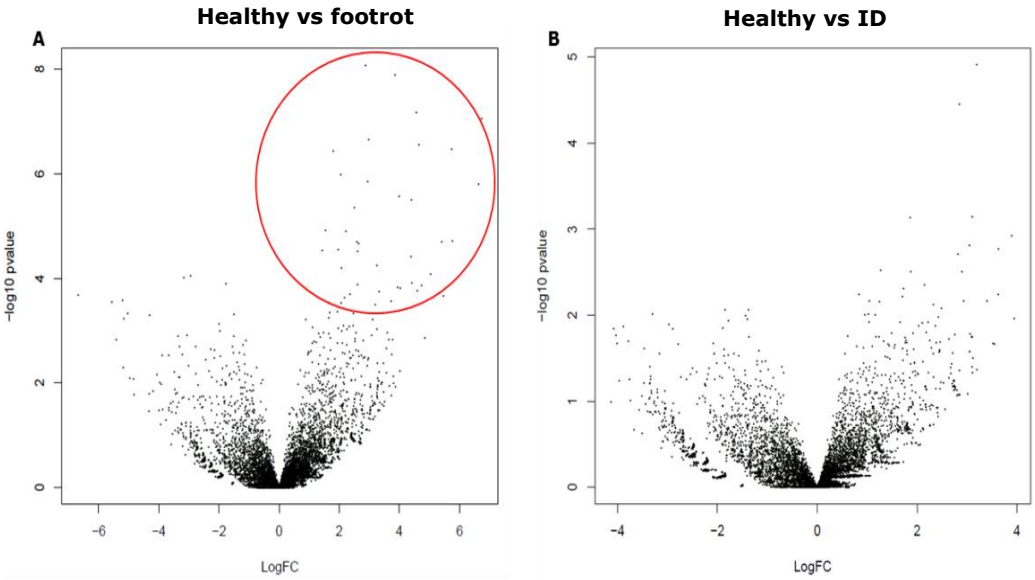


Figure 7.1 Volcano plot showing the relationship between the –log10 P-value for each gene and the magnitude of the difference in expression values of the samples in healthy, interdigital dermatitis (ID) and footrot groups. A: all healthy samples and all footrot samples highlighting the cluster of genes with high statistical difference between the two clinical conditions. B: all healthy and all ID samples (Data provided by Advanced Data Analysis Centre, University of Nottingham).

Table 7.3 List of differentially expressed genes in healthy and footrot samples (n=18) from RNAseq.

Official symbol	Description	Log FC	P value	Ensembl ID
Upregulated transcripts				
NT5DC4	*5'-nucleotidase domain containing 4*	6.73	8.72E-08	ENSOARG00000020871
OVCA2	*Ovarian tumour suppressor candidate 2*	6.63	1.56E-06	ENSOARG00000014808
NFAM1	*NFAT activating protein with ITAM motif 1*	5.76	1.94E-05	ENSOARG00000018955
	*Uncharacterized protein (Ovis aries)**	5.74	3.40E-07	ENSOARG00000015893
COPZ1	*Coatomer protein complex, subunit zeta 1*	5.41	2.04E-05	ENSOARG00000016220
PLBD2	*Phospholipase B domain containing 2*	5.04	8.30E-05	ENSOARG00000007553
ADORA3	*Adenosine A3 receptor*	4.73	1.37E-04	ENSOARG00000019630
MVD	*Mevalonate (diphospho) decarboxylase*	4.65	2.84E-07	ENSOARG00000013010
DDX39A	*DEAD (Asp-Glu-Ala-Asp) box polypeptide 39A*	4.56	6.65E-08	ENSOARG00000005744
	*Uncharacterized protein (Ovis aries)**	4.41	1.23E-04	ENSOARG00000012832
LOC100744607	*TAF5-like RNA polymeraseII p300/CBP-associated factor-associated factor*	88% identity (*Bos taurus*)		
TMEM51	*Transmembrane protein 51*	4.40	3.20E-06	ENSOARG00000010392
STAT2	*Signal transducer and activator of transcription 2*	4.38	3.86E-05	ENSOARG00000009154
RPS4X	*Ribosomal protein S4, X-linked*	4.03	1.51E-04	ENSOARG00000008692
KLK6	*Kallikrein-related peptidase 6*	3.93	1.51E-04	ENSOARG00000014290
CYBA	*Cytochrome B-245 Alpha Chain*	3.86	1.30E-08	ENSOARG00000012901
CTSW	*Cathepsin W*	3.25	5.68E-05	ENSOARG00000018487
	*Uncharacterized protein (Ovis aries)**	2.97	2.21E-07	ENSOARG00000009143
IGHG3	*Immunoglobulin heavy constant gamma 3*	79% identity (*Bos taurus*)		

ANXA1	*Annexin A1*	2.94	1.40E-06	ENSOARG00000012672
HDAC1	*Histone deacetylase 1*	2.88	8.47E-09	ENSOARG00000020951
HSPA5	*Heat shock 70kDa protein 5 (glucose-regulated protein, 78kDa)*	2.61	1.33E-04	ENSOARG00000012928
ZC3H12A	*Zinc finger CCCH-type containing 12A*	2.61	3.07E-05	ENSOARG00000019760
CRABP2	*Cellular retinoic acid binding protein 2*	2.59	2.01E-05	ENSOARG00000006212
	*Uncharacterized protein (Ovis aries)**	2.51	4.52E-06	ENSOARG00000012585
IGL	*Immunoglobulin lambda light chain*	80% identity (*Capra hircus*)		
TNIP1	*TNFAIP3 interacting protein 1*	2.22	1.26E-05	ENSOARG00000008016
TMEM176A	*Transmembrane protein 176A*	2.07	6.31E-05	ENSOARG00000001756
	*Uncharacterized protein (Ovis aries)**	2.05	1.04E-06	ENSOARG00000013462
PIK3R2	*Phosphatidylinositol 3-kinase regulatory subunit beta*	82% identity (*Bos taurus*)		
C19orf71[#]	*Chromosome 19 open reading frame 71*	1.80	3.61E-07	ENSOARG00000012488
CHKA[#]	*Choline kinase alpha*	1.54	1.22E-05	ENSOARG00000014868
TCP1[#]	*T-complex 1*	1.43	2.95E-05	ENSOARG00000004554
Downregulated transcripts				
GYLTL1B	*Glycosyltransferase-like 1B*	-1.76	1.28E-04	ENSOARG00000002854
MAP6	*Microtubule-associated protein 6*	-2.93	9.04E-05	ENSOARG00000011875
PLCXD2	*Phosphatidylinositol-specific phospholipase C, X domain containing 2*	-3.16	9.70E-05	ENSOARG00000019192

[#]Genes not included in the functional and pathway analysis since their Log Fold Change (FC) values are below the stablished cut-off criteria (FC>2) for this particular analysis. (*Ovis aries*)*: ovine uncharacterized proteins were further investigated using NCBI Blast Protein to identify whether they were caractherized in other animal species and their % of identity with ovine.

7.3.3 Validation of differently expressed genes of RNAseq using RT-qPCR

Three genes of interest were selected from the list of differently expressed genes for validation using RT-qPCR. *ANXA1, KLK6* (upregulated) and *PLCXD2* (downregulated). Genes were selected based on their association with inflammatory response and level of expression (upregulation or downregulation). RT-qPCR was successfully optimized and all targets showed amplification efficiencies within the ranges of an optimised RT-qPCR assay (90%-105%, Table 7.4). No template controls did not show any amplification and melt curves showed single peaks of amplification. Results obtained from RT-qPCR confirmed that the mRNA expression of *ANXA1* ($P \leq 0.005$) and *KLK6* ($P \leq 0.05$) were consistent with the results obtained by RNAseq since the expression of both genes was significantly increased in footrot samples (Figure 7.2 A and B). The expression of the downregulated gene *PLCXD2* was slightly but not significantly higher in healthy samples than in footrot samples ($P=0.363$) (Figure 7.2 C). In summary, the RNAseq data was validated using RT-PCR with a statistical significant association between results from both techniques for both upregulated genes tested in this analysis (*ANXA1* and *KLK6*).

Table 7.4 Standard curve data for RT-qPCR assays used to validate RNAseq results.

Gene	Cq values range	Slope	R^2	Efficiency	Melt curve peaks
ANXA1	20-27	-3.426	0.997	95.8%	Single
KLK6	22–30	-3.467	0.999	94.27%	Single
PLCXD2	27-35	-3.365	0.962	98.2%	Single

Cq: quantification cycles. Slope/Efficiency: Ideally the efficiency (E) of a PCR should be 100%, meaning that for each cycle the amount of product doubles (E=2). The efficiency was calculated from the slope of the standard curve according to the following formula: E = 10(-1/slope)-1. R^2 is the coefficient of correlation obtained from the standard curve and should ideally be >0.99.

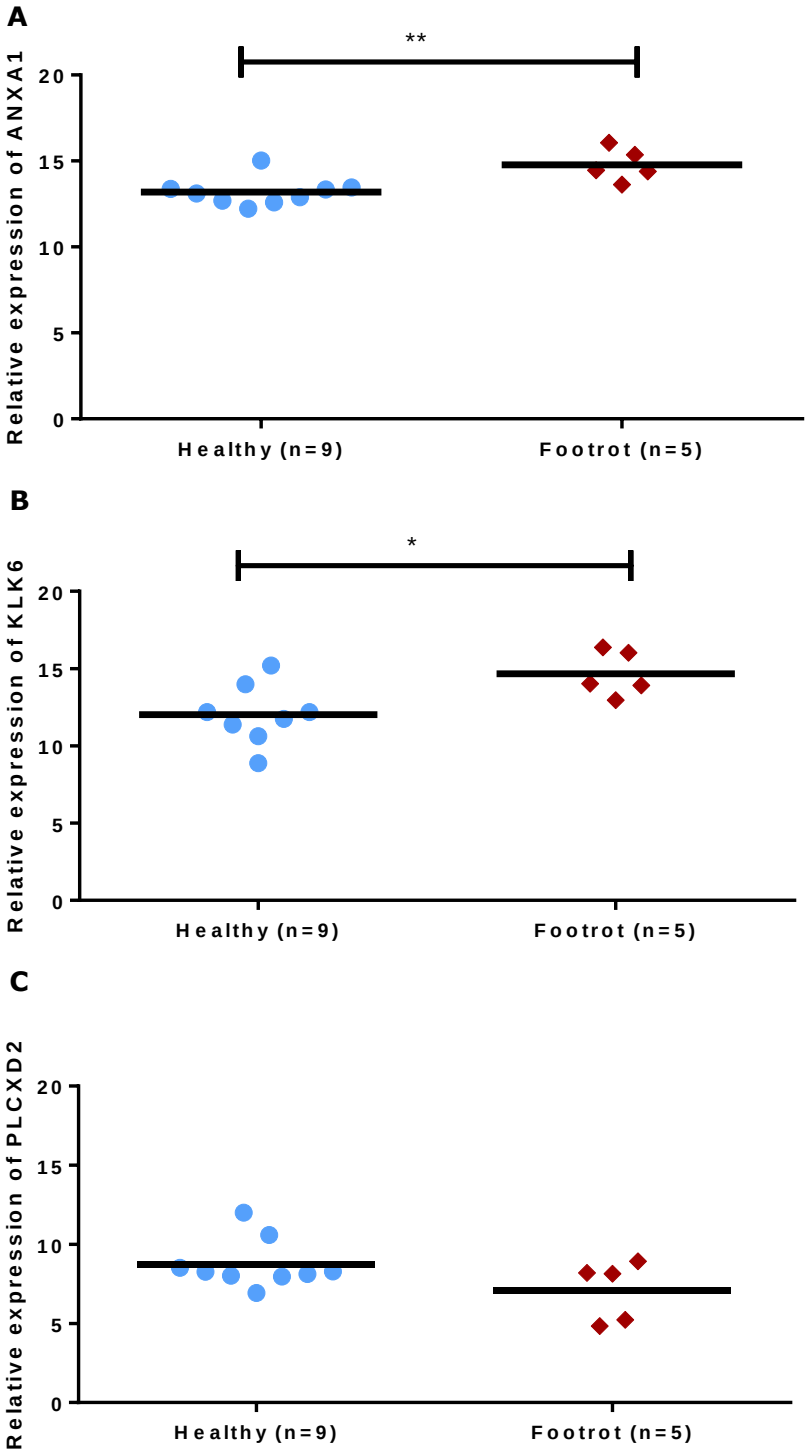


Figure 7.2 RT-qPCR validation of RNAseq data for differently expressed genes between healthy and footrot samples. *ANXA1* (A) and *KLK6* (B) (upregulated genes in the RNAseq), and *PLCXD2* (downregulated gene in the RNAseq). These results were consistent with RNAseq (A and B), except for *PLCXD2* (C). Data were normalised with *ACTB* and *PPIA* (reference genes) and analysed by Kruskal-Wallis test (Mann Whitney test) using Graphpad Prism. *P ≤0.05, **P ≤0.005.

7.3.4 Hierarchical cluster analysis

For the hierarchical cluster analysis a heat-map was generated based on differently expressed genes among healthy, ID and footrot samples (Figure 7.3). Two distinct clusters corresponding to footrot and healthy samples were identified confirming that samples from the same clinical condition more closely resembled each other. However, ID samples did not cluster well together. In addition, the heat-map illustrates that one footrot sample (MM209) showed a different expression profile presenting many upregulated genes compared with other footrot samples. This analysis also revealed that neither samples with similar levels of *IL1β*, presence nor absence of *D. nodosus* as well as samples collected from the same animal resembled each other in terms of gene expression. Dendrograms were added for both the transcripts and the samples to indicate the level of similarity in the groupings (Figure 7.3).

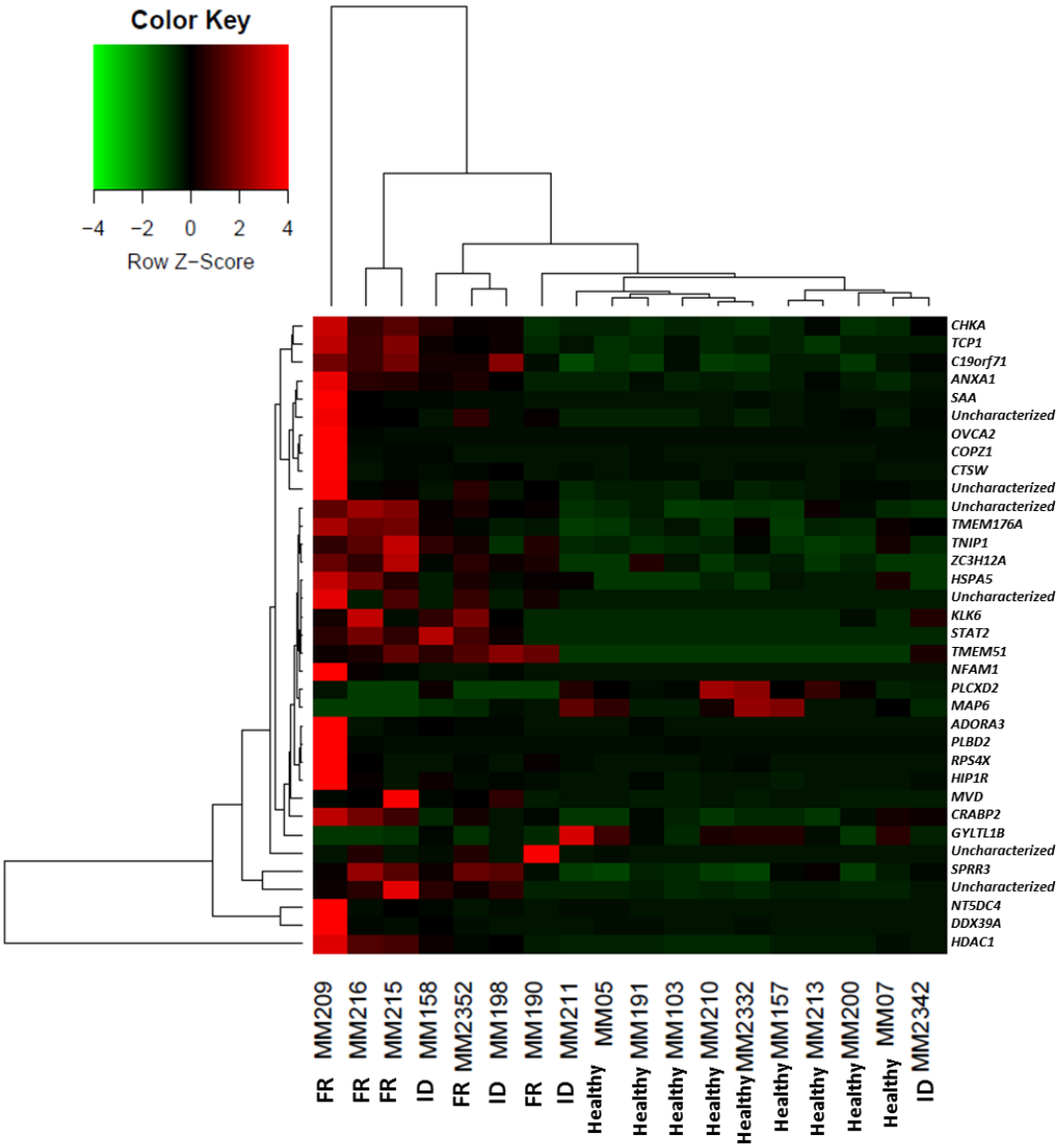


Figure 7.3 Heat-map showing hierarchical clustering of global gene expression detected through RNAseq in healthy, interdigital dermatitis (ID) and footrot (FR) ovine interdigital skin samples. Heat map shows genes differentially expressed between clinical conditions: red represents upregulated genes and green the downregulated genes. Columns correspond to samples and rows correspond to genes.

7.3.5 Grouping of differently expressed genes according to biological function using Ingenuity Pathway Analysis

Data were analysed through the use of IPA, which generated gene networks and the diseases associated with the 34 genes differently expressed between healthy and footrot samples. In this study, the most enriched diseases and biological functions of the differently expressed genes shown by IPA were (a) inflammatory response, (b) cancer, (c) dermatological diseases and conditions, (d) organismal injury and abnormalities and (e) haematological diseases. Further investigation focused exclusively on the inflammatory response and dermatological diseases, which are categories of interest in the context of ovine footrot. *ANXA1* was the most associated gene with inflammatory functions. The majority of these functions were related to acute inflammatory response such as recruitment of granulocytes (i.e. neutrophils, basophils and eosinophils), degranulation of mast cells and neutrophils, and emigration of neutrophils from blood vessels (Table 7.5). Some functions of *ANXA1* were also associated with the transition from acute to chronic inflammation, for instance the recruitment of monocytes to the lesion site and adhesion of $CD4^+$ and $CD8^+$ T lymphocytes. In addition, *ANXA1* was highly associated with unspecified anti-inflammatory responses. Similar to *ANXA1*, *ADORA3* was another gene predicted to be associated with inflammation, which functions were mainly related to an acute inflammatory response such as recruitment of granulocytes, degranulation of mast cells and unspecified inflammatory responses, and acute inflammation of tissue (Table 7.5).

Some of the differently expressed genes in footrot samples such as *DDX39A*, *HDAC1*, *SPRR1B*, *DDX39A*, *SPRR1B* and *HDAC1*, were also linked with dermatological functions that are mainly human-associated conditions such as hyperplasia of skin, hyperplasia of epidermis and hyperplasia of epidermal cells (Table 7.6).

Table 7.5 Functional analysis of the genes differently expressed in healthy and footrot samples by Ingenuity Pathway Analysis. Category: inflammatory response.

Inflammatory response		
Diseases or Functions Annotation	**P value**	**Molecules**
Anti-inflammatory response	1.50E-04	ADORA3, ANXA1
Phagocytosis of glioblastoma cells	1.02E-03	ANXA1
Adhesion of CD4+ T lymphocytes	1.02E-03	ANXA1
Adhesion of CD8+ T lymphocytes	1.02E-03	ANXA1
Recruitment of granulocytes	2.01E-03	ADORA3,ANXA1,HDAC1
Detachment of neutrophils	2.04E-03	ANXA1
Chemoattraction of peripheral blood monocytes	4.07E-03	ANXA1
Degranulation of mast cells	9.32E-03	ADORA3, ANXA1
Emigration of neutrophils	1.22E-02	ANXA1
Disruption of tight junctions	1.52E-02	ANXA1
Recruitment of neutrophils	1.94E-02	ADORA3, ANXA1
Degranulation of neutrophils	3.11E-02	ANXA1
Contact growth inhibition of fibroblast cell lines	3.21E-02	COPZ1
Acute inflammation of tissue	4.19E-02	ADORA3, KLK6

P-value ≤0.05 indicate a statistically significant association (Fisher Exact Test)

Table 7.6 Functional analysis of the genes differently expressed in healthy and footrot samples by Ingenuity Pathways Analysis. Category: dermatological diseases and conditions.

Dermatological diseases and conditions		
Diseases or Functions Annotation	**P value**	**Molecules**
Hyperplasia of skin	4.04E-04	DDX39A,HDAC1,SPRR1B
Hyperplasia of epidermis	6.35E-03	DDX39A,SPRR1B
Hyperplasia of epidermal cells	2.02E-02	HDAC1

P-value ≤0.05 indicate a statistically significant association (Fisher Exact Test)

Further analysis using IPA arranged the differently expressed genes into a network of interest. The cut-off criteria used in the IPA analysis was changed to log fold change>2 in order to increase stringency of differential expression (genes included in this analysis are highlighted in Table 7.3). The network generated by IPA contained upregulated genes with well-defined roles in inflammatory responses such as *ANXA1* (Gastardelo et al. 2009; Neymeyer et al. 2015), *STAT2* (Park et al. 2000), *KLK6* (Bayani et al. 2013; Schrader et al. 2015), *CTSW* (Conus & Simon 2008; Edinger et al. 2015), *ZC3H12A* (Liu et al. 2013) and *TNIP* (Matsuzawa et al. 2015). Moreover, the molecules were predicted to interact with key inflammatory complexes such as NFkβ and P38 MAPK, both signalling pathways involved in the induction and activation of cytokines (Lawrence 2009; Cuadrado & Nebreda 2010) (Figure 7.4). The genes were mainly associated with the innate immune response, whereas the adaptive immune response was less involved in the network with a predicted inhibition of IgG molecule (Figure 7.4). The only downregulated gene present in the network is *MAP6*, while *GYLTL1B* and *PLCXD2* were not predicted to be involved in this network. In summary, the network analysis

confirms the upregulation and downregulation of the genes differently expressed between healthy and footrot samples, and provides further insights into a potential role of these genes and their interactions with other molecules.

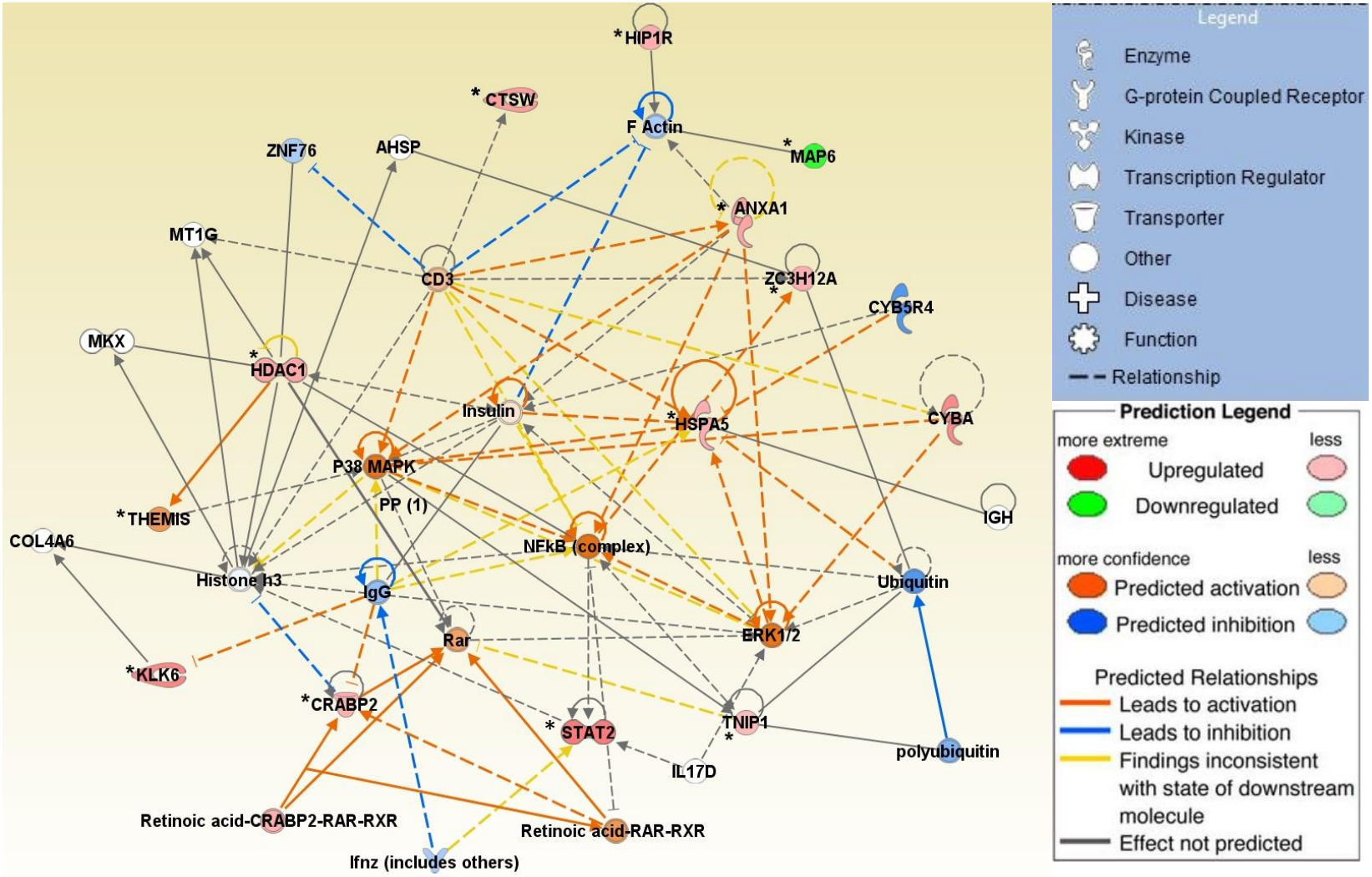


Figure 7.4 Differentially expressed genes (P<0.05 and fold change >2) grouped by Ingenuity Pathway Analysis to identify affected pathways and key central regulatory genes involved in ovine footrot. *Genes found to be differently expressed in the RNAseq dataset analysis; other non-marked genes were predicted by IPA knowledge base to interact with the differently expressed genes.

7.4 Discussion

This study provided information on global ovine gene expression through the characterization of the transcriptomic profile of healthy, ID and footrot interdigital skin samples using RNAseq. The analysis focused on molecules involved in the inflammatory response against footrot. Little is known regarding the mechanisms by which the infection is instigated. Hence, the genes identified in this study may provide further understanding of footrot pathogenesis, which in the long term may underpin the development of new vaccines and drug targets. RNAseq was used in preference to other genome-wide methods, such as microarray, since it provides an assessment of all transcripts with a greater dynamic range on a transcriptome-wide scale not relying on genome annotation for prior probe selection and avoiding biases introduced during hybridization as in microarray (Wang et al. 2009). In terms of RNAseq data analysis, every RNAseq experiments performed by different research groups may have their optimal methods for transcript quantification, normalization, and analysis of differently expressed genes. In this study, all methods used to analyse the dataset are described in the best practice guidelines for RNAseq analysis recently published by Conesa et al. (2016).

Sample selection

RNA samples were carefully selected and several criteria were taken into consideration (Table 7.1). The first criteria was the quality and

yield of RNA to ensure sufficient cDNA libraries and consequently transcriptome reads of good quality (Conesa et al. 2016). As the results of the first attempt to investigate the expression of targeted molecules by RT-qPCR showed similar inflammatory background between healthy and diseased samples, healthy samples with low expression of *IL1β* (inflammatory marker) were cautiously selected to ensure they would display different inflammatory background than footrot samples. Moreover, a higher number of healthy samples (n=9) than ID (n=4) and footrot (n=5) was chosen to strength the comparative analysis between healthy and clinically affected biopsies. Other criteria employed to select samples included the clinical condition of all four feet of each animal (Table 7.1, animal 1, 2 and 3) in order to further investigate whether global gene expression is dependent on the disease state of the individual feet or of the animal. A similar investigation was previously performed by our group using a targeted set of genes, where *IL1β*, *TLR2* and *TLR4* expression was found to be dependent on the disease state of individual ovine feet rather than the animal (Davenport et al. 2014). Similar analysis was not performed with the RNAseq dataset due to time limitations; hence, future studies of global gene expression in ovine interdigital skin could further examine this question.

Differential expression analysis identified 34 genes differently expressed in footrot samples

In a complex disease involving several different bacterial species such as footrot, it was expected that increased expression of many genes

would be involved. In an RNAseq study of bovine digital dermatitis, which is a similar condition to ovine footrot, more than 500 differently expressed genes were found between 5 controls and 5 digital dermatitis samples (Scholey et al. 2013). Another RNAseq study on skin tissues from mice revealed that over 1000 genes exhibited increased expression on skin experimentally infected with *Staphylococcus aureus* (Brady et al. 2015). RNAseq analysis on human skin from diabetic patients identified 182 differently expressed genes (Wu et al. 2017). Skin of raccoon dogs were also analysed by RNAseq to explore melanin biosynthesis and the differential expression analysis showed that a total of 187 genes were significantly differentially expressed between two different skin types (Du et al. 2017). In contrast with these erlier studies, the present study found only 34 genes significantly differentially expressed between healthy and footrot samples, and no differences were found between healthy and ID. Despite all the criteria employed to select healthy samples for RNAseq, these results suggest that healthy samples and ID/footrot samples may have a similar inflammatory background. Inflammation in apparently healthy interdigital skin might be explained by several reasons, for instance (i) the presence of *D. nodosus* that might be associated with subclinical disease that may have developed into ID and footrot in the next few days; (ii) wet environmental conditions might impact on the basal levels of inflammation and may favour inflammation in the interdigital skin of apparently healthy samples; and (iii) these sheep might have had footrot previously and inflammation could be related to a healing

process. Therefore, a major limitation of this study was the availability of healthy samples with assured low inflammatory levels to be used as controls. All these factors may explain the low number of differently expressed genes among healthy and footrot samples. One footrot sample (MM209) showed a different expression profile presenting many upregulated genes if compared with other footrot samples, as illustrated in the heat map (Figure 7.3). This sample was classified as footrot score 3 (severe lesions), which may explain the increased gene expression and indicates that further RNAseq studies should therefore include a higher number of samples with this lesion stage. Here, it is essential to highlight that any gene expression experiment using lesion samples from field animals could reveal unexpected results compared to outcomes obtained from *in vitro* infection of cell lines. However, this approach is a more realistic way to raise relevant information on gene expression profiles involved *in vivo*.

Regarding the similar gene expression levels of healthy and ID samples, it is important to note that all ID samples included in the RNAseq analysis were classified as ID score 1 (mild) or 2 (moderate), representing a possible reason for this similar expression. Since these stages of ID are characterized by slight inflammation, this might not reflect in a strong inflammatory response. This is in agreement with a previous study where similar levels of immune molecule expression was found between healthy and mild ID samples (Davenport et al. 2014).

Technical arguments to explain the low number of differently expressed genes may also include lack of predicted biological function of some uncharacterised proteins (Table 7.3). Indeed, from the present dataset 34 genes were differentially expressed, but 6 of these had uncharacterised proteins in the databank. These uncharacterised proteins are predicted to exist in sheep, but their functions are not biochemically characterized or they cannot be linked to a known gene (Nadzirin & Firdaus-Raih 2012). Importantly, it can be argued that uncharacterised proteins are worth studying in future studies since they may represent molecules with novel functions in ovine footrot.

Further investigations were performed to compare the level of expression found for the differently expressed genes on ovine footrot samples and in skin samples from other species and conditions. *GYLTL1B* was found to be downregulated in ovine footrot samples (present study) and in bovine digital dermatitis samples (Scholey et al. 2013); however, this gene was found to be upregulated in human melanocytes (Reemann et al. 2014). Another divergent result was found for *STAT2*, which was upregulated in footrot samples (present study) and in human skin from diabetic patients (Wu et al. 2017), but downregulated in human melanocytes (Reemann et al. 2014). Moreover, the same study on human melanocytes found *DDX39A*, *MVD*, *CYBA*, *COPZ1*, *ANXA1*, *HDAC1*, *HSPA5*, *C19ORF71*, *CHKA* and

TCP1 to be downregulated while they were upregulated on the ovine interdigital skin.

Validation of differently expressed genes using RT-qPCR

mRNA expression of 3 differently expressed genes from the RNAseq dataset was validated using RT-qPCR. A strong association between results from both techniques could be seen for both upregulated genes (*ANXA1* and *KLK6*). The gene of which the expression level did not fully match is a downregulated in the RNAseq (*PLCXD2*), suggesting a possible reduced sensitivity of the RNAseq technique at low expression levels. Nevertheless, as RNAseq is reported to be a sensitive technology with a strong correlation with RT-qPCR (Wang et al. 2009; Brooks et al. 2011), the unmatched result found in this validation analysis might be a single effect of this particular gene.

Differently expressed genes were mostly associated with inflammatory functions

Differently expressed genes ($P<0.05$ and fold change >2) were grouped to find biological functions and pathways involved in footrot using systems biology analysis (IPA software knowledgebase). The top predicted diseases and bio functions of interest in ovine footrot included inflammatory response and dermatological diseases. *ANXA1*, *ADORA3, HDAC1, COPZ1 and KLK6* were the genes in the inflammatory response category (Table 7.5), highlighting a potential role of these genes in the immune mechanisms involved in footrot.

Previous studies have associated *ANXA1* to anti-inflammatory reactions since this gene encodes an anti-inflammatory protein that prevents fibrosis by modulating the activity of fibroblasts in human skin (Neymeyer et al. 2015). In contrast to our study, ANXA1 was found to be downregulated in human melanocytes (Reemann et al. 2014). Importantly, the enzyme encoded by *ANXA1* was predicted to be associated with disruption of tight junctions, which are intercellular junctions that seal adjacent keratinocytes in the stratum granulosum and are considered a major epidermal barrier (Kirschner & Brandner 2012). We could postulate that bacteria involved in footrot may induce a host mechanism, i.e upregulation of *ANXA1*, in order to invade the skin through the disrupted tight junctions, or bacteria could directly act in the disruption of tight junctions. This disruption may potentially represent one of the mechanisms that leads to separation of the skin from the hoof, hence initiating footrot lesions.

ADORA3 was another gene predicted to be associated with inflammation, with functions mainly related to acute inflammatory response. *ADORA3* was previously reported to have anti-inflammatory roles (Ren et al. 2014) through the inhibition of neutrophil degranulation, and inhibition of NF-κB signalling pathway associated with inhibition of downstream *CXCL8* and *IL1β* expression (Ren et al. 2014). Some of the top upregulated genes in footrot samples, as *NFAM1, KLK6* and *CTSW*, did not have a predicted function in the IPA analysis, but they are well-reported in the literature as molecules involved in inflammatory responses. *NFAM1* was one of the top 3 most expressed genes in footrot samples and

was shown to activate the transcription of IL13 and TNFα promoters. Moreover, *NFAM1* plays a role in the immune system as a receptor which activates via the calcineurin/NFAT-signaling pathway the downstream cytokine gene promoters (Plager et al. 2012). *NFAM1* is part of a wide inflammatory cascade process. *KLK6* is a gene that encodes an enzyme reported to degrade components of the extracellular matrix (Bayani et al. 2013), which may potentially be part of the mechanisms of separation of the skin from the hoof, then initiating footrot underrunning lesions. *KLK6* also participates in cellular processes such as inflammation, receptor activation, and regulation of apoptosis (Prassas et al. 2015; Schrader et al. 2015; Bayani et al. 2013). *CTSW* was also among the top genes upregulated in footrot samples and plays a role in both innate and adaptive immune responses (Conus & Simon 2008; Edinger et al. 2015). *CTSW* encodes cathepsins, which are proteases mainly expressed in NK cells and $CD8^{+}$T cells. They are involved in the main apoptotic pathways, keratinocyte differentiation and antigen processing, hence they are significant modulators of adaptive immunity (Conus & Simon 2008; Edinger et al. 2015).

7.5 Conclusions

The results of the RNAseq analysis of ovine interdigital skin revealed 34 significantly expressed genes in footrot samples indicating upregulation of the local inflammatory and innate immune responses, whilst little association of the local adaptive immune response. Based on the current data, it is notable that there is a potential role of the

innate immune response in footrot mechanisms. Moreover, *ANXA1* and *ADORA3* genes were highly associated with inflammation and could be considered possible molecules of relevance in footrot in terms of pathogenesis elucidation as well as treatment strategies. Importantly, further studies on global gene expression of ovine interdigital skin using an increased number of samples are warranted. More samples per clinical condition, mainly in the footrot group, could provide a more representative list of genes with increased expression in footrot and their predicted functions and pathways.

Chapter 8

8. Development of a 3D skin model culture to investigate ovine footrot

8.1 Introduction

The ovine interdigital skin space is a complex microenvironment difficult to replicate *in vitro*, hence *in vivo* sheep experimentation creates the ideal scenario to investigate host-pathogen interactions and mechanisms of pathogenicity of footrot. Previous *in vivo* experiments contributed substantially to the understanding of these mechanisms (Beveridge, 1941; Egerton et al. 1969; Roberts & Egerton 1969; Kennan et al. 2010). However, *in vivo* models raise ethical and legal issues due to the use of animals in research. In this context, *in vitro* approaches could be used as alternatives aiming to replace or at least minimize the necessity of *in vivo* sheep experiments. A single cell type culture model using ovine fibroblasts was previously developed and published by our group, where an increased expression of *IL1β* was measured in fibroblasts stimulated with both heat-killed *D. nodosus* and *F. necrophorum* (Davenport et al. 2014). It is important to highlight that 2D monolayer cultures do not reflect complex *in vivo* cellular processes due to the lack of multicellular interactions (MacNeil, 2007) and may differ in gene and protein expression from *in vivo* models (Gurski et al. 2010; Price et

al. 2012). Therefore, it is imperative to develop new alternatives to provide physiologically relevant conditions in a system that can realistically simulate the sheep interdigital skin.

An *in vitro* alternative that could be applied to investigate footrot is an *Ex vivo* organ culture (EVOC), which is a three-dimensional (3D) model based on tissue explants cultured *in vitro*. This enables the reproduction of key events of disease processes in an *in vitro* controlled environment preserving cellular elements and tissue architecture (Dutta & Dutta 2009; Steinstraesser et al. 2010). 3D models are considered to be phenotypically and histologically similar to the organs and tissues of the *in vivo* situation and its importance in the development of relevant tissue models has been widely recognized (Ren et al. 2006; Edmondson et al. 2014). Despite the advantages of 3D models, its limitations include the lack of integration of the vascular, nervous and lymphatic system (Lebonvallet et al. 2010).

Skin cultured in *ex vivo* 3D models is well established, using explants acquired from neonatal foreskin, surgical, or *post mortem* tissues from humans or animals. The skin explants contain all resident cells and skin appendages of the epidermis and dermis (Popov et al. 2014). 3D skin models have been used in a variety of purposes including (i) the investigation of the skin immune response to bacterial infection and wound healing (Steinstraesser et al. 2010), (ii) studies of normal skin cell pigmentation (Bessou et al. 1996) and (iii) the pathology of

how melanoma cells interact with skin (Eves et al. 2003). Bacterial infection studies have been performed previously using human 3D skin models (Steinstraesser et al. 2010; Popov et al. 2014), but not using ovine skin. Developing an *ex vivo* model for the ovine interdigital skin will allow the investigation of the pathogenesis of footrot, especially the local cellular response elucidating the early stages of infection. In addition, the EVOC model using sheep skin explants also addresses the 3Rs (Replacement, Reduction and Refinement) of animal experimentation, as explants can be collected from abattoirs, where they are by-products of the slaughter process. The 3Rs were first published by William Russell and Rex Burch in the "The Principles of Humane Experimental Technique" (1959). They proposed that if animals were to be used in experiments, every effort should be made to replace animals with other alternatives, to reduce to a minimum the number of animals used, and to refine experiments which used animals so that they caused the minimum pain and distress. The 3Rs have become established as essential considerations when animals are used in research. They have influenced new legislation aimed at controlling the use of experimental animals. In the UK, the 3Rs have become formally incorporated into the Animal (Scientific Procedures) Act, which regulates the use of animals for research (Flecknell, 2002).

In this context, the aim of this study was to develop an effective model for the *ex vivo* investigation of the ovine interdigital skin infection with *D. nodosus*. This will enable the investigation of the

bacterial invasion within the interdigital skin layers and the early local inflammatory response to this bacterium. Moreover, the model viability was assessed during the model incubation time, and the early local cellular response to *D. nodosus* was investigated by quantification of IL1β and CXCL8 present in the media supernatant.

This project was initiated through undergraduate research projects at SVMS (Davenport, 2011; Sessford, 2012). Sample collection, media composition, conditions to simulate the natural footrot infection and EVOC model assembly were previously optimized. Moreover, putative *D. nodosus* was found in the EVOC biopsies using *in tissue* Gram stain (Davenport, 2011; Sessford, 2012). The present study extended this project aiming to investigate tissue integrity in detail, confirm and quantify infection with *D. nodosus.*

8.2 Materials and methods

Isolation of *D. nodosus* strains used for model infection is decribed in section 2.8, DNA extraction of biopsies in section 2.2 and qPCR to quantify *D. nodosus* within the EVOC biopsies is described in section 2.3 (Chapter 2).

8.2.1 EVOC model optimization

Healthy ovine feet were collected from sheep at an abattoir post-slaughter. Only feet with perfect hoof conformation and integrity with apparently healthy interdigital skin were selected. Environmental

contaminants were removed from the foot and from the interdigital space using 70% ethanol and antimicrobial skin cleanser (Hibiscrub, Oldham, UK) before removal of the hair using scissors. The entire ovine interdigital skin was removed using a sterile scalpel, then it was immersed in transport media stored on ice (Table 8.1), and transported to the laboratory.

Table 8.1 Transport medium components.

Components (final concentration)	**Manufacturer (stock concentration)**
DMEM-HAM`S F12 (1:1)	Sigma Aldrich (1:1)
Penicillin + Streptomycin (0.01µg/mL)	Gibco (5,000U/mL Penicillin) (5000µg/mL Streptomycin)
Amphotericin B (0.01µg/mL)	Lonza (250µg/mL)
Gentamicin (5µg/mL)	Sigma Aldrich (47µg/mL)
L-glutamine (0.01 µg/mL)	Gibco (200mM)

Biopsies (n=4) were collected aseptically from each interdigital skin fragment using an 8mm punch biopsy (National Veterinary Service, UK) (Figure 8.1). The base region of the biopsy was flatten using scissors in order to increase stability in the model. The surface of the biopsy was incised with a scalpel blade to simulate naturally occurring damage to the skin (required for the invasion of *D. nodosus*) prior to further washing steps.

In addition to the 8mm biopsies, skin sections of 1.5 x 1.5cm were also collected from the entire skin fragments to investigate whether a larger explant area would provide a better stability of the biopsies in the model.

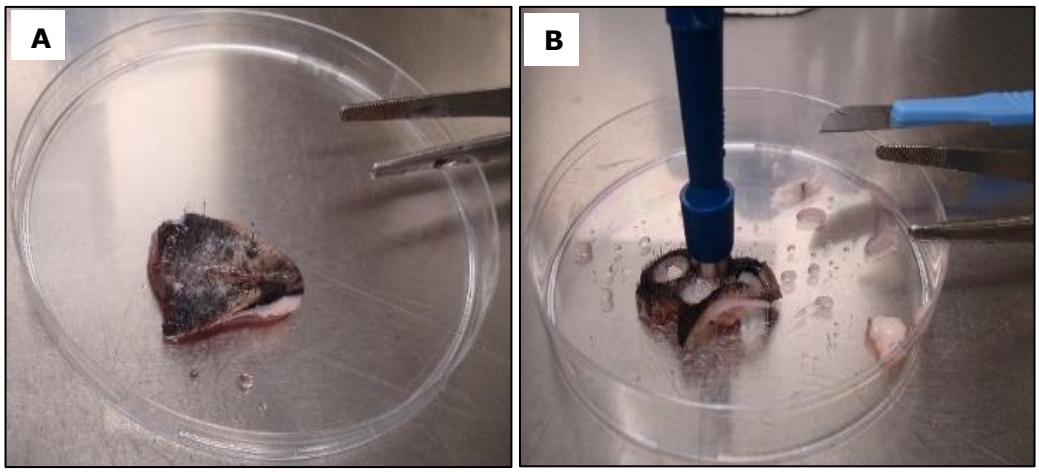


Figure 8.1 Aseptic collection of biopsies from the ovine interdigital skin under a laminar flow cabinet. Entire ovine interdigital skin fragment collected few minutes after animal slaughter (A); 3-4 biopsies were collected from the entire skin fragment using an 8mm punch biopsy (B).

Biopsies were immersed in wash medium (Table 8.2), pre-heated to 37°C, and incubated at room temperature for 15 minutes. The media change and incubation steps were repeated 3 times.

Table 8.2 Washing medium components.

Components (final concentration)	**Manufacturer (stock concentration)**
DMEM-HAM`S F12 (1:1)	Sigma Aldrich (1:1)
Penicillin + Streptomycin (20µg/mL)	Gibco (5,000U/mL Penicillin) (5000µg/mL Streptomycin)
Amphotericin B (20µg/mL)	Lonza (250µg/mL)
Gentamicin (2µg/mL)	Sigma Aldrich (47µg/mL)

Agarose pedestal and top plug: To provide a physical support for the biopsies, an agarose pedestal (500µl of 1.2% w/v agarose (Thermo Scientific, Paisley, UK) in DMEM-HAM`S F12 1:1 (Sigma-Aldrich) was added to each well of a 24 well plate (Thermo Scientific) and covered with 0.5cm^2 sterile surgical gauze (Figure 8.2). To create a semi-anaerobic environment on the surface of the biopsy and to prevent it

from drying out, an agarose top plug (300µl of 0.8% w/v agarose in DMEM-HAM`S F12 1:1) was added on the top of each biopsy.

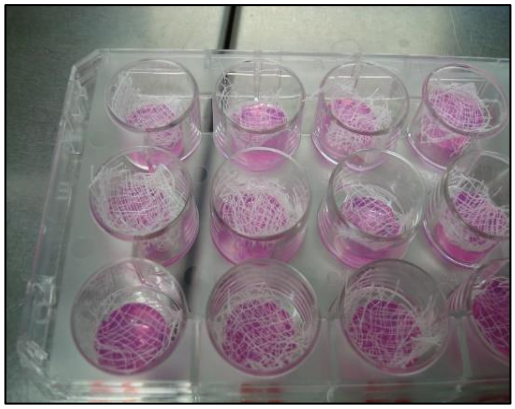


Figure 8.2 Assembling the EVOC model. An agarose pedestal was placed into each well. A surgical gauze was placed on the top of each agarose pedestal. Both were used to provide support and stability for the biopsy.

8.2.2 EVOC model viability

The viability of the model was verified over 76h of MOCK infection. Five time points were assessed; biopsy collection at the abattoir (-8h) (~30 minutes after slaughter), at mock infection (0h), 28h, 52h and 76h post mock infection. Two biopsies were collected from each time point; one placed into RNA later for RNA extraction and the other one was fixed in 10% v/v Neutral Buffer Formalin (NBF) for histological investigation (Figure 8.3). Experiments were performed in the presence and absence of 2% v/v HEPES buffer (4-(2-hydroxyethyl)-1-piperazineethanesulfonic acid) (Sigma-Aldrich) added in the culture media to investigate the impact of maintained pH. The biopsy viability was analysed assessing tissue integrity (scoring of H&E stained sections), cell viability by TUNEL staining and RNA yield.

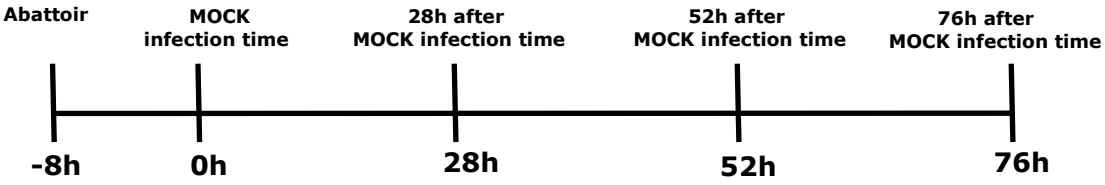


Figure 8.3 Timeline of the EVOC model viability experiment. 2 biopsies were fixed in each time point, one in RNA later for further RNA/DNA extraction and one in 10% Neutral Buffered Formalin for histological proposes. Medium without antibiotics was used from -4h to 4h.

8.2.2.1 Tissue fixing, processing & staining

Prior to embedding in wax, all samples were fixed in 10% (v/v) NBF. In order to obtain optimal tissue integrity, biopsies were fixed for 48h at 4°C and an extended tissue processing protocol was used (60 minutes in dH_2O, 4h in 50% ethanol, 4h in 70% ethanol, 16h in 90% ethanol, 4h in 100% ethanol, 4h in xylene). Biopsies were then immersed in wax (in scintillation vials) for 2h at 60°C for paraffin infiltration and then embedded in histology cassettes. Paraffin wax embedded tissues were soaked in 10% (v/v) ammoniated water for further cutting. 3µm and 6µm thick sections were cut from each block by microtome (Leica RM2255, Wetzlar, Germany) using polystyrene microscope slides (Thermo Scientific, Paisley, UK). Tissues were cut by a laboratory technician (Aziza Alibhai). Haematoxylin and eosin (H&E) stain (Sigma-Aldrich) was used to allow visual assessment of the tissue sections cut at 6µm (Appendix 3 for optimized H&E protocol). All slides were mounted with DPX (Sigma-Aldrich) after staining and were analysed by microscopy using a Heracell 150i microscope (Thermo Scientific, Paisley, UK). A trained pathologist (Dr

Kerstin Baiker), blinded to slide identity, evaluated 54 H&E-stained biopsy sections to assess tissue integrity and architecture. A qualitative, semi-quantitative scoring system was developed by the examiner to grade the tissue integrity and architecture according to histopathological features (Table 8.3 and Figure 8.4).

Table 8.3 Qualitative, semi-quantitative scoring system used to evaluate skin tissue viability for both epidermis and dermis. Developed by Dr Kerstin Baiker.

Score	**Histopathology (changes observed)**	**Tissue Viability**
0	- Acute ischaemic damage to epidermis at sample margins (necrosis) - Severe extent of all epidermal and dermal changes described below	Tissue is not viable
1 Marked:	- Multifocal subepidermal clefting - Basal cell vacuolisation (epidermal degeneration) - Nuclear pyknosis and detachment of eccrine glands, leukocytes and epidermal cells showing signs of autolysis - Multifocal pyknosis of basal cells with degenerating neutrophils, vacuolisation, supepidermal clefting, sloughed cells in glands	Tissue is viable
1.5 Moderate to marked:	- Apoptotic keratinocytes - Vacuolation of basal cells - Supepidermal clefting - Follicular epithelial cell slough - Eccrine glands and peripheral nerves show signs of autolysis, as do some follicular epithelial cells (detached)	Tissue is viable
2 Moderate:	- Subepidermal clefting - Prominent pyknotic nuclei in stratum spinosum - Some subasilar clefting around follicles - Few sloughed epithelial cells in glands	Tissue is viable
2.5 Mild to moderate:	- Scattered apoptotic keratinocytes	Tissue is viable
3 Mild:	- Normal tissue architecture and viability and occasionally few sloughed epithelial cells within eccrine glands	Tissue is viable

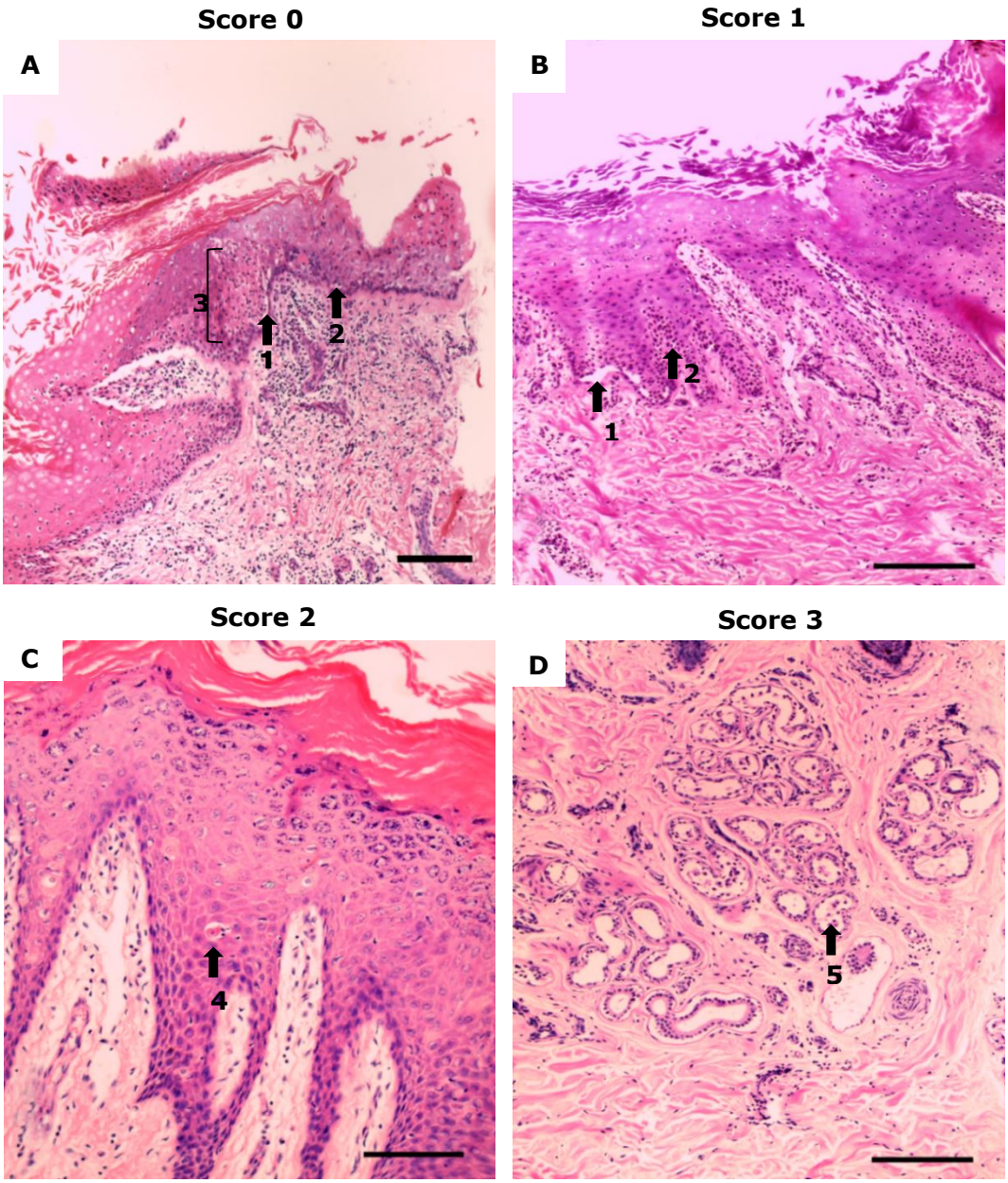


Figure 8.4 H&E images illustrating examples of the qualitative, semi-quantitative scoring system used to evaluate skin explants viability. Histological score 0 (tissue not viable) 1= subepidermal clefting, 2= basal cell vacuolisation, 3= necrotic area (A). Histological score 1 (viable tissue), marked 1= subepidermal clefting, 2= basal cell vacuolisation (B). Histological score 2 (viable tissue), mild to moderate, 4= apoptotic keratinocyte (C). Histological score 3 (viable tissue), mild, 5= (single) few sloughed cells within eccrine gland (D). Scale bar: a=200μm b=100μm c=100μm d=100μm.Scores 1.5 and 2.5 are not illustrated in this figure (for details see table 8.3). Scale bars: A=200μm B=100μm C=100μm D=100μm. Images were taken by the author of this thesis and Dr Kerstin Baiker.

8.2.2.2 TUNEL staining for cell viability detection

Detection of DNA fragments *in situ* was performed using the modified TUNEL assay (DeadEnd Colorimetric TUNEL System, Promega) in order to investigate cell death (apoptosis, necrosis and/or autolysis) (Grasl-Kraupp et al., 1995). The assays were performed according to the manufacturer's instructions using 6µm tissue sections. Cells were stripped of proteins and made permeable by incubation with 20µg/mL of proteinase K solution for 20 minutes (Promega). DAB 20x chromogen solution (Promega) incubation was performed for 3 minutes. The sections were counterstained with haematoxylin solution for 5 seconds, rinsed in tap and deionized water. All slides were mounted with DPX after staining. Negative controls were obtained by omitting the TdT enzyme from the TdT mix in the reaction (according to manufacturer's instructions). Positive controls were generated by treating a skin section with DNAse (Promega), which forced DNA fragmentation of the tissue section cells. In order to assess the number of dead and live cells, 5 non-overlapping fields from the epidermis and 5 fields from the dermis of each biopsy tissue section were used. Images were captured and analysed on a microscope using polarised light on a Leica CTR500 microscope (Leica Microsystems, Germany). All cells from all 10 images (epidermis and dermis) from each sample were counted using Fiji/ImageJ-win64 software (https://fiji.sc/, October 2016) and percentage of dead and live cells were calculated for all 10 images/sample. Brown stained nuclei were assessed as dead cells, whereas blue stained nuclei were assessed as live cells and counterstained with haematoxylin.

8.2.3 EVOC exposure to *D. nodosus*

Four experiments using explants from different sheep collected on different occasions were performed (1 experiment with HEPES buffer). Firstly, a semi-anaerobic microenvironment was produced for the model where a sterile agarose plug was placed on the top of the biopsy and incubated in a humidified tissue incubator at 37ºC (Heracell 150i, Thermo Fisher Scientific) with 5% CO_2 for 4h. 1mL of infection media without antibiotics (Table 8.4) was placed in each well. The volume of media did not flood the entire biopsy.

Table 8.4 Components of infection media without antibiotics.

Components (final concentration)	**Manufacturer (stock concentration)**
DMEM high glucose*	Gibco
DMEM-HAM`S F12*	Sigma Aldrich (1:1)
Amphotericin B (0.25µg/mL)	Lonza (250µg/mL)
L-glutamine (0.01 µg/mL)	Gibco (200mM)
10% Foetal Bovine Serum	Gibco
2% HEPES ≥99.5% (titration)	Sigma Aldrich

*DMEM high glucose + DMEM-HAM`S F12 in a proportion 3:1 (Modified from Sanders et al. 2002)

The second step involved the biopsy exposure to *D. nodosus*. To achieve that, an 8mm punch biopsy (same size of the biopsy) was used to collect aseptically a hoof agar plug confluent with *D. nodosus* on its surface (virulent strain MM261 and benign strain MM277, Appendix 4). The agar plug with confluent *D. nodosus* was placed on the top of the biopsy and 1mL of infection media without antibiotics was added into each well. The plate was incubated anaerobically

(Oxoid AnaeroGen, Thermo Scientific, Paisley, UK) for 4h at 37ºC. The third step involved the maintenance of the model with infection media containing antibiotics (Table 8.5) for 24h in a humidified tissue incubator with 5% $C0_2$.

Table 8.5 Components of infection media with antibiotics.

Components (final concentration)	**Manufacturer (stock concentration)**
DMEM high glucose*	Gibco
DMEM-HAM`S F12*	Sigma Aldrich (1:1)
Penicillin+Streptomycin (0.01µg/mL)	Gibco (5,000U/mL Penicillin) (5000µg/mL Streptomycin)
Amphotericin B (0.25µg/mL)	Lonza (250µg/mL)
Gentamicin (5µg/mL)	Sigma Aldrich (47µg/mL)
L-glutamine (0.01 µg/mL)	Gibco (200mM)
10% Foetal Bovine Serum	Gibco
2% HEPES ≥99.5% (titration)	Sigma Aldrich

*DMEM high glucose + DMEM HAM`S F12 in a proportion 3:1 (Modified from Sanders et al. 2002)

The media was changed 4h post infection and then every 12h keeping the same agar plug with *D. nodosus* on the top of the biopsy. Media supernatants were collected and stored at -80ºC for further cytokine analysis by ELISA assay. The biopsies were placed into RNA later (for DNA/RNA extraction) or 10% v/v NBF (for histology) 28h post infection with *D. nodosus* (See Figure 8.5 illustrating the timeline of the EVOC infection experiment). In all steps of this experiment, media were pre-warmed to 37ºC before being added into the well plate. Mock infected biopsies were prepared for each sheep skin fragment to determine that the tissue was negative for *D. nodosus* prior to inclusion in the EVOC model. Biopsies were divided in three groups; infected with virulent *D. nodosus*, infected with benign *D. nodosus*

and mock-infected biopsies. DNA extraction from EVOC biopsies was performed and used for the quantification of *D. nodosus* by qPCR targeting the 1*6S rRNA* gene (as described in Chapter 2). In order to calculate the load of *D. nodosus* that actually infected the model, DNA was extracted from *D. nodosus* colonies present on 8mm of hoof agar surface using the QIAamp cador kit (QIAGEN) (described in Chapter 2). The *D. nodosus* load that infected the model was estimated using the total DNA extracted from *D. nodosus* confluent on 8mm of agar surface confirmed by qPCR, as previously described (Frosth et al., 2012; Maboni et al., 2016).

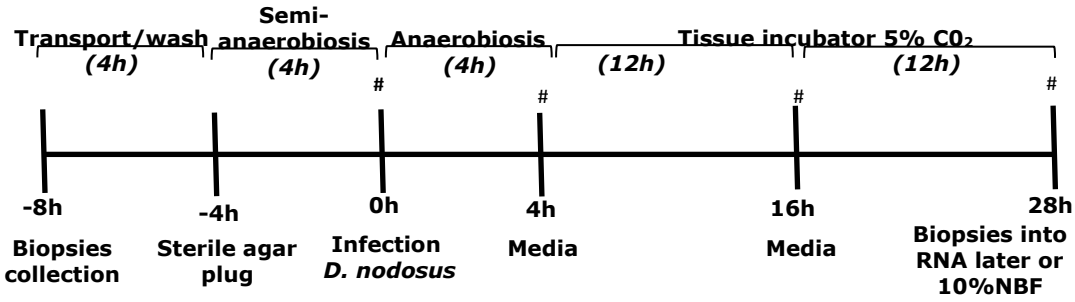


Figure 8.5 Timeline of the EVOC infection experiments. (#) Media were changed and supernatants were collected for ELISA detection of IL1β and CXCL8. Medium without antibiotics was used from -4h to 4h after infection with *Dichelobacter nodosus*.

8.2.3.1 Fluorescent *in situ* Hybridization (FISH) for *D. nodosus*

FISH analysis was performed at the Department of Pathology and Bacteriology of the Technical University of Denmark (DTU), Copenhagen. All FISH assays were performed by the author of this thesis and a laboratory technician (Annie Ravn). Moreover, all slides were analysed and scored by the author and a trained pathologist (Dr

Tim Jensen). The 16S rRNA-targeting oligonucleotide probes for *D. nodosus* (S-S-D.nodosus-443 5'-CATGCACCGTTCTTCACT-3') and eubacteria domain (S-D-eub-338-alexa 5´-GTCATTCCATCGAAACATA-3´) labelled with fluorescein isothiocyanate (FITC) or Cy3 were used on 3µm tissue sections (Rasmussen et al. 2012). Hybridization was carried out at 45°C with hybridization buffer (100mM Tris, pH 7.2, 0.9M NaCl, 0.1% sodium dodecyl sulphate) containing 5ng/ml of each oligonucleotide probe (usually double hybridizations with a FITC and CY3 labelled probe) for 16h in a Sequenza slide rack (Thermo Shandon, Cheshire, UK). After that, slides were washed with prewarmed (45°C) hybridisation buffer for 3 x 3 minutes followed by wash with prewarmed (45°C) washing buffer (100mM Tris, pH 7.2, 0.9M NaCl) for 3 x 3 minutes. Finally, they were rinsed in ultrapure water, air dried and mounted with Vectashield (Vector Laboratories Inc., Burlingame, CA). An Axioimager M1 epifluorescence microscope equipped for epifluorescence with a 100-W HBO lamp and filter sets 43 and 38 were used to visualize Cy3 and FITC, respectively. Images were obtained using an AxioCam MRm version 3 FireWiremonocrome camera and AxioVision software, version 4.5 (Carl Zeiss, Oberkochen, Germany). The total bacterial invasion of the epidermis was scored from 0 to 3 (0= no invasive bacteria, 1= low number of invasive bacteria from 1-20, 2= moderate number of invasive bacteria from 20-200, 3= high number of invasive bacteria from 200 to uncountable bacterial cells) (Modified from Rasmussen et al. 2012). Positive control tissue sample was previously prepared by the DTU group using

1ml suspension of *D. nodosus* (CCUG 27824) reference strain injected into a small sample of healthy porcine lung tissue. A negative control lung tissue without *D. nodosus* injection was also included in the analysis.

8.2.3.2 Cytokine measurement by ELISA

As part of a preliminary study, IL1β and CXCL8 were measured in supernatants harvested at 28h (12h of cytokine accumulation) at the Roslin Institute (Edinburgh) by research collaborators. Both, IL1β and CXCL8 were analysed as previously described (Doull et al. 2015). Recombinant ovine IL1β (Kingfisher Biotech, U.S.A) and CXCL8 (Wattegedera et al., 2004) were used as standards. Further assays were performed targeting only IL1β and not CXCL8 due to time limitations. All ELISA assays for IL1β were performed by a laboratory technician at SVMS (Ceri Staley). IL1β measurement was performed as previously using mouse anti-sheep IL1β monoclonal antibody (Bio-RaD, Watford, UK). Recombinant ovine IL1β was diluted from 30000mg/mL, 15000mg/mL, 7500mg/mL, 3250mg/mL, 3000mg/mL, 1500mg/mL, 750 mg/mL to 325mg/mL. The supernatants were thawed, assayed on a 96-well plate and tested in triplicates. SureBlue TMB Microwell Peroxidase Substrate Kit (KPL, Milford, USA) was used throughout. The optical density (OD) was measured using a LT-4000 microplate ELISA reader (Labtech, Hopkinton, USA) equipped with a 450-nm filter. Cytokine concentrations were extrapolated from a standard curve, which was calculated by polynomial quadratic regression using GraphPad Prism.

8.2.4 Statistical analysis

One-way analysis of variance followed by Dunn's multiple comparisons test was applied for *D. nodosus* load in infected and uninfected groups as well as for percentage of TUNEL negative cells in infected and uninfected groups. Mann Whitney (non-parametric test) was used for *D. nodosus* load and TUNEL negative cells between groups treated with HEPES buffer and for IL1β release between infected and uninfected biopsies in each specific time point. All analysis were performed using Prism (V.6.0, La Jolla, USA). A P value ≤0.05 was considered significant. *D. nodosus* qPCR data were normalised as pg of *D. nodosus* DNA present in the total DNA extracted from the skin biopsy.

8.3 Results

8.3.1 Optimisation of EVOC model

Model optimisation targeted mainly the EVOC assembly since biopsies tended to fall over in the medium during the 28h of incubation. One attempt was to use a squared skin fragment (1.5 x 1.5cm) instead of 8mm circular biopsies considering that a larger tissue area would provide a better support for the tissue. The 3 squared skin fragments used in the model over 28h of incubation demonstrated that a larger tissue area improves the EVOC assembly. The disadvantage of using skin fragments is the lack of precision of the size of fragments. Another attempt to improve the EVOC assembly was to use a squared

agar fragment (1.5 x 1.5cm) with confluent *D. nodosus* instead of a circular agar plug of 8mm (same biopsy size). A larger agar fragment than 8mm tended to balance the biopsy (8mm) and it improved EVOC assembly; however, it was difficult to cut the same agar size for all biopsies. Therefore, the calculation of the load of *D. nodosus* that infected the model and reproducibility between EVOC model set ups was not precise. RNA yield and quality deteriorated during transport and EVOC incubation. Low RNA yield and quality was measured in all EVOC biopsies ranging from 0.1–35ng/µl, except for the biopsy palced into RNA later at the abattoir few minutes after slaughter (132.3 ng/µl). In an attempt to improve the RNA quality and yield, as well as cell/tissue viability, HEPES buffer was added in the culture media in order to maintain physiological Ph, however, the addition of HEPES buffer did not improve the RNA quality and yield of the EVOC biopsies. A schematic overview of the EVOC optimization and improvements is displayed in Figure 8.6.

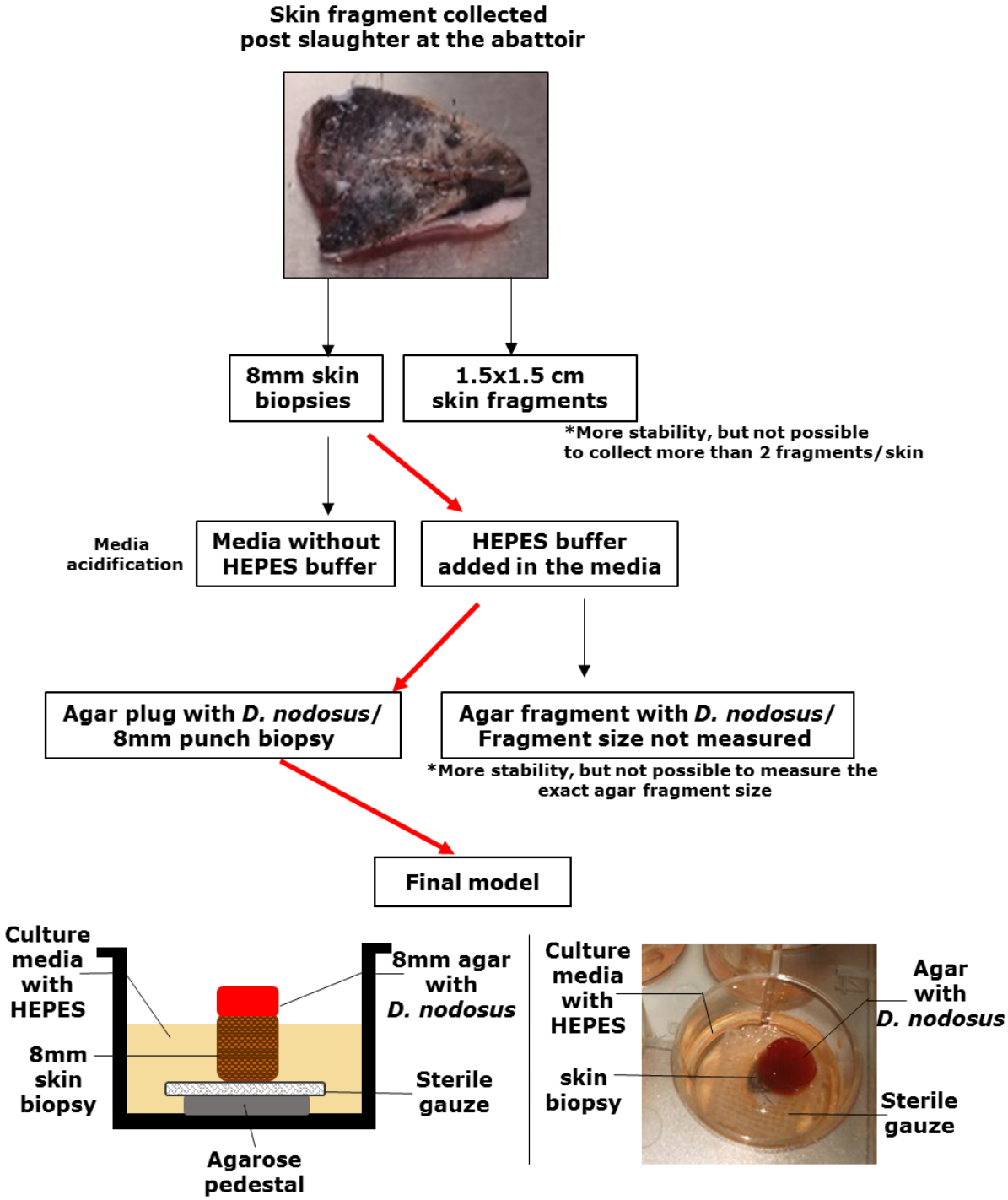


Figure 8.6 Schematic overview of EVOC model optimization and improvements. Red arrows lead to improved methods.

The final and complete procedures used to assemble and infect the EVOC model with *D. nodosus* are summarised in Figure 8.7.

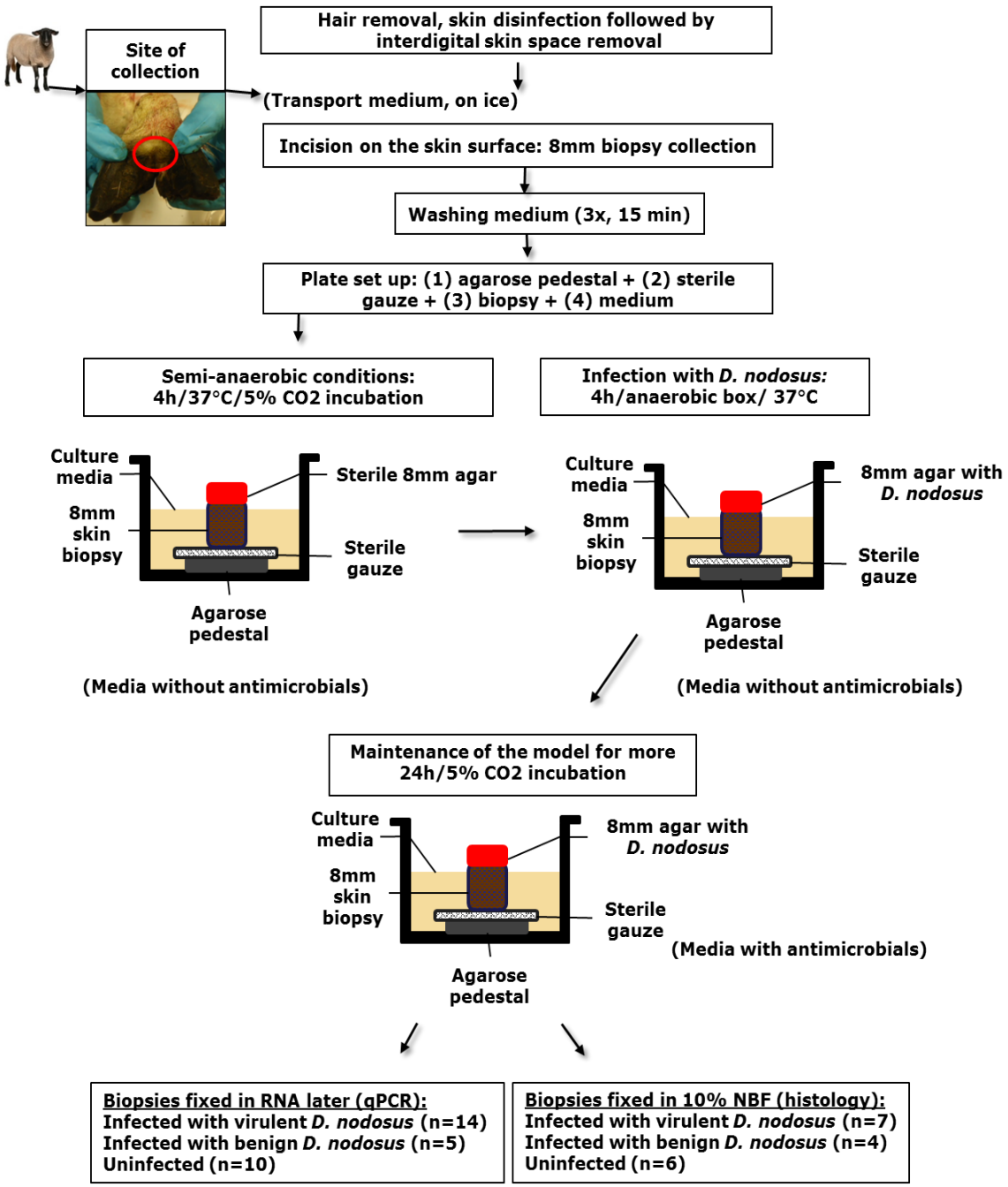


Figure 8.7 Final EVOC protocol. Steps from biopsy collection at the abattoir to infection with *Dichelobacter nodosus* and fixation of biopsies in 10% NBF and RNA later.

8.3.2 Tissue integrity and cell viability over a 76h mock infection

Tissue integrity (H&E) and cell viability (TUNEL staining) were assessed over a 76h mock infection time course (-8h (at abattoir), 0h, 28h, 52h and 76h) in order to investigate the maintenance of tissue viability during incubation (Figure 8.3 for timeline of model viability experiment). Overall, tissue biopsies maintained the normal architecture for up to 76h of culture. However early signs of lack of tissue viability, such as basal cell vacuolisation, subepidermal clefting, sloughed cells in glands and follicular epithelial cells were observed in biopsies cultured for 52h and 76h (histopathological scores 1-1.5).

Regarding the TUNEL staining, the percentage of live cells in the epidermis decreased from -8h (abattoir; 99% (2497/2524)) to 76h of incubation (45% (296/660)) (Figure 8.8, and 8.9 A). In contrast, a higher percentage of live cells was found in the dermis in all time points, with a slight decrease from -8h (99.3% (2092/2105)) to 76h (84% (952/1131)) (Figure 8.9 B). Biopsies fixed at the abattoir had a low level of dead cells, which was expected to be the normal process of cell cycle. An observation made during the TUNEL staining analysis was that tissue sections presented a higher concentration of cell death in the core tissue cells while the margin cells tended to be more viable; this effect was not quantified. The comparison of cell viability and tissue integrity revealed samples with epidermis and dermis presenting high percentage of live cells (TUNEL) also presented with a well preserved tissue architecture (H&E tissue viability scores)

(Figure 8.9). In summary, at 28h of incubation more than 50% of the epidermal as well as dermal cells presented live cells and the tissue architecture was preserved. Hence this time point was decided as the most suitable for further EVOC infection with *D. nodosus*.

HEPES buffer was added in the culture media in an attempt to improve the tissue maintenance during incubation since this buffer helps to stabilize the medium pH. Regarding the model viability experiment, biopsies treated with HEPES presented a higher percentage of live cells in the epidermis than those not treated with this buffer in the time course of 0h (81% (598/737)), 28h (85%(662/779)), 52h (83% (920/1105)) and 76h (45% (296/660)) (Figure 8.9 A). This positive effect of HEPES buffer was observed in both epidermal and dermal cells, but more evident in epidermal cells (Figure 8.9 A-B).

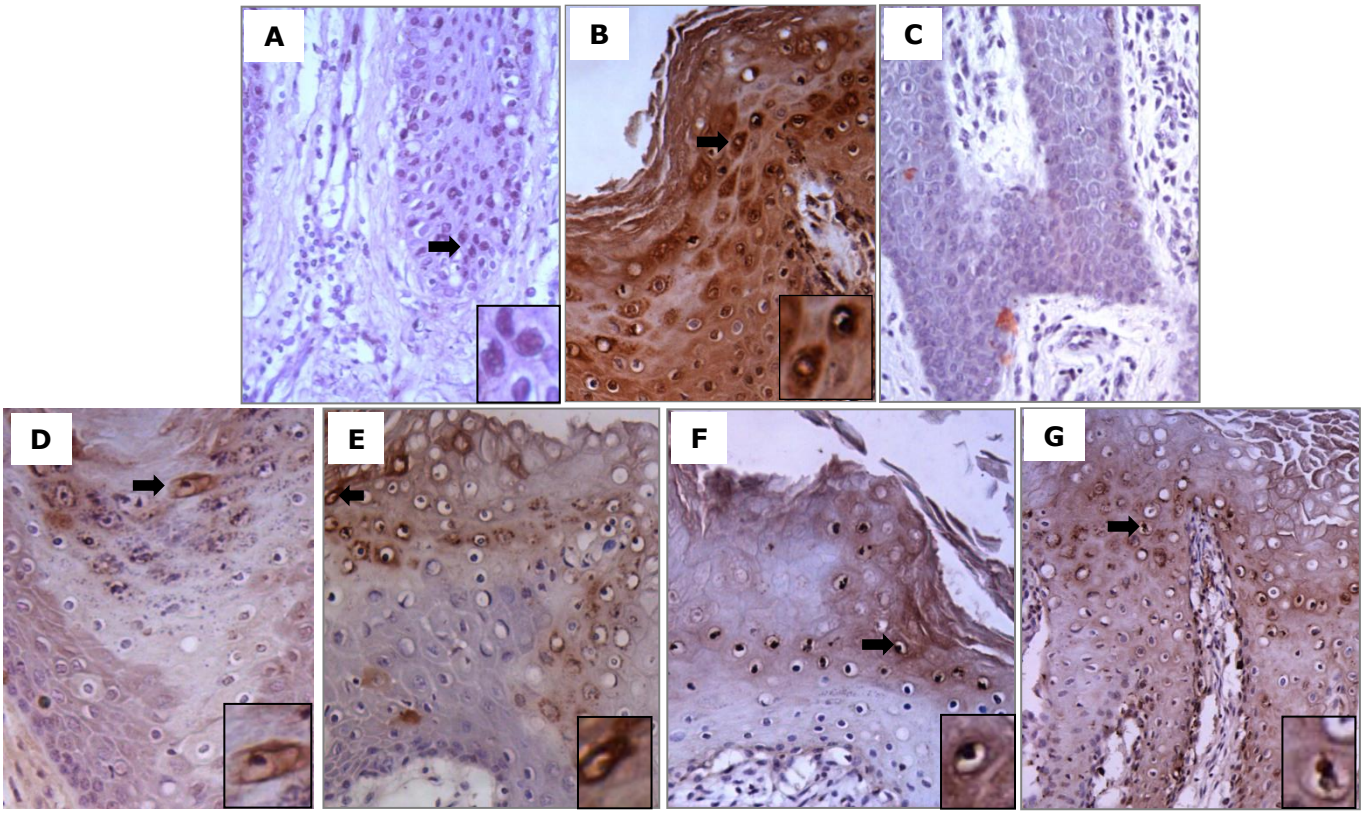


Figure 8.8 Demonstration of DNA fragmentation (TUNEL) in epidermal cells of the skin explants over a time course of 76h. (A) Negative control slide of the TUNEL assay (tissue section not treated with DNAse); (B) Positive control slide of the TUNEL assay (tissue section treated with DNAse); (C) Skin explant fixed in NBF10% at -8h (biopsy fixed at the abattoir); (D) 0h (biopsy fixed at MOCK infection time); (E) 28h (biopsy fixed 28h after MOCK infection time); (F) 52h (biopsy fixed 52h after MOCK infection time); (G) 76h (biopsy fixed 76h after MOCK infection time). Purple nuclei: live cell (TUNEL negative suggesting there was no DNA fragmentation); Brown nuclei: dead cell (TUNEL positive revealing DNA fragmentation).

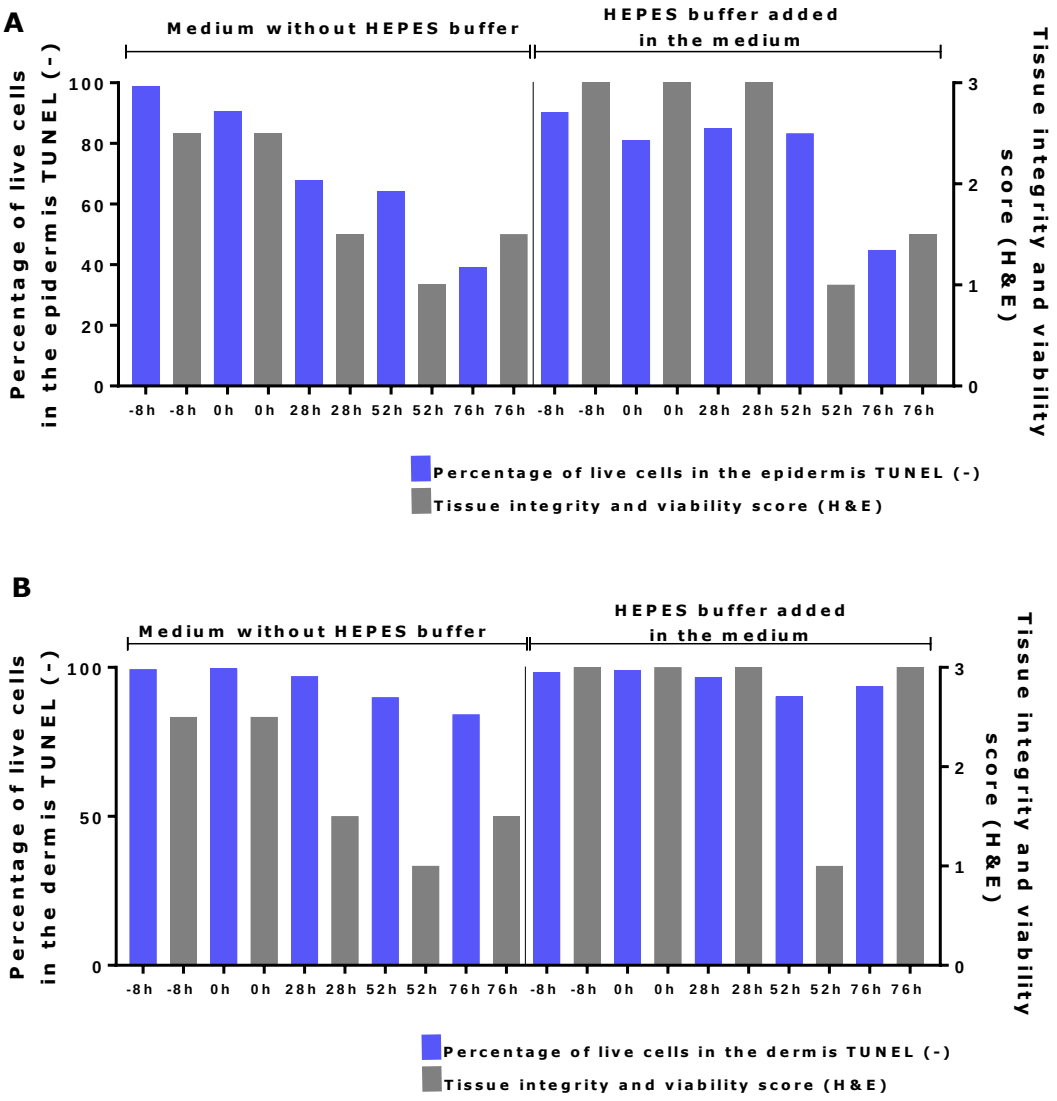


Figure 8.9 Comparison of cell viability (TUNEL) and tissue integrity (H&E scores). Percentage of TUNEL-negative (live cells) in the epidermis (A) and dermis (B) of ovine interdigital skin biopsies incubated in the EVOC model in different time points in comparison with tissue integrity scores obtained by H&E stain (histological scoring system in Table 8.3). Blue bar graphs indicate percentage number of TUNEL-negative cells. Grey bar graphs indicate tissue integrity and viability score (H&E). Each bar indicates single biopsies. -8h (biopsy fixed at the abattoir); 0h (biopsy fixed at MOCK infection time); 28h (biopsy fixed 28h after MOCK infection time); 52h (biopsy fixed 52h after MOCK infection time); 76h (biopsy fixed 76h after MOCK infection time).

8.3.3 Ovine interdigital skin explant as an infection model for *D. nodosus*

The ovine interdigital skin explants of the EVOC model were infected with both virulent and benign *D. nodosus* during 28h (Figure 8.7 for final infection protocol). Further analysis included the measurement of cytokines in the media supernatant. The *D. nodosus* load varied in each 8mm agar area from the same plate since *D. nodosus* growth is not confluent on the entire agar area. Therefore, it was not possible to assure that all biopsies were exposed to the same *D. nodosus* load. It was estimated that 1.14pg/ul of virulent *D. nodosus* DNA (strain MM261) was present was present on 8mm agar area, and 1.8pg/ul of benign *D. nodosus* DNA (strain MM277) was present in 8mm agar area.

Detection of D. nodosus by qPCR

The presence of *D. nodosus* DNA was investigated in infected and uninfected control biopsies using qPCR to confirm the model infection. All infected biopsies with virulent (n=6) and benign *D. nodosus* (n=6) strains were positive in the qPCR targeting the *16S rRNA* gene of *D. nodosus*. In contrast, all uninfected biopsies (n=7) were negative for *D. nodosus*. A higher but not statistically significant difference was found for the load of *D. nodosus* in biopsies infected with a benign strain in comparison with biopsies infected with a virulent strain; however, no further conclusions can be made since it was not possible

to assure that the same bacterial load was used to infect all biopsies (Figure 8.10 A). Biopsies treated with HEPES buffer (n=8) had a higher load of *D. nodosus* than biopsies treated without HEPES buffer (n=12) ($P \leq 0.0001$).

Detection of D. nodosus by FISH

We used FISH to further investigate whether the *D. nodosus* cells were mainly localised on the skin surface or within the tissue. Hybridized *D. nodosus* cells were identified in the positive lung tissue control and in all EVOC biopsies infected with either virulent (n=7) or benign *D. nodosus* (n=4). Negative lung tissue control and all uninfected EVOC biopsies were negative for *D. nodosus* (n=5) (Figure 8.11). *D. nodosus* cells were identified on the skin surface (Figure 8.11 C, D), and invading the superficial layers of the epidermis (Figure 8.11 E, F and G). When present on the surface, *D. nodosus* tended to be organised in clusters of cells while within the tissue it was identified as single cells invading the superficial epidermal layer. *D. nodosus* cells were not identified in the dermis. In order to have a quantitative approach for the FISH results, a scoring system adopted from Rasmussen et al. (2012) was used. *D. nodosus* cells were counted and then scored according to the number of cells present in the entire tissue section (Appendix 5). A general eubacterial domain probe did not detect the presence of other bacteria in any infected or uninfected tissues. In summary, ovine interdigital skin explants were used as a model for *D. nodosus* infection. Both virulent and benign strains of *D.*

nodosus could successfully infect and penetrate the skin biopsies during 28h of model incubation.

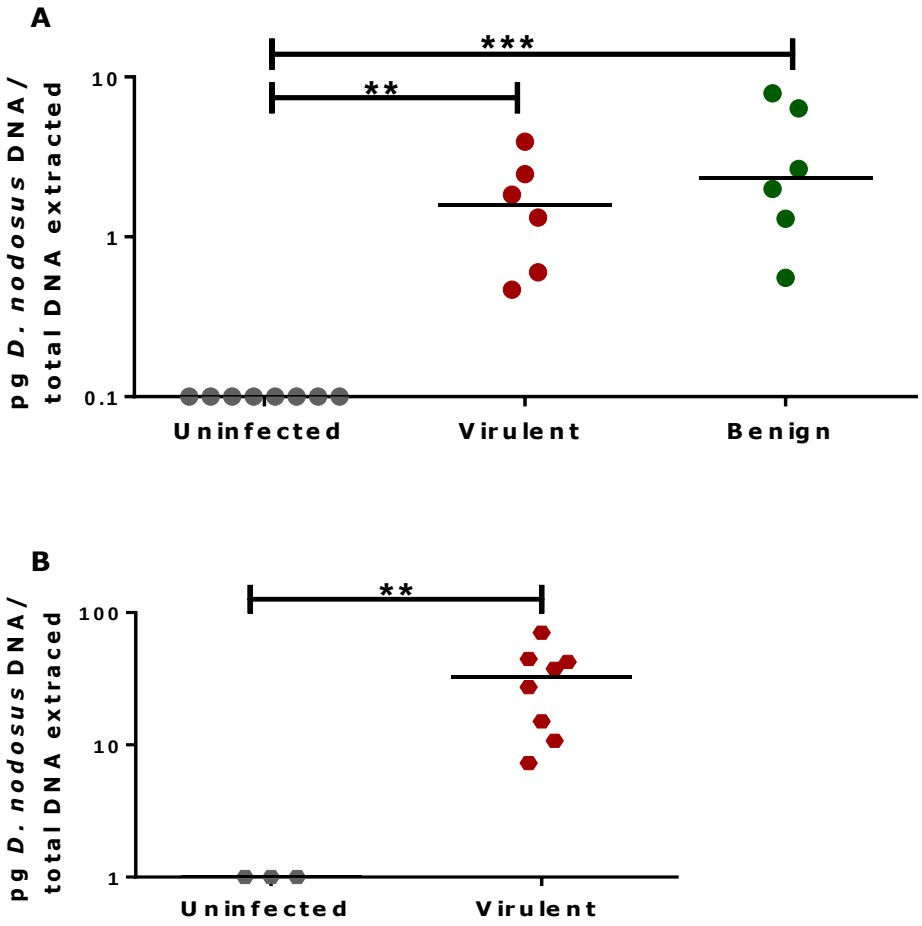


Figure 8.10 EVOC model infection with *Dichelobacter nodosus* virulent and benign strains. All infected biopsies were positive for *D. nodosus* using a qPCR assay targeting the *16S rRNA* gene. All uninfected biopsies were negative for *D. nodosus (*0.1 and 1= results below of the detection limit). Experiment without HEPES buffer (A) and with HEPES buffer (B). Data were analysed by Dunn's multiple comparisons test (A) and Mann Whitney (non-parametric) (B) using GraphPad Prism. *P≤0.05, **P≤0.01. Each point indicates single biopsies. Strains used to infect the model: virulent *D. nodosus* MM261 and benign *D. nodosus* MM277.

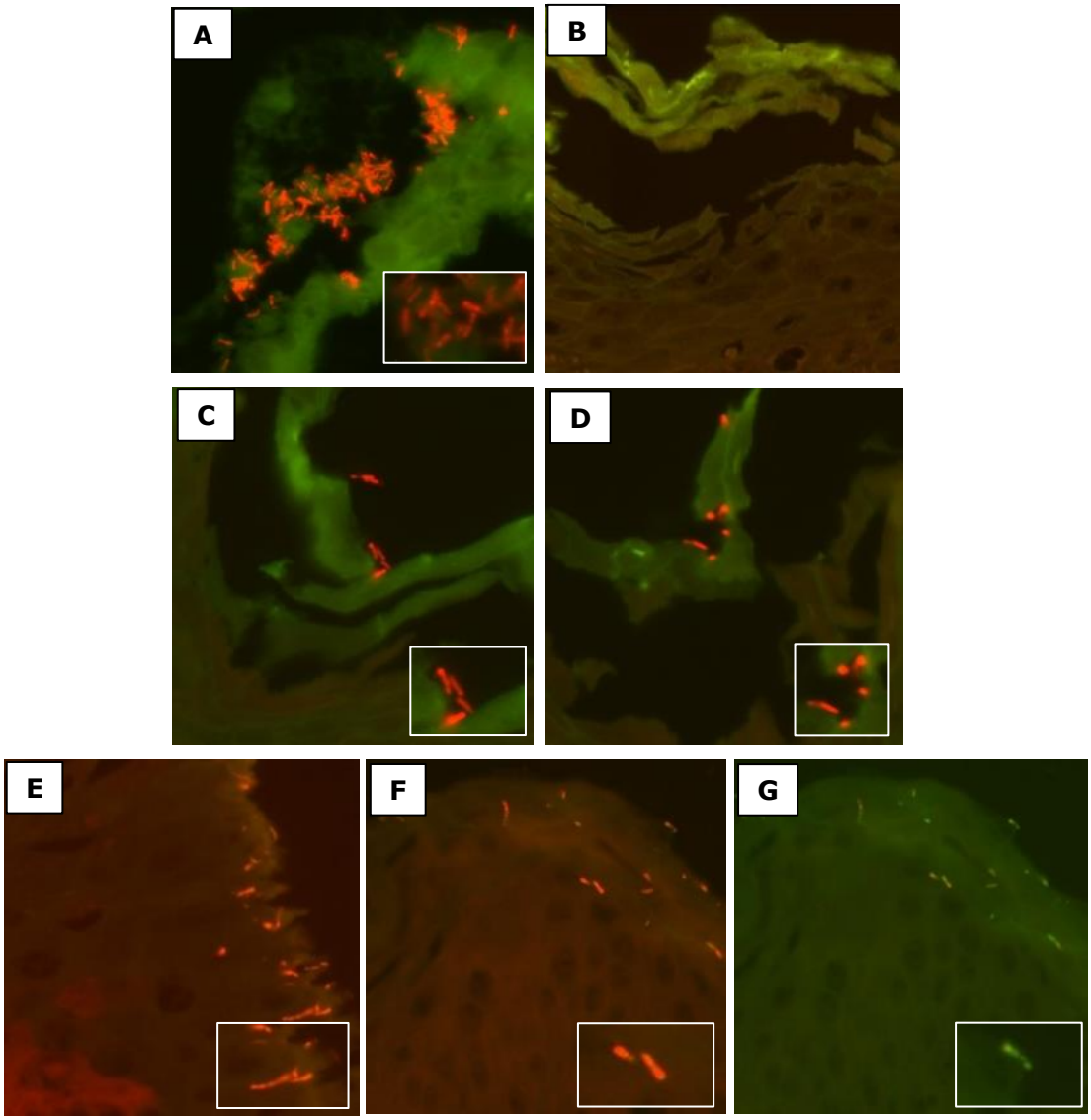


Figure 8.11 Fluorescent *in situ* Hybridization (FISH) on ovine interdigital skin biopsies from the EVOC model (B, C, D, E, F and G). Positive control using a healthy porcine lung tissue injected with *D. nodosus* reference strain (CCUG 27824) (red/orange) (A); EVOC uninfected negative control (B); Demonstration of benign *Dichelobacter nodosus* (red/orange) (C, D) and virulent *D. nodosus* (E, F red/orange and G green) infecting the epidermis of biopsies from the EVOC model. 40x magnification. Strains used to infect the model: virulent *D. nodosus* MM261 and benign *D. nodosus* MM277. Images correspond to biopsies not treated with HEPES buffer.

8.3.3.1 Tissue integrity and cell viability after 28h of bacterial infection

Tissue integrity and cell viability from infected and uninfected biopsies were assessed in order to investigate the effect of bacterial infection on model viability and maintenance. In the histopathology analysis, all uninfected control biopsies presented viable epidermis and dermis (median histopathology score 2.5, range 1.5-3), except for one biopsy (score 1.5) (Figure 8.12 A). Similarly, all infected biopsies with either virulent or benign *D. nodosus* presented viable tissues (median histopathology score 2), except two biopsies (1 and 1.5 scores) (Figure 8.12 A). Additionally, all infected and uninfected control biopsies presented more than 50% of epidermal and dermal live cells, except one biopsy infected with a virulent *D. nodosus* strain (Figure 8.12 B). There was no statistical significant difference between infected and uninfected biopsies for the percentage of live cells in the epidermis and dermis (Figure 8.12 B-C). In summary, 28h of *D. nodosus* infection showed no negative effect on tissue integrity/architecture and in the cell viability.

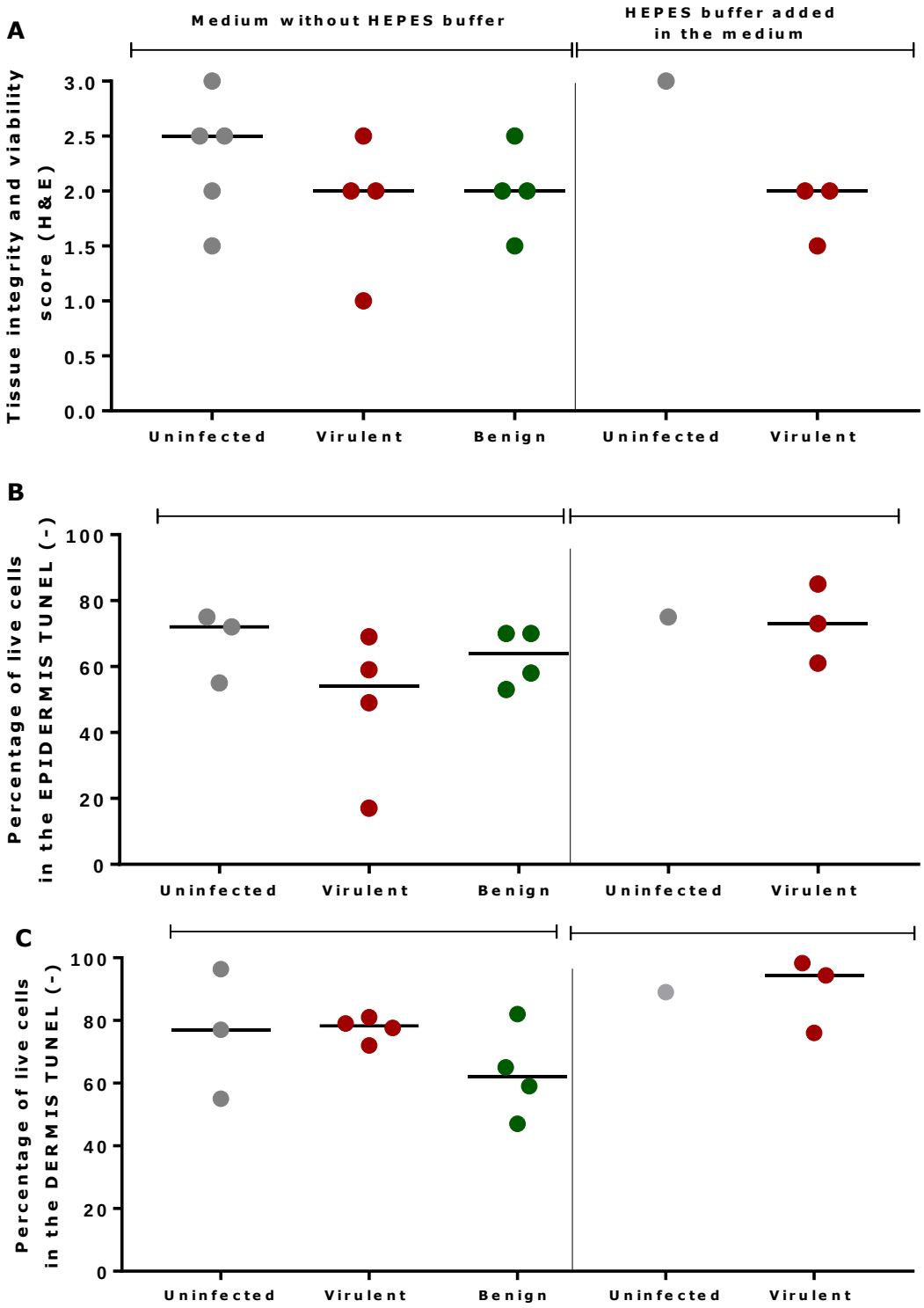


Figure 8.12 Tissue integrity and cell viability after 28h of infection with *D. nodosus*. Tissue integrity scores of EVOC biopsies (A). Percentage of live cells (TUNEL-negative) in the epidermis (B) and dermis (C) of EVOC biopsies. Each point indicates single biopsies. Black bars indicate median. Strains used to infect the model: virulent *D. nodosus* MM261 and benign *D. nodosus* MM277. Data were analysed by Dunn's multiple comparisons test (B and C, medium without HEPES buffer) and Mann Whitney (non-parametric) (B and C, medium with HEPES). $P \leq 0.05$ was considered significant. Data were analysed using GraphPad Prism.

8.3.3.2 Release of cytokine in the media supernatants following infection with *D. nodosus*

Results from the EVOC preliminary experiment showed that all biopsies infected with virulent and benign *D. nodosus* released IL1β and CXCL8 in the supernatants harvested at 28h after *D. nodosus* infection (12h of cytokine accumulation in the media). All supernatants from uninfected controls were negative for both IL1β and CXCL8 (Figure 8.13). (ELISA performed by research collaborators at the Roslin Institute, Edinburgh).

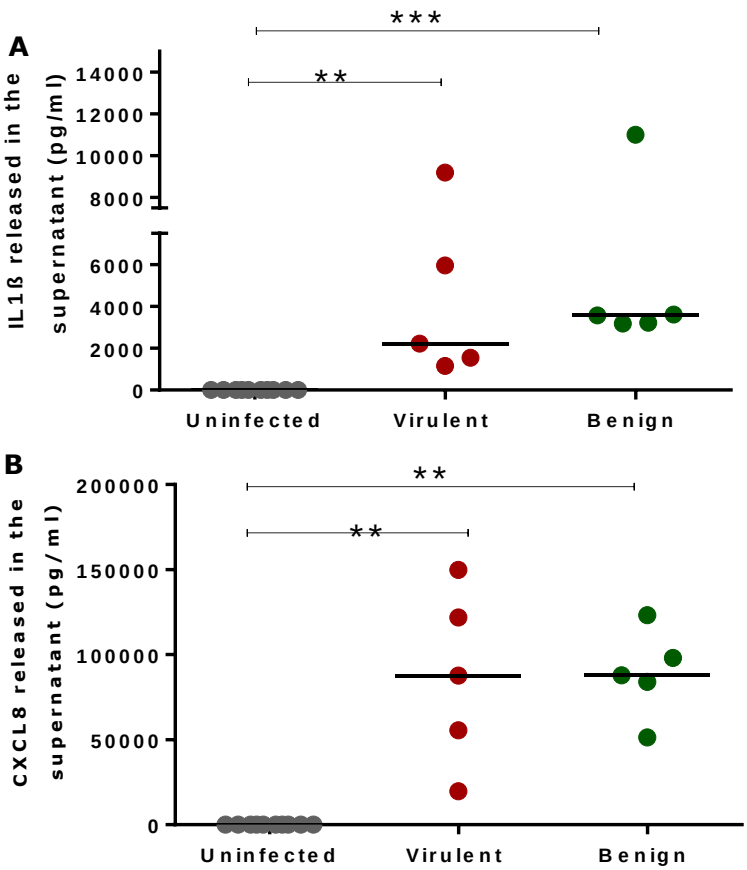


Figure 8.13 Preliminary experiment. Release of IL1β (A) and CXCL8 (B) in the media supernatants following infection with *D. nodosus*. Supernatants were harvested at 28h after infection= 12h of accumulation of IL1β during model maintenance in a tissue incubator with 5% CO_2. Each point indicates single biopsies. Data were analysed by Dunn's multiple comparisons test. **P ≤0.01, ***P ≤0.001. Strains used to infect the model: virulent *D. nodosus* MM261 and benign *D. nodosus* MM277. Data were analysed using GraphPad Prism. Uninfected biopsies n=7; biopsies infected with virulent *D. nodosus* n=5; biopsies infected with benign *D. nodosus* n=5.

The optimized ELISA protocol was then applied to measure IL1β in the media supernatants from two EVOC experiments, one without addition of HEPES buffer in the culture media (Figure 8.14 B), and one with HEPES buffer in the media (Figure 8.14 C). A total of 4 uninfected control biopsies and 8 infected biopsies with *D. nodosus* were included in the experiment without HEPES buffer. From this experiment, EVOC biopsies infected with both virulent and benign *D. nodosus* released IL1β in the media supernatants that were accumulated between 4-16h and 16-28h post infection (12h of accumulation each time point). At 16h, IL1β concentration in infected biopsies was significantly greater than in uninfected controls ($P \leq 0.05$) (Figure 8.14 B). At 28h, the accumulation of IL1β was higher than in uninfected controls, but this difference was not statistically significant (Figure 8.14 B). All supernatants from uninfected and infected biopsies harvested at -4h mock infection and 4h after infection (4h of accumulation) were negative or showed very low concentration of IL1β. In addition, biopsies treated with HEPES buffer released higher amounts of IL1β than the untreated ones (Figure 8.14 C), which might be associated with a higher *D. nodosus* load present in these biopsies. The detection of CXCL8 was not investigated in these samples due to time limitations.

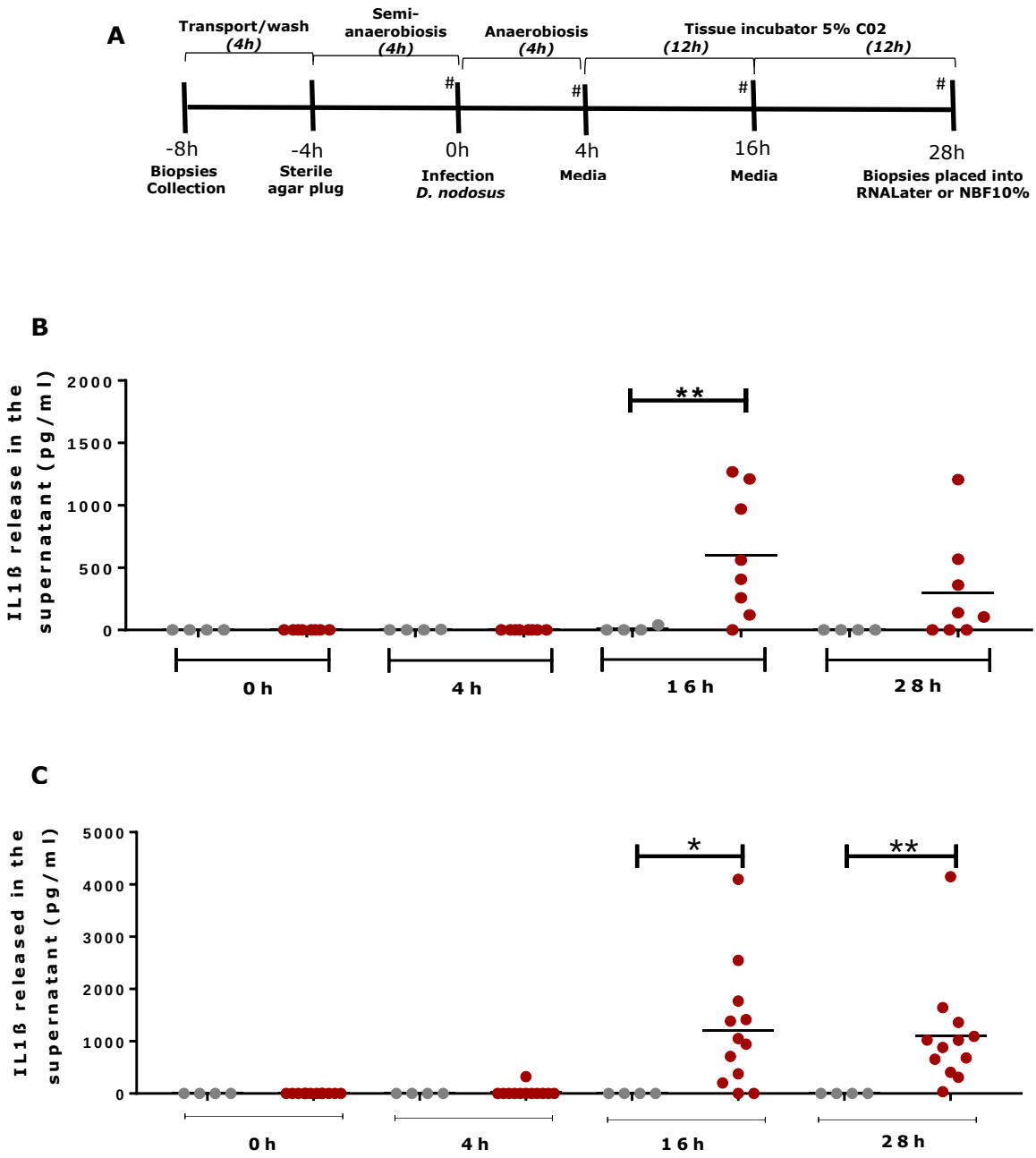


Figure 8.14 Detection of IL1β in the media supernatants of the EVOC model by ELISA. Timeline of the EVOC model infection highlighting the time points where the media supernatants were collected (#) (A). Accumulative detection of IL1β in uninfected and infected biopsies with *D. nodosus* in different time points. 0h= total accumulation of IL1β in the media supernatant during -4h to 0h of semi-anaerobic conditions (mock infection); 4h= total accumulation of IL1β in the media supernatant from 0h to 4h post infection with *D. nodosus*; 16h and 28h= total accumulation of IL1β post infection with *D. nodosus* during model maintenance in a tissue incubator (B). Experiment performed with the addition of HEPES buffer in the culture medium (C). Mann Whitney (non-parametric) was performed for comparison between uninfected and infected biopsies, *P≤0.05, **P≤0.01. Grey circles represent mock infected biopsies (controls n=4) and red circles represent infected biopsies with *D. nodosus* (n=8 B) (n=12 C).

8.4 Discussion

This project optimized a 3D skin culture model using *ex vivo* skin explants collected from sheep post slaughter, hence developing a model with original host explants without relying on the use of rodents to study a sheep disease. The key findings of this study include the presence of both virulent and benign strains of *D. nodosus* in tissues after 28h of infection, and the release of cytokines in the media supernatant highlighting an initial inflammatory response to *D. nodosus*. In this context, considering the limited amount of information on the host immune response to footrot, this study provides further evidence on early local inflammatory responses to *D. nodosus*. To our knowledge, this is the first study to establish a 3D culture model using skin explants to investigate ovine footrot.

Replicating the natural in vivo conditions leading to footrot occurrence

Preliminary damage of the epidermis is necessary for *D. nodosus* to establish itself in the interdigital skin microenvironment and then initiate footrot lesions (Beveridge, 1941; Kennan et al. 2001). Hence, the epidermis of EVOC biopsies were lacerated using a scalpel before infection with *D. nodosus* in order to replicate conditions as found *in vivo.* Wet environmental conditions are another risk factor for interdigital skin damage (Beveridge, 1941; Wassink et al. 2004). In the UK, sheep are likely to graze on muddy pastures throughout the year since there is no specific seasonality for wet conditions (Smith

et al. 2014). The mud-covered damp skin microenvironment may provide the necessary semi-anaerobic conditions for *D. nodosus* survival. For *in vivo* studies, sheep were kept for four days upon wet foam mats leading the interdigital skin to macerate and providing wet conditions prior to infection with *D. nodosus* (Kennan et al. 2001; Kennan et al. 2010). In the present study, skin explants were never allowed to dry out during transport and were kept moist and semi-anaerobic through agarose and agar plugs prior and throughout the infection model. Moreover, footrot has been reported to be a localised foot infection with little or unknown involvement of the ovine systemic response (Davenport et al. 2014). In this context, this model represents a suitable approach to investigate footrot in local cellular components since biological processes may be observed without any systemic influence. As the model was not connected to the vascular or lymphatic system, all responses observed were solely due to the skin cells present in the tissue biopsies and the conditions they were exposed to during experimentation.

Factors affecting the maintenance of EVOC skin biopsies in vitro

Histological assessment and TUNEL assay have shown that tissue structure and cell viability were maintained over 76h of incubation, with only minor signs of tissue degeneration in biopsies incubated for more than 52h. Aspects that may have affected tissue survivability include animal age and breed, equal distribution of nutrients within the tissue, culture media pH and antimicrobial toxicity in the tissue

explants. In this study, a heterogeneous population of sheep feet collected at the abattoir of unknown breeding, age, and previous feet clinical status were used. It may have influenced the tissue viability, however this study lacks this information since the animals were sampled in the processing line of an abattoir. Previous studies observed that animal age, measured from 5 to 10 weeks, may influence porcine gut explant survival time, most likely due to diet differences and their impact on gut commensal microorganisms (Costa et al. 2016). Also foetal explants have been reported to maintain tissue viability for prolonged periods of *in vitro* incubation due to their physiological state of morphogenesis, which contributes to survival under *in vitro* condition with low levels of oxygen (Abud et al. 2005; Quinlan et al. 2006).

3D tissue culture models may also be affected by different cell viability in outer layers compared to core cells. The outer layers of an explant, which is highly exposed to the medium, are mainly comprised of viable, proliferating cells; however, the core cells receive less oxygen, growth factors and nutrients from the medium, and tend to be in a quiescent or hypoxic state (Khaitan et al. 2006). This effect was also observed (though not quantified) in the present study. TUNEL staining of tissue sections appeared to have a higher level of cell death in the core tissue cells while the margin cells tended to be more viable. Future work on this model is necessary to accurately quantify and therefore confirm this observation. HEPES addition in the culture media improved cell survivability over time with increased cell

viability and less marked signs of early tissue degeneration. This is most likely due to the increase in buffer capacity and hence more stable physiological pH. Mammalian primary cells need a stable pH (~7) to survive *in vitro* conditions. Previous publications on ovine skin cell culture have mentioned the use of HEPES in the culture media (Withers et al. 1986); however, the influences of buffer systems in ovine cell culture models have not been analysed in detail. Reports on bovine chondrocytes (Xu et al., 2007) and human lymphocytoid cell lines (Chagnon & Corbeil 1973) showed that the presence of HEPES in culture medium improved cell viability. Further experiments with a higher number of samples and repeated experiments are necessary to establish further conclusions on the effect of HEPES buffer in tissue viability and maintenance.

Antibiotics and antifungal agents were essential in the washing medium in order to eliminate microorganisms from the ovine biopsies to prevent contamination. However, a detrimental effect of antibiotics has been described in human keratinocyte culture (Gibson et al. 2008), and in porcine gut explants cultured *in vitro* (Costa et al. 2016), which presented a lower epithelium coverage when compared with explants not treated with antimicrobials (Costa et al. 2016). Since 3D models lack circulatory and excretion systems, it is likely that cytotoxic effects may happen due to accumulation of antimicrobials in the tissue explants (Levy, 2000). Moreover, the addition of antimicrobials in the incubation media has an effect on the interdigital skin microbiota. The role of the ovine interdigital skin

microbiota in footrot remains unclear, but it has been suggested that *D. nodosus* and other microorganisms might have a synergistic relationship in the pathogenesis of footrot (Maboni et al. 2016; Maboni et al. 2017). Therefore, the absence of these microorganisms may affect mechanisms of *D. nodosus* establishment in the skin biopsies. However, these disadvantages can be minimized but not completely avoided since the use of antibiotics is imperative to control overgrowth of bacteria and fungi in the EVOC model (Davenport, 2011).

Moreover, to investigate factors related to EVOC viability, TUNEL staining was used to measure DNA fragmentation on skin cells. Several reports highlight the usefulness of this method (Jarvis et al. 2002; Lu et al. 2007; Garrido-Fariña et al. 2008). It is well established that the TUNEL method fails to discriminate between apoptosis, necrosis and autolysis processes of cell death (Grasl-Kraupp et al. 1995). For clarity, the present study reported `cell death' as a general term for any cell death that leads to DNA fragmentation. The lack of apoptosis specificity of the TUNEL assay could represent an advantage for this study considering that other cell death processes might be more prominent under the experimental conditions of the EVOC model. Autolysis, for instance, is the degradation of the parts of a cell by its own enzymes mainly after death (Kumar et al. 2014) and it is likely to be the most prominent cell death process occurring in the *post mortem* skin explants used in the EVOC model. Importantly, a certain level of apoptosis was mainly expected in the epidermis of the

skin explants due to the natural life cycle of keratinocytes (Lippens et al., 2005).

EVOC model infection with D. nodosus

The EVOC model was effectively infected with both virulent and benign strains of *D. nodosus*, as shown by the results from qPCR and FISH. The presence of *D. nodosus* in healthy ovine interdigital skin tissues has been reported (Calvo-Bado et al. 2011; Maboni et al. 2016), hence there was no guarantee that apparently healthy ovine feet would be free of *D. nodosus* colonisation prior to model infection. The absence of *D. nodosus*, under the limit of the qPCR detection, in all uninfected control biopsies suggests that the washing time and antibiotic concentrations used in the model likely destroyed any *D. nodosus* in the interdigital skin. FISH was an invaluable tool to prove that *D. nodosus* cells were present not only on the skin surface, but also invading the tissue. Multiple *D. nodosus* cells invading the epidermis were detected in all infected biopsies localised in the stratum corneum and most superficially in the stratum granulosum. The findings of the current study are similar to those by Witcomb et al. (2015), which also localized *D. nodosus* within the superficial epidermal layer of sheep affected with interdigital dermatitis and footrot. A previous study hypothesized that the initial site of *D. nodosus* attachment during infection was at the superficial epidermal layer, and degradation of keratin in this area by virulent *D. nodosus* was likely to be required to break through the skin horn junction.

Hence, this allowed the subsequent underrunning of the horn by *D. nodosus* (Kennan et al. 2010). Therefore, the visualization of *D. nodosus* organisms in the superficial epidermal layer of the EVOC biopsies provides additional evidence for this hypothesis. Whether *D. nodosus* cells would have been located in deeper epidermal layers if the model was incubated for longer than 28h is a question to be further investigated. A general eubacterial domain probe did not detect the presence of other bacteria in any infected or uninfected tissues. It could be postulated that the antimicrobial washing incubation might have eliminated most of the bacterial community present on the surface and likely within the tissue biopsies.

Tissue inflammatory response to D. nodosus infection

We further investigated the inflammatory response after bacterial challenge to determine the immunological functionality of the cultured skin. Moreover, identification of cytokines released by the EVOC tissues in response to bacterial invasion is essential to our understanding of disease pathogenesis and the development of innate immunity. In this study, the cytokine patterns and concentrations released varied between biopsies infected with benign and virulent *D. nodosus*. Importantly, all uninfected controls did not release cytokines in the media supernatants. Taken these results together, it was demonstrated that IL1β and CXCL8 molecules released in the media are specifically associated with a local early inflammatory response to *D. nodosus* after 16-28h of challenge. Similar results

were found using a human skin EVOC model, where mRNA expression of *IL1α*, also from the interleukin 1 family, and *CXCL8* were significantly high in response to *Staphylococcus aureus* and *Pseudomonas aeruginosa* skin infection (Steinstraesser et al. 2010). Similarly, mRNA expression levels of *IL1β* and *CXCL8* were increased after human skin equivalents exposure to *Acinetobacter* spp., but IL1β protein, however, was undetectable in the media supernatant (de Breij et al., 2012). In this context, our findings provide additional evidence on the role of IL1β and CXCL8 in skin bacterial infections and more specifically in response to *D. nodosus* and pathogenesis of ovine footrot. As described in Chapter 6, high mRNA expression of *IL1β* and *CXCL8* were associated with high *D. nodosus* load in footrot samples collected from naturally infected sheep. Moreover, an increased mRNA expression of *IL1β* in biopsies from affected feet as well as an increased mRNA expression of *IL1β* in ovine fibroblasts challenged with heat-killed extracts of *D. nodosus* was previously reported (Davenport et al. 2014). These previous studies were all based on transcriptional level of immune molecules, hence the detection of cytokines in the media supernatants using ELISA suggests the viability of the EVOC model to analyse inflammatory response to bacterial infection at the protein translational level.

8.5 Future work and EVOC applications

Several experiments could be performed using the EVOC model in order to generate new insights into the pathogenesis of ovine footrot.

Due to time limitations, this study was restricted to investigate whether the model could be infected with *D. nodosus* and whether there was an initial immune response to bacterial infection after 28h of infection.

Future work to improve model viability and stability

In terms of model incubation period, a time longer than 28h of model exposure to bacteria would more realistically mimic the chronic development of footrot, but this extended period of bacterial exposure would need close monitoring of tissue architecture and cell viability. Taking into account that HEPES buffer improved the tissue viability at 76h of a MOCK experiment (without infection), we can postulate that the tissue would maintain its integrity and cell viability up to 76h of bacterial infection. Importantly, more experiments with HEPES buffer are necessary to precisely measure the effect of this buffer on tissue preservation. In addition, considering the toxic-tissue effects of antimicrobials, further attempts to reduce their concentrations in the culture media may improve the tissue/cell viability. Reducing the concentrations of Penicillin/Streptomycin, Gentamicin and Amphotericin B may allow bacterial and fungal contamination in the model as previously shown (Davenport, 2011), hence experiments could be performed testing a new set of antimicrobials. The capacity to avoid contamination as well as the effect in the tissue and cell viability could be factors to be compared between the previously used and the new set of antimicrobials. In terms of biopsy stability, the use

of 10mm biopsy punches instead of 8mm biopsy would likely improve the model stability due to the larger skin area provided. Importantly, the advantage of using biopsy punches instead of large skin fragments could standardize the size of all biopsies as well as the size of the agar plug with *D. nodosus* used for model infection.

TUNEL allows the assessment of different cell death processes through DNA fragmentation, however, it may be interesting to specifically detect apoptosis using other methods in combination with TUNEL staining. For instance, immunohistochemical staining methods for monoclonal antibodies to FasL, TNFα, granzyme β and caspase enzymes could all be used to detect the products associated with apoptosis. Moreover, it was observed that TUNEL staining tissue sections presented a higher concentration of cell death in the core epidermal cells while the margin epidermal cells tended to be more viable. Khaitan et al. (2006) reported that this happens in 3D tissue culture because the core cells receive less oxygen, growth factors, and nutrients from the medium. This observation could be accurately investigated by the quantification of TUNEL positive cells in the stained tissue sections where this effect was observed. In order to achieve that, the epidermis could be divided in four image-sections, two images from the margins and two images from the core tissue. Similar quantitative TUNEL analysis, as described in this chapter, could be performed and then margin and core cells viability could be further compared.

Future work to investigate bacterial colonisation and tissue inflammatory response

The EVOC model could be used to investigate the synergistic role of *D. nodosus*, *F. necrophorum* and *Treponema* spp. Each bacterial species could be used to infect the model individually or in combination with *D. nodosus*. Moreover, the EVOC model could also be infected with *F. necrophorum* subspecies *necrophorum* and *funduliforme* in order to raise further insights into the pathogenesis and diversity of the two subspecies. In addition, the model could be used to further validate the results of microbiome studies and hence investigate the role of other bacterial communities in footrot pathogenesis. For instance, *Mycoplasma* spp. was highly abundant in footrot samples as shown by 16S rRNA sequencing (Maboni et al. 2017), hence this bacterium could be used in a model co-infection to investigate potential synergistic relationship with *D. nodosus.* Other future work would be the detection of total eubacteria in the EVOC biopsies, which would indicate whether the washing steps removed the commensal bacterial communities of the skin explants. Further investigation of *D. nodosus* virulence could be performed comparing the ability of *D. nodosus* wild-type and AprV2, AprB2, AprV5 and AprB5 protease mutants to invade the interdigital skin. The EVOC model could be infected with mutant strains that were previously constructed by Kennan et al. (2010), and were offered to our group. Moreover, FISH could be applied to reveal whether *D. nodosus* would

be located in deeper epidermal or dermal layers after 52 and/or 76h of infection.

8.6 Conclusions

The key findings of this study include that the model can be infected with both, virulent and benign strains of *D. nodosus* for 28h leading to the release of IL1β and CXCL8 in the media. These results suggest the EVOC model can realistically simulate the interdigital skin microenvironment providing relevant information on how *D. nodosus* infects the skin and the early local cellular response to infection. Importantly, HEPES buffer should be added to culture media of further experiments using ovine interdigital skin explants, as this buffer appeared to have a positive effect on the tissue viability. This novel model is the first of its kind for investigating ovine footrot using sheep skin explants in alignment with the 3Rs of animal experimentation.

Chapter 9

9. General discussion

9.1 Overview

This thesis aimed to investigate host-pathogen interactions in ovine footrot. This was based on the hypothesis that the pathology of the disease is a host mediated expression of local immune responses in association with bacterial colonisation, leading to severe inflammation that can progress to underrunning footrot. All experiments were performed using biopsies and skin explants from post slaughter sheep collected in a local abattoir. Firstly, the prevalence and load of the main bacteria involved in footrot was investigated, considering the lack of current information on bacterial prevalence in the UK flocks. The latest cross sectional field study on bacterial prevalence in the UK was performed in 2005 by Moore et al. necessitating an investigation to provide more current data. A small pilot study was performed to compare the bacterial prevalence obtained by swabs and biopsies, hence advancing information on bacterial localization on the surface or within the skin and comparing swabs and biopsies as methods for sampling the ovine interdigital skin. Secondly, this project also investigated the host response to footrot in healthy, ID and footrot affected feet by the application of RT-qPCR for cytokines/ TLRs, and RNAseq for global gene expression analysis. How do the infectious bacteria and host immune response interact during the disease

process? In attempt to answer this question we combined information obtained from the gene expression analysis and bacterial load associating high and low levels of IL1β expression (host mechanism) and high and low load of virulent *D. nodosus* (pathogen mechanism). Finally, this project developed a 3D skin model culture using ovine interdigital skin explants cultured *in vitro*. This model was successfully infected with virulent and benign strains of *D. nodosus*. Moreover, the initial local tissue response to *D. nodosus* infection was confirmed through the detection of IL1β and CXCL8 in the media supernatant. The 3D skin model provided relevant information on host-pathogen interactions of footrot and confirmed the potential role of IL1β and CXCL8.

Egerton et al. (1969) investigated the role of bacteria and inflammatory response in the development of underrunning footrot lesions. They hypothesized that the destruction of the epidermal matrix, resulting in the separation of the hoof horn from the skin, was not dependent on the direct bacterial attack on the horn itself, but it was rather caused by the intense host inflammatory response to the infection (Egerton et al. 1969). The present thesis extended this hypothesis adding that the host expression of local immune responses, in association with bacterial colonisation, leads to severe inflammation that can progress to the hoof-skin separation. The results obtained in this project partially supported this hypothesis providing novel evidence of host-bacterial interaction. This evidence is summarized in Figure 9.1, which illustrates key events leading to

the development of underrunning footrot based on our results and data from the literature. However, there are still several questions to be further elucidated, mainly regarding the (i) disease aetiology and the role of bacteria in healthy, ID and footrot, (ii) immune molecules and inflammatory mechanisms triggered by the bacterial infection, and (iii) the main factors leading to hoof-skin separation.

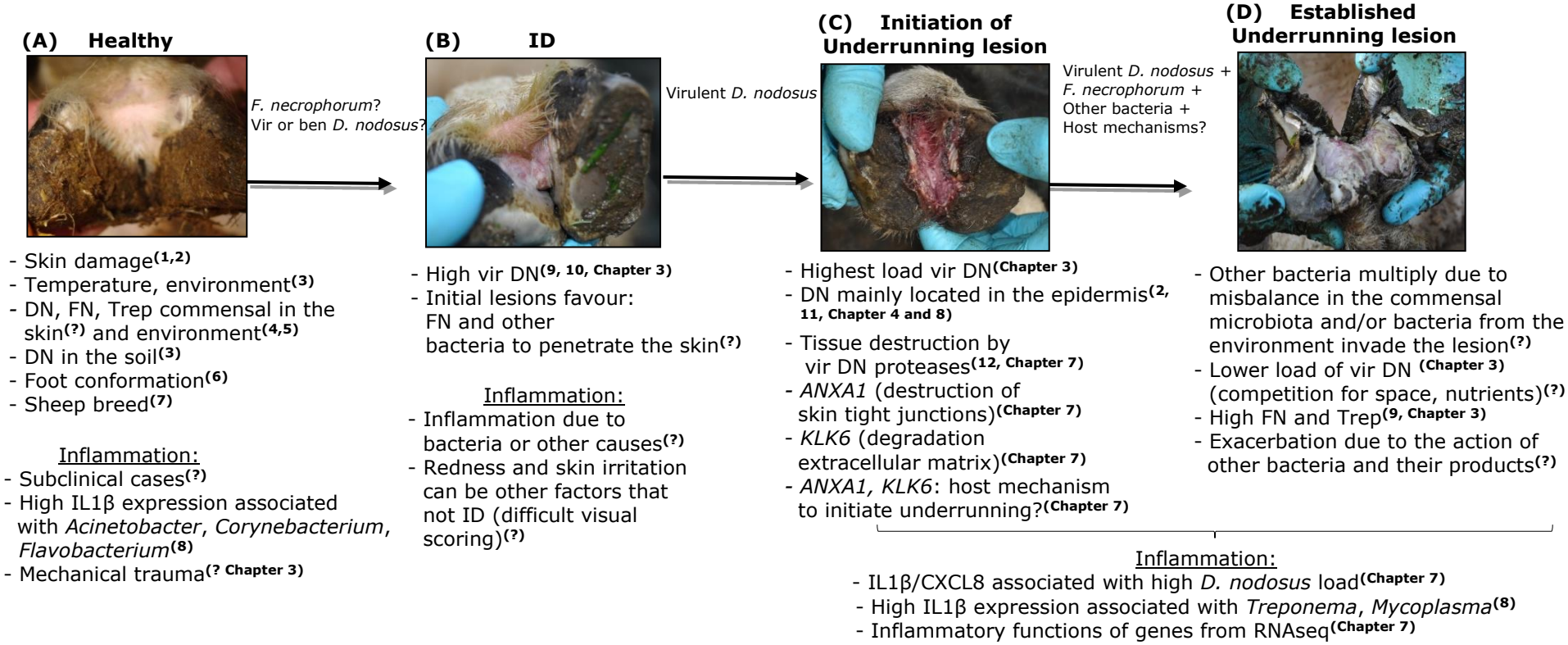


Figure 9.1 Key events involved in the host-pathogen mechanisms leading to ovine footrot in the presence of virulent *D. nodosus*. (A) Healthy: means undamaged sole and heel area with no visual skin inflammation, no fetid smell and no underrunning lesion. (B) ID (interdigital dermatitis): means any ID case with scores 1 to 4 (scores in Table 2.1, Chapter 2). (C) Initiation of underrunning lesion= means the transition between ID score 4 and footrot score 1. (D) Established underrunning lesion: means clear separation of the hoof from the skin, footrot scores 2-3. vir DN: virulent *Dichelobacter nodosus*; ben DN: benign *Dichelobacter nodosus*; FN: *Fusobacterium necrophorum*; Trep: *Treponema* spp. Question marks (?) indicate possible events involved in the disease pathogenesis. Information obtained from this thesis is indicated by respective chapters. References as indicated by numbers: [1]Beveridge, 1941; [2]Egerton et al. 1969; [3]Muzafar et al. 2016; [4]Garcia et al., 1971; [5]Cockburn 1961; [6]Kaler et al. 2010; [7]Emery et al. 1984; [8]Maboni et al. 2017; [9]Witcomb et al. 2014; [10]Frosth et al. 2015; [11]Witcomb et al. 2015; [12]Kennan et al. 2010.

9.1.1 Events involved in healthy ovine feet leading to disease initiation (Figure 9.1 A)

Damage in the epidermis is a major factor involved in healthy ovine feet since it allows bacteria to penetrate the skin. *In vivo* trials replicated this infection by causing initial damage to the skin before bacterial exposure and consequent establishment of footrot lesions (Beveridge, 1941; Egerton et al. 1969; Roberts & Egerton 1969; Egerton & Roberts 1971; Kennan et al. 2001; Kennan et al. 2010). In the field, skin damage in a healthy interdigital skin can be triggered by several factors such as mechanical trauma by small stones, pieces of wood and grass present between the digits. In addition, skin maceration is reported to be necessary for disease initiation (Egerton et al. 1969). In the UK context the damp skin microenvironment might constantly cause skin maceration since sheep are likely to graze on muddy pastures throughout the year. However, maceration with mild skin damage was reported to be insufficient to initiate footrot *in vivo* (Egerton et al. 1969). Infection was established in sheep feet that were macerated for 3 to 4 days on wet mats contaminated with faeces (Egerton et al. 1969). Faecal materials are likely to be the source of environmental microorganisms such as *F. necrophorum* (Garcia et al. 1971), highlighting the role played by the environment in footrot pathogenesis. Moreover, a definite association between faecal contamination and invasion of *F. necrophorum* was also suggested (Roberts & Egerton 1969). Based on these previous studies, *F. necrophorum* has been recognised as an important

pathogen to initiate interdigital dermatitis; however, this hypothesis was not further investigated or confirmed.

The presence of *D. nodosus* in the environment is another factor contributing to the initiation of the disease. In the UK, *D. nodosus* has been detected in the soil where sheep were kept for grazing as well as in the sheep oral cavity (Witcomb, 2012), suggesting a potential cross contamination between the pasture and sheep mouth. *D. nodosus* was also detected in soil, faecal balls, within the interdigital space and in fresh hoof prints (Witcomb, 2012). These findings further support the hypothesis that the environment is a potential source of *D. nodosus*. Environmental factors such as wet conditions and temperature is also reported to facilitate disease occurrence. Under optimal in vitro conditions of temperature and humidity, *D. nodosus* was detected in soil samples for up to 40 days (Muzafar et al. 2016).

Another factor that might contribute to the disease initiation is the co-colonisation by *F. necrophorum*, *D. nodosus*, *Treponema* spp. and other microorganisms in healthy ovine interdigital skin. The three bacteria were detected by qPCR in healthy ovine skin biopsies analysed in this study (Chapter 3) and by Calvo-Bado et al. (2011). Furthermore, other bacteria as *Corynebacterium*, *Psychrobacter* and *Acinetobacter* were highly abundant in the same set of healthy biopsies using 16S rRNA sequencing (Maboni et al. 2017). The role of commensal bacteria has been previously investigated in an *in vivo* trial where *Corynebacterium pyogenes* was applied to the feet with *D.*

nodosus and *F. necrophorum* (Roberts & Egerton 1969). Sheep infected with the three bacteria developed footrot lesions faster and with a higher incidence of footrot than sheep only infected with *D. nodosus* and *F. necrophorum* (Roberts & Egerton 1969). The authors proposed it might be associated with a possible effect of *C. pyogenes* on the growth and invasiveness of *F. necrophorum*. Taken together, these data suggest that different bacterial communities present in healthy ovine feet might also play a role in the disease initiation. This will require further investigation by future studies to elucidate their role.

The wide range of inflammatory background present in healthy interdigital skin samples (Chapter 6) is a potential factor associated with disease initiation. In this study, healthy, ID and footrot samples displayed similar levels of mRNA expression of *IL1β*, *CXCL8*, *IL17*, *IL6*, *TLR2* and *TLR4* (Chapter 6). Interestingly, the same healthy samples were positive for virulent *D. nodosus* detected by qPCR (58%, 46/79) (Chapter 3). Here, the question raised was why visually healthy samples presented with these wide levels of inflammatory background? A possible explanation is that footrot might have a subclinical stage where *D. nodosus* is present in the interdigital skin as well as other bacteria, but without any visual sign of the infection. Currently there is no definitive evidence on whether the presence of bacteria and high inflammatory background are indicative of subclinical cases of footrot. Also, there is no information on how the

host controls the infection or how bacteria evade the host control mechanisms.

9.3 Events involved in ID stage (Figure 9.1 B)

Key events involved in ID include the high prevalence of *D. nodosus*, suggesting it drives the development of the early stages of the disease (Witcomb et al. 2014). This hypothesis can be supported by findings in cross sectional (Chapter 3, Witcomb et al. 2015) and longitudinal studies (Witcomb et al. 2014), where *D. nodosus* was highly detected in ID samples. Our findings in addition to the data present in the literature support the claim from Witcomb et al. (2014) that ID should be treated as well as footrot since it is likely a highly infective stage of the disease. In contrast, *F. necrophorum* was detected in very few ID samples (11%, 7/65) (Chapter 3) and was found not to be associated with ID stage (Witcomb et al. 2014).

Feet presenting with clinical signs of ID were classified using 4 different scores according to the area and severity of lesions (Table 2.1, Chapter 2). Initial stages of ID are characterized by dry and irritated skin (score 1), and slight irritation with a fetid smell with ≤5% of the interdigital space affected (score 2). The initial clinical signs of ID can be easily confused with any other inflammatory process in the interdigital skin, hence limiting the scoring system for ID score 1 and 2. Interestingly, the global gene expression analysis did not reveal any upregulated genes in ID samples in comparison to

healthy samples. It is important to note that all ID samples included in the RNAseq analysis were classified as ID score 1 or 2, representing a possible reason for this similar expression. Further studies are necessary to advance our understanding of the role of inflammation in ID and clarify whether the initial skin inflammatory response allows environmental bacteria to invade the skin (i), or if the initial skin inflammation affects the proliferation of certain bacterial communities of the skin microbiota (ii).

9.4 Events leading to the separation of the hoof from the sensitive underlying tissue (Figure 9.1 C)

The scoring system used in this study categorises footrot according to lesion area based on the fact that footrot score 1 begins when underrunning lesions appear in the ovine foot. However, there is a transitional stage between ID score 4 and footrot score 1. Here, we analysed this stage separately considering unique events involved in the transitional process.

In the transition from ID to footrot, the essential factor to initiate underrunning lesions is the presence of virulent *D. nodosus*. An *in vivo* sheep trial proved that AprV2 protease present in virulent *D. nodosus* strains is essential in footrot initiation, hence fulfilling Koch's postulates (Kennan et al., 2010). AprV2 proteases are involved in the degradation of keratin, collagen and elastin of the interdigital skin and hoof (Kennan et al., 2010). We could therefore claim a direct bacterial attack on the horn and skin aiding to initiate hoof-skin separation.

Could the host inflammatory response be a subsequent factor responsible for the development of the lesions? The data from our RNAseq study may provide novel insights to clarify this question. For instance, genes with inflammatory functions such as *ANXA1* and *KLK6* were upregulated in footrot samples (Chapter 7). *ANXA1* encodes an enzyme predicted to be associated with disruption of tight junctions, and KLK6 encodes an enzyme reported to degrade components of the extracellular matrix (Bayani et al. 2013). We could then postulate that bacteria involved in footrot may induce a host mechanism (i.e upregulation of *ANXA1* and *KLK6*) in order to invade the skin through the disrupted tight junctions and extracellular matrix, or that bacteria could directly act in the disruption of tight junctions and extracellular matrix. These may potentially represent mechanisms that lead to separation of the skin from the hoof, hence initiating underrunning footrot. These results may potentially endorse our hypothesis that the separation of the hoof horn from the sensitive underlying tissue is led by the host mediated expression of local immune responses in association with bacterial colonisation.

9.5 Events involved in established footrot lesion (Figure 9.1 C)

Important events involved in established and well-developed underrunning footrot lesions include the reduced load of *D. nodosus* and the high abundance of other microbial communities. In this study, a lower prevalence of virulent *D. nodosus* was found in footrot than in ID samples (Chapter 3). Similarly, a slightly lower abundance of *D.*

nodosus was found in the same footrot biopsies compared to ID using 16S rRNA sequencing analysis (Maboni et al. 2017). Our data confirm the findings from a longitudinal study where the load of *D. nodosus* was increased a week prior to disease onset and decreased once footrot lesions had developed (Witcomb et al. 2014). In contrast, *F. necrophorum* was more frequently detected in footrot samples than in ID and healthy samples (Chapter 3). The 16S rRNA sequencing revealed other bacterial populations such as *Mycoplasma*, *Corynebacterium*, *Psychrobacter*, *Treponema*, *Porphyromonas*, *Anaerococcus* and *Brachybacterium* to be more abundant than *D. nodosus* in the same footrot biopsies (Maboni et al. 2017). These findings suggest the load and abundance of bacteria in footrot affected feet differ from ID and healthy stages. Some factors may explain the lower load of *D. nodosus* in footrot than in ID. For instance, *D. nodosus* may be outcompeted by the most abundant commensal populations for space and nutrients. Furthermore, since *D. nodosus* multiplies slowly (Roberts & Egerton 1969), this may allow other bacteria to thrive and proliferate faster within the tissue. Moreover, the separation of the hoof horn and skin might expose the lesion to increased levels of oxygen within the tissue and/or *D. nodosus* could be removed via the sloughing of necrotic tissue (Egerton et al. 1969).

The higher detection of *F. necrophorum* in footrot samples (Chapter 3) possibly indicates that this bacterium thrives in a process favoured by the misbalance in the commensal microbiota and then aid disease

persistence; a process previously suggested by Witcomb (2012). Egerton et al. (1969) described a severe inflammatory process and destruction of the ovine interdigital skin in response to *in vivo* exposure to *F. necrophorum*. In addition, *F. necrophorum* injected into rabbit's skin caused a much stronger inflammatory reaction than *D. nodosus*, seeing visual oedematous skin swelling and also necrotic areas histologically (Roberts & Egerton 1969). Taken together, these data indicate that *F. necrophorum* contributes to the severity of footrot lesions. These contribution might be associated with exotoxin action, hence being responsible for high inflammation. Further studies could investigate the association between high and low levels of *F. necrophorum* load and cytokine expression in healthy, ID and footrot affected feet.

There is little information in the literature regarding the inflammatory process involved in footrot lesions. Information obtained in this thesis helped to expand our understanding of local inflammatory responses. We found that inflammation, as marked by mRNA expression levels of *CXCL8* and *IL1β*, central mediators of the immune response in the skin, were associated with virulent *D. nodosus* in footrot-affected feet (Chapter 6). Moreover, the results of the RNAseq analysis indicated upregulation of the local inflammatory and innate immune responses in footrot samples, whilst there was little evidence of the local adaptive immune response. Some of these genes, *ANXA1*, *ADORA3*, *KLK6*, *NFAM1* and *CTSW,* have inflammatory functions and could be considered possible molecules of relevance in footrot in terms of

pathogenesis elucidation (Chapter 7). The association between skin inflammation and bacterial abundance in the same footrot samples used in this thesis was shown in a 16S rRNA sequencing analysis. *Treponema* (34%), *Mycoplasma* (29%) and *Porphyromonas* (15%) were the most abundant genera associated with high levels of *IL1β* expression in footrot samples (Maboni et al. 2017). This provides further evidence that the presence of *Treponema* spp. could influence the infection.

In summary, the misbalance of the microbiota and increased load of specific microorganisms in association with local skin inflammatory responses could therefore allow the invasion of bacteria from the environment or proliferation of skin resident microorganisms. The combination of these factors could eventually play a role in the exacerbation of underrunning footrot lesions.

Abbott, K.A. & Lewis, C.J., 2005. Current approaches to the management of ovine footrot. *Veterinary Journal*, 169(1), pp.28–41.

Abud, H.E., Watson, N. & Heath, J.K., 2005. Growth of intestinal epithelium in organ culture is dependent on EGF signalling. *Experimental Cell Research*, (303), pp.252–262.

Afshar, M. & Gallo, R.L., 2013. Innate immune defense system of the skin. *Veterinary Dermatology*, 24(1).

Aguiar, G.M. et al., 2011. Foot rot and other foot diseases of goat and sheep in the semiarid region of northeastern Brazil. *Pesquisa Veterinaria Brasileira*, 31(10), pp.879–884.

Albanesi, C. et al., 2005. Keratinocytes in inflammatory skin diseases. *Current Drug Targets - Inflammation & Allergy*, 4, 329-334.

Andersen, C.L., Jensen, J.L. & Ørntoft, T.F., 2004. Normalization of real-time quantitative reverse transcription-PCR data: A model-based variance estimation approach to identify genes suited for normalization, applied to bladder and colon cancer data sets. *Cancer Research*, 64(15), pp.5245–5250.

Arend, W. P., Palmer, G. & Gabay, C., 2008. IL-1, IL-18, and IL-33 families of cytokines. *Immunology Reviews*, (223), pp.20–38.

Aughey, E. & Frye, F., 2001. Comparative veterinary histology with clinical correlates. Manson Publishing, The Veterinary Press.

Bayani, J. et al., 2013. Copy number and expression alterations of miRNAs in the ovarian cancer cell line OVCAR-3: Impact on kallikrein 6 protein expression. *Clinical Chemistry*, 59(1), pp.296–305.

Bennett, G. et al., 2009. *Dichelobacter nodosus*, *Fusobacterium necrophorum* and the epidemiology of footrot. *Anaerobe*, 15(4), pp.173–176.

Bessou, S. et al., 1996. *Ex vivo* study of skin phototypes. *Journal of Investigative Dermatology*, (107), pp.684–688.

Beveridge, W. I. B., 1941. Foot-rot in sheep: a transmissable disease due to infection with Fusiformis nodosus (n. sp.): studies on its cause, epidemiology and control. *CSIRO Australian Bulletin*, (140), pp.1-56.

Bhardwaj, V. et al., 2014. Investigation of immunity in sheep following footrot infection and vaccination. *Vaccine*, 32(51), pp.6979–6985.

Bolger, A.M., Lohse, M. & Usadel, B., 2014. Trimmomatic: A flexible trimmer for Illumina sequence data. *Bioinformatics*, 30(15), pp.2114–2120.

Borish, L.C. & Steinke, J.W., 2003. Cytokines and chemokines. *Journal of Allergy and Clinical Immunology*, 111(2), pp.460–475.

Brady, A.R. et al., 2015. RNA-Seq analysis of the host response to *Staphylococcus aureus* skin and soft tissue infection in a mouse model. *Plos One*, 10(4):e0124877

Brooks, M.J. et al., 2011. Next-generation sequencing facilitates quantitative analysis of wild-type and Nrl(-/-) retinal transcriptomes. *Molecular vision*, (17), pp.3034–54.

Buckley, C.D. et al., 2001. Fibroblasts regulate the switch from acute resolving to chronic persistent inflammation. *Trends in Immunology*, 22(4), pp.199–204.

Bustin, S., 2000. Absolute quantification of mRNA using real-time reverse transcription polymerase chain reaction assays. *Journal of Molecular Endocrinology*, 25, pp.169–193.

Bustin, S.A., 2002. Quantification of mRNA using real-time reverse transcription PCR (RT-PCR): Trends and problems. *Journal of Molecular Endocrinology*, 29(1), pp.23–39.

Bustin, S. a et al., 2010. MIQE précis: Practical implementation of minimum standard guidelines for fluorescence-based quantitative real-time PCR experiments. *BMC Molecular Biology*, 11, p.74.

Bustin, S. a. et al., 2009. The MIQE guidelines:Minimum Information for publication of quantitative real-time PCR experiments. *Clinical Chemistry*, 55(4), pp.611–622.

Calvo-Bado, L.A. et al., 2011. Detection and diversity of a putative novel heterogeneous polymorphic proline-glycine repeat (Pgr) protein in the footrot pathogen *Dichelobacter nodosus*. *Veterinary Microbiology*, 147(3–4), pp.358–366.

Cederlöf, S.E. et al., 2013. An evaluation of the ability of *Dichelobacter nodosus* to survive in soil. *Acta veterinaria Scandinavica*, 55(1), p.4.

Chagnon, A. & Corbeil, M., 1973. Use of an organic buffer (hepes) in human lymphocytoid cell line cultures. *In Vitro*, (8), pp283-287.

Chan, C. Y. et al., 2013. Mast Cell Interleukin-10 drives localized tolerance in chronic bladder infection. *Immunity*, 38, 349-359.

Chang, J.S. et al., 2009. Molecular cloning and characterization of Toll-like receptors 1-10 in sheep. *Veterinary Immunology and*

Immunopathology, 127(1–2), pp.94–105.

Cheetham, B.F. et al., 2006. Improved diagnosis of virulent ovine footrot using the intA gene. *Veterinary Microbiology*, 116(1–3), pp.166–174.

Chopra-Dewasthaly, R. et al., 2017. Comprehensive RNA-Seq profiling to evaluate the sheep mammary gland transcriptome in response to experimental *Mycoplasma agalactiae* infection. *Plos One*, 12(1), p.e0170015.

Claxton, P.D., 1989. Antigenic classification of *Bacteroides nodosus.* In: Egerton, J.R., Yong, W.K. & Riffkin, G.G. (eds) Footrot and Foot Abscess of Ruminants. Boca Raton, FL: CRC Press, pp. 155-66.

Clements, R.H. & Stoye, S.C., 2014. The "Five Point Plan": a successful tool for reducing lameness in sheep. *The Veterinary record*, (2014), p.vetrec-2013-102161.

Clifton, R. & Green, L., 2016. Pathogenesis of ovine footrot disease: a complex picture. *The Veterinary record*, 179(9), pp.225–7.

Cockburn, T.A., 1961. The origin of the treponematoses. *Bulletin of World Health Organisation*, (24), pp.221–228.

Commins, S.P., Borish, L. & Steinke, J.W., 2010. Immunologic messenger molecules: Cytokines, interferons, and chemokines. *Journal of Allergy and Clinical Immunology*, (125), pp.S53–S72.

Conesa, A. et al., 2016. A survey of best practices for RNA-seq data analysis. *Genome Biology*, 17(1), p.13.

Conus, S. & Simon, H.U., 2008. Cathepsins: Key modulators of cell death and inflammatory responses. *Biochemical Pharmacology*,

76(11), pp.1374–1382.

Costa, M.O. et al., 2016. Development and evaluation of a porcine *in vitro* colon organ culture technique. *In Vitro Cellular and Developmental Biology - Animal*, 52(9), pp.942–952.

Cuadrado, A. & Nebreda, A.R., 2010. Mechanisms and functions of p38 MAPK signalling. *The Biochemical journal*, 429, pp.403–417.

Dalpke, A. et al., 2006. Activation of Toll-Like Receptor 9 by DNA from different bacterial species. *Infection and Immunity*, 74(2), pp.940–946.

Darlay, R.J. et al., 2011. Novel polymorphisms in ovine immune response genes and their association with abortion. *Animal Genetics*, 42(5), pp.535–543.

Davenport, R. 2011. Development of an *Ex vivo* organ culture to explore the innate immune response to footrot in sheep. Year 3 research project dissertation. School of Veterinary Medicine and Science, University of Nottingham, UK.

Davenport, R. et al., 2014. Differential expression of Toll-like receptors and inflammatory cytokines in ovine interdigital dermatitis and footrot. *Veterinary Immunology and Immunopathology*, 161(1–2), pp.90–98.

de Breij, A. et al., 2012. Differences in *Acinetobacter baumannii* strains and host innate immune response determine morbidity and mortality in experimental pneumonia. PLoS One, (7), p.e30673.

Delavary, B. M., et al., 2011. Macrophages in skin injury and repair. *Immunobiology*, 216, 753-762.

Dhanasekaran, S. et al., 2010. Differential expression of toll-like receptor mRNA in corneal epithelium of ruminants. *Veterinary Ophthalmology*, 13(4), pp.270–274.

Dhungyel, O. et al., 2013. Outbreak-specific monovalent/bivalent vaccination to control and eradicate virulent ovine footrot. *Vaccine*, 31(13), pp.1701–1706.

Doull, L. et al., 2015. Late production of CXCL8 in ruminant oro-nasal turbinate cells in response to *Chlamydia abortus* infection. *Veterinary Immunology and Immunopathology*, 168(1–2), pp.97–102.

Du, Z. et al., 2017. Comparative transcriptome analysis of raccoon dog skin to determine melanin content in hair and melanin distribution in skin. *Scientific Reports*, (7), p.40903.

Duncan, J.S. et al., 2012. Impact of footrot vaccination and antibiotic therapy on footrot and contagious ovine digital dermatitis. *The Veterinary Record*, 170(18), p.462.

Dutta, R.C. & Dutta, A.K., 2009. Cell-interactive 3D-scaffold; advances and applications. *Biotechnology Advances*, 27(4), pp.334–339.

Dyce, K.M., Sack, W.O. & Wensing, C.J.G., 2002. Texbook of Veterinary Anatomy. Third edition. Saunders, Philadelphia.

Edinger, T. et al., 2015. Cathepsin W Is required for escape of influenza a virus from late endosomes. *mBio*, 6(3), pp.1–12.

Edmondson, R. et al., 2014. Three-dimensional cell culture systems and their applications in drug discovery and cell-based biosensors. *Assay and drug development technologies*, 12(4),

pp.207–18.

Edwards, A.M. et al., 2003. Genetic relatedness and phenotypic characteristics of *Treponema* associated with human periodontal tissues and ruminant foot disease. *Microbiology*, 149(5), pp.1083–1093.

Edwards, A.M., Dymock, D. & Jenkinson, H.F., 2003. From tooth to hoof: Treponemes in tissue-destructive diseases. *Journal of Applied Microbiology*, 94(5), pp.767–780.

Egerton, J., 2014. Aetiology of ovine footrot. *Preventive Veterinary Medicine*, 117(1), p.313.

Egerton, J.R., Roberts, D.S. & Parsonson, I.M., 1969. The aetiology and pathogenesis of ovine foot-rot. *Journal of Comparative Pathology*, 79(2), p.207–IN7.

Emery, D.L., Stewart, D.J. & Clark, B.L., 1984. The comparative susceptibility of five breeds of sheep to foot-rot. *Australian Veterinary Journal*, 61(3), pp. 85-8.

Emmert-Streib, F. & Glazko, G. V., 2011. Pathway analysis of expression data: Deciphering functional building blocks of complex diseases. *PLoS Computational Biology*, 7(5), pp.1–6.

Entrican, G. et al., 1999. Cytokine release by ovine macrophages following infection with *Chlamydia psittaci*. *Clinical and Experimental Immunology*, 117(2), pp.309–315.

Eves, P. et al., 2003. Melanoma invasion in reconstructed human skin is influenced by skin cells - Investigation of the role of proteolytic enzymes. *Clinical and Experimental Metastasis*, 20(8), pp.685–700.

Fieber, C. et al., 2015. Innate immune response to *Streptococcus pyogenes* depends on the combined activation of TLR13 and TLR2. *PLoS ONE*, 10(3), pp.1–20.

Flacher, V. et al., 2006. Human Langerhans cells express a specific TLR profile and differentially respond to viruses and Gram-positive bacteria. *Journal of immunology*, 177(11), pp.7959–67.

Flecknell, P. 2002. Replacement, reduction and refinement. *Altex*, 19(2), pp.73-78.

Frandson, D.R., Lee, Wilke, W. & Dee Fails, A., 2009. Anatomy and Physiology of Farms Animals. Seventh edition. Wiley-Blackwell.

Frosth, S. et al., 2015. Characterisation of *Dichelobacter nodosus* and detection of *Fusobacterium necrophorum* and *Treponema* spp. in sheep with different clinical manifestations of footrot. *Veterinary Microbiology*, 179(1–2), pp.82–90.

Frosth, S. et al., 2012. Development and comparison of a real-time PCR assay for detection of *Dichelobacter nodosus* with culturing and conventional PCR: harmonisation between three laboratories. *Acta Veterinaria Scandinavica*, 54(1), p.6.

Frosth, S., 2016. *Dichelobacter nodosus* and footrot in Swedish sheep. Increased knowledge and improved laboratory diagnostics. Swedish University of Agricultural Sciences, Uppsala, Sweden.

Fu, Y. et al., 2016. Transcriptomic study on ovine immune responses to *Fasciola hepatica* infection. *PLoS Neglected Tropical Diseases,* 10(9), p. e0005015.

Gao, B. & Tsan, M.F., 2003. Recombinant human heat shock protein

60 does not induce the release of tumor necrosis factor alpha from murine macrophages. *The Journal of biological chemistry*, 278(25), pp.22523–22529.

Garcia, M.M. et al., 1971. Application of immunofluorescence to studies on the ecology of *Sphaerophorus necrophorus*. *Applied Microbiology*, (21), pp.809–814.

Garrido-Fariña, G.I. et al., 2008. A study of the process of apoptosis in animals infected with the contagious ecthyma virus. *Veterinary Microbiology*, 129(1–2), pp.28–39.

Gastardelo, T.S. et al., 2009. Functional and ultrastructural analysis of annexin A1 and its receptor in extravasating neutrophils during acute inflammation. *The American Journal of Pathology*, 174(1), pp.177–83.

Gawkrodger, J.D., 2002. Dermatology, an Illustrated Colour Text. Third edition. Churchill Livingstone.

Ghimire, S.C. et al., 1998. Identification and characterisation of serogroup M among Nepalese isolates of *Dichelobacter nodosus*, the transmitting agent of footrot in small ruminants. *Veterinary Microbiology*, 62(3), pp.217–233.

Gibson, A.L. et al., 2008. Comparison of therapeutic antibiotic treatments on tissue-engineered human skin substitutes. *Tissue Engineering Part A*, (14), pp.629–638.

Gilhuus, M. et al., 2013. Characterisation of *Dichelobacter nodosus* isolates from Norway. *Veterinary Microbiology*, 163(1–2), pp.142–148.

Goddard, P. et al., 2006. The perception of the welfare of sheep in

extensive systems. *Small Ruminant Research*, 62(3), pp.215–225.

Gomez, A. et al., 2012. An experimental infection model to induce digital dermatitis infection in cattle. *Journal of Dairy Science*, 95(4), pp.1821–30.

Gorbachev, A. V. & Fairchild, R.L., 2006. Activated NKT cells increase dendritic cell migration and enhance CD8+ T cell responses in the skin. *European Journal of Immunology*, 36(9), pp.2494–2503.

Graham, N. P. H. & Egerton, J. R., 1968. Pathogenesis of ovine foot-rot: the role of some environmental factors. *Australian Veterinary Journal*, 44(5), 235-240.

Grasl-Kraupp B., et al. 1995. *In situ* detection of fragmented DNA (TUNEL assay) fails to discriminate among apoptosis, necrosis, and autolytic cell death; a cautionary note. *Hepatology*, (21), pp.1465–1468.

Green, L.E. et al., 2007. Looking after the individual to reduce disease in the flock: A binomial mixed effects model investigating the impact of individual sheep management of footrot and interdigital dermatitis in a prospective longitudinal study on one farm. *Preventive Veterinary Medicine*, 78(2), pp.172–178.

Green, L.E. & George, T.R.N., 2008. Assessment of current knowledge of footrot in sheep with particular reference to *Dichelobacter nodosus* and implications for elimination or control strategies for sheep in Great Britain. *Veterinary Journal*, 175(2), pp.173–180.

Grøneng, G.M. et al., 2014. A longitudinal study of the risks for introduction of severe footrot into sheep flocks in the south west

of Norway. *Preventive Veterinary Medicine*, 113(2), pp.241–248.

Guo, Z. et al., 2016. Possible mechanisms of host resistance to Haemonchus contortus infection in sheep breeds native to the Canary Islands. *Scientific Reports*, (6), pp.1–14.

Gurski, L. a et al., 2010. 3D Matrices for anti-cancer drug testing and development. *Oncology Issues*, (25), pp.20–25.

Gurung, R.B. et al., 2006. Distribution and prevalence of footrot in Bhutan. *Veterinary Journal*, 171(2), pp.346–351.

Guttman, M. et al., 2010. Ab initio reconstruction of cell type-specific transcriptomes in mouse reveals the conserved multi-exonic structure of lincRNAs. *Nature biotechnology*, 28(5), pp.503–10.

Hagedorn, T., 2007. [photograph]. Winning the war on sheep footrot. Sheep Canada. 5-9.

Han, X. et al., 2008. Twitching motility is essential for virulence in *Dichelobacter nodosus*. *Journal of Bacteriology*, 190(9), pp.3323–3335.

Hänel, K.H. et al., 2013. Cytokines and the skin barrier. *International Journal of Molecular Sciences*, 14(4), pp.6720–6745.

Hruz, T. et al., 2011. RefGenes: identification of reliable and condition specific reference genes for RT-qPCR data normalization. *BMC Genomics*, 12(1), p.156.

Hughes, J. et al., 2011. Effects of omega-3 and -6 polyunsaturated fatty acids on ovine follicular cell steroidogenesis, embryo development and molecular markers of fatty acid metabolism. *Reproduction*, 141(1), pp.105–118.

Hughes, S. et al., 2007. Re-evaluation of the chicken MIP family of

chemokines and their receptors suggests that CCL5 is the prototypic MIP family chemokine, and that different species have developed different repertoires of both the CC chemokines and their receptors. *Developmental and Comparative Immunology,* 31(1), pp.72–86.

Hunt, J. D. et al., 1994. Antigenic competition in a multivalent footrot vaccine. *Vaccine*, (12), pp.457-464.

Igyártó, B.Z. & Kaplan, D.H., 2013. Antigen presentation by Langerhans cells. *Current Opinion in Immunology*, 25(1), pp.115–119.

Jarvis, M. et al., 2002. The detection of apoptosis in a human *in vitro* skin explant assay for graft versus host reactions. *Journal of Clinical Pathology*, 55(2), pp.127–32.

Jiang, X. et al., 2015. Evaluation of reference gene suitability for quantitative expression analysis by quantitative polymerase chain reaction in the mandibular condyle of sheep. *Molecular Medicine Reports*, pp.5633–5640.

Jiménez, R. et al., 2004. Minimum inhibitory concentrations for 25 selected antimicrobial agents against *Dichelobacter nodosus* and *Fusobacterium* strains isolated from footrot in sheep of Portugal and Spain. *Journal of Veterinary Medicine Series B: Infectious Diseases and Veterinary Public Health*, 51(5), pp.245–248.

Jin, W. & Dong, C., 2013. IL-17 cytokines in immunity and inflammation. *Emerging Microbes & Infections*, 2(9), p.e60.

Kaler, J. et al., 2010. Factors associated with changes of state of foot conformation and lameness in a flock of sheep. *Preventive*

Veterinary Medicine, 97(3–4), pp.237–244.

Kaler, J. & Green, L.E., 2009. Farmers' practices and factors associated with the prevalence of all lameness and lameness attributed to interdigital dermatitis and footrot in sheep flocks in England in 2004. *Preventive Veterinary Medicine*, 92(1–2), pp.52–59.

Kaplan, D.H., 2010. *In vivo* Function of Langerhans Cells and Dermal DC. *Trends in Immunology*, 31(12), pp.446–451.

Katz, M.E. et al., 1991. Identification of three gene regions associated with virulence in *Dichelobacter nodosus*, the causative agent of ovine footrot. *Journal of General Microbiology*, 137(9), pp.2117–24.

Kawai, T. & Akira, S., 2006. TLR signaling. *Seminars in Immunology*, (19), pp.24–32.

Kemp, M.W. et al., 2011. Exposure to *in utero* lipopolysaccharide induces inflammation in the fetal ovine skin. *Reproductive Sciences*, 18(1), pp.88–98.

Kennan, R.M. et al., 2010. The subtilisin-like protease AprV2 is required for virulence and uses a novel disulphide-tethered exosite to bind substrates. *PLoS Pathogens*, 6(11), p. e1001210.

Kennan, R.M. et al., 2001. The type IV fimbrial subunit gene (*fimA*) of *Dichelobacter nodosus* is essential for virulence, protease secretion, and natural competence. *Journal of Bacteriology*, 183(15), pp. 4451-8.

Kennan, R.M. et al., 2014. Genomic evidence for a globally distributed, bimodal population in the ovine footrot pathogen

Dichelobacter nodosus. *mBio*, 5(5).

Khaitan, D. et al. 2006. Establishment and characterization of multicellular spheroids from a human glioma cell line; Implications for tumor therapy. *Journal of Translational Medicine*, 4(1), pp.12.

Kikkert, R. et al., 2007. Activation of toll-like receptors 2 and 4 by gram-negative periodontal bacteria. *Oral Microbiology and Immunology*, 22(3), pp.145–151.

Kirschner, N. & Brandner, J.M., 2012. Barriers and more: Functions of tight junction proteins in the skin. *Annals of the New York Academy of Sciences*, 1257(1), pp.158–166.

Klindworth, A. et al., 2013. Evaluation of general 16S ribosomal RNA gene PCR primers for classical and next-generation sequencing based diversity studies. *Nucleic Acids Research*, (41), pp.1–11.

Kumar, V. et al., 2014. Robbins and Cotran pathologic basis of disease. Elsevier Health Sciences, 2014.

Kupper, T. & Fuhlbrigge, R., 2004. Immune surveillance in the skin: mechanisms and clinical consequences. *Nature Reviews. Immunology*, 4(3), pp.211–222.

Lai, Y. & Gallo, R.L., 2008. Toll-like receptors in skin infections and inflammatory diseases. *Infectious Disorders Drug Targets*, 8(3), pp.144–55.

Lalonde, E. et al., 2011. RNA sequencing reveals the role of splicing polymorphisms in regulating human gene expression. *Genome Research*, pp.545–554.

Lawrence, T., 2009. The nuclear factor NF-kappaB pathway in

inflammation. *Cold Spring Harbor Perspectives in Biology*, 1(6), pp.1–10.

Lebonvallet, N. et al., 2010. The evolution and use of skin explants: potential and limitations for dermatological research. *European Journal of Dermatology*, (20), pp.671–684.

Levy, J., 2000. The effects of antibiotic use on gastrointestinal function. *American Journal of Gastroenterology*, (95), pp.S8–S10

Li, X.D. & Chen, Z.J., 2012. Sequence specific detection of bacterial 23S ribosomal RNA by TLR13. *eLife*, 1, p.e00102.

Lippens, S., et al. 2005. Death penalty for keratinocytes: apoptosis versus cornification. *Cell Death & Differentiation*, (12), pp.1497–508.

Liu, L. et al., 2013. Zc3h12c inhibits vascular inflammation by repressing NF-κB activation and pro-inflammatory gene expression in endothelial cells. *The Biochemical Journal*, 451(1), pp.55–60.

Lloyd, L.J. et al., 2012. Protein-energy malnutrition during early gestation in sheep blunts fetal renal vascular and nephron development and compromises adult renal function. *The Journal of Physiology*, 590(2), pp.377–93.

Locati, M., Bonecchi, R. & Corsi, M.M., 2005. Chemokines and their receptors: roles in specific clinical conditions and measurement in the clinical laboratory. *American Journal of Clinical Pathology*, (123), pp.82–95.

Lorenzo, M. et al., 2012. Antimicrobial resistance determinants among anaerobic bacteria isolated from footrot. *Veterinary*

Microbiology, 157(1–2), pp.112–118.

Lu, Z. et al., 2007. Towards the development of a simplified long-term organ culture method for human scalp skin and its appendages under serum-free conditions. *Experimental Dermatology*, 16(1), pp.37–44.

Ma, Y. et al., 2016. A species-specific activation of Toll-like receptor signaling in bovine and sheep bronchial epithelial cells triggered by mycobacterial infections. *Molecular Immunology*, (71), pp.23-33.

Maboni, G. et al., 2017. A distinct bacterial dysbiosis associated skin inflammation in ovine footrot. *Scientific Reports*, (7), p.45220.

Maboni, G. et al., 2016. Ovine footrot: new insights into bacterial colonisation. *Veterinary Record*, p.vetrec-2015-103610.

MacNeil, S., 2007. Progress and opportunities for tissue-engineered skin. *Nature*, 445(7130), pp.874–80.

Mahakapuge, T.A.N. et al., 2016. Assessment of reference genes for reliable analysis of gene transcription by RT-qPCR in ovine leukocytes. *Veterinary Immunology and Immunopathology*, (171), pp.1–6.

Mandell, L. et al., 2004. Intact gram-negative *Helicobacter pylori*, *Helicobacter felis*, and *Helicobacter hepaticus* bacteria activate innate immunity via toll-like receptor 2 but not toll-like receptor 4. *Infection and Immunity*, 72(11), pp.6446–6454.

Mathur, R. et al., 2012. A mouse model of *Salmonella typhi* infection. *Cell*, 151(3), pp.590–602.

Matsuzawa, Y., S. et al., 2015. TNFAIP3 promotes survival of CD4 T

cells by restricting MTOR and promoting autophagy. *Autophagy*, (11), pp.1052–1062.

Maxie M.G. & Youssef S., 2007. Skin and Appendages. In: Ginn, P., Mansel, E. K. L., Rakich, M. P. Jubb, Kennedy and Palmer's Pathology of Domestic Animals. Fifth edition. Saunders Elsevier, Philadelphia.

McPherson, A.S., Dhungyel, O.P. & Whittington, R.J., 2017. Evaluation of genotypic and phenotypic protease virulence tests for *Dichelobacter nodosus* infection in sheep. *Journal of Clinical Microbiology*, p.JCM.02403-16.

Medzhitov, R., 2001. Toll-like receptors and innate immunity. *Nature reviews. Immunology*, 1(2), pp.135–145.

Menzies, M. & Ingham, A., 2006. Identification and expression of Toll-like receptors 1-10 in selected bovine and ovine tissues. *Veterinary Immunology and Immunopathology*, 109(1–2), pp.23–30.

Miller, L.S. & Modlin, R.L., 2007. Toll-like receptors in the skin. *Seminars in Immunopathology*, 29(1), pp.15–26.

Mills, S.E., 2007. Histology for Pathologists. Third edition. Lippincott Williams & Wilkins.

Mills, K.H.G., 2011. TLR-dependent T cell activation in autoimmunity. *Nature Reviews Immunology*, 11(12), pp.807–22.

Mizutani, H., Black, R. & Kupper, T.S., 1991. Human keratinocytes produce but do not process pro-interleukin-1 (IL-1) beta different strategies of IL-1 production and processing in monocytes and keratinocytes. *Journal of Clinical Investigation*, 87(3), pp.1066–

1071.

Moore, L.J. et al., 2005. The detection and characterisation of Dichelobacter nodosus from cases of ovine footrot in England and Wales. *Veterinary Microbiology*, 108(1–2), pp.57–67.

Morrison, D.C. & Ryan, J.L., 1980. Bacterial endotoxins and host immune responses. *Advances in Immunology*, (28), pp.293–450.

Mraz, O., 1963. Nomina und Synonyma der pathogenen und saprophytaren Mikroben, isoliert aus den wirtschaftlich oder epidemiologisch bedeutenden Wirbeltieren und Lebensmitteen tierischer Herkunf. In: Mraz, O., Tesarcik, J. & Varejka, F. Schizomycetes. Jena: VEB Gustav Fischer Verlag, pp. 53-334.

Muzafar, M. et al., 2016. Survival of the ovine footrot pathogen *Dichelobacter nodosus* in different soils. *Anaerobe*, (38), pp.81–87.

Muzafar, M. et al., 2015. The role of the environment in transmission of *Dichelobacter nodosus* between ewes and their lambs. *Veterinary Microbiology*, 179(1–2), pp.53–59.

Myers, G.S. a et al., 2007. Genome sequence and identification of candidate vaccine antigens from the animal pathogen *Dichelobacter nodosus*. *Nature Biotechnology*, 25(5), pp.569–575.

Nadzirin, N. & Firdaus-Raih, M., 2012. Proteins of unknown function in the protein data bank (PDB): An inventory of true uncharacterized proteins and computational tools for their analysis. *International Journal of Molecular Sciences*, 13(10), pp.12761–12772.

Nakatsuji, T. et al., 2013. The microbiome extends to subepidermal compartments of normal skin. *Nature Communications*, (4), p.1431.

Nalubamba, K.S. et al., 2008. Differential expression of pattern recognition receptors during the development of foetal sheep. *Developmental and Comparative Immunology*, 32(7), pp.869–874.

Nalubamba, K.S. et al., 2007. Differential expression of pattern recognition receptors in sheep tissues and leukocyte subsets. *Veterinary Immunology and Immunopathology*, 118(3–4), pp.252–262.

Nestle, F.O. et al., 2009. Skin immune sentinels in health and disease. *Nature reviews. Immunology*, 9(10), pp.679–91.

Neymeyer, H. et al., 2015. Activation of annexin A1 signalling in renal fibroblasts exerts antifibrotic effects. *Acta Physiologica*, 215(3), pp.144–158.

Nieuwhof, G.J. & Bishop, S.C., 2005. Costs of the major endemic diseases of sheep in Great Britain and the potential benefits of reduction in disease impact. *Animal Science*, (81), pp.23–29.

Nishifuji, K. & YOON, J. S. 2013. The stratum corneum: the rampart of the mammalian body. *Veterinary Dermatology*, (24), 60-e16.

O'Connor, T., Wilmut, I. & Taylor, J., 2013. Quantitative evaluation of reference genes for real-time pcr during *in vitro* maturation of ovine oocytes. *Reproduction in Domestic Animals*, 48(3), pp.477–483.

Palmer, M.A., 1993. A gelatin test to detect activity and stability of

proteases produced by *Dichelobacter* (bacteroides) *nodosus*. *Veterinary Microbiology*, 36(1–2), pp.113–122.

Parsonson, I.M. et al., 1967. Ovine interdigital dermatitis. *Journal of Comparative Pathology*, 77(3), pp.309-13.

Park, C. et al., 2000. Immune response in Stat2 knockout mice. *Immunity*, 13(6), pp.795–804.

Passmore, M., Nataatmadja, M. & Fraser, J.F., 2009. Selection of reference genes for normalisation of real-time RT-PCR in brain-stem death injury in *Ovis aries*. *BMC Molecular Biology*, (10), p.72.

Peletto, S. et al., 2011. Evaluation of internal reference genes for quantitative expression analysis by real-time PCR in ovine whole blood. *International Journal of Molecular Sciences*, 12(11), pp.7732–7747.

Pépin, M., et al., 1997. Cytokine gene expression in sheep following experimental infection with various strains of *Corynebacterium pseudotuberculosis* differing in virulence. *Veterinary Research*, (28), pp.149-163.

Persson-Waller, K., Colditz, I.. & Seow, H.F., 1997. Accumulation of leucocytes and cytokines in the lactating ovine udder during mastitis due to *Staphylococcus aureus* and *Escherichia coli*. *Research in Veterinary Science*, 62(1), pp.63–66.

Pfaffl, M.W. et al., 2004. Determination of stable housekeeping genes, differentially regulated target genes and sample integrity: BestKeeper-Excel-based tool using pair-wise correlations. *Biotechnology Letters*, 26(6), pp.509–15.

Plager, D.A. et al., 2012. Gene transcription abnormalities in canine atopic dermatitis and related human eosinophilic allergic diseases. *Veterinary Immunology and Immunopathology*, 149(1–2), pp.136–142.

Plain, K.M. et al., 2010. Toll-like receptor (TLR)6 and TLR1 differentiation in gene expression studies of Johne's disease. *Veterinary Immunology and Immunopathology*, 137(1–2), pp.142–148.

Popov, L. et al., 2014. Three-dimensional human skin models to understand *Staphylococcus aureus* skin colonization and infection. *Frontiers in Immunology*, (5), pp.1–6.

Prassas, I. et al., 2015. Unleashing the therapeutic potential of human kallikrein-related serine proteases. *Nature Reviews. Drug Discovery*, 14(3), pp.183–202.

Price, K.J. et al., 2012. Matrigel basement membrane matrix influences expression of microRNAs in cancer cell lines. *Biochemical and Biophysical Research Communications*, 427(2), pp.343–348.

Puech, C. et al., 2015. Design and evaluation of a unique SYBR Green real-time RT-PCR assay for quantification of five major cytokines in cattle, sheep and goats. *BMC Veterinary Research*, 11(1), p.65.

Quinlan, J.M. et al., 2006. *In vitro* culture of embryonic mouse intestinal epithelium: cell differentiation and introduction of reporter genes. *BMC Developmental Biology,* (6), p24.

Raadsma, H.W. et al., 1994. Protective antibody titres and antigenic competition in multivalent *Dichelobacter nodosus* fimbrial

vaccines using characterised rDNA antigens. *Veterinary Immunology and Immunopathology*, 40(3), pp.253–274.

Raadsma, H.W. & Dhungyel, O.P., 2013. A review of footrot in sheep: New approaches for control of virulent footrot. *Livestock Science*, 156(1–3), pp.115–125.

Rasmussen, M. et al., 2012. Bovine digital dermatitis: Possible pathogenic consortium consisting of *Dichelobacter nodosus* and multiple *Treponema* species. *Veterinary Microbiology*, 160(1–2), pp.151–161.

Reber, L.L. & Frossard, N., 2014. Targeting mast cells in inflammatory diseases. *Pharmacology & Therapeutics*, 142(3), pp.416–35.

Refaai, W. et al., 2013. Digital dermatitis in cattle is associated with an excessive innate immune response triggered by the keratinocytes. *BMC Veterinary Research*, 9(1), p.193.

Regan, T. et al., 2013. Identification of TLR10 as a key mediator of the inflammatory response to *Listeria monocytogenes* in intestinal epithelial cells and macrophages. *The Journal of Immunology*, 191(12), pp.6084–6092.

Ren, T. et al., 2014. Activation of Adenosine A3 Receptor Alleviates TNFα-induced inflammation through Inhibition of the NF-kB signaling pathway in human colonic epithelial cells. *Mediators of Inflammation*, pp.1–11.

Ren, Y. et al., 2006. Inhibition of tumor growth and metastasis *in vitro* and *in vivo* by targeting macrophage migration inhibitory factor in human neuroblastoma. *Oncogene*, (25), pp.3501–3508.

Reemann, P. et al., 2014. Melanocytes in the skin–comparative whole

transcriptome analysis of main skin cell types. *PloS one*, 9(12), e115717.

Riffkin, M.C. et al., 1995. A single amino-acid change between the antigenically different extracellular serine proteases V2 and B2 from *Dichelobacter nodosus*. *Gene*, 167(1–2), pp.279–283.

Roberts, D. S. & Egerton. J. R., 1969. The aetiology and pathogenesis of ovine foot-rot. The pathogenic association of *Fusiformis nodosus* and *F. necrophorus*. *Journal of Comparative Pathology*, (79), pp.217-227.

Rood, J.I. et al., 1996. Comparison of gene probe and conventional methods for the differentiation of ovine footrot isolates of *Dichelobacter nodosus*. *Veterinary Microbiology*, 52(1–2), pp.127–141.

Ross, H.M. & Pawlina, W. 2006. Histology, a text and atlas. Fifth edition. Lippincott Williams & Wilkins.

Russell, W.M.S., & Burch, R.L. 1959. The principles of humane experimental technique. *The principles of humane experimental technique.*

Sanders, J. E., et al., 2002. An explant model for the investigation of skin adaptation to mechanical stress. *Biomedical Engineering, IEEE Transactions on*, (49), pp.1626-1631.

Scarlet, D. et al., 2015. The orthology clause in the next generation sequencing era: Novel reference genes identified by RNA-seq in humans improve normalization of neonatal equine ovary RT-qPCR data. *PLoS ONE*, 10(11), pp.1–16.

Scheller, J. et al., 2011. The pro- and anti-inflammatory properties of

the cytokine interleukin-6. *Biochimica et Biophysica Acta*, (1813), pp.878–888.

Scholey, R.A. et al., 2013. Identifying host pathogenic pathways in bovine digital dermatitis by RNA-Seq analysis. *Veterinary Journal*, 197(3), pp.699–706.

Schrader, C.H. et al., 2015. Kallikrein-related peptidase 6 regulates epithelial-to-mesenchymal transition and serves as prognostic biomarker for head and neck squamous cell carcinoma patients. *Molecular Cancer*, (14), pp.1–14.

Schromm, A.B. et al., 2001. Molecular genetic analysis of an endotoxin nonresponder mutant cell line. *The Journal of Experimental Medicine*, 194(1), pp.79–88.

Schwartzkoff, C.L. et al., 1993. The effects of antigenic competition of the efficacy of multivalent footrot vaccines. *Australian Veteterinary Journal*, (70), pp.123–126.

Seow, H.F. et al., 1994. Cloning, sequencing, expression and inflammatory activity in skin of ovine interleukin-8. *Immunology & Cell Biology*, 72(5), pp.398–405.

Sessford, K., 2012. The histopathological characterisation of the ovine interdigital space to develop and Ex vivo organ culture model for infection with *Dichelobacter nodosus*. Year 3 research project dissertation. School of Veterinary Medicine and Science, University of Nottingham, UK.

Serrano, M. et al., 2011. Use of Maximum Likelihood-Mixed Models to select stable reference genes: a case of heat stress response in sheep. *BMC Molecular Biology*, 12(1), p.36.

Silver, N. et al., 2006. Selection of housekeeping genes for gene expression studies in human reticulocytes using real-time PCR. *BMC Molecular Biology*, 7(1), p.33.

Skerman, T.M. 1975. Determination of some *in vitro* growth requirements of *Bacteroides nodosus*. *Journal of General Microbiology*, 87(1), pp. 107-19.

Smeed, J.A. et al., 2007. Differential cytokine gene expression profiles in the three pathological forms of sheep paratuberculosis. *BMC Veterinary Research*, 3(1), p.18.

Smith, E. M. et al., 2014. Dynamics and impact of footrot and climate on hoof horn length in 50 ewes from one farm over a period of 10 months. *The Veterinary Journal*, 201(3), pp.295-301.

Smith, R.S. et al., 1997. Fibroblasts as sentinel cells. Synthesis of chemokines and regulation of inflammation. *The American Journal of Pathology*, 151(2), pp.317–22.

Smith, G. R. & Thornton, E. A., 1997. Classification of human and animal strains of *Fusobacterium necrophorum* by their pathogenic effects in mice. *Journal of Medical Microbiology,* (46), pp.879–882

Stäuble, A. et al., 2014. Simultaneous detection and discrimination of virulent and benign *Dichelobacter nodosus* in sheep of flocks affected by foot rot and in clinically healthy flocks by competitive real-time PCR. *Journal of Clinical Microbiology*, 52(4), pp.1228–1231.

Steinstraesser, L. et al., 2010. A novel human skin chamber model to study wound infection *ex vivo*. *Archives of Dermatological*

Research, 302(5), pp.357–365.

Strub, S. et al., 2007. Quantitation of *Guggenheimella bovis* and *treponemes* in bovine tissues related to digital dermatitis. *FEMS Microbiology Letters*, 269(1), pp.48–53.

Stewart, D.J. & Claxton, P.D., 1993. Ovine foot rot: clinical diagnosis and bacteriology. In: Corner LA & Bagust TJ (eds) Australian Standard Diagnostic Techniques for Animal Diseases. East Melbourne: CSIRO, pp. 1-27.

Stewart, D.J., 1979. The role of elastase in the differentiation of *Bacteroides nodosus* infections in sheep and cattle. *Research in Veterinary Science*, 27(1), pp. 99-105.

Sullivan, L.E. et al., 2015. High-level association of bovine digital dermatitis *Treponema* spp. with contagious ovine digital dermatitis lesions and presence of *Fusobacterium necrophorum* and *Dichelobacter nodosus*. *Journal of Clinical Microbiology*, 53(5), pp.1628–1638.

Suresh, R. & Mosser, D.M., 2013. Pattern recognition receptors in innate immunity, host defense, and immunopathology. *Advances in Physiology Education*, 37(4), pp.284–91.

Takeda, K. 2004. Toll-like receptors in innate immunity. *International Immunology*, 17(1), pp.1–14.

Takeuchi, O. et al., 2002. Cutting edge: role of Toll-like receptor 1 in mediating immune response to microbial lipoproteins. *Journal of Immunology*, 169(1), pp.10–14.

Takeuchi, O. et al., 2001. Discrimination of bacterial lipoproteins by Toll-like receptor 6. *International immunology*, 13(7), pp.933–

940.

Tan, Z.L., Nagaraja, T.G. & Chengappa, M.M., 1996. *Fusobacterium necrophorum* infections: virulence factors, pathogenic mechanism and control measures. *Veterinary Research Communications*, 20(2), pp.113–140.

Taylor, D.L. et al., 2008. Toll-like receptor genes are differentially expressed at the sites of infection during the progression of Johne's disease in outbred sheep. *Veterinary Immunology and Immunopathology*, 124(1–2), pp.132–151.

Thellin, O. et al., 1999. Housekeeping genes as internal standards: Use and limits. *Journal of Biotechnology*, 75(2–3), pp.291–295.

Thomas, J. H. 1962. The bacteriology and histopathology of footrot in sheep. *Australian Journal of Agricultural Research,* (13), p.725

Thorley, C.M. 1976. A simplified method for the isolation of Bacteroides nodusus from ovine foot-rot and studies on its colony morphology and serology. *Journal of Applied Bacteriology*, 40(3), pp. 301-9.

Tong, Z. et al., 2009. Selection of reliable reference genes for gene expression studies in peach using real-time PCR. *BMC Molecular Biology*, (10), p.71.

Tuschil, A. et al., 1992. Interleukin-8 stimulates calcium transients and promotes epidermal cell proliferation. *Journal of Investigative Dermatology,* (99), pp.294–298.

van der Aar, A.M.G. et al., 2007. Loss of TLR2, TLR4, and TLR5 on Langerhans cells abolishes bacterial recognition. *Journal of Immunology*, 178(4), pp.1986–90.

Vandesompele, J. et al., 2002. Accurate normalization of real-time quantitative RT-PCR data by geometric averaging of multiple internal control genes. *Genome Biology*, 3(7), p.0034.

Vinod Kumar, N., Sreenivasulu, D. & Karthik, A., 2016. Identification and characterization of *Dichelobacter nodosus* serogroup H from ovine footrot in India. *Anaerobe*, 40, pp.100–102.

Vorachek, W.R. et al., 2013. Reference gene selection for quantitative PCR studies in sheep neutrophils. *International Journal of Molecular Sciences*, 14(6), pp.11484–11495.

Wang, Q. et al., 2007. Naive Bayesian classifier for rapid assignment of rRNA sequences into the new bacterial taxonomy. *Applied and Environmental Microbiology*, 73(16), pp.5261–5267.

Wang, Z., Gerstein, M. & Snyder, M., 2009. RNA-Seq: a revolutionary tool for transcriptomics. *Nature Reviews. Genetics*, 10(1), pp.57–63.

Wassink, G. J. et al., 2004. Risk factors associated with the prevalence of interdigital dermatitis in sheep from 1999 to 2000. *Veterinary Record,* (154), pp.551-555.

Wassink, G.J. et al., 2010. A within farm clinical trial to compare two treatments (parenteral antibacterials and hoof trimming) for sheep lame with footrot. *Preventive Veterinary Medicine*, 96(1–2), pp.93–103.

Wassink, G.J. et al., 2005. Footrot and interdigital dermatitis in sheep: farmers' practices, opinions and attitudes. *The Veterinary Record*, 157(24), pp.761–765.

Wattegedera, S. et al., 2004. Variability in cytokine production and

cell proliferation by mitogen-activated ovine peripheral blood mononuclear cells: Modulation by interleukin (IL)-10 and IL-12. *Veterinary Immunology and Immunopathology,* (102), pp.67–76.

Werts, C. et al., 2001. Leptospiral lipopolysaccharide activates cells through a TLR2-dependent mechanism. *Nature Immunology*, 2(4), pp.346–52.

Whittington, R. J. 1995. Observations of the indirect transmission of virulent ovine footrot in sheep yards and its spread in sheep on unimproved pasture. *Australian Veterinary Journal,* 72 (4), 132-134.

Winter, A. et al., 2004. Lameness in sheep 1. Diagnosis. *In Practice*, pp.58–63.

Witcomb, L.A. et al., 2014. A longitudinal study of the role of *Dichelobacter nodosus* and *Fusobacterium necrophorum* load in initiation and severity of footrot in sheep. *Preventive Veterinary Medicine*, 115(1–2), pp.48–55.

Witcomb, L.A. et al., 2015. First study of pathogen load and localisation of ovine footrot using fluorescence *in situ* hybridisation (FISH). *Veterinary Microbiology*, 176(3–4), pp.321–327.

Withers, A.P. et al., 1986. Culture of wool follicle dermal papilla cells from two breeds of sheep. *Archives of Dermatological Research*, (279), pp.140-142.

Wu, C. et al., 2017. Whole-genome expression analyses of type 2 diabetes in human skin reveal altered immune function and

burden of infection. *Oncotarget*.

Xie, F. et al., 2012. miRDeepFinder: A miRNA analysis tool for deep sequencing of plant small RNAs. *Plant Molecular Biology*, 80(1), pp.75–84.

Xu, X. et al., 2007. Influences of buffer systems on chondrocyte growth during long-term culture in alginate. *Osteoarthritis and Cartilage*, 15(4), pp.396-402.

Xu, H. et al., 2015. Genome-Wide identification of new reference genes for qRT-PCR normalization under high temperature stress in rice endosperm. *Plos One*, 10(11), p.e0142015.

Xue, D. et al., 2015. *Mycoplasma ovipneumoniae* induces inflammatory response in sheep airway epithelial cells via a MyD88-dependent TLR signaling pathway. *Veterinary Immunology and Immunopathology*, 163(1–2), pp.57–66.

Yue, Y.J. et al., 2015. De novo assembly and characterization of skin transcriptome using RNAseq in sheep (*Ovis aries*). *Genetics and Molecular Research*, 14(1), pp.1371–1384.

Zhang, D. et al., 2004. A Toll-like Receptor that prevents infection by uropathogenic bacteria. *Science*, (303), pp.1522–1527.

Zhang, L. et al., 2012. Intra-amniotic administration of *E. coli* lipopolysaccharides causes sustained inflammation of the fetal skin in sheep. *Reproductive Sciences*, 19(11), pp.1181–1189.

Zuber Shaikh, P., 2011. Cytokines and their physiologic and pharmacologic functions in inflammation: *International Journal of Pharmacy and Life Sciences*, 2(11), pp.1247–1263.

Appendix 1

(Maboni et al. 2016 – Chapter 3)

Downloaded from http://veterinaryrecord.bmj.com/ on April 18, 2017 - Published by group.bmj.com

Paper

Ovine footrot: new insights into bacterial colonisation

G. Maboni, S. Frosth, A. Aspán, S. Tötemeyer

Ovine footrot is characterised by interdigital dermatitis (ID) and by the separation of the skin and hoof horn (under-running footrot). *Dichelobacter nodosus* is the essential pathogen causing footrot; the role of other microorganisms in this disease remains unclear. The aims of this study were (i) to investigate the colonisation of *D nodosus, Fusobacterium necrophorum* and *Treponema* species in biopsies from the ovine interdigital skin of healthy, ID and footrot-affected feet and (ii) to characterise the virulence of *D nodosus* strains in those biopsies. Postslaughter biopsy samples (n=241) were collected and analysed by real-time PCR to determine prevalence and load of the different bacterial species. The highest prevalence and load of *D nodosus* were found on feet with ID. The vast majority of samples contained virulent *D nodosus* and some samples contained both virulent and benign *D nodosus*. Notably, the more pathogenic subspecies of *F necrophorum* was found in samples from UK sheep. Our findings provide further insights into the role bacterial colonisation may play in the early stage of ID and in the progression towards footrot.

Ovine footrot is a major cause of lameness affecting sheep welfare worldwide (Goddard and others 2006); it is characterised by two different clinical presentations, interdigital dermatitis (ID) and under-running footrot. ID is an initial inflammation of the interdigital skin where the superficial epidermal layers are inflamed, damaged and slough off irregularly and it may develop into under-running footrot, which is characterised by the separation of the hoof horn from the sensitive underlying tissue (Beveridge 1941, Egerton and others 1969). In Australia, mild/benign footrot is also used synonymously for ID and under-running footrot is called virulent footrot (Raadsma and Dhungyel 2013).

Footrot is a complex disease with *Dichelobacter nodosus,* a Gram-negative anaerobic bacterium, as the essential pathogen causing under-running footrot (Egerton and others 1969, Kennan and others 2001, 2010, Han and others 2008). *D nodosus* load was found to be already increased in ID before the development of under-running footrot, thereby suggesting that *D nodosus* load drives the early stages of infection (Witcomb and others 2014, 2015). Additionally, the occurrence of this disease is associated with different factors such as the virulence of *D nodosus* strains (Kennan and others 2010), farm management (Green and others 2007), environmental conditions (Wassink and others 2005, Muzafar and others 2016) and initial damage in the epithelium of the interdigital skin (Beveridge 1941, Egerton and others 1969).

Whole-genome sequencing demonstrated that *D nodosus* has a global conserved bimodal population, correlating with virulent and benign phenotypes (Kennan and others 2014). A large number of virulent *D nodosus* strains were identified in Australia (Kennan and others 2014), while in Scandinavian countries, such as Sweden, mainly benign strains have been found (Frosth and others 2015). In UK flocks, virulent *D nodosus* was more prevalent than benign in swabs from sheep with ID and footrot (Moore and others 2005). Virulent and benign *D nodosus* strains differ in their ability to degrade the extracellular matrix of the host due to enzymatic activity of extracellular proteases (Riffkin and others 1995). The acidic protease AprV2 is responsible for the overall elastase activity of virulent strains and was shown to be essential for the development of footrot, while the acidic protease AprB2 is associated with a benign phenotype (Kennan and others 2010). Importantly, presence of virulent *D nodosus* strains does not always correlate with severity of clinical presentations since virulent *D nodosus* has also been identified in sheep without any clinical sign and in ID cases (Moore and others 2005, Stäuble and others 2014).

In addition, *Fusobacterium necrophorum*, *Treponema* species and a range of other bacterial genera have been identified in the ovine interdigital skin (Roberts and Egerton 1969, Bennett and others 2009, Calvo-Bado and others 2011, Frosth and others 2015). The role of *F necrophorum* in this disease still needs to be fully understood, with two hypothesis currently discussed: (i) *F necrophorum* is important to establish ID before *D nodosus* infection and hence initiates the disease (Egerton and others 1969) or (ii) *F necrophorum* is involved in the persistence and severity of footrot, once the under-running lesion has developed, playing a role as an opportunistic, secondary pathogen (Witcomb and others 2014, 2015). *F necrophorum* is divided into subspecies *necrophorum* and *funduliforme*, the first is described to be more pathogenic (Tan and others 1996).

Veterinary Record (2016) doi: 10.1136/vr.103610

G. Maboni, BVetMed, MSc,
S. Tötemeyer, DiplBiol, PhD,
School of Veterinary Medicine and Science, University of Nottingham, Sutton Bonington, UK
S. Frosth, MSc,
Department of Biomedical Sciences and Veterinary Public Health, Swedish University of Agricultural Sciences, Uppsala, Sweden
A. Aspán, MSc, PhD,
Department of Microbiology, National Veterinary Institute (SVA), Uppsala, Sweden
S. Frosth is also at Department of Microbiology, National Veterinary Institute (SVA), Uppsala, Sweden
E-mail for correspondence: sabine.totemeyer@nottingham.ac.uk

Provenance: not commissioned; externally peer reviewed
Accepted May 27, 2016

Downloaded from http://veterinaryrecord.bmj.com/ on April 18, 2017 - Published by group.bmj.com

Treponema species are usually free-living spirochetes, but they have been associated with contagious ovine digital dermatitis (CODD) (Sullivan and others 2015) and bovine digital dermatitis (BDD) (Gomez and others 2012). BDD and CODD have polytreponemal aetiology with different *Treponema* species involved in their pathogenesis (Sayers and others 2009, Sullivan and others 2015). Initial identification of spirochetes in ovine footrot lesions was reported by Beveridge (1941). Recent studies identified *Treponema* species in a sheep with ID lesions from a flock with footrot history (Calvo-Bado and others 2011) and were found in both flocks and feet, with and without footrot (Frosth and others 2015). Hence, it suggests that further investigation to elucidate their role and whether different species of *Treponema* can be identified in ovine footrot is warranted.

Taken together, current data suggest that footrot is a polymicrobial disease and *D nodosus* and other microorganisms might have a synergistic relationship. However, the role of bacterial diversity and load and how that differ between healthy, ID and footrot feet remains unclear. In this context, the aims of this study were (i) to investigate the colonisation of *D nodosus, F necrophorum, Treponema* species and eubacteria, and (ii) to characterise the virulence of *D nodosus* strains in a cross section of healthy, ID and footrot abattoir biopsies from the ovine interdigital skin.

Materials and methods

Collection of tissue biopsies

This study included 241 ovine interdigital postslaughter biopsies collected at an abattoir using a convenience sampling approach due to variable availability of the clinical conditions at slaughter. The entire sample set included 79 healthy, 39 mild ID (slight lesion with ≤5 per cent of the interdigital skin space affected), 26 moderate/severe ID (interdigital skin lesions with ≥5 per cent of the interdigital space affected) and 97 footrot samples (Table 1). Of these, 40 animals had all four feet sampled, total of 160 samples. During two visits to the abattoir (November 1, 2013, and November 4, 2013), it was not possible to follow the same animal on the processing line; therefore, 78 feet biopsies were collected without the information if they belonged to the same sheep (Table 1). Since the animals were sampled in the processing line of the abattoir, no information regarding sheep breed or other characteristics was available for this study.

At the abattoir, all feet disease status was scored by two different scorers with one of the scorers present during all visits in order to standardise the sampling and scoring method; for details, see Table 1. The scoring system was adapted from Parsonson and others (1967), allowing classification into healthy, ID or footrot feet according to established scoring criteria: absence of interdigital skin lesion=healthy; slight interdigital skin lesion (≤5 per cent affected)=mild ID; moderate-to-severe ID lesion (>5 per cent affected); presence of under-running lesion=footrot.

Tissues were collected as described previously (Davenport and others 2014) and placed into RNALater (Sigma-Aldrich, Saint Louis, USA) at 4°C before long-term storage at −20°C.

DNA extraction and real-time PCR assays

For enzymatic digestion, each tissue was cut into small pieces and incubated with 180 µl of tissue lysis buffer (ATL) and 20 µl of proteinase K (20 mg/ml) (Qiagen, Hilden, Germany) at 56°C for three hours. DNA was isolated using the QIAamp cador kit according to manufacturer's recommendations and eluted in 50 µl AVE buffer (Qiagen). The final DNA concentration was determined using NanoDrop (ND-1000 (Thermo Fisher Scientific, Waltham, USA). Bacterial load was quantified using real-time PCR based on *16S rRNA* gene for eubacteria (Strub and others 2007) and *D nodosus* (Frosth and others 2012) and the intergenic spacer region 2 containing a tRNAIle gene for *Treponema* species (Frosth and others 2015). Real-time PCR for *F n* subspecies *necrophorum* and *F n* subspecies *funduliforme* targeted the *gyrB* gene (Frosth and others 2015). Differentiation between virulent and benign *D nodosus* was performed based on the presence of *aprV2* (virulent) and *aprB2* (benign) genes (Frosth and others 2015). *D nodosus* and eubacteria assays were performed using PCR Lightcycler 480 (Roche Applied Science, Penzberg, Germany). Virulent and benign *D nodosus*, *F necrophorum* and *Treponema* species assays were carried out in an Applied Biosystems 7500 Fast Real-Time PCR System (Thermo Fisher Scientific).

Statistical analysis

Fisher's exact test was performed for bacterial prevalence and one-way analysis of variance followed by Dunn's multiple comparisons test for bacterial load using GraphPad Prism (V.6.0, La Jolla, USA). CIs of the prevalence data were calculated using GraphPad Software (http://graphpad.com/quickcalcs/confInterval2/). A P value ≤0.05 was considered significant.

Results

Prevalence and load of *D nodosus*, *F necrophorum* and *Treponema* species in tissues from the ovine interdigital skin

The prevalence of *D nodosus*, *F necrophorum*, *Treponema* species and eubacteria was investigated in the ovine interdigital skin biopsies. All samples were positive for eubacteria (100 per cent of prevalence). Both total *D nodosus* and virulent *D nodosus* were significantly more prevalent in mild ID ($P<0.05$ and <0.01, respectively), moderate/severe ID ($P<0.001$ and <0.0001, respectively) and footrot ($P<0.05$ and <0.01, respectively) in comparison with healthy feet, with highest prevalence in moderate/severe ID samples. Moreover, total *D nodosus* and virulent *D nodosus* were significantly more prevalent in moderate-to-severe ID than in footrot samples (Fig 1a; see online supplementary appendix 1). In contrast, benign *D nodosus* was only detected in 7 per cent (17/241) of the samples (Fig 1b). Mixed populations of benign and virulent *D nodosus* strains were found in a small number of samples across all clinical conditions (Fig 1b).

F necrophorum was detected in 15 per cent (36/241) of the samples, with 14.5 per cent (35/241) positive for *F necrophorum* subspecies *necrophorum*, only two samples positive for *F necrophorum* subspecies *funduliforme* and one sample positive for both

TABLE 1: Number of visits to the abattoir and number of biopsies collected from healthy, interdigital dermatitis and footrot ovine feet

Date of visit to abattoir	Number of healthy feet	Number of interdigital dermatitis feet	Number of footrot feet	Number of sheep with all four feet sampled	Total number of samples collected
October 21, 2013[1,2]	32	6	2	10	40
November 1, 2013*[1,2]	0	20	20	0	40
November 4, 2013*[1,2]	4	4	30	0	38
December 13, 2013[1,2]	14	7	19	10	40
December 16, 2013[1,2]	10	19	10	10	39
January 19, 2015[1,3]	19	9	16	10	44
Total	79	65	97	40	241

*It was not possible to follow the same animal in the processing line
[1–3]Scorer 1 (GM), scorer 2 (MB), scorer 3 (MA)

Downloaded from http://veterinaryrecord.bmj.com/ on April 18, 2017 - Published by group.bmj.com

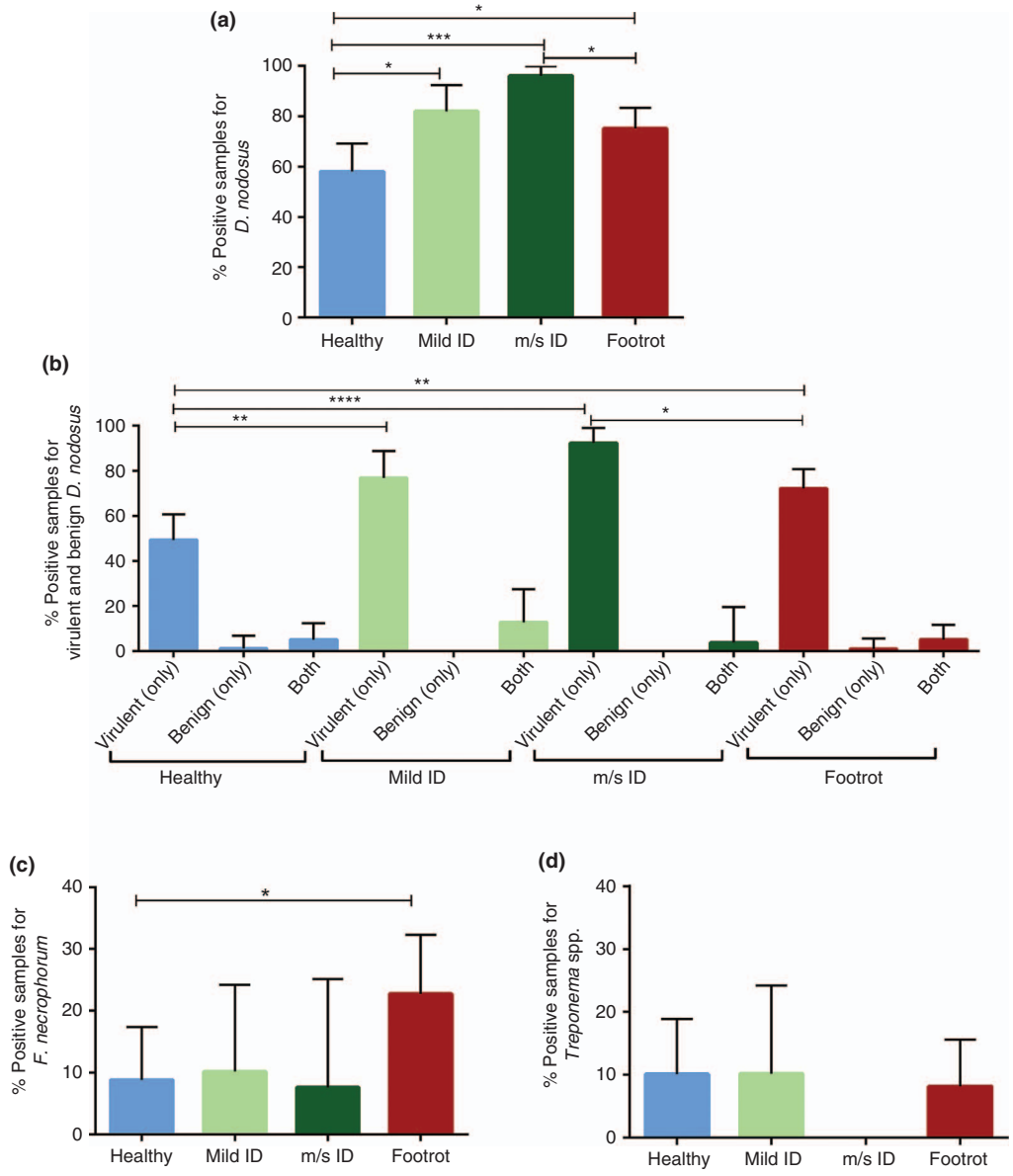


FIG 1: Bacterial prevalence in the ovine interdigital skin from healthy, interdigital dermatitis (ID) and footrot feet biopsies. Prevalence and CIs (95 per cent) are shown for total *Dichelobacter nodosus* (a); virulent and benign *D nodosus* (b); *Fusobacterium necrophorum* (c); *Treponema* species (d). Mild ID (ID score 1); m/s ID (moderate-to-severe ID scores 2, 3 and 4). Data were analysed by Fisher's exact test. *P≤0.05, **P≤0.01, ***P≤0.001, ****P≤0.0001

subspecies. *F necrophorum* was significantly more prevalent in footrot than in healthy feet (P<0.05) (Fig 1c). Presence of both *D nodosus* and *F necrophorum* in the same tissue sample or virulent *D nodosus* and *F necrophorum* in the same tissue was significantly higher in footrot compared with healthy feet (P<0.01 and <0.01, respectively). *Treponema* species prevalence was very low (8 per cent, 20/241) and similar across all clinical conditions (Fig 1d) (see online supplementary appendix 1).

Similar proportion of eubacterial DNA was detected at around 0.06 per cent±0.020 (mean±se of the mean) of total DNA for all samples, with 0.07 per cent±0.041 for healthy samples, 0.028 per cent±0.007 mild ID, 0.027±0.011 for moderate/severe ID and 0.073±0.039 for footrot samples. *D nodosus* load was significantly higher in moderate/severe ID and footrot in comparison to healthy feet (P<0.0001 for both) (Fig 2a). Virulent *D nodosus* load was significantly increased in mild ID, moderate/severe ID and footrot compared with a healthy feet (P=0.001, P<0.0001 and P<0.0001, respectively), with highest load in moderate/severe ID (Fig 2b). *F necrophorum* load was significantly increased in footrot but not in ID samples (P=0.022) (Fig 2c). The highest *Treponema* species load was found in footrot followed by healthy feet (Fig 2d).

In summary, while eubacterial loads were similar in all feet, both prevalence and load of total and virulent *D nodosus* were highest in moderate-to-severe ID, while *F necrophorum* were highest in footrot samples.

Discussion

In this study, the authors provided further insights into the bacterial colonisation present in healthy, ID and footrot ovine feet. The authors found similar patterns regarding the prevalence and load of *D nodosus* and *F necrophorum* in postslaughter biopsies from the interdigital space as previous studies in UK sheep flocks using swabs and biopsies (Moore and others 2005, Calvo-Bado and others 2011, Witcomb and others 2014, 2015).

As expected, the highest *D nodosus* prevalence and load found in this study was in ID samples, hence supporting the hypothesis that *D nodosus* drives the development of the early stages of footrot (Witcomb and others 2014, 2015). Interestingly, *D nodosus* was found in a large proportion of biopsy samples from healthy feet (58 per cent, 46/79), suggesting it might be present in the stratum corneum (horny layer) but not necessarily causing disease. It is also possible that these visibly healthy feet might have had subclinical footrot and may have developed

Downloaded from http://veterinaryrecord.bmj.com/ on April 18, 2017 - Published by group.bmj.com

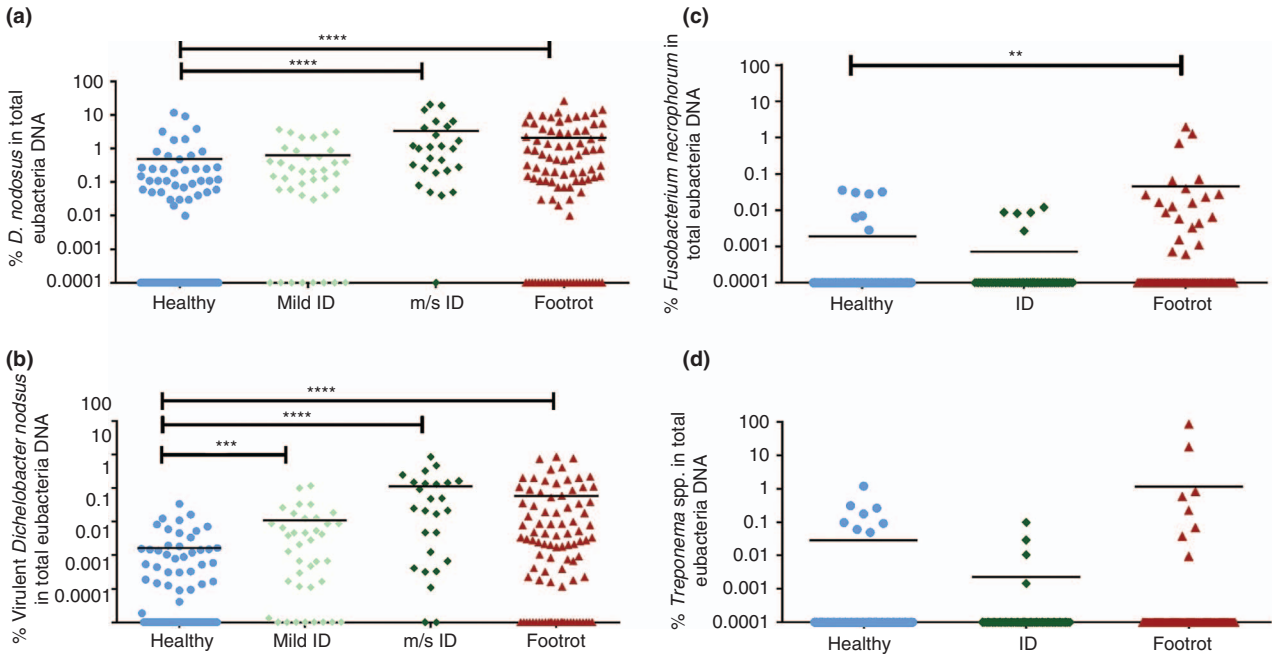


FIG 2: Bacterial load in the ovine interdigital skin from healthy, interdigital dermatitis (ID) and footrot feet biopsies. Load of total *Dichelobacter nodosus* (a), virulent *D nodosus* (b), *Fusobacterium necrophorum* (c) and *Treponema* species (d) as percentage of total eubacterial DNA. Due to very low numbers of positive samples, mild ID and ms ID have been pooled together as ID for *F necrophorum* (c) and for *Treponema* species (d). Healthy=79 samples; mild ID=39 samples; m/s ID=26 samples; footrot=97 samples. Mean is indicated by a black horizontal line. Data were analysed by Dunn's multiple comparisons test. *P≤0.05, **P≤0.01, ***P≤0.001, ****P≤0.0001. Number 0.001 (y axis): results below of the detection limit. mild ID score 1; ms ID: moderate-to-severe ID scores 2, 3 and 4

under-running lesions in the following days. Risk factors for the development of under-running footrot in addition to the presence of virulent *D nodosus* include poor foot conformation (Kaler and others 2010), superficial skin damage (Egerton and others 1969), sheep breed (Emery and others 1984) and presence of co-infecting bacteria such as *F necrophorum* (Egerton and others 1969, Roberts and Egerton 1969).

In this study, the majority of *D nodosus* present in the ovine interdigital skin biopsies were virulent strains. Similarly, high prevalence of virulent *D nodosus* in the UK sheep was identified previously using gelatinase gel protease assay (Moore and others 2005). Therefore, these studies demonstrate that virulent strains are currently circulating in UK flocks. In contrast, in Sweden where under-running footrot is not endemic, most of the *D nodosus* were found to be benign (Frosth and others 2015). The authors found a mixed population of benign and virulent *D nodosus* strains in the same feet; a potential synergistic role of benign and virulent strains still needs to be investigated.

F necrophorum prevalence and load were higher in footrot than in ID and healthy samples. These results, together with other published data that also found an increased presence of *F necrophorum* in footrot lesions (Beveridge 1941, Bennett and others 2009, Witcomb and others 2014, 2015), support the hypothesis that *F necrophorum* contributes to the pathogenesis of under-running footrot. *F necrophorum* was presumed to facilitate *D nodosus* invasion (Egerton and others 1969); in the present study, the authors found that the presence of both *D nodosus* and *F necrophorum* in the same tissue was significantly higher in footrot than in healthy feet; nevertheless, the exact nature and the role of the synergy between *F necrophorum* and *D nodosus* remains unclear.

Only a small number (9 per cent, 7/79) of healthy biopsy samples were positive for *F necrophorum* in this study. Similarly, Witcomb and others (2015) found low prevalence of *F necrophorum* in swabs (8 per cent, 1/12) and biopsies (8 per cent, 1/12) from healthy feet, but in an earlier study where swabs were repeatedly collected from 18 sheep during five weeks, *F necrophorum* was found in 62 per cent (140/225) of healthy feet (Witcomb and others 2014). This suggests that the prevalence of *F necrophorum* in healthy feet varies according to sampling structure and collection methods. *F necrophorum* is a commensal in the alimentary tract (Smith and Thornton 1997) and might be present in faeces contaminating ovine feet. Moreover, it was also detected on swabs taken from the oral cavity of sheep and suggested it might be transmitted from the mouth of sheep to the paddock (Bennett and others 2009); hence, the significance of *F necrophorum* in healthy ovine interdigital skin remains unclear; it may colonise healthy skin as a commensal microorganism without causing any skin disease, while in damaged skin, *F necrophorum* colonisation may initiate ID and, thus, predispose the invasion of *D nodosus*. Whether *D nodosus* essentially requires *F necrophorum* colonisation to facilitate its skin invasion remains unclear.

F necrophorum is divided into subspecies *necrophorum* and *funduliforme*, the first is described to be more pathogenic due to a higher lipopolysaccharide content and higher production of leukotoxin (Tan and others 1996). In this study, the majority of positive samples for *F necrophorum* was subspecies *necrophorum*. Previous studies investigating this bacterium in UK flocks did not differentiate the subspecies of *F necrophorum* (Witcomb and others 2014, 2015). Therefore, despite the fact that this sample set is small, this is the first study suggesting that *F necrophorum* subspecies *necrophorum* may be the more prevalent subspecies circulating in UK flocks. Since *F n* subspecies *necrophorum* is described to be more virulent than *F n* subspecies *funduliforme* (Tan and others 1996) and considering the fact that this bacterium may exacerbate footrot lesions, there might be an association between the high prevalence of severe footrot lesions in the UK and the presence of *F n* subspecies *necrophorum*. In contrast, in Swedish flocks where most of the footrot lesions were associated with mild footrot, *F n* subspecies *funduliforme* was more prevalent than *F n* subspecies *necrophorum* (Frosth and others 2015).

Spirochaetes have also been identified in ID and/or footrot lesions (Beveridge 1941, Calvo-Bado and others 2011, Frosth and others 2015). In the present study, a small number of biopsies

Downloaded from http://veterinaryrecord.bmj.com/ on April 18, 2017 - Published by group.bmj.com

were positive for *Treponema* species with similar prevalence in healthy, ID and footrot feet. Similarly, low detection of *Treponema* species in ovine biopsies from UK sheep was also reported by Calvo-Bado and others (2011); moreover, no significant association between *Treponema* species and footrot was reported by Frosth and others (2015). Hence, whether the low detection of *Treponema* species reflects its importance in the footrot pathogenesis remains an open question to be further elucidated. The authors amplified treponemal DNA using a genus-specific qPCR and not a species-specific assay, hence detecting free living as well as pathogenic *Treponema* species; therefore, more studies are warranted to characterise the *Treponema* species commonly present in ovine footrot. In contrast to early investigations reporting that an initial infection with *D nodosus* is often followed by an infection with *Treponema* species (Beveridge 1941, Thomas 1962), the authors only found 3 per cent of the biopsies (8/241) positive for both virulent *D nodosus* and *Treponema* species.

A limitation of using abattoir samples is that it is impossible to investigate the progression of the disease and thus verify whether healthy or ID feet positive for *D nodosus* would develop footrot lesions. On the other hand, an advantage of using abattoir samples is the ability to collect biopsies from animals that are slaughtered for other purposes than this study and detect bacteria localised within tissues.

Conclusions

The results presented in this study, together with other published data, confirm that *D nodosus* is mainly associated with ID stage and *F necrophorum* with footrot stage, thereby supporting that *D nodosus* drives the early stages of footrot and *F necrophorum* plays a role in the pathogenesis of ovine footrot. Moreover, virulent *D nodosus* population is more prevalent than benign in UK flocks. *Treponema* species were detected in few samples; hence, further studies are warranted to provide more detailed information about the role *Treponema* species may have in ovine footrot. Additionally, this study reports novel results regarding the higher prevalence of *F necrophorum* subspecies *necrophorum* than subspecies *funduliforme* in sheep from the UK, and a mixed population of virulent and benign *D nodosus* present in the same skin biopsy.

Acknowledgements

We thank Marianne Gilhuus for kindly providing DNA from *D nodosus*.

Correction notice This article has been corrected since it was published Online First. The asterisks indicating p values have been added into Figure 2.

Funding This work was funded by the University of Nottingham, and Swedish Farmers' Foundation for Agricultural Research is also acknowledged for financial support. GM had a fellowship from the Coordination for the Improvement of Higher Education (CAPES, Brazil).

► Additional material is available. To view please visit the journal (http://dx.doi.org/10.1136/vr.103610).

References

BENNETT, G., HICKFORD, J., ZHOU, H., LAPORTE, J. & GIBBS, J. (2009) Detection of *Fusobacterium necrophorum* and *Dichelobacter nodosus* in lame cattle on dairy farms in New Zealand. *Research in Veterinary Science* **87**, 413–415

BEVERIDGE, W. I. B. (1941) Foot-rot in sheep: a transmissible disease due to infection with *Fusiformis nodosus* (n. sp.): studies on its cause, epidemiology and control. *CSIRO Australian Bulletin* **140**, 1–56

CALVO-BADO, L. A., OAKLEY, B. B., DOWD, S. E., GREEN, L. E., MEDLEY, G. F., UL-HASSAN, A., BATEMAN, V., GAZE, W., WITCOMB, L., GROGONO-THOMAS, R., KALER, J., RUSSELL, C. L. & WELLINGTON, E. M. H. (2011) Ovine pedomics: the first study of the ovine foot 16S rRNA-based microbiome. *The ISME Journal* **5**, 1426–1437

DAVENPORT, R., HEAWOOD, C., SESSFORD, K., BAKER, M., BAIKER, K., BLACKLAWS, B., KALER, J., GREEN, L. & TÖTEMEYER, S. (2014) Differential expression of Toll-like receptors and inflammatory cytokines in ovine interdigital dermatitis and footrot. *Veterinary Immunology and Immunopathology* **161**, 90–98

EGERTON, J. R., ROBERTS, D. S. & PARSONSON, I. M. (1969) The aetiology and pathogenesis of ovine foot-rot. A histological study of the bacterial invasion. *Journal of Comparative Pathology* **79**, 207–215

EMERY, D. L., STEWART, D. J. & CLARK, B. L. (1984) The comparative susceptibility of five breeds of sheep to foot-rot. *Australian Veterinary Journal* **61**, 85–88

FROSTH, S., KÖNIG, U., NYMAN, A. K., PRINGLE, M. & ASPÁN, A. (2015) Characterisation of *Dichelobacter nodosus* and detection of *Fusobacterium necrophorum* and *Treponema* spp. in sheep with different clinical manifestations of footrot. *Veterinary Microbiology* **179**, 82–90

FROSTH, S., SLETTEMEÅS, J. S., JØRGENSEN, H. J., ANGEN, Ø. & ASPÁN, A. (2012) Development and comparison of a real-time PCR assay for detection of *Dichelobacter nodosus* with culturing and conventional PCR: harmonisation between three laboratories. *Acta Veterinaria Scandinavica* **54**, 6

GODDARD, P., WATERHOUSE, T., DWYER, C. & STOTT, A. (2006) The perception of the welfare of sheep in extensive systems. *Small Ruminant Research* **62**, 215–225

GOMEZ, A., COOK, N. B., BERNARDONI, N. D., RIEMAN, J., DUSICK, A. F., HARTSHORN, R., SOCHA, M. T., READ, D. H. & DÖPFER, D. (2012) An experimental infection model to induce digital dermatitis infection in cattle. *Journal of Dairy Science* **95**, 1821–1830

GREEN, L. E., WASSINK, G. J., GROGONO-THOMAS, R., MOORE, L. J. & MEDLEY, G. F. (2007) Looking after the individual to reduce disease in the flock: a binomial mixed effects model investigating the impact of individual sheep management of footrot and interdigital dermatitis in a prospective longitudinal study on one farm. *Preventive Veterinary Medicine* **78**, 172–178

HAN, X., KENNAN, R. M., DAVIES, J. K., REDDACLIFF, L. A., DHUNGYEL, O. P., WHITTINGTON, R. J., TURNBULL, L., WHITCHURCH, C. B. & ROOD, J. I. (2008) Twitching motility is essential for virulence in *Dichelobacter nodosus*. *Journal of Bacteriology* **190**, 3323–3335

KALER, J., MEDLEY, G. F., GROGONO-THOMAS, R., WELLINGTON, E. M., CALVO-BADO, L. A., WASSINK, G. J., KING, E. M., MOORE, L. J., RUSSELL, C. & GREEN, L. E. (2010) Factors associated with changes of state of foot conformation and lameness in a flock of sheep. *Preventive Veterinary Medicine* **97**, 237–244

KENNAN, R. M., DHUNGYEL, O. P., WHITTINGTON, R. J., EGERTON, J. R. & ROOD, J. I. (2001) The type IV fimbrial subunit gene (fimA) of *Dichelobacter nodosus* is essential for virulence, protease secretion, and natural competence. *Journal of Bacteriology* **183**, 4451–4458

KENNAN, R. M., GILHUUS, M., FROSTH, S., SEEMANN, T., DHUNGYEL, O. P., WHITTINGTON, R. J., BOYCE, J. D., POWELL, D. R., ASPÁN, A., JØRGENSEN, H. J., BULACH, D. M. & ROOD, J. I. (2014) Genomic evidence for a globally distributed, bimodal population in the ovine footrot pathogen *Dichelobacter nodosus*. *mBio* **5**, e01821–14

KENNAN, R. M., WONG, W., DHUNGYEL, O. P., HAN, X., WONG, D., PARKER, D., ROSADO, C. J., LAW, R. H., MCGOWAN, S., REEVE, S. B., LEVINA, V., POWERS, G. A., PIKE, R. N., BOTTOMLEY, S. P., SMITH, A. I., MARSH, I., WHITTINGTON, R. J., WHISSTOCK, J. C., PORTER, C. J., ROOD, J. I. (2010) The subtilisin-like protease AprV2 is required for virulence and uses a novel disulphide-tethered exosite to bind substrates. *PLoS Pathogens* **6**, e1001210

MOORE, L. J., WASSINK, G. J., GREEN, L. E. & GROGONO-THOMAS, R. (2005) The detection and characterisation of *Dichelobacter nodosus* from cases of ovine footrot in England and Wales. *Veterinary Microbiology* **108**, 57–67

MUZAFAR, M., GREEN, L. E., CALVO-BADO, L. A., TICHAUER, E., KING, H., JAMES, P. & WELLINGTON, E. M. (2016) Survival of the ovine footrot pathogen *Dichelobacter nodosus* in different soils. *Anaerobe* **38**, 81–87

PARSONSON, I. M., EGERTON, J. R. & ROBERTS, D. S. (1967) Ovine interdigital dermatitis. *Journal of Comparative Pathology* **77**, 309–313

RAADSMA, H. W. & DHUNGYEL, O. P. (2013) A review of footrot in sheep: new approaches for control of virulent footrot. *Livestock Science* **156**, 115–125

RIFFKIN, M. C., WANG, L. F., KORTT, A. A. & STEWART, D. J. (1995) A single amino-acid change between the antigenically different extracellular serine proteases V2 and B2 from *Dichelobacter nodosus*. *Gene* **167**, 279–283

ROBERTS, D. S. & EGERTON, J. R. (1969) The aetiology and pathogenesis of ovine foot-rot. The pathogenic association of *Fusiformis nodosus* and *F. necrophorus*. *Journal of Comparative Pathology* **79**, 217–227

SAYERS, G., MARQUES, P. X., EVANS, N. J., O'GRADY, L., DOHERTY, M. L., CARTER, S. D. & NALLY, J. E. (2009) Identification of spirochetes associated with contagious ovine digital dermatitis. *Journal of Clinical Microbiology* **47**, 1199–1201

SMITH, G. R. & THORNTON, E. A. (1997) Classification of human and animal strains of *Fusobacterium necrophorum* by their pathogenic effects in mice. *Journal of Medical Microbiology* **46**, 879–882

STÄUBLE, A., STEINER, A., NORMAND, L., KUHNERT, P. & FREY, J. (2014) Molecular genetic analysis of *Dichelobacter nodosus* proteases AprV2/B2, AprV5/B5 and BprV/B in clinical material from European sheep flocks. *Veterinary Microbiology* **168**, 177–184

STRUB, S., VAN DER PLOEG, J., NUSS, K., WYSS, C., LUGINBÜHL, A. & STEINER, A. (2007) Quantitation of *Guggenheimella bovis* and treponemes in bovine tissues related to digital dermatitis. *FEMS Microbiology Letters* **269**, 48–53

SULLIVAN, L. E., CLEGG, S. R., ANGELL, J. W, NEWBROOK, K., BLOWEY, R. W., CARTER, S. D., BELL, J., DUNCAN, J. S., GROVE-WHITE, D. H., MURRAY, R. D. & EVANS, N. J. (2015) High-level association of bovine digital dermatitis *Treponema* spp. with contagious ovine digital dermatitis lesions and presence of *Fusobacterium necrophorum* and *Dichelobacter nodosus*. *Journal of Clinical Microbiology* **53**, 1628–1638

TAN, Z. L., NAGARAJA, T. G. & CHENGAPPA, M. M. (1996) *Fusobacterium necrophorum* infections: virulence factors, pathogenic mechanism, and control measures. *Veterinary Research Communications* **20**, 113–140

THOMAS, J. H. (1962) The bacteriology and histopathology of footrot in sheep. *Australian Journal of Agricultural Research* **13**, 725

Downloaded from http://veterinaryrecord.bmj.com/ on April 18, 2017 - Published by group.bmj.com

WASSINK, G. J., MOORE, L. J., GROGONO-THOMAS, R. & GREEN, L. E. (2005) Footrot and interdigital dermatitis in sheep: farmers' practices, opinions and attitudes. *Veterinary Record* **157**, 761–765

WITCOMB, L. A., GREEN, L. E., CALVO-BADO, L. A., RUSSELL, C. L., SMITH, E. M., GROGONO-THOMAS, R. & WELLINGTON, E. M. (2015) First study of pathogen load and localisation of ovine footrot using fluorescence in situ hybridisation (FISH). *Veterinary Microbiology* **176**, 321–327

WITCOMB, L. A., GREEN, L. E., KALER, J., UL-HASSAN, A., CALVO-BADO, L. A., MEDLEY, G. F., GROGONO-THOMAS, R. & WELLINGTON, E. M. (2014) A longitudinal study of the role of *Dichelobacter nodosus* and *Fusobacterium necrophorum* load in initiation and severity of footrot in sheep. *Preventive Veterinary Medicine* **115**, 48–55

Downloaded from http://veterinaryrecord.bmj.com/ on April 18, 2017 - Published by group.bmj.com

Veterinary Record

Ovine footrot: new insights into bacterial colonisation

G. Maboni, S. Frosth, A. Aspán and S. Tötemeyer

Veterinary Record 2016 179: 228 originally published online June 17, 2016
doi: 10.1136/vr.103610

Updated information and services can be found at:
http://veterinaryrecord.bmj.com/content/179/9/228

These include:

References This article cites 32 articles, 6 of which you can access for free at:
http://veterinaryrecord.bmj.com/content/179/9/228#BIBL

Email alerting service Receive free email alerts when new articles cite this article. Sign up in the box at the top right corner of the online article.

Notes

To request permissions go to:
http://group.bmj.com/group/rights-licensing/permissions

To order reprints go to:
http://journals.bmj.com/cgi/reprintform

To subscribe to BMJ go to:
http://group.bmj.com/subscribe/

Maboni et al. 2016 (Ovine footrot: new insights into bacterial colonisation). TABLE 1 supplementary appendix: Fisher exact test of the bacterial prevalence in the ovine interdigital skin biopsies.

	Dichelobacter nodosus		**virulent *D. nodosus***	
	Yes	**No**	**Yes**	**No**
Healthy	46 (58.2%[95%CI: 46.6-69.2%])	33 (41.8%[95%CI: 30.7-53.4%])	39 (49.3%[95%CI: 37.9-60.8%])	40 (50.6%[95%CI: 39.1-62.1%])
Mild interdigital dermatitis (ID)	32 (82%[95%CI: 66.4-92.4%])	7 (17.9%[95%CI: 7.5-33.5%])	30 (76.9%[95%CI: 60.6-88.9%])	9 (23%[95%CI: 11.1-39.3%])
Moderate to Severe ID	25 (96.1%[95%CI: 80.3-99.9%])	1 (3.8%[95%CI: 0.1-19.6%])	24 (92.3%[95%CI: 74.8-99%])	2 (7.6%[95%CI: 0.95-25.1%])
Footrot	73 (75.2%[95%CI: 65.4-83.4%])	24 (24.7%[95%CI: 16.5-34.5%])	70 (72.1%[95%CI: 62.1-80.8%])	27 (27.8%[95%CI: 19.2-37.8%])
Healthy vs. mild ID p-value:	**0.013**		**0.005**	
Healthy vs. moderate/severe ID p-value:	**0.0002**		**<0.0001**	
Healthy vs. footrot p-value:	**0.023**		**0.003**	
moderate /severe ID vs. footrot p-value:	**0.025**		**0.037**	

Bold values: statistically significant (P≤0.05)

Healthy (n=79); mild interdigital dermatitis (n=39); moderate to severe interdigital dermatitis (n=26); footrot (n=97)
Fisher's exact test was performed using GraphPad Prism (Version 6.0, La Jolla, USA).

Continuous from Appendix 1 TABLE 1 supplementary appendix: Fisher exact test of the bacterial prevalence in the ovine interdigital skin biopsies.

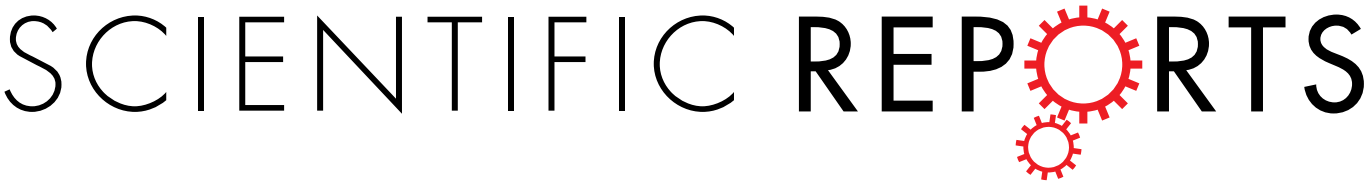
	F. necrophorum* and *D. nodosus		***F. necrophorum* and virulent *D. nodosus***		***Treponema* spp.**	
	Yes	**No**	**Yes**	**No**	**Yes**	**No**
Healthy	4 (5.1%[95%CI: 1.4%-12.4%])	75 (94.9%[95%CI: 87.5-98.6%])	5 (6.33%[95%CI: 2.1-14.1%])	74 (93.6%[95%CI: 85.8-97.9%])	8 (10.1%[95%CI: 4.4-18.9%])	71(89.9%[95%CI: 81-95.5%])
Mild interdigital dermatitis (ID)	5 (12.8%[95%CI: 4.3-27.4%])	34 (87.1%[95%CI: 72.6-95.7%])	3 (7.69%[95%CI: 1.6-20.9%])	36 (92.3%[95%CI: 79.1-98.3%])	4 (10.2%[95%CI: 2.8-24.2%])	35 (89.7%[95%CI: 75.8-97.1%])
Moderate to Severe ID	2 (7.6%[95%CI: 0.95-25.1%])	24 (92.3%[95%CI: 74.8-99%])	2 (7.6%[95%CI: 0.95-25.1%])	24 (92.3%[95%CI: 74.8-99%])	0	26
Footrot	19 (19.5%[95%CI: 12.2-28.9%])	78 (80.4%[95%CI: 71.1-87.8%])	20 (20.6%[95%CI: 13-30%])	77 (79.3%[95%CI: 70-86.9%])	8 (8.2%[95%CI: 3.6-15.6%])	89 (91.7%[95%CI: 84.3-96.3%])
Healthy vs. mild ID p-value:	0.155		1		1	
Healthy vs. moderate/severe ID p-value:	0.636		1		0.196	
Healthy vs. footrot p-value:	**0.006**		**0.009**		0.793	

Continuous from Appendix 1 TABLE 1 supplementary appendix: Fisher exact test of the bacterial prevalence in the ovine interdigital skin biopsies.

	***D. nodosus* and *Treponema* spp.**		**virulent *D. nodosus* and *Treponema* spp.**		***D. nodosus* + *F. necrophorum* + *Treponema* spp.**	
	Yes	**No**	**Yes**	**No**	**Yes**	**No**
Healthy	7 (8.8%[95%CI: 3.64-17.4%])	72 (91.4%[95%CI: 82.6-96.3%])	4 (5.1%[95%CI: 1.4%-12.4%])	75 (94.9%[95%CI: 87.5-98.6%])	3 (3.8%[95%CI: 0.8-10.7%])	
Mild interdigital dermatitis (ID)	4 (10.2%[95%CI: 2.8-24.2%])	35 (89.7%[95%CI: 75.8-97.1%])	1 (2.5%[95%CI: 0.06%-13.4%])	38 (97.4%[95%CI: 86.5%-99.9%])	3 (7.69%[95%CI: 1.6-20.9%])	36 (92.3%[95%CI: 79.1-98.3%])
Moderate to Severe ID	0	26	0	26	0	26
Footrot	7 (7.2%[95%CI: 2.9-14.3%])	90 (92.8%[95%CI: 85.7-97%])	3 (3%[95%CI: 0.64-8.7%])	94 (97%[95%CI: 91.2-99.3%])	0	97
Healthy vs. mild ID p-value:	1		1		0.395	
Healthy vs. moderate/severe ID p-value:	0.189		0.570		0.573	
Healthy vs. footrot p-value:	0.782		0.702		0.0885	

Appendix 2

(Maboni et al. 2017 – Chapter 5 and 6)



OPEN

A distinct bacterial dysbiosis associated skin inflammation in ovine footrot

Received: 09 December 2016
Accepted: 21 February 2017
Published: 24 March 2017

Grazieli Maboni[1,*], Adam Blanchard[1,*], Sara Frosth[2,3], Ceri Stewart[1], Richard Emes[1,4] & Sabine Tötemeyer[1]

Ovine footrot is a highly prevalent bacterial disease caused by *Dichelobacter nodosus* and characterised by the separation of the hoof horn from the underlying skin. The role of innate immune molecules and other bacterial communities in the development of footrot lesions remains unclear. This study shows a significant association between the high expression of IL1β and high *D. nodosus* load in footrot samples. Investigation of the microbial population identified distinct bacterial populations in the different disease stages and also depending on the level of inflammation. *Treponema* (34%), *Mycoplasma* (29%) and *Porphyromonas* (15%) were the most abundant genera associated with high levels of inflammation in footrot. In contrast, *Acinetobacter* (25%), *Corynebacteria* (17%) and *Flavobacterium* (17%) were the most abundant genera associated with high levels of inflammation in healthy feet. This demonstrates for the first time there is a distinct microbial community associated with footrot and high cytokine expression.

Footrot is an infectious disease and a major cause of lameness affecting sheep welfare worldwide[1,2]. The disease causes a significant financial impact, estimated to be £24 to £80 million in annual losses within the United Kingdom alone[2]. Footrot is the progression of interdigital dermatitis (ID) due to the presence and effect of *D. nodosus*. ID is characterised by inflammation of the superficial epidermal layers, which slough off irregularly. This potentially leads to underrunning footrot, characterised by the separation of the hoof horn from the sensitive underlying tissue[1].

Virulent *D. nodosus,* a Gram negative bacterium, is essential to initiate underrunning footrot lesions[3,4]. *Fusobacterium necrophorum,* also a Gram negative bacterium, is attributed to play a role in the initiation of ID prior to *D. nodosus* infection[1], and/or in the exacerbation of footrot lesions once it is established[5]. Other bacteria such as *Treponema* have also been detected in footrot cases, but its role in the disease process remains unclear[6–8]. A microbiota study, using a pyrosequencing approach, found 27 different bacterial genera in the ovine interdigital skin where *Peptostreptococcus* was the most abundant genus in healthy interdigital skin, *Corynebacterium* was mainly associated with ID and *Staphylococcus* was the most abundant read genus in footrot samples[6]. A similar disease in cattle, bovine digital dermatitis (BDD), also presents a complex aetiology and is considered a polymicrobial disease[9,10]. *Treponema* are the predominantly identified microorganism with *Fusobacterium necrophorum*, *Porphyromonas, Bacteroides*, *Campylobacter*, *Guggenheimella*, and *D. nodosus* also present in these lesions[9–12]. Research on footrot has been mainly focused on bacterial colonisation targeting *D. nodosus* and *F. necrophorum* to understand virulence mechanisms and disease progression. However, little is known about the role of other bacterial groups within skin or the ovine immune response to footrot, which may also play a fundamental role in the disease process. Advice regarding prevention of footrot in the U.K. is covered by the Agriculture and Horticulture Development Board Five point plan for tackling lameness in sheep, which includes the use of the Footvax vaccination[13]. This vaccine alone is not a standalone preventative measure and has to be used in coordination with the remaining four aspects of the suggested Five point plan[14]. Also, the efficacy of this multivalent vaccine is often questioned due to antigenic competition[14,15] and limited uptake is often attributed to additional cost and time

[1]University of Nottingham, School of Veterinary Medicine and Science, Sutton Bonington, United Kingdom. [2]Department of Biomedical Sciences and Veterinary Public Health, Swedish University of Agricultural Sciences, Uppsala, Sweden. [3]Department of Microbiology, National Veterinary Institute (SVA), Uppsala, Sweden. [4]Advanced Data Analysis Centre (ADAC), University of Nottingham, United Kingdom. *These authors contributed equally to this work. Correspondence and requests for materials should be addressed to S.T. (email: sabine.totemeyer@nottingham.ac.uk)

factors for farmers[2]. Current treatment of footrot is limited to parenteral antibiotics and topical bactericides[16]. Information on the immune response is an essential step for the establishment of new methods for prevention and control of footrot including the design of an efficacious and affordable vaccine. Several pro-inflammatory cytokines and chemokines are expressed in the skin including IL6, CXCL8, IL1β[17] and IL17[18]. IL1β has a range of stimulatory effects on immune cells playing a key role in the innate immunity of the skin[19]. Similarly, IL6 is involved in key immune processes such as monocyte and T-cell recruitment, survival and differentiation[20], and IL17 leads to release of pro-inflammatory cytokines and immune cell recruitment[18]. CXCL8 is a classical chemokine involved in the recruitment of neutrophils and proliferation of keratinocytes[21,22]. In the ovine interdigital space, the mRNA expression of TLR2, TLR4 and IL1β was found to be significantly elevated in severe ID and footrot[23]. Other studies so far have been focused on the investigation of the systemic ovine inflammatory response to footrot in the context of vaccination or experimental infection with *D. nodosus*[24–26]. Following experimental infection with *D. nodosus* and vaccination no changes in TLR4 mRNA expression in peripheral blood leukocytes was observed; in contrast, TLR2 mRNA expression levels increased in peripheral blood in leukocytes response to both, infection or vaccination[27]. In this context, we hypothesise that the pathology of footrot is a host mediated expression of local immune responses, in association with bacterial colonisation, leading to severe inflammation that can progress to underrunning footrot. This study aimed to investigate whether high virulent *D. nodosus* load and abundance of bacterial populations are associated with high levels of inflammation in the ovine interdigital skin.

Results

Identification of reliable reference genes for the normalization of RT-qPCR data from the ovine interdigital skin. To improve robustness of the reference gene identified in our previous study[23], we increased sample size for each clinical condition (10 healthy, 10 mild ID, 10 moderate/severe ID and 10 footrot), the number of potential reference genes included and multiple algorithms to assess stability. In addition, we also included a co-regulation analysis. mRNA expression levels of *ACTB, GAPDH, TUBA*, *PPIA*, *18S rRNA*, *TMEM79, ASCC2, C3ORF58, BHLHE40* and *DDX54* were examined in all 40 biopsies by RT-qPCR to verify their reliability as potential reference genes. The amplification efficiencies were between 90–105%, except for *TUBA* (122%) (Supplementary Table 1). The RefFinder web based tool[28] was used to analyse gene expression stability in accordance with the MIQE guidelines[29,30]. Comprehensive analysis identified that *ACTB, DDX54* and *PPIA* were the most stably expressed genes and *TUBA*, *18S rRNA and GAPDH* were ranked as the least stably expressed genes (Supplementary Table 2). The four algorithms incorporated by RefFinder showed slightly different gene ranking orders individually; however, *ACTB, PPIA* and *DDX54* were consistently ranked as the most stably expressed genes in all algorithms (Supplementary Table 2) with no major differences among the different clinical conditions observed. The co-regulation analysis showed that two groups of the selected reference genes had common upstream regulators: (1) *C3ORF58* and *DDX54* and (2) *ACTB, GAPDH* & *TUBA*. No direct co-regulator was known between *ACTB*, *PPIA* and *DDX54*, which were identified as reliably stable genes by RefFinder software.

To investigate the host immune response to interdigital dermatitis and footrot, the mRNA expression levels of IL1β, IL6, CXCL8 and IL17 were analysed in 53 visually healthy, 55 ID samples and 83 footrot samples. PCR products were confirmed by sequencing and all targets showed amplification efficiencies within the ranges of an optimised RT-qPCR assay (90–105%, Supplementary Table 1). Expression of all targets was detected. Surprisingly, healthy samples showed a wide and marked inflammatory background and no differential gene expression of any inflammatory mediator in the context of clinical conditions was identified (Fig. 1a,d,g,j). This suggests that expression of the cytokines targeted in this study is not affected by ID and footrot alone, but may relate to bacterial colonisation or other non-infectious causes. In this context, we investigated whether foot conformation and integrity could affect the expression levels of cytokines in the ovine interdigital skin. There was no difference in the mRNA expression levels of IL1β, IL6 IL17 and CXCL8 in samples from feet with conformation scores 2 and 3 (Supplementary Fig. 1).

Microbial diversity associated with disease condition. The microbial population analysis was carried out on tissue biopsies from 40 healthy, 30 ID and 36 footrot samples. The healthy pool of samples contained 10,655,297 sequences, ID had 7,606,638 and footrot had 11,103,063. Post quality filtering the healthy pool of samples contained 8,609,842 (81%) sequences, ID had 6,625,304 (87%) and footrot had 8,999,482 (81%). After taxonomic classification using the Ribosomal database project RDPTools classifier[31] 6,734,875 (78%) sequences were classified for healthy samples, 4,474,178 (68%) for ID and 6,030,053 (67%) for footrot (Supplementary Fig. 2). Pielou's evenness test showed a significant difference between healthy and footrot affected samples at each taxonomic level assessed (phylum $p = \leq 0.0001$, family $p = \leq 0.05$ and genus $p = \leq 0.0001$), and a significant difference between healthy and ID at phylum ($p = \leq 0.01$) and genus ($p = \leq 0.01$) levels. The Shannon index showed a significant difference at the genus level between healthy and footrot affected samples ($p = \leq 0.01$) (Supplementary Fig. 3). The two main bacterial families across all three disease states were Moraxellaceae (20–36%) and Corynebacteriacae (14–20%) (Fig. 2a). The main bacterial families significantly increased in abundance in footrot compared to both, healthy and ID samples, were Mycoplasmatacae ($p < 0.0001$ for both), Spirochaetaceae ($p < 0.0001$ for both) and Fusobacteriacae ($p < 0.0001$ for both). Bacterial families with significantly increased abundance in healthy samples compared to footrot included Flavobacteriaceae ($p < 0.0001$) and Staphylococcaceae ($p = 0.017$) (Fig. 2a). At genus level the three most abundant bacterial genera in healthy and ID samples were *Corynebacterium* (H: 26%, ID: 31%), *Psychrobacter* (H: 26%, ID: 19%) and *Acinetobacter* (H: 11%, ID: 8%). In contrast, in footrot samples, four genera were highly represented: *Mycoplasma* (20%, $p = 0.0009$ vs healthy, $p = 0.007$ vs ID), *Corynebacterium* (19%), *Psychrobacter* (18%) and *Treponema* (14%, $p < 0.0001$ vs both, H and ID) (Fig. 2b,c). As expected, *D. nodosus* abundance was low (0.5–1.9%) but significantly higher in ID ($p = 0.0005$) and footrot samples ($p < 0.0001$) compared to healthy samples (Fig. 2c). Taken together the microbial community of tissue samples from the interdigital space of footrot affected feet is significantly different to that of healthy and ID affected feet.

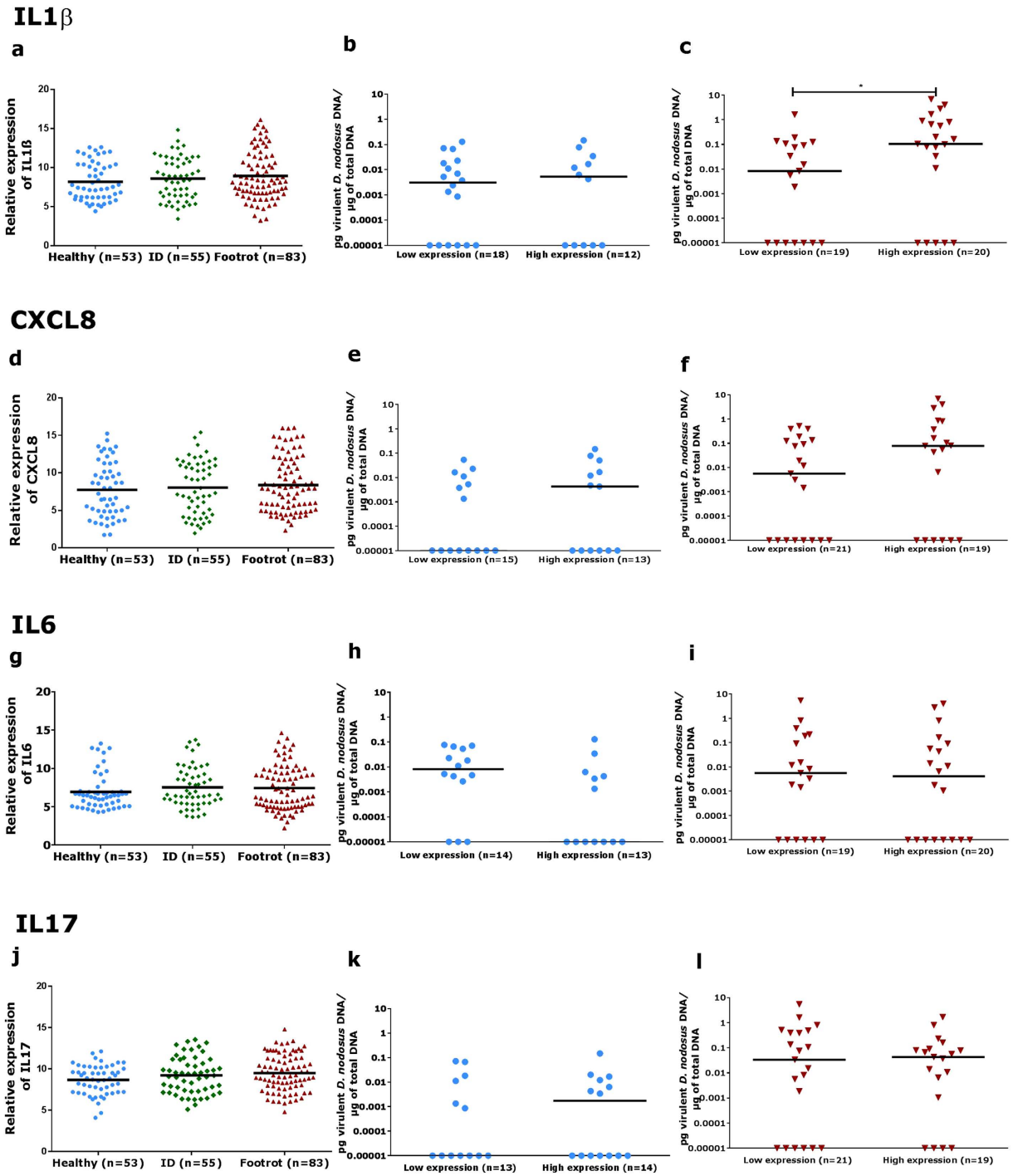


Figure 1. Relative mRNA expression levels of IL1β (**a**), CXCL8 (**d**), IL6 (**g**) and IL17 (**j**) in healthy, interdigital dermatitis (ID) and footrot biopsies from the ovine interdigital skin. Association between virulent *Dichelobacter nodosus* load and relative mRNA expression of IL1β (**b**), CXCL8 (**e**), IL6 (**h**) and IL17 (**k**) in healthy samples with low and high expression levels of these cytokines (blue symbols). Association between virulent *D. nodosus* load and relative mRNA expression of IL1β (**c**), CXCL8 (**f**), IL6 (**i**) and IL17 (**l**) in footrot samples with low and high expression levels of these cytokines (red symbols). Median is represented by black bars. Kruskal-Wallis test (Mann Whitney test, non-parametric) was performed to verify the association between virulent *D. nodosus* load and expression of IL1β, IL6, CXCL8 and IL17. Kruskal-Wallis test (Dunn's multiple comparison test, non-parametric) was used to verify the association between cytokines relative mRNA expression levels with clinical conditions, $^{*}p < 0.037$.

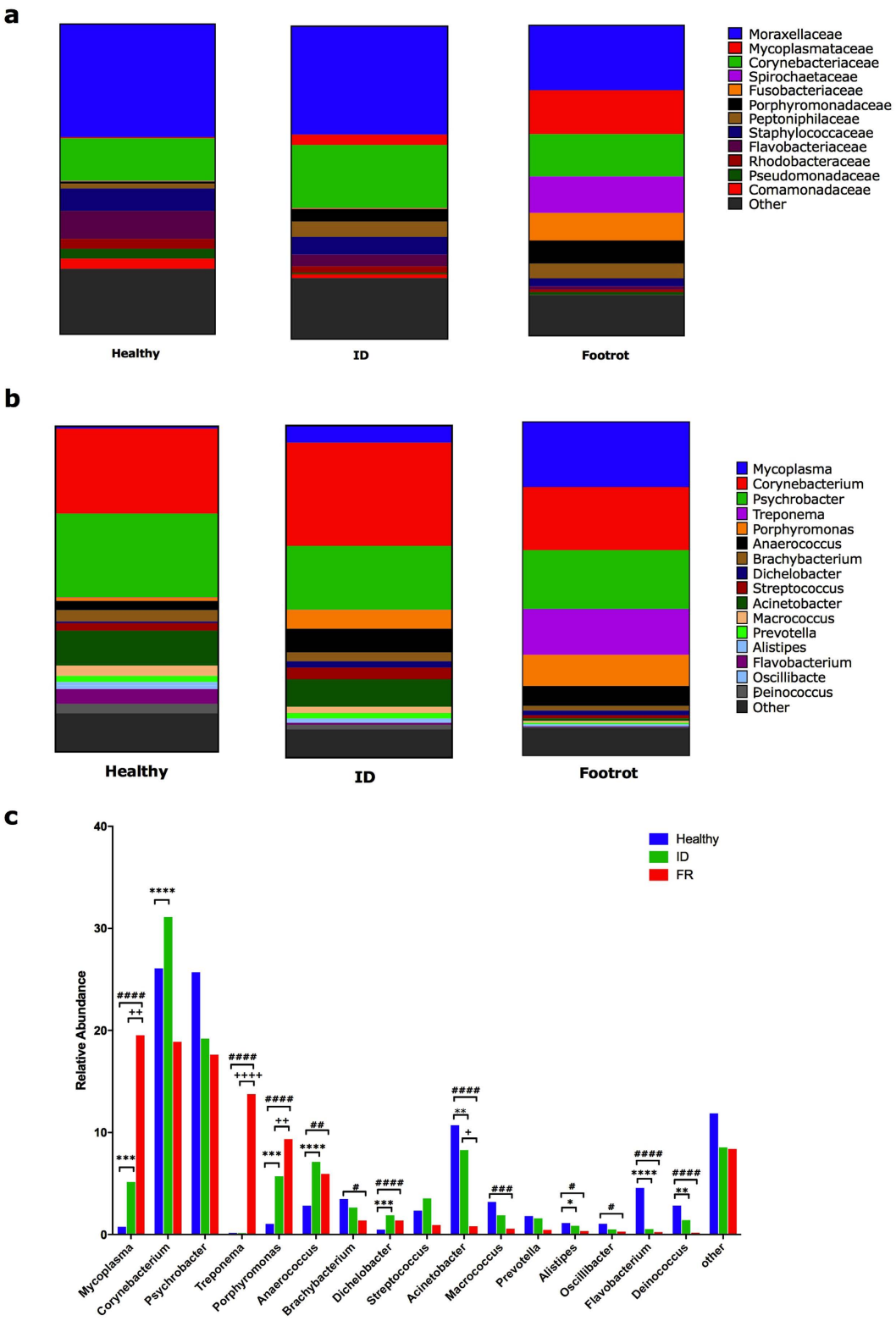


Figure 2. Microbial communities in ovine interdigital skin tissues from healthy, interdigital dermatitis (ID) and footrot affected feet. Relative abundance of taxonomic bacterial groups in healthy (n = 40), ID (n = 30) and footrot (n = 36) affected feet using 16 S rRNA gene based metagenomics. (**a**) at the family level (**b**) at the genus level, (**c**) at genus level with ≥1 relative abundance. 'ID' significantly different to 'Healthy' $^{*}p < 0.05$, $^{**}p < 0.01$, $^{***}p < 0.001$, $^{****}P < 0.0001$; 'FR ' significantly different to 'Healthy' $^{\#}p < 0.05$, $^{\#\#}p < 0.01$, $^{\#\#\#\#}p < 0.0001$; 'FR' significantly different to 'ID ' $^{++}P < 0.01$, $^{+++}P < 0.001$, $^{++++}P < 0.0001$.

	IL1β vs. D. nodosus		CXCL8 vs. D. nodosus		IL6 vs. D. nodosus		IL17 vs. D. nodosus	
	r	P value	r	P value	r	P value	r	P value
Healthy	0.029	0.839	0.096	0.492	−0.042	0.764	0.202	0.152
Footrot	0.229	**0.040**	0.221	**0.046**	−0.082	0.558	0.025	0.858

Table 1. Correlation analysis between pro-inflammatory cytokines relative mRNA expression and virulent *Dichelobacter nodosus* load. Bold values: statistically significant P value (<0.05). r: Pearson's correlation coefficient.

Association of the host immune response and virulent *D. nodosus* colonisation. Considering that clinical conditions and foot conformation were not significantly associated with higher expression of the investigated pro-inflammatory cytokines, we investigated whether the load of the causative bacterium of underrunning footrot, virulent *D. nodosus*, is associated with high expression of inflammatory markers. Low but significant correlations of virulent *D. nodosus* load and cytokine mRNA expression were identified for IL1ß ($p = 0.039$) and CXCL8 ($p = 0.046$) in samples from footrot affected feet (Table 1). To investigate this further, samples with IL1β, IL6, CXCL8 and IL17 expression values within the 25th (low) and 75th (high) quartiles were selected to investigate the *D. nodosus* load (Fig. 1b,c,e,f,h,i,k,l). While in healthy samples the *D. nodosus* load is similar in the low and high inflammation groups, in footrot samples with high levels of IL1β expressions also have significantly higher *D. nodosus* load (Fig. 1b,c).

Microbial diversity associated with low and high levels of inflammation in the ovine interdigital skin. In the context of footrot being a polymicrobial infection and the main microorganism, *D. nodosus,* being significantly associated with high levels of IL1β in footrot samples, we further investigated whether the microbial community composition differs depending on high (75th quartile) and low (25th quartile) levels of inflammation using IL1β expression as a marker of inflammation. Sequence reads from the previous analysis were pooled according to IL1β expression level and corresponding disease state. A total of 21 samples were associated with healthy animals (12 low IL1β expression and 9 high IL1β expression) and 15 footrot affected samples (7 low IL1β expression and 8 high IL1β expression). The number of sequence reads were 2,273,223 and 2,699,979 for healthy low and high IL1β expression and 2,536,826 and 3,671,436 for footrot low and high respectively. After quality filtering, there were 2,032,217 (89%) and 2,182,260 (81%) for healthy low and high IL1β expression and 1,904,295 (75%) and 2,826,028 (77%) for footrot low and high, respectively. Post taxonomic classification, using the Ribosomal database project RDPTools classifier[31], there were 1,860,595 (92%) designation for healthy low samples, 1,725,874 (79%) for healthy high, 1,783,436 (94%) for footrot low and 1,650,951 (58%) for footrot high (for individual samples see Supplementary Fig. 2). Pielou's evenness test showed a significant difference between healthy samples with low IL1β expression and footrot affected samples with high IL1β expression (phylum $p = \leq 0.001$ and genus $p = \leq 0.05$) and between healthy sample with low IL1β expression and healthy samples with high IL1β expression (phylum $p = \leq 0.05$) and footrot affected with low IL1β expression and footrot affect with high IL1β expression (phylum $p = \leq 0.05$ and genus $p = \leq 0.05$). Shannon index also highlighted a significant difference between healthy samples with low IL1β expression and footrot affected samples with high IL1β expression (phylum $p = \leq 0.01$). There were no significant differences at the family taxonomic level (Supplementary Fig. 4). Surprisingly, at the taxonomic levels investigated the bacterial communities from low inflammation healthy and low inflammation footrot samples were very similar (Fig. 3a–c). On family level the main groups were Moraxellaceae (31–44% abundance) and Corynebacteriacae (23–27% abundance) (Fig. 3b); and at genus level the three most abundant bacterial genera were *Psychrobacter* (27–40%), *Corynebacterium* (30–39%) and *Anaerococcus* (8%) (Fig. 3c,d). In contrast, the microbial communities from high inflammation healthy and high inflammation footrot are very different to each other as well as to the low inflammation samples from the same disease state (Fig. 3a–c). Comparing those two microbial communities, on family level the highly abundant groups in high inflammation healthy samples are Moraxellaceae (30%) and Flavobacteriaecae (20%, $p = 0.001$), and in high inflammation footrot samples are Spirochaetaceae (33%, $p < 0.0001$), Mycoplasmataecae (26%, $p = 0.0002$) and Porphyromonadaecae (14%, $p < 0.0001$) (Fig. 3b). At genus level the most abundant genera in high inflammation healthy samples were *Acinetobacter* (25%), *Corynebacteria* (17%) and *Flavobacterium* (17%), which are all significantly less abundant in low inflammation healthy samples ($p < 0.0001$, $p = 0.035$ and $p < 0.0001$, respectively) (Fig. 3c,d). In high inflammation footrot samples, *Acinetobacter* (0.05%) and *Flavobacterium* (0.05%) are significantly less abundant ($p < 0.0001$ for both) (Fig. 3c,d). In contrast, the most abundant genera in those high inflammation footrot samples are *Treponema* (34%), *Mycoplasma* (29%) and *Porphyromonas* (15%), which are significantly less abundant in both, low inflammation footrot samples ($p < 0.0001$, $p < 0.0001$, $p = 0.0006$, $p = 0.039$, respectively) and high inflammation healthy samples ($p < 0.0001$ for all 4 genera) (Fig. 3c,d). Taken together this demonstrates while the bacteria communities are very similar in low inflammation healthy and footrot samples, high inflammation samples from healthy as well as from footrot samples have distinct and very different bacterial communities.

Discussion

This study investigated the microbial community in the context of inflammation in healthy and footrot affected ovine feet and showed for the first time that inflammation, as marked by high mRNA expression levels of IL1β, a central mediator of immune response in the skin, is associated with a distinct microbial community in the ovine interdigital skin. Analysis of the microbial community showed distinct bacterial populations in tissues from healthy, ID and footrot affected feet. The four most abundant phyla in all skin samples, irrespective of

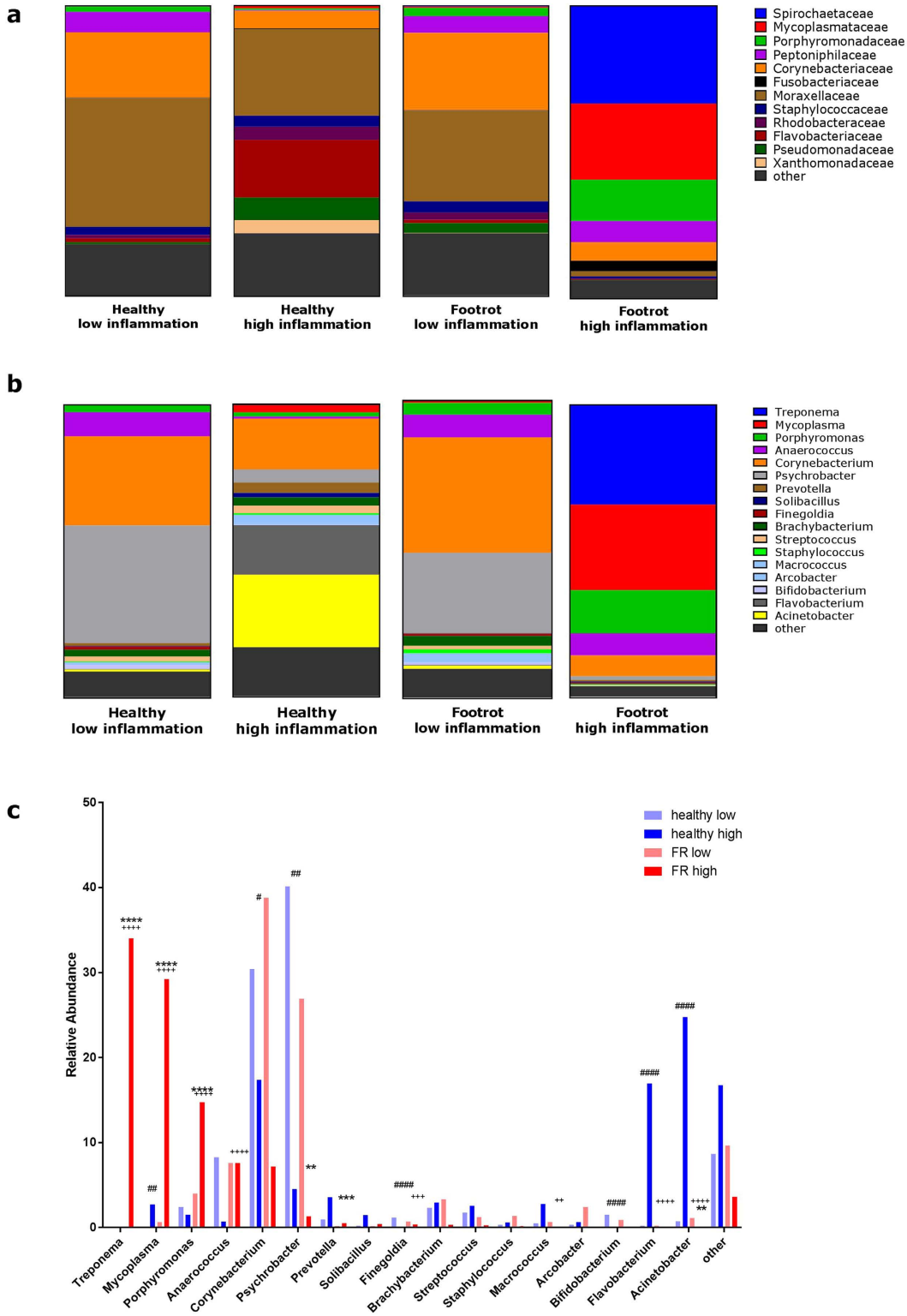


Figure 3. Microbial communities in ovine interdigital skin tissues with high and low levels of inflammation from healthy and footrot affected feet. Relative abundance of taxonomic bacterial groups in tissue with low and high levels of inflammation from healthy (H, n = 12 and n = 9) and footrot (FR, n = 7 and n = 8) affected feet, respectively using a 16 S rRNA amplicon survey. (**a**) at the family level (**b**) at the genus level, (**c**) at genus level with ≥1 relative abundance. 'FR high' significantly different to 'FR low' $^{**}p < 0.01$, $^{***}p < 0.001$, $^{****}P < 0.0001$; 'H high' significantly different to 'H low' $^{\#}p < 0.05$, $^{\#\#}p < 0.01$, $^{\#\#\#\#}p < 0.0001$; + 'FR high' significantly different to 'H high' $^{++}P < 0.01$, $^{+++}P < 0.001$, $^{++++}P < 0.0001$.

clinical conditions, were Actinobaceria, Firmicutes, Proteobacteria and Bacteriodetes, which were also found to be the most abundant phyla in the interdigital space of healthy dogs[32] and in healthy bovine skin of the claw area[10,33]. The same phyla were found in bovine DD lesions[33] at differing proportions, whilst Tenericutes, Spirochaetes and Fusobacteria are enriched in footrot samples. In healthy and ID feet the most abundant genera were *Corynebacteria*, *Psychrobacter* and *Acinetobacter*, while in footrot the most abundant genera were *Mycoplasma*, *Corynebacteria*, *Psychrobacter* and *Treponema*. However, these populations differ from a small study that was the first publication of the 16S based ovine foot microbiome, where *Macrococcus*, *Peptostreptococcus* and *Corynebacteria* were most abundant in healthy, *Macrococcus* and *Corynebacteria* were most abundant in ID and *Macrococcus*, *Staphylococcus* and *Corynebacteria* most abundant in footrot affected feet[6]. There are several factors that explain those differences, in our study the sample number was higher (40 healthy, 30 ID and 36 footrot versus 3 healthy, 2 ID, 1 footrot), each of our samples was from an individual foot and not pooled from all feet per sheep. This could affect the footrot specific community identified if the individual animal only had one foot affected. In addition, the sequencing technology and data processing pipelines have significantly changed in the last few years. As expected, *D. nodosus* had greater abundance in footrot samples as was also shown by qPCR to have a higher load. Surprisingly, the microbial community composition appears to show a stronger correlation with inflammation level rather than disease state since there is very little difference between the microbiome of healthy and footrot low inflammation biopsies while the microbial community and the dominant genera differed greatly between healthy high inflammation (*Acinetobacter*, *Corynebacterium*, *Flavobacterium*) and footrot high inflammation tissues (*Treponema*, *Mycoplasma*, *Porphyromonas*). Increased proportions of *Corynebacteria* were also observed in canine atopic dermatitis[34]. Of the bacterial genera identified, *Dichelobacter*, *Fusobacteria* and *Treponema* all linked to ovine or bovine foot disease[4,6–8,10]. *Prevotella* and *Porphyromonas* were isolated from footrot cases in goats[35] and were recently reclassified from *Bacteriodes melaninogenicus*[36], a species regularly isolated from bovine interdigital necrobacillosis (bovine footrot)[37]. *Corynebacterium*, a non-motile and facultative anaerobic bacterium, has been reported to be abundant in tissue biopsies from ID affected feet[6], but also near the surface of the interdigital skin of sheep and in footrot lesions[38]. In addition, *Corynebacterium* has been found in ovine heel abscesses[39]. *Psychrobacter* species are rarely associated with disease in animals. Two subspecies have been isolated from congested lungs from two different lambs (ages 20 days & 1 year) after sudden death[40]. *Mycoplasma* species are linked to lameness, generally associated with polyarthritis in a wide range of animals, mainly pigs and poultry[41,42], but also cattle[43,44] and occasionally in sheep[45].

The methodology we used, a 16S rRNA amplicon survey, has some inherent limitations associated with the data generated and the way in which they are analysed and how the results are interpreted. However, through experimental design and robust data analysis tools we have reduced those limitations where possible. While metagenomic whole genome sequencing is often the favoured methodology, with in-tissue samples like our interdigital post slaughter biopsies, microbial DNA typically accounts for less than 1% of the total DNA yield and methods of enrichment are required as host DNA would greatly overwhelm the microbial DNA present[46]. This is normally achieved by either host DNA depletion, increased sequencing depth or microbial enrichment like 16S rRNA amplification. In this situation, an amplicon approach is preferred because the required increase in sequencing depth would be cost prohibitive and current methods of host DNA depletion are more suited to biological fluid samples, where the host to microbe DNA ratio is more favourable. Short read sequencing requires targeting of a variable region. This may introduce bias due to poor resolution between bacteria[47], under representation of some genera[48] and positive selection for others[49,50]. Here the V3/V4 region was used as they are incorporated into the Illumina library prep workflow and are suggested to be a good primer pair for 16S rRNA discrimination[51]. However, this paring may not be the most optimal, and V4/V6 has now been shown to provide superior resolution[50]. Recently, contamination issues have been identified relating to the laboratory environment, reagents and preparation kit[52]. It is therefore important to be aware that some contaminants may be present in the data set, however most are common water or soil bacteria, which in context of this study it seems drastic to discount their presence completely as damaged interdigital skin is in close contact with soil and water. A pragmatic approach must be used to determine if their presence could be of any importance and abundance calculations used with some scepticism. Sequencing read number and quantity of input DNA need to be taken into account as low numbers of reads and low quality DNA can artificially exaggerate abundance within a sample due to poor amplification[53]. All DNA extractions used in this study were compared for uniformity and have average quantity of bacterial DNA; healthy samples 0.12 ng/μl (SD 0.7), ID 0.08 ng/μl (SD 0.5) and footrot 0.17 ng/μl (SD 3.6).

The host immune response was investigated through the mRNA expression of a panel of six inflammatory genes likely to have a role in skin immune responses in sheep and cattle[23,54,55]. Surprisingly, in the context of foot disease, no differential expression of IL1β, IL6, CXCL8 and IL17 was identified in ID and footrot compared to healthy samples. Using a smaller sample set ($n = 28$), our previous work has shown IL1β to be elevated in severe ID and footrot in relation to healthy samples[23]. These divergent results can be associated with a higher expression of IL1β in healthy samples found in this study than was observed by Davenport *et al.*[23]. Samples for the present study were collected between autumn and winter and it was noted that the weather had been significantly wetter than when samples were collected for the previous study. Wetter environmental conditions have been shown to increase the prevalence of interdigital dermatitis and footrot[15,38,39,56,57], therefore this might also impact on the basal levels of inflammation and may favour inflammation in the interdigital skin of apparently healthy samples. The wide inflammatory background seen in healthy samples might also be associated with the presence of subclinical disease that may have developed into ID and footrot in the next few days. However, using abattoir samples makes it impossible to investigate the progression of the disease and thus verify whether healthy feet would develop footrot lesions. These sheep might also have had footrot previously and the wide inflammatory response could be related to a healing process.

Infectious as well as non-infectious factors might be associated with inflammatory responses in the skin. Particularly in the context of footrot, poor foot conformation could be a non-infectious factor leading to a higher

expression of inflammatory genes indicating underlying damage and disease. Sheep with damaged sole and heel area have an increased susceptibility to become lame and consequently develop footrot[16]. In the present study, we showed that the effects of poor foot conformation were not directly associated with a higher inflammatory response, since slightly higher but not significant mRNA expression levels of cytokines was present in feet with poor conformation.

A significant association between samples with high expression of IL1β and high *D. nodosus* load in footrot samples as well as significant correlations between CXCL8 and IL1β with *D. nodosus* in footrot samples, but not in healthy samples, further confirmed that *D. nodosus* infection could play a key role in the development of an inflammatory microenvironment characterised by those pro-inflammatory cytokines. It is important to highlight that based on these experiments, it is not possible to conclude whether *D. nodosus* triggers the expression of CXCL8 and IL1β or the inflammation in the skin may facilitate the invasion of this bacterium. In our previous study, IL1β levels were elevated in ovine dermal fibroblasts stimulated with LPS or heat-killed extracts of *D. nodosus*, suggesting that both IL1β and fibroblasts play a key role in the host response to footrot[23]. CXCL8 production is part of the initial immune response and plays a role in the recruitment of neutrophils, as well as having an effect on the proliferation of keratinocytes[22]. Keratinocytes are key cells synthesising the potent pro-inflammatory cytokine IL1β[58]. This may explain the thickened epidermal layer of ovine interdigital skin observed in histological studies of footrot[1]. Both cytokines, CXCL8 and IL1β, were highly expressed in sheep with skin pyogranulomas[59], in response to inflamed foetal ovine skin[60] and also in bovine digital dermatitis lesions in cattle feet[54].

In summary, this study has shown distinct dysbiosis evident across disease states and the association with inflammation, highlighting the importance of the microbial population in relation to the local inflammatory response within the context of the healthy or footrot affected ovine foot.

Material and Methods

Study design and sample collection. Ovine interdigital post-slaughter biopsies were collected at an abattoir (Leicestershire, U.K.) at various time points (Oct 2013-Jan 2015) using a convenience sampling approach due to variable availability of the clinical conditions at slaughter. Firstly, ovine feet were scored for conformation/integrity of the sole and heel/wall of each digit: 0 = undamaged sole and heel area with a perfect shape. 1 = mildly damaged/misshapen sole and/or heel area of the digit (<25%). 2 = moderately damaged/misshapen sole and/or heel area of the digit (>25% and <75%). 3 = severely damaged/misshapen sole and/or heel area of the digit (>75%). Then, ovine feet disease status was scored as described previously[16], allowing classification into healthy, ID or footrot feet according to established scoring criteria: absence of interdigital skin lesion = healthy; slight interdigital skin lesion (≤5% affected) = mild ID; moderate to severe ID lesion (>5% affected); presence of underrunning lesion = footrot[8]. The sample set (n = 191) included 53 healthy, 55 interdigital dermatitis (ID) and 83 footrot biopsy samples. Biopsies were collected using disposable 6mm biopsy punches (National Veterinary Services) and then stored in 2 ml of RNALater® (Sigma-Aldrich, St. Luis, USA) according to manufacturer's instructions. Each biopsy was cut in half; one piece was used for DNA extraction and the other one for RNA extraction.

Quantification of virulent *D. nodosus*. Tissue homogenisation and DNA extractions were performed as described previously using QIAamp cador® kit (QIAGEN, Hilden, Germany)[8]. Virulent *D. nodosus* was quantified based on the presence of *aprV2* gene by quantitative PCR in an Applied Biosystems® 7500 Fast Real-Time PCR System (Thermo Fisher Scientific Inc., Waltham, USA) as previously described[7]. The data were normalised as pg of virulent *D. nodosus* DNA present in the total μg of DNA extracted from each tissue biopsy.

Microbial Diversity. Extracted DNA was subjected to a 16S rRNA V3/V4 variable region amplification by standard PCR using the Illumina metagenomic library preparation kit and primers 341F and 534R (Supplementary Table 3). The libraries were sequenced using an Illumina MiSeq at the National Veterinary Institute (SVA), Sweden. Sequencing consisted of four 2 × 300 bp runs, resulting in approximately 33 Gb of data (All raw sequence reads are available in the NCBI SRA Project number PRJNA369597). The generated reads where parsed through Trimmomatic (version 0.36)[61] to remove Illumina sequencing adaptors and 16S rRNA primer contamination based on Klindworth *et al.*[62]. Remaining sequences were also assessed and filtered using a 15 bp sliding window approach for quality scores (phred >30) and were required to be of a minimum length of 50 bp. The trimmed high quality reads where analysed using a local installation of the RDPTools 16S supervised taxonomic classification workflow[31] (https://github.com/rdpstaff/classifier). Briefly, UCHIME[63] was used to identify putative chimeric reads to be removed from the quality trimmed sequence file. Taxonomy was then assigned using the naïve Bayesian RDP classifier[31], with the default assignment cutoff of 0.8 and with the 16S SSU rRNA gene copy number adjustment enabled. Based on the qPCR data, the assigned samples were concatenated in 25th and 75th quartiles of IL1β expression for healthy and footrot affected samples allowing for population comparison. The counts (normalised for 16S rRNA copy number) per taxonomic level were imported into R for analysis using Vegan and Fossil packages[64,65]. Microbial diversity at phylum, family and genus taxonomic levels were assessed by calculating the Shannon index and Pielou's Evenness test.

RNA extraction & cDNA synthesis. Half biopsies were homogenised as described previously[23]. RNA was isolated using NucleoSpin RNA isolation kit (Machery-Nagel, Germany) following the manufacturer's recommendations. RNA concentration and quality were analysed using RNA 6000 Nano Kit Bioanalyser (Agilent technologies, Germany). RNA was diluted in water and cDNA was synthesised using M-MLV Reverse Transcriptase (Promega, Madison, USA) according to manufacturer's instructions. The final volume of each reaction was diluted in RNAse/DNAse free water (Fisher Scientific, UK).

Quantification of ovine gene expression. Ovine mRNA expression levels of β-Actin (*ACTB*), Glyceraldehyde-3-Phosphate Dehydrogenase (*GAPDH*), α-Tubulin (*TUBA*), Cyclophilin (*PPIA*) and Eukaryotic 18S ribosomal RNA (18S rRNA), Activating signal cointegrator 1 complex subunit 2 (*ASCC2*), basic helix-loop-helix family, member e40 (*BBHEL*), Transmembrane protein 79 (*TMEM79*), DEAD (Asp-Glu-Ala-Asp) box polypeptide 54 (*DDX54*) and chromosome 3 open reading frame 58 (*C3ORF58*), Interleukins IL1β, IL6, CXCL8 and IL17 were investigated by RT-qPCR using a LightCycler® 480 system (Roche Applied Science, UK). Primers for *ASCC2, BBHEL, TMEM79, DDX54* and *C3ORF58* genes were designed using Primer3Plus (version 0.4.0). For each gene, a minimum of three forward and three reverse primers were designed and assessed by RT-qPCR (Supplementary Table 2). All assays were performed with manual reaction setup using the LightCycler 480 system (Roche Applied Science, UK). Reactions contained 5 μl of cDNA (1/100 dilutions) in 1 × SYBR green qPCR master mix (Sigma-Aldrich, UK) with 1 μM of forward and reverse primers (Sigma Aldrich, UK). All standard dilutions, samples and no template controls (NTC) were performed in triplicates. For *ASCC2, BBHEL, TMEM79, DDX54* and *C3ORF58*, samples were subjected to initial denaturation at 95 °C for 20 minutes, followed by 45 cycles at 95 °C for 5 seconds, 60 °C for 20 seconds and 72 °C for 30 seconds and a continuous dissociation step at 97 °C to obtain a melt curve. For *ACTB, GAPDH, TUBA*, *PPIA*, 18S rRNA, IL1β, IL6, CXCL8 and IL17 the samples were subjected to initial denaturation at 95 °C for 10 minutes, followed by 45 cycles at 95 °C for 10 seconds, 60 °C for 50 seconds and 72 °C for 1 minute and a final dissociation step at 97 °C.

Analysis of reference genes stability and normalisation analysis. Analysis of reference genes stability was performed using RefFinder[28], integrating geNorm[66], Normfinder[67], BestKeeper[68], and a comparative ΔCq method, to compare and rank the tested candidate reference genes[69]. Upstream regulators were identified using the Ingenuity Pathway Analysis knowledgebase (IPA®, QIAGEN Redwood City). Normalised expression of RT-qPCR data of cytokines was calculated using the following formula: $CT + (NT\text{-}CT') * S/S'$ with S = target gene slope; S′ = reference gene slope; CT = Cq value of targeted gene for each sample; CT′ = Cq value of reference gene for each sample; NT = mean of Cq values of reference gene for all samples[70].

Richness and diversity analysis. The concatenated taxonomic assignment data was imported into R[71] to calculate diversity and richness statistics. Relative abundance was used at each taxonomic level to calculate the Shannon index and Pielous evenness using the vegan package[64] Kruskal-Wallis test (Dunn's multiple comparison test, non-parametric) was used to assess statistical differences in the diversity statistics. All analyses were performed using GraphPad Prism® (Version 6.0, La Jolla, USA) and a P-value ≤ 0.05 was considered significant. Determination of statistically significant differences in populations was carried out using R[71] with the edgeR[72] wrapper as part of phyloseq 1.6.1 package[73].

References

1. Egerton, J. R., Roberts, D. S. & Parsonson, I. The Aetiology and Pathogenesis of ovine Footrot. *J. comp. Pathol.* **79,** 207–217 (1969).
2. Wassink, G. J., George, T. R., Kaler, J. & Green, L. E. Footrot and interdigital dermatitis in sheep: farmer satisfaction with current management, their ideal management and sources used to adopt new strategies. *Prev Vet Med* **96,** 65–73 (2010).
3. Kennan, R. M., Dhungyel, O. P., Whittington, R. J., Egerton, J. R. & Rood, J. I. The type IV fimbrial subunit gene (*fimA*) of *Dichelobacter nodosus* is essential for virulence, protease secretion, and natural competence. *J Bacteriol* **183,** 4451–4458 (2001).
4. Kennan, R. M. *et al.* The subtilisin-like protease AprV2 is required for virulence and uses a novel disulphide-tethered exosite to bind substrates. *PLoS Pathog* **6,** e1001210 (2010).
5. Witcomb, L. A. *et al.* A longitudinal study of the role of *Dichelobacter nodosus* and *Fusobacterium necrophorum* load in initiation and severity of footrot in sheep. *Prev Vet Med* **115,** 48–55 (2014).
6. Calvo-Bado, L. a. *et al.* Ovine pedomics: the first study of the ovine foot 16S rRNA-based microbiome. *ISME J.* **5,** 1426–1437 (2011).
7. Frosth, S. *et al.* Characterisation of *Dichelobacter nodosus* and detection of *Fusobacterium necrophorum* and *Treponema* spp. in sheep with different clinical manifestations of footrot. *Vet. Microbiol.* **179,** 82–90 (2015).
8. Maboni, G., Frosth, S., Aspan, A. & Totemeyer, S. Ovine footrot: new insights into bacterial colonisation. *Vet Rec*, doi: 10.1136/vr.103610 (2016).
9. Krull, A. C. *et al.* Deep sequencing analysis reveals temporal microbiota changes associated with development of bovine digital dermatitis. *Infect. Immun.* **82,** 3359–3373 (2014).
10. Zinicola, M. *et al.* Altered microbiomes in bovine digital dermatitis lesions, and the gut as a pathogen reservoir. *PLoS One* **10,** e0120504 (2015).
11. Rasmussen, M. *et al.* Bovine digital dermatitis: possible pathogenic consortium consisting of *Dichelobacter nodosus* and multiple *Treponema* species. *Vet Microbiol* **160,** 151–161 (2012).
12. Schlafer, S. *et al.* Involvement of *Guggenheimella bovis* in digital dermatitis lesions of dairy cows. *Vet Microbiol* **128,** 118–125 (2008).
13. The Agriculture and Horticulture Development Board. The five-point plan for tackling lameness in sheep. at http://beefandlamb.ahdb.org.uk/wp/wp-content/uploads/2015/06/BRP-Lameness-five-point-plan-110615.pdf (2015).
14. Duncan, J. S. *et al.* Impact of footrot vaccination and antibiotic therapy on footrot and contagious ovine digital dermatitis. *Vet. Rec.* **170,** 462 (2012).
15. Wassink, G. J., Grogono-Thomas, R., Moore, L. J. & Green, L. E. Risk factors associated with the prevalence of interdigital dermatitis in sheep from 1999 to 2000. *Vet. Rec.* **154,** 551–555 (2004).
16. Kaler, J. *et al.* Factors associated with changes of state of foot conformation and lameness in a flock of sheep. *Prev Vet Med* **97,** 237–244 (2010).
17. Lai, Y. & Gallo, R. L. Toll-like receptors in skin infections and inflammatory diseases. *Infect Disord Drug Targets* **8,** 144–155 (2008).
18. Jin, W. & Dong, C. IL-17 cytokines in immunity and inflammation. *Emerg Microbes Infect* **2,** e60 (2013).
19. Arend, W. P., Palmer, G. & Gabay, C. IL-1, IL-18, and IL-33 families of cytokines. *Immunol Rev* **223,** 20–38 (2008).
20. Scheller, J., Chalaris, A., Schmidt-Arras, D. & Rose-John, S. The pro- and anti-inflammatory properties of the cytokine interleukin-6. *Biochim Biophys Acta* **1813,** 878–888 (2011).
21. Seow, H. F., Yoshimura, T., Wood, P. R. & Colditz, I. G. Cloning, sequencing, expression and inflammatory activity in skin of ovine interleukin-8. *Immunol Cell Biol* **72,** 398–405 (1994).
22. Tuschil, A., Lam, C., Haslberger, A. & Lindley, I. Interleukin-8 stimulates calcium transients and promotes epidermal cell proliferation. *J Invest Dermatol* **99,** 294–298 (1992).

23. Davenport, R. *et al.* Differential expression of Toll-like receptors and inflammatory cytokines in ovine interdigital dermatitis and footrot. *Vet. Immunol. Immunopathol.* **161,** 90–98 (2014).
24. Bhardwaj, V., Dhungyel, O., de Silva, K. & Whittington, R. J. Investigation of immunity in sheep following footrot infection and vaccination. *Vaccine* **32,** 6979–6985 (2014).
25. Raadsma, H. W., O'Meara, T. J., Egerton, J. R., Lehrbach, P. R. & Schwartzkoff, C. L. Protective antibody titres and antigenic competition in multivalent *Dichelobacter nodosus* fimbrial vaccines using characterised rDNA antigens. *Vet Immunol Immunopathol* **40,** 253–274 (1994).
26. Schwartzkoff, C. L. *et al.* The effects of antigenic competition of the efficacy of multivalent footrot vaccines. *Aust. Vet. J.* **70,** 123–126 (1993).
27. Bhardwaj, V. The role of the host in the pathogenesis of ovine footrot. PhD thesis (The University of Sydney 2012).
28. Fu, W. *et al.* Exploring valid reference genes for quantitative real-time PCR analysis in *Plutella xylostella* (Lepidoptera: Plutellidae). *Int. J. Biol. Sci.* **9,** 792–802 (2013).
29. Bustin, S. A. *et al.* The MIQE guidelines: minimum information for publication of quantitative real-time PCR experiments. *Clin Chem* **55,** 611–622 (2009).
30. Bustin, S. A. *et al.* MIQE precis: Practical implementation of minimum standard guidelines for fluorescence-based quantitative real-time PCR experiments. *BMC Mol Biol* **11,** 74 (2010).
31. Wang, Q., Garrity, G. M., Tiedje, J. M. & Cole, J. R. Naive Bayesian classifier for rapid assignment of rRNA sequences into the new bacterial taxonomy. *Appl Env. Microbiol* **73,** 5261–5267 (2007).
32. Hoffmann, A. R. *et al.* The skin microbiome in healthy and allergic dogs. *PLoS One* **9** (2014).
33. Nielsen, M. W. *et al.* Potential bacterial core species associated with digital dermatitis in cattle herds identified by molecular profiling of interdigital skin samples. *Vet. Microbiol.* **186,** 139–149 (2016).
34. Bradley, C. W. *et al.* Longitudinal evaluation of the skin microbiome and association with microenvironment and treatment in canine atopic dermatitis. *J. Invest. Dermatol.* 1–9, doi: 10.1016/j.jid.2016.01.023 (2016).
35. Lacombe-Antoneli, A., Piriz, S. & Vadillo, S. Aetiology of caprine footrot in Extremadura region, Spain. *Acta Vet Hung* **54,** 313–320 (2006).
36. Paster, B. J., Dewhirst, F. E., Olsen, I. & Fraser, G. J. Phylogeny of *Bacteroides*, *Prevotella*, and *Porphyromonas* spp. and related bacteria. *J. Bacteriol.* **176,** 725–732 (1994).
37. Berg, J. N. & Loan, R. W. *Fusobacterium necrophorum* and *Bacteroides melaninogenicus* as etiologic agents of foot rot in cattle. *Am J Vet Res* **36,** 1115–1122 (1975).
38. Beveridge, W. I. B. Foot-rot in sheep: a transmissible disease due to infection with *Fusiformis nodosus* (n. sp.): studies on its cause, epidemiology and control. *CSIRO Aust. Bull.* **140,** 1–56 (1941).
39. Graham, N. P. H. & Egerton, J. R. Pathogenesis of Ovine footrot: The role of some environmental factors. in *Australian Veterinary Journal* **44,** 235–240 (1968).
40. Vela, A. I. *et al. Psychrobacter pulmonis* sp. *nov*., isolated from the lungs of lambs. *Int J Syst Evol Microbiol* **53,** 415–419 (2003).
41. Nielsen, E. O., Nielsen, N. C. & Friis, N. F. *Mycoplasma hyosynoviae* arthritis in grower-finisher pigs. *J Vet Med A Physiol Pathol Clin Med* **48,** 475–486 (2001).
42. Sullivan, T. W. Skeletal problems in poultry: estimated annual cost and descriptions. *Poult Sci* **73,** 879–882 (1994).
43. Stokka, G. L. *et al.* Lameness in feedlot cattle. *Vet Clin North Am Food Anim Pr.* **17,** 189–207, viii (2001).
44. Wilson, D. J. *et al.* Unusual history and initial clinical signs of *Mycoplasma bovis* mastitis and arthritis in first-lactation cows in a closed commercial dairy herd. *J Am Vet Med Assoc* **230,** 1519–1523 (2007).
45. Johnstone, A. C. & King, C. M. Bovine and ovine Mycoplasmal arthritis and synovitis (abstract). *N Z Vet J* **51,** 46 (2003).
46. Meisel, J. S. *et al.* Skin microbiome surveys are strongly influenced by experimental design. *J. Invest. Dermatol.* **136,** 947–956 (2016).
47. Schloss, P. D., Gevers, D. & Westcott, S. L. Reducing the effects of PCR amplification and sequencing artifacts on 16S rRNA-based studies. *PLoS One* **6,** e27310 (2011).
48. Baker, G. C., Smith, J. J. & Cowan, D. A. Review and re-analysis of domain-specific 16S primers. *J Microbiol Methods* **55,** 541–555 (2003).
49. Tringe, S. G. & Hugenholtz, P. A renaissance for the pioneering 16S rRNA gene. *Curr Opin Microbiol* **11,** 442–446 (2008).
50. Yang, B., Wang, Y. & Qian, P.-Y. Y. Sensitivity and correlation of hypervariable regions in 16S rRNA genes in phylogenetic analysis. *BMC Bioinformatics* **17,** 135 (2016).
51. Klindworth, A. *et al.* Evaluation of general 16S ribosomal RNA gene PCR primers for classical and next-generation sequencing-based diversity studies. *Nucleic Acids Res.* **41,** e1 (2013).
52. Salter, S. J. *et al.* Reagent and laboratory contamination can critically impact sequence-based microbiome analyses. *BMC Biol* **12,** 87 (2014).
53. Kennedy, K., Hall, M. W., Lynch, M. D. J., Moreno-Hagelsieb, G. & Neufeld, J. D. Evaluating bias of Illumina-based bacterial 16S rRNA gene profiles. *Appl. Environ. Microbiol.*, doi: 10.1128/AEM.01451-14 (2014).
54. Refaai, W. *et al.* Digital dermatitis in cattle is associated with an excessive innate immune response triggered by the keratinocytes. *BMC Vet Res* **9,** 193 (2013).
55. Scholey, R. A. *et al.* Identifying host pathogenic pathways in bovine digital dermatitis by RNA-Seq analysis. *Vet J* **197,** 699–706 (2013).
56. Emery, D. L., Stewart, D. J. & Clark, B. L. The comparative susceptibility of five breeds of sheep to footrot. *Aust. Vet. J.* **61,** 85–88 (1984).
57. Wassink, G. J., Grogono-Thomas, R., Moore, L. J. & Green, L. E. Risk factors associated with the prevalence of footrot in sheep from 1999 to 2000. *Vet. Rec.* **152,** 551–555 (2003).
58. Mizutani, H., Black, R. & Kupper, T. S. Human keratinocytes produce but do not process pro-interleukin-1 (IL-1) beta. Different strategies of IL-1 production and processing in monocytes and keratinocytes. *J Clin Invest* **87,** 1066–1071 (1991).
59. Pepin, M. *et al.* Cytokine gene expression in sheep following experimental infection with various strains of *Corynebacterium pseudotuberculosis* differing in virulence. *Vet Res* **28,** 149–163 (1997).
60. Zhang, L. *et al.* Intra-amniotic administration of *E coli* lipopolysaccharides causes sustained inflammation of the fetal skin in sheep. *Reprod Sci* **19,** 1181–1189 (2012).
61. Bolger, A. M., Lohse, M. & Usadel, B. Trimmomatic: A flexible trimmer for Illumina sequence data. *Bioinformatics* **30,** 2114–2120 (2014).
62. Klindworth, A. *et al.* Evaluation of general 16S ribosomal RNA gene PCR primers for classical and next-generation sequencing-based diversity studies. *Nucleic Acids Res.* **41,** 1–11 (2013).
63. Edgar, R. C., Haas, B. J., Clemente, J. C., Quince, C. & Knight, R. UCHIME improves sensitivity and speed of chimera detection. *Bioinformatics* **27,** 2194–2200 (2011).
64. Oksanen, J. *et al. vegan: Community Ecology Package* (2016).
65. Vavrek, M. J. Fossil: Palaoecological and Palaeogeographical Analysis Tools. *Palaeontol. Electron.* **14** (2011).
66. Mestdagh, P. *et al.* A novel and universal method for microRNA RT-qPCR data normalization. *Genome Biol* **10,** R64 (2009).
67. Andersen, C., Jensen, J. & Orntoft, T. Normalization of Real Time Quantitative Reverse Transcription PCR Data : A Model Based Variance Estimation Approach to Identify Genes Suited for Normalization, Applied to Bladder and Colon Cancer Data Sets. *Cancer Res.* **64,** 5245 (2004).

68. Pfaffl, M. W., Tichopad, A., Prgomet, C. & Neuvians, T. P. Determination of stable housekeeping genes, differentially regulated target genes and sample integrity: BestKeeper–Excel-based tool using pair-wise correlations. *Biotechnol. Lett.* **26,** 509–15 (2004).
69. Xie, F., Xiao, P., Chen, D., Xu, L. & Zhang, B. miRDeepFinder: a miRNA analysis tool for deep sequencing of plant small RNAs. *Plant Mol Biol*, doi: 10.1007/s11103-012-9885-2 (2012).
70. Hughes, S., Poh, T. Y., Bumstead, N. & Kaiser, P. Re-evaluation of the chicken MIP family of chemokines and their receptors suggests that CCL5 is the prototypic MIP family chemokine, and that different species have developed different repertoires of both the CC chemokines and their receptors. *Dev Comp Immunol* **31,** 72–86 (2007).
71. Ihaka, R. & Gentleman, R. R: A language for data analysis and graphics. *J. Comput. Graph. Stat.* **5,** 299–314 (1996).
72. Robinson, M., McCarthy, D., Chen, Y. & Smyth, G. *edgeR: differential expression analysis of digital gene expression data* (2010).
73. McMurdie, P. J. & Holmes, S. phyloseq: an R package for reproducible interactive analysis and graphics of microbiome census data. *PLoS One* **8,** e61217 (2013).

Acknowledgements

This work was supported by the Biotechnology and Biological Sciences Research Council (BBSRC) Animal Health Research Club 2014, grant numbers BB/M012085/1 (University of Nottingham), the University of Nottingham and the Swedish Farmers' Foundation for Agricultural Research. GM had a fellowship from the Coordination for the Improvement of Higher Education (CAPES, Brazil). We thank Marianne Gilhuus for kindly providing DNA from *D. nodosus* and Dr Anna Aspán (SVA) for critical reading of the manuscript.

Author Contributions

G.M., A.M.B. and S.T. all wrote the manuscript and generated the figures. A.M.B. and R.D.E. provided bioinformatic analysis. G.M., C.S. and S.F. generated qPCR data. All authors have reviewed the manuscript.

Additional Information

Supplementary information accompanies this paper at http://www.nature.com/srep

Competing Interests: The authors declare no competing financial interests.

How to cite this article: Maboni, G. *et al.* A distinct bacterial dysbiosis associated skin inflammation in ovine footrot. *Sci. Rep.* **7**, 45220; doi: 10.1038/srep45220 (2017).

Publisher's note: Springer Nature remains neutral with regard to jurisdictional claims in published maps and institutional affiliations.

This work is licensed under a Creative Commons Attribution 4.0 International License. The images or other third party material in this article are included in the article's Creative Commons license, unless indicated otherwise in the credit line; if the material is not included under the Creative Commons license, users will need to obtain permission from the license holder to reproduce the material. To view a copy of this license, visit http://creativecommons.org/licenses/by/4.0/

© The Author(s) 2017

Appendix 3

Ovine interdigital skin tissue processing for histological proposes.

Bath	Medium	Time (minutes)	Process
1	dH_2O	60	Progressive dehydration
2	50% ethanol	240	
3	70% ethanol	240	
4	90% ethanol	Overnight	
5	100% ethanol	240	
6	Xylene	240	Preparation for wax bath and embedding

Haematoxylin and Eosin staining protocol for ovine interdigital skin.

Reagent	Time
Xylene	5 minutes
100% ethanol	5 minutes
90% ethanol	5 minutes
70% ethanol	5 minutes
dH_2O	5 minutes
Haematoxylin	Quick dip
Wash under running water	
1% acid IMS	2 dips (2-4 seconds each)
Wash under running water	
Ammoniated water	2 dips
Wash under running water	
Eosin	3 minutes
Wash under running water	
dH_2O	5 minutes
70% ethanol	5 minutes
90% ethanol	5 minutes
100% ethanol	5 minutes
Xylene	5 minutes
Mount using DPX	

Appendix 4

Instructions for preparation of 4% Hoof Agar provided by the National Veterinary Institute (SVA), Sweden.

Ingredients	Manufacture	Quantity/L
Sodium chloride	Merck	5g/L
Proteose Peptone	Difco	10g/L
Beef Extract Desiccate	Difco	10g/L
Yeast extract	Difco	1g/L
Bacto Agar	Difco	40g/L
Hoof powder	`Prepared in the SVA`	15g/L
Water		1L

Dichelobacter nodosus strains isolated from interdigital skin swabs.

***D. nodosus* ID strain**	**Foot disease status**	**Virulence**
MM242	Footrot	Virulent
MM247	Footrot	Virulent
MM248	ID	Virulent
MM260	ID	Virulent
MM261*	**ID**	**Virulent**
MM262	ID	Virulent
MM266	ID	Virulent
MM267	ID	Virulent
MM268	ID	Virulent
MM270	ID	Virulent
MM272	Footrot	Virulent
MM273	ID	Virulent
MM274	ID	Virulent
MM277*	**ID**	**Benign**

ID= interdigital dermatitis; * Strains used to infect the EVOC model. All strains were maintained in glycerol and cryobeads.

Appendix 5

Counts of fluorescently targeted *D. nodosus* cells by FISH method. Score system: 0= no invasive bacteria; 1= low number of invasive bacteria from 1-20; 2= moderate number of invasive bacteria from 20-200; 3= high number of invasive bacteria from 200 to uncountable bacterial cells.

Biopsy tissue ID	**Number of *D. nodosus* cells – slide section 1**	**Number of *D. nodosus* cells- slide section 2**	**Score**
Virulent biopsy 1	73	45	2
Virulent biopsy 2	16	15	1
Virulent biopsy 3	15	20	1
Virulent biopsy 4	26	20	2
Virulent biopsy 1.4*	>200	>200	3
Virulent biopsy 2.4*	>200	>200	3
Virulent biopsy 3.4*	>200	>200	3
Benign biopsy 1	151	176	2
Benign biopsy 2	>200	>200	3
Benign biopsy 3	79	89	3
Benign biopsy 4	10	17	1
Uninfected control 1	0	0	0
Uninfected control 2	0	0	0
Uninfected control 3	0	0	0
Uninfected control 4	0	0	0
Uninfected control 3.5*	0	0	0

*Biopsies treated with HEPES buffer in the culture media

Appendix 6

R scripts used in the RNAseq analysis

(Provided by ADAC, University of Nottingham)

```
source("http://bioconductor.org/biocLite.R")

#biocLite("edgeR")

library(edgeR)

library(limma)

biocLite("dplyr")

library(biomaRt)

library(dplyr)


##############################################################################################

## USER TO CHANGE


x <- read.table("test",sep='\t',head=TRUE)

x <- x[- grep("__", x$GENE),]


group <- factor(c(1,1,1,1,1,1,1,1,1,1,1,1,1,1,1,1,1))


all_results_table = "combined.counts.xls"

de_ids_table = "combined.counts.EdgeR.xls"

FDR.lt0.05_table = "combined.counts.DE_edgeR.xls"

FDR.lt0.05_FC2.table = "combined.counts_DE_FC2.edgeR.xls"


mds.plot.name = "combined.counts.MDS.plot.pdf"
```

```
smear.plot.name = "combined.counts.smear.plot.pdf"

volcano.plot.name = "combined.counts.volcano.plot.pdf"



all.RPKM.table = "combined.counts.RPKM.table"

##############################################################################################

# determine gene lengths



ensembl = useMart("ensembl", dataset="oaries_gene_ensembl")

ensembl_lookup <-
getBM(attributes=c("ensembl_gene_id","transcript_length"),values=x$GEN
E, mart=ensembl)



ensembl_lookup_match <- merge(x, ensembl_lookup, by.x="GENE",
by.y="ensembl_gene_id", all=TRUE)

ensembl_lookup_match <- ensembl_lookup_match[c(1,20)]

ensembl_lookup_match[is.na(ensembl_lookup_match)] <- 50



# average for replicate genes is different lengths

ensembl_lookup_match.norm <- ensembl_lookup_match %>%
group_by(GENE) %>% summarize(length = mean(transcript_length))

ensembl_lookup_match.norm <-
ensembl_lookup_match.norm[ensembl_lookup_match.norm$GENE %in%
x$GENE ,]



# make rownames column 1

rownames(x) <- x[,1]

x <- x[-1] #remove extra "GENE" column

y <- DGEList(counts=x,group=group,genes =
ensembl_lookup_match.norm)
```

```
## Since the smallest group size is TWO, we keep genes that achieve at least one count per million (cpm) in at least TWO samples:\n";

keep <- rowSums(cpm(y)>1) >= 2

y <- y[keep,]

# Re-compute the library sizes

y$samples$lib.size <- colSums(y$counts)


# Compute effective library sizes using TMM normalization:\n";

y <- calcNormFactors(y)

y$samples


############### generate RPKM values
##############################

rpkm.table <- rpkm(y)

rpkm.table <- as.data.frame(format(rpkm.table, scientific=FALSE))

rpkm.table.genes<- rownames(rpkm.table)

rpkm.table <- cbind(rpkm.table.genes, rpkm.table)


write.table(rpkm.table,
file=all.RPKM.table,row.names=FALSE,col.names=TRUE,quote=FALSE,sep='\t')


#  Output plot as a pdf

pdf(mds.plot.name)

plotMDS(y)

dev.off()


y <- estimateCommonDisp(y)

y <- estimateTagwiseDisp(y)

#plotBCV(y)

et <- exactTest(y)
```

```
top <- topTags(et)


pdf(smear.plot.name)

plotSmear(y, de.tags=top, main="Differential expression using the
common dispersion")

dev.off()


## Check the individual cpm values for the top genes:

cpm(y)[rownames(top), ]

## The total number of DE genes at 5% FDR is given by:

summary(de <- decideTestsDGE(et))

## Plot the log-fold-changes, highlighting the DE genes:

detags <- rownames(y)[as.logical(de)]


# volcano plot

pdf(volcano.plot.name)

plot(et$table$logFC, -log10(et$table$PValue), pch=19, cex=0.2, main
="Volcano Plot", xlab = "LogFC", ylab = "-log10 pvalue")

dev.off()


allResults <- topTags( et , n = nrow( et$table ) )$table

gene.counts <- y$counts

combined.results <- merge(allResults, gene.counts, by=0, all=TRUE)

combined.results.UP.G2 <- subset(combined.results, logFC > 0)

combined.results.DOWN.G2 <- subset(combined.results, logFC <= 0)


combined.results.UP.G2[, "G2vsG1"] <- "UP"

combined.results.DOWN.G2[, "G2vsG1"] <- "DOWN"
```

```
combined.results <-
rbind(combined.results.UP.G2,combined.results.DOWN.G2)


significant.results <- subset(combined.results, FDR <= 0.05)

significant.results.FC2.UP.G2 <- subset(significant.results, logFC >= 1)

significant.results.FC2.DOWN.G2 <- subset(significant.results, logFC <= -
1)


combined.significant.FC2 <-
rbind(significant.results.FC2.UP.G2,significant.results.FC2.DOWN.G2)


write.table(combined.results,
file=all_results_table,row.names=FALSE,col.names=TRUE,quote=FALSE)

write.table(significant.results,
file=FDR.lt0.05_table,row.names=FALSE,col.names=TRUE,quote=FALSE)

write.table(detags,
file=de_ids_table,row.names=FALSE,col.names=FALSE,quote=FALSE)

write.table(combined.significant.FC2,
file=FDR.lt0.05_FC2.table,row.names=FALSE,col.names=TRUE,quote=FAL
SE)
```